CENTRO DE INVESTIGACIÓN Y DE ESTUDIOS AVANZADOS
DEL INSTITUTO POLITÉCNICO NACIONAL

UNIDAD ZACATENCO
DEPARTAMENTO DE FÍSICA

“Decaimientos exclusivos hadrónicos del leptón τ como pruebas de interacciones no estándar”

Tesis que presenta

Jesús Javier Rendón Castañeda

para obtener el Grado de

Doctor en Ciencias

en la Especialidad de

Física

Director de tesis: Dr. Pablo Roig Garcés

Ciudad de México Octubre, 2021

CENTER FOR RESEARCH AND ADVANCED STUDIES OF THE
NATIONAL POLYTECHNIC INSTITUTE

PHYSICS DEPARTMENT

“Exclusive hadronic τ decays as probes of non-SM interactions”

by

Jesús Javier Rendón Castañeda

In order to obtain the

Doctor of Science

degree, speciality in

Physics

Advisor: Ph. D. Pablo Roig Gacés

Mexico City October, 2021

CENTRO DE INVESTIGACIÓN Y DE ESTUDIOS AVANZADOS DEL INSTITUTO POLITÉCNICO NACIONAL

DEPARTAMENTO DE FÍSICA

THESIS: Exclusive hadronic τ decays as probes of non-SM interactions.

A Thesis submitted by Jesús Javier Rendón Castañeda as partial fullfilment to obtain the degree of Doctor in Science.

Advisor:
Dr. Pablo Roig Garcés

A mis padres.

Agradecimientos

A mis padres agradezco el haberme brindado la educación que ha hecho todo esto posible, sin esos primeros esfuerzos y sin esa motivación primordial, los logros y las alegrías que la física ha traído a mi vida no habrían podido concretarse. El sentido de progreso que me han inculcado es uno de sus regalos más grandes.

A mi asesor Pablo Roig le agradezco la formación que me ha brindado, gracias por haberme guiado de la mejor manera posible estos maravillosos seis años. Junto con mis años de infancia, estos últimos seis que comprenden mi formación académica de maestría y doctorado han sido los más felices de mi vida y es que bien podría decirse que esta ha sido mi segunda infancia.

A mis sinodales; Genaro Toledo, Omar Miranda, Eduard De La Cruz, Pedro Podesta y Alonso Contreras, les agrandezco primero su tiempo y su disposición y también sus preguntas, comentarios y consejos. Gracias a todos por haber enriquecido enormemente esta tesis.

Agradezco también la amistad de mucha gente valiosa que conocí en esta etapa de mi vida, a mis amigos de generación; Marcela, Luis, Héctor, Fernando, José Luis Gaona, Armando, Saúl, José Luis Bonilla, Ángel y Luis Enrique, a los del cubo; Miguel y Lalo, a los que tenían más experiencia y siempre brindaron un buen consejo; Adolfo, Gerardo, Chepe, Gus y Jorge Luis y a mis hermanitos académicos; de nuevo Marcela y Adolfo, Alex, Faby, Enrique, Pacheco, Saray y Luis Fernando.

Agradezco también a mis viejos amigos de Sinaloa; a los de la facultad, a Irene, Ralihe, Argelia, Verónica, Yoanna, Solángel y Adriana; a mi querido amigo de infancia Bryan; y a los prepos, Edgar y Ernesto. A todos ellos por estar siempre al pendiente de como me iba y por mostrar siempre una curiosidad genuina hacia mis aventuras de posgrado.

Agradezco infinitamente la formación que recibí en CINVESTAV y en la UAS. Como olvidar esas clases magistrales de Pepe Méndez y de Abdel Pérez. Como olvidar los coloquios y seminarios y todas esas discusiones y valiosas preguntas que se generaban. Muchas gracias a los organizadores de las cátedras Augusto García, aprendí de ellas a montones. Gracias a Gaby

por el magnífico programa de laboratorio de idiomas que maneja en CINVESTAV, aprendí muchísimo de esos clubes de conversación de inglés. Gracias al Ingeniero Aurelio Espíritu por ayudarme cada vez que tenía un problema ténico con mi computadora, y muchas gracias también a Rosemary y a Mariana por toda su ayuda administrativa y por su trato amable. En mi vida nunca he visto otra institución más eficiente que CINVESTAV.

Gracias a la Red FAE por todo el apoyo que se me brindó siempre para asistir a escuelas y workshops. A los organizadores del programa de veranos en laboratorios extranjeros les agradezo todo su apoyo al brindarme la oportunidad de visitar FERMILAB aquél lejano 2013. Esa experiencia fue inolvidable.

Agradezco a ICTP el haberme ofrecido ayuda económica para asistir a la escuela de verano de partículas 2019 en Trieste. Este evento marcó mi vida, jamás olvidaré el curso de flavor physics de Yuval Grossman ni el de física de neutrinos de André de Gouvea, además de haber tenido la oportunidad de conocer a estudiantes brillantes. Yo sólo sé que a ICTP vuelvo.

Gracias a mis profesores de la UAS por haber sembrado la primer semilla. Estaré muy agradecido siempre con Ildefonso, Pedro e Isabel por haberme introducido en la física de partículas. Muchas gracias también al profe Leyva, a Raúl Félix y a Gelacio por sus maravillosas clases de física general, con ellos di mis primeros pasos.

Gracias de nuevo a CINVESTAV por el apoyo de obtención de grado, y por último, pero no menos importante, quiero agradecer a CONACYT por haberme otorgado las becas que hicieron esto posible y al pueblo de México porque es este el que finalmente aporta para que se desarrolle algo de ciencia básica en nuestro país.

Resumen

El modelo estándar de la física de partículas (SM) es la teoría física más poderosa que tenemos en la ciencia. Pese a su enorme poder de predicción, existen fenómenos que se escapan del alcance explicativo del SM y a los que conocemos como física más allá del modelo estándar o simplemente como nueva física (NP). Este trabajo de tesis tiene como objetivo estudiar potenciales efectos de nueva física usando para ello decaimientos hadrónicos del leptón Tau a uno y dos mesones pseudoscalares. Se estudian a detalle particularmente los decaimientos a un mesón pseudoescalar: $\tau^- \to \pi^-\nu_\tau$ y $\tau^- \to K^-\nu_\tau$ y los decaimientos a dos mesones pseudoescalares $\tau^- \to (K\pi)^-\nu_\tau$ y $\tau^- \to K^-K^0\nu_\tau$, además nos beneficiamos mucho de los decaimientos $\tau^- \to K\eta^{(\prime)}\nu_\tau$ y $\tau^- \to \pi^-\pi^0\nu_\tau$.

Nuestros análisis están basados en el uso de teorías efectivas, concretamente en el uso del SMEFT a bajas energías, donde hemos empleado operadores de dimensión seis.

Para el estudio de los factores de forma relevantes hacemos uso de la Teoría Quiral de Perturbaciones (ChPT), de relaciones de dispersión y de datos de lattice.

Nuestra búsqueda se centrará en el estudio de interacciones no estándar y para ello estudiaremos distintos observebles como Dalitz plots, espectros, branching ratios y asimetrías forward-backward. Estudiaremos también los posibles efectos que pudiera tener nueva físca pesada en la violación de CP.

La finalidad de este trabajo es hacer notar que la física del Tau no es sólo un laboratorio muy limpio para estudiar QCD a bajas energías (hecho por el que es bien conocida) sino que además resulta sumamente útil para explorar posibles señales de nueva física. Esta es una razón más para considerar a los decaimientos hadrónicos del Tau como canales fundamentales de estudio en el experimento Belle-II.

Abstract

The Standard model of particle physics (SM) is the most powerful physical theory that we have in science. Despite its predictive power, we have phenomena that are not understood in the framework of the SM to which we refer as physics beyond the standard model or as new physics (NP). The purpose of this thesis work is to study potential new physics effects using one- and two-pseudoscalar meson hadronic Tau decays. We study in detail the one-meson decay modes: $\tau^- \to \pi^-\nu_\tau$ and $\tau^- \to K^-\nu_\tau$, and the two-meson decay modes: $\tau^- \to (K\pi)^-\nu_\tau$ y $\tau^- \to K^-K^0\nu_\tau$. We also benefit a lot from the decays $\tau^- \to K\eta^{(\prime)}\nu_\tau$ and $\tau^- \to \pi^-\pi^0\nu_\tau$.

Our analysis is based on effective field theories, particularly in the SMEFT at low energies. We have used dimension six operators.

For our study of the relevant form factors we have used Chiral Perturbation Theory (ChPT), dispersion relations and lattice data.

Our research focuses in the study of non-standard interactions. With this in mind, we will study several observables like Dalitz plots, spectra, branching ratios and forward-backward asymmetries. We will also study the potential effects of heavy new physics in CP violation.

The aim of this work is to point out that Tau physics is more than a clean low energy QCD laboratory (for which is very well known). We want to show that the Tau lepton can also be used as a probe of NP. This is yet another reason for considering hadronic Tau decays as golden modes at the Belle-II experiment.

Contents

1 The Tau Lepton: an invaluable tool in the search for new physics **6**
- 1.1 General introduction . . . 6
- 1.2 Tau Physics . . . 8
  - 1.2.1 Leptonic decays of the Tau lepton . . . 9
  - 1.2.2 Hadronic decays of the Tau lepton . . . 10
- 1.3 Different searches for new physics . . . 12
- 1.4 Organization of the Thesis . . . 13

2 Effective Field Theories **15**
- 2.1 Introduction . . . 15
- 2.2 Standard Model Effective Field Theory (SMEFT) . . . 21
  - 2.2.1 Standard Model . . . 21
  - 2.2.2 SMEFT . . . 31
- 2.3 QCD and Chiral Perturbation Theory . . . 33
  - 2.3.1 Quantum Chromodynamics . . . 33
  - 2.3.2 Chiral Perturbation Theory (ChPT) . . . 39
  - 2.3.3 Resonance Chiral Theory . . . 47

3 Effective-field theory analysis of the $\tau^- \to (K\pi)^- \nu_\tau$ decays **49**
- 3.1 Summary . . . 49
- 3.2 Introduction . . . 50
- 3.3 Effective theory analysis of $\tau^- \to \nu_\tau \bar{u} s$ . . . 52
- 3.4 Semileptonic τ decay amplitude . . . 54
- 3.5 Hadronization of the scalar, vector and tensor currents . . . 56
- 3.6 Decay observables . . . 60
  - 3.6.1 Dalitz plots . . . 60
  - 3.6.2 Angular distribution . . . 63
  - 3.6.3 Decay rate . . . 66
  - 3.6.4 Forward-backward asymmetry . . . 66
  - 3.6.5 Limits on $\hat{\epsilon}_S$ and $\hat{\epsilon}_T$ . . . 68

3.7 CP violation 72

4 Effective-field theory analysis of the $\tau^- \to K^-(\eta^{(\prime)}, K^0)\nu_\tau$ decays 74
4.1 Summary of the chapter 74
4.2 Introduction 75
4.3 Effective field theory analysis and decay amplitude of $\tau^- \to \nu_\tau \bar{u} D$ $(D = d, s)$ 76
4.4 Hadronization of the scalar, vector and tensor currents 78
4.5 Decay observables 81
4.5.1 Dalitz plot 81
4.5.2 Angular distribution 83
4.5.3 Decay rate 84
4.5.4 Forward-backward asymmetry 86
4.5.5 Limits on $\hat{\epsilon}_S$ and $\hat{\epsilon}_T$ 88

5 Global analysis of exclusive hadronic tau decays 92
5.1 Introduction 92
5.2 SMEFT Lagrangian and decay rate 93
5.3 New Physics bounds from $\Delta S = 0$ decays 95
5.4 New Physics bounds from $|\Delta S| = 1$ decays 97
5.5 New Physics bounds from a global fit to both $\Delta S = 0$ and $|\Delta S| = 1$ sectors 99

6 Summary and conclusions 101
6.1 Conclusions for chapter 3 101
6.2 Conclusions for chapter 4 102
6.3 Conclusions for chapter 5 103

Appendices 105

A The CCWZ Formalism 106
A.1 Application of the formalism to the QCD Chiral Lagrangian . 107

B Spin and parity of hadronic currents 110

C Form Factors 113

D Polarization effects in the decay $\tau^- \to \pi^- \ell^+ \ell^- \nu_\tau$ 118

E Global constraints on neutral-current generalized neutrino interactions 132

Chapter 1

The Tau Lepton: an invaluable tool in the search for new physics

"Ars longa, vita brevis"

Hipócrates

1.1 General introduction

The Standard Model (SM) of particle physics [1, 2, 3] is without question the most successful physical theory that we have and probably the most beautiful intellectual construction conceived by humankind, but even with all its predictive power and beauty, we know that the SM cannot be the whole story. Despite its success, there are many open questions in high energy physics that the SM does not answer. In many of those cases, the failure comes from the fact that the theoretical framework of the SM was not even constructed to handle such questions, that is why the SM must be extended somehow. Some of the problems within the SM are the following:

- Neutrino masses: This is the most obvious of the problems since in the SM neutrinos are assumed to be massless by definition, but, on the other hand, we know from oscillation experiments that they do have mass, although this mass is unusually small. This fact must be incorporated in the SM and there are several ways to do it that we will discuss very briefly along this thesis.

- Matter-Antimatter asymmetry: There is much more matter than antimatter in the universe and we do not fully understand why this is so.

- Dark sector: The SM particles compose only the 5% of the matter/energy content of the universe, the other 95% is called the dark sector and we do not know exactly what it is. This dark sector has one component known as dark matter, which is needed to explain at least three different phenomena: the rotational speeds of galaxies, gravitational lensing in dark regions, and the anisotropies in the cosmic microwave background. The other component, known as dark energy -about which we know even less than about dark matter-, is needed to explain the acceleration of the universe among other things.

Finding an answer to any of these open questions is the main concern of the high energy physics community and the general theoretical physics community nowadays. As we have anticipated before, the solution to those problems is beyond the scope of the SM and belongs to what we call New Physics, or NP for short, this is an appropriate name since we do not fully understand what is behind those processes and in this respect the laws of physics governing them are in some sense 'new'.

There are basically two approaches when one deals with NP problems, one is to construct specific models to try to answer very specific questions, this approach is really elegant and it is usually ambitious, in the sense that one needs to assume many things like the symmetries and degrees of freedom that play a role at the relevant energy scale assumed in the model. The other approach is to work with the problems in a model independent way, this is achieved with the help of the so called Effective Field Theories (EFTs), in this approach one does not assume heavy degrees of freedom or symmetries realized at high energy scales, one just starts with what is fully known and from there by extending the Lagrangian of the theory with more terms allowed by the low energy symmetries one tries to 'guess' what is happening at higher energy scales. The second approach is more conservative than the first one, and the fact that it is essentially model-independent makes it specially suitable and powerful to handle NP searches. This is why we chose to follow the second approach in this thesis. We will discuss Effective Field Theories in great detail in chapter 2 and throughout the whole work.

There are of course other open questions that need physics beyond the standard model besides the three that were pointed out previously, as for example: why are the forces of nature of such different strengths?, why are there three generations of particles?, and how can we stabilize the electroweak scale under radiative corrections?, just to mention a few, however we chose

the neutrino mass problem, the matter-antimatter asymmetry and the dark sector as the most fundamental problems and the most urgent priorities in particle physics nowadays.

1.2 Tau Physics

The Tau lepton was discovered by Martin Perl at the SLAC-LBL collaboration using e^+e^- collisions [4, 5]. The name they chose for the new particle [5] Tau or τ comes from the first letter of the greek word $\tau\rho\iota\tau o\varsigma$ which means 'the third', in allusion to the three charged leptons e, μ, and τ.

The Tau lepton is the heaviest lepton and it belongs to the third generation of particles. Being the mass the only difference between generations, the tau lepton is similar to the electron and muon in any other respect, so that, electrons, muons and taus have the same interactions with the photon, the W and the Z bosons, or in other words, they all have the same electric and weak interactions.

There is one more fundamental interaction present in the SM, the strong force, what can we say about it? of course leptons do not 'feel' it, so again, electrons, muons and Taus behave in a similar way. They are all 'blind' to the strong force, but here there is something that makes the Tau lepton really special. Given its large mass ($M_\tau \approx 1.777$ GeV [6]), unlike electrons and muons, Taus are capable of decaying into hadrons, this fact makes the Tau lepton a really helpful tool when one studies low energy QCD. Although it does not feel the strong force by itself, it serves as a bridge to study low energy QCD phenomena in a rather clean environment.

The decays of the Tau lepton to hadrons referred previously are known as semileptonic decays, note that in this special case when we say hadrons we really mean mesons because the Tau cannot decay into baryons. The reason is very simple, although the mass of the Tau is enough to decay into one proton which is the lightest of the baryons, this process is forbidden by the conservation of baryon number, it would necessarily have to decay into a proton-antiproton pair, but the Tau is not massive enough to do that.

The study of the Tau lepton or Tau physics as we will say from now on is not only important as a tool to study low energy QCD phenomena, although that by itself is so fundamental that it deserves special attention, Tau physics is much broader and deeper. It is useful in many areas of particle physics, for example in the determination of the value of the strong coupling constant α_S at low energies. We will see this in great detail in section 2.3 (see figure 2.3). Tau physics is also very useful in a determination of the value of the Cabibbo-Kobayashi-Maskawa matrix parameter V_{us}, which is competi-

tive with the results from kaon decays. It is also fundamental in the study of lepton universality and in new physics searches like the study of lepton flavor and lepton number violations, CP violation, and potential modifications of the Lorentz structure of the fundamental interactions. As a matter of fact, one of the main purposes in this thesis work is to use Tau physics to study possible NP scenarios.

Before we start our searches for NP signals, it is important to discuss the things that are already well established, so we are going to discuss how leptonic and hadronic decays of the Tau lepton proceed according to the SM of particle physics.

1.2.1 Leptonic decays of the Tau lepton

Due to its large mass, the Tau lepton has many different ways to decay, or many open channels as we like to say. Some of those channels are purely leptonic and some of them have hadrons in the final state, these are the semileptonic decays we mentioned previously. From all these possibilities, leptonic decays are special in the sense that they are really easy to calculate. They are basically an extension of muon decay and proceed trough the exchange of a W-boson. This is the so called weak charged-current interaction and is governed by the following Lagrangian [1]

$$\mathcal{L}_{cc} = -\frac{g}{2\sqrt{2}} \sum_{\ell} W_{\mu} \bar{\nu}_{\ell} \gamma^{\mu} (1 - \gamma_5) \ell + h.c. \,, \tag{1.1}$$

where $W_{\mu} = \frac{W^1_{\mu} - i W^2_{\mu}}{\sqrt{2}}$ [2] creates a physical W^- boson. From the previous expression we see that the W boson couples to the leptons with the same strength, so that lepton universality for the charged weak interactions is evident.

According to the Feynman rules, the generic form for an amplitude that comes from eq. (1.1) is given by,

$$\mathcal{M} = \left(\frac{-ig}{2\sqrt{2}} \right)^2 J^{\nu\dagger}_W \left(g_{\nu\mu} - \frac{q_\nu q_\mu}{M^2_W} \right) \left(\frac{-i}{q^2 - M^2_W} \right) J^{\mu}_W \,, \tag{1.2}$$

where,

$$\begin{aligned} J^{\mu}_W &= \bar{\nu}_{\ell} \gamma^{\mu} (1 - \gamma_5) \ell \,, \\ J^{\mu\dagger}_W &= \bar{\ell}' \gamma^{\mu} (1 - \gamma_5) \nu_{\ell'} \,. \end{aligned} \tag{1.3}$$

[1] See chapter 2 for a general discussion of the weak charged-current interaction and a complete discussion of the SM.

[2] W^i_{μ} refer to the weak isospin components of this gauge boson.

For a small momentum transfer, $|q^\mu| \ll M_W$, the W-boson propagator reduces to an effective four-fermion interaction just as in the Fermi Theory of muon and beta decays. As a result the effective Hamiltonian density becomes,

$$\mathcal{H}_{eff} = \frac{G_F}{\sqrt{2}} J^\dagger_{W\mu} J^\mu_W \,, \tag{1.4}$$

where $G_F/\sqrt{2} = g^2/(8M_W^2)$.

Even though one has the SM, which is the full theory in this case, it is sometimes convenient to work with effective theories. For Tau decays, one uses the Fermi theory for practical reasons just as occurs with the muon decay. We basically do not lose anything considering the W-propagator shrunk to a point while we gain a lot of operational power. We will see shortly that the same effective field theory ideas can also be applied to the hadronic decays, where it turns out to be even more convenient to use effective Lagrangians since we will always be working in the low energy regime of QCD.

The partial width for the $\tau^- \to \nu_\tau \ell^- \bar{\nu}_\ell$ decays is given by,

$$\Gamma(\tau^- \to \nu_\tau \ell^- \bar{\nu}_\ell) = \frac{G_F^2 M_\tau^5 S_{EW}}{192\pi^3} f\left(\frac{m_\ell^2}{M_\tau^2}\right)(1 + \delta^{\ell\tau}_{RC}) \,, \tag{1.5}$$

where S_{EW} resums the short-distance electroweak corrections [7, 8, 9, 10, 11, 12, 13, 14], $f(x) = 1 - 8x + 8x^3 - x^4 - 12x^2\log(x)$, and

$$\delta^{\ell\tau}_{RC} = \frac{\alpha}{2\pi}\left[\frac{25}{4} - \pi^2 + \mathcal{O}\left(\frac{m_\ell^2}{M_\tau^2}\right)\right] + ... \tag{1.6}$$

takes into account QED radiative corrections.

1.2.2 Hadronic decays of the Tau lepton

Hadronic or semileptonic Tau decays are decays of the Tau lepton that have hadrons (really mesons) in the final state. These decays have proved to be of fundamental importance in the study of low energy QCD, this is a well known fact. In this work we want to show that semileptonic Tau decays are much more than a clean low energy QCD laboratory. We will see that they are also very useful in the search for new physics effects and for this reason they will have a leading role in this thesis work.

The mass of the Tau lepton is really large compared with the mass of light mesons like pions and kaons, therefore, the Tau has many semileptonic channels open, starting with the simple decays into one meson (two body decays) like $\tau^- \to \pi^-\nu_\tau$ and $\tau^- \to K^-\nu_\tau$, passing to decays into two mesons (three

body decays) like $\tau^- \to \pi^-\pi^0\nu_\tau$ and $\tau^- \to (K\pi)^-\nu_\tau$, to higher multiplicities like decays into 3, 4 and 5 mesons. Multiplicities higher than 5 mesons are kinematically allowed, but they do not have too much phenomenological interest.

The semileptonic decays of the Tau lepton proceed through the exchange of a W-boson according to the SM, just as purely leptonic decays. The interaction is again given by the weak charged-current Lagrangian,

$$\mathcal{L}_{cc} = -\frac{g}{2\sqrt{2}} W_\mu \bar{u}\gamma^\mu(1-\gamma_5)(V_{ud}d + V_{us}s) + h.c.\,, \tag{1.7}$$

where V_{ud} and V_{us} are elements of the CKM (or quark-mixing) matrix, V_{ud} mediates the strangeness conserving decays while V_{us} mediates the strangeness changing decays, both will be very useful in our studies along this work.

The simplest hadronic decays are the one-meson decay modes $\tau^- \to P^-\nu_\tau$ where $P = \pi, K$. Here the kinematics is fixed since these are two-body decays, then the decay rates can be trivially calculated and are given by the following expression,

$$\Gamma(\tau^- \to \pi^-\nu_\tau) = \frac{G_F^2 |V_{ud}|^2 f_\pi^2 M_\tau^3 S_{EW}}{8\pi}\left(1 - \frac{m_\pi^2}{M_\tau^2}\right)(1 + \delta_{em}^{\tau\pi})\,, \tag{1.8}$$

where f_π is the pion decay constant and the quantity $\delta_{em}^{\tau\pi}$ accounts for the electromagnetic radiative corrections. For the channel $\tau^- \to K^-\nu_\tau$, the decay rate is exactly as in eq. (1.8) but replacing $V_{ud} \to V_{us}$, $f_\pi \to f_K$, $m_\pi \to m_K$ and $\delta_{em}^{\tau\pi} \to \delta_{em}^{\tau K}$.

The constants f_π and f_K come from the relevant matrix elements

$$\langle \pi^-(p)|\bar{d}\gamma^\mu\gamma^5 u|0\rangle = -i\sqrt{2} f_\pi p^\mu\,, \quad \langle K^-(p)|\bar{s}\gamma^\mu\gamma^5 u|0\rangle = -i\sqrt{2} f_K p^\mu\,, \tag{1.9}$$

where $f_\pi \sim 92$ MeV and $f_K \sim 110$ MeV, whose values are measured from the decays $\pi^- \to \mu^-\bar{\nu}_\mu$ and $K^- \to \mu^-\bar{\nu}_\mu$, respectively. Note that the values for f_π and f_K can also be determined from Lattice QCD [15] and in fact we will use the lattice values for f_π and f_K in chapter 5 when we discuss a global effective field theory analysis for tau decays.

For the two-meson decay modes $\tau^- \to (PP')\nu_\tau$, the matrix elements are more complicated than the simple one-meson formulas (1.9) since in this case the matrix elements are parametrized in terms of functions and not just constants. These functions that parametrize the hadronization process are known as form factors and they appear inside the matrix elements in the following way

$$\langle P^- P'^0|\bar{d}_i\gamma^\mu u|0\rangle = C_{PP'}\left[\left(p_- - p_0 - \frac{\Delta_{PP'}}{s}q\right)^\mu F_V^{PP'}(s) + \frac{\Delta_{PP'}}{s}q^\mu F_S^{PP'}(s)\right], \tag{1.10}$$

where $\bar{d}_i$ is either $\bar{d}$ or $\bar{s}$, p_-^μ and p_0^μ are the momenta of the charged and neutral pseudoscalars, $\Delta_{PP'} = m_P^2 - m_{P'0}^2$, $q^\mu = (p_- + p_0)^\mu$ is the momentum transfer, $s = q^2$ and $F_V^{PP'}(s)$ and $F_S^{PP'}(s)$ are the vector and the scalar form factors, respectively. In chapters 3, 4 and 5, we will discuss in more detail the scalar and vector form factors, additionally, we will add a tensor form factor to our analysis which will play a key role, specially in chapter 3. Also in appendix C you will find more information about all the form factors that we will discuss in the text. The global normalization coefficients $C_{PP'}$ are chosen so that the vector form factor $F_V^{PP'}(s)$ is one at lowest order in Chiral Perturbation Theory (see section 2.3.2), the values for $C_{PP'}$ for each of the channels are [3] ,

$$C_{\pi\pi} = \sqrt{2}\,,\; C_{K\bar{K}} = -1\,,\; C_{K\pi} = \frac{1}{\sqrt{2}}\,,\; C_{\pi\bar{K}} = -1\,, C_{K\eta} = \sqrt{\frac{3}{2}}\,. \tag{1.11}$$

The hadronic invariant mass distribution for the two-meson decay modes is given by

$$\begin{aligned}\frac{d\Gamma}{ds} =& \frac{G_F^2 |V_{ui}|^2 M_\tau^3}{768\pi^3} S_{EW} C_{PP'}^2 \left(1 - \frac{s}{M_\tau^2}\right) \\ &\times \left[\left(1 + \frac{2s}{M_\tau^2}\right) \lambda_{PP'}^{3/2} |F_V^{PP'}(s)|^2 + 3\frac{\Delta_{PP'}^2}{s^2} \lambda_{PP'}^{1/2} |F_S^{PP'}(s)|^2\right]\,,\end{aligned} \tag{1.12}$$

where $\lambda_{PP'} \equiv \lambda(s, m_{P^-}^2, m_{P'0}^2)/s^2$, S_{EW} resums the short-distance electroweak corrections and $\lambda(x,y,z) = x^2 + y^2 + z^2 - 2xy - 2xz - 2yz$ is the usual Kallen function.

In chapters 3, 4 and 5 we will see how expressions (1.8) and (1.12) are modified in the presence of new physics.

1.3 Different searches for new physics

There are two different ways to look for new particles and new interactions beyond the SM. One is to produce the new particles directly and the other is to measure the effects of these new particles indirectly through quantum effects. In the following two points we explain exactly what we mean by this:

- Direct detection: according to Einstein's famous formula $E = mc^2$, new particles could be produced in collider experiments if the energy of the collisions is high enough. This has been the route that led to the

[3] For simplicity, the physical η meson was identified with the η_8 of flavor $SU(3)$.

discovery of many of the elementary particles of the SM like the $W^{\pm}$ and Z bosons in 1983 at CERN, and more recently the Higgs boson in 2012, also at CERN. Since the discovery of the Higgs, the SM is complete, so that we do not know exactly what we are looking for, in the sense that we do not know how many new particles and interactions are present at higher energies, or if they exist at all. On the one hand, we have the possibility that they are just around the corner waiting to be discovered by the next generation of particle accelerators, but on the other hand, we have the possibility that these particles are so massive that they are very far to be produced directly.

- Indirect detection: new heavy particles and potential new interactions could be observed indirectly through quantum corrections (loop effects) if the measurements are sufficiently precise. As a matter of fact, some particles were postulated to explain several observables before they were actually produced in collider experiments. A famous example is the charm quark, which was first proposed to explain the branching ratio for the process $K_L \to \mu^+\mu^-$. Without the charm quark the calculation for the branching ratio of $K_L \to \mu^+\mu^-$ was predicted to be much larger than experimentally measured. This is a consequence of the GIM mechanism which states that there are no flavor-changing neutral currents in the SM. We will briefly discuss the GIM mechanism in chapter 2.

Since the new physics energy scale could be extraordinarily high, the second point is particularly useful in the current searches. In fact, this indirect approach fits perfectly within the EFT tools and techniques that we have mentioned before and it is the one that we will follow in this thesis.

1.4 Organization of the Thesis

So far, we have discussed some important aspects of Tau physics in this chapter. In chapter 2 we will discuss in detail the fundamentals of effective field theories, first, we will explain some generalities of EFTs and then we will review meticulously two fundamental examples, namely: the Standard Model Effective Field Theory (SMEFT) and Chiral Perturbation Theory (ChPT). These two examples will serve to illustrate the main ideas behind EFTs, and will also serve as the basic ingredients of this thesis.

In chapters 3 to 5, we present our results. In chapter 3, we analyze in detail the decays $\tau^- \to (K\pi)^-\nu_\tau$. In chapter 4 we study the decay $\tau^- \to K^-K^0\nu_\tau$ and also discuss very briefly the decays $\tau^- \to K^-\eta^{(\prime)}\nu_\tau$.

In chapter 5 we take advantage of our results in chapters 3 and 4 and perform a global analysis of hadronic Tau decays.

Finally, in chapter 6 we summarize our main findings and present our conclusions.

Several appendices complement this thesis: the first three of them include necessary technical details on the formalism used to describe the pseudoGoldstone bosons in chiral Lagrangians, the hadronic currents and their corresponding form factors. Appendix D includes the main results on polarization observables in the $\tau^- \to \pi^- \ell^+ \ell^- \nu_\tau$ decays (this work was started in my master thesis) and Appendix E summarizes my most recent results, on neutral-current generalized neutrino interactions, within a global analysis.

Before concluding this chapter, we want to say that Tau physics is in a golden age. The precise measurements achieved mainly thanks to the Z and B factories [16, 17] have promoted this area to the level of precision necessary to test the SM and its possible extensions in a manner which is complementary or even competitive with other usual low-energy probes, such as nuclear β decays or semileptonic pion and kaon decays and also with the high-energy measurements at LHC scales. We expect that the analysis carried out in this work can serve as a motivation for the experimental Tau Physics groups at Belle(-II) [18].

This chapter was mostly based in refs. [19, 20], and ref. [21] was very helpful. Finally, the recent book on weak decays [22] by Buras was also extremely useful.

While writing this work I benefited a lot from previous PhD theses that inspired me and helped me to clarify many concepts and ideas, the following works were specially helpful [23, 24, 25, 26].

Chapter 2

Effective Field Theories

2.1 Introduction

Effective Theories are ubiquitous in physics and are the poster child approach in the construction of physical theories. By this we mean that they are always the first step when modeling physical phenomena. We can track back the use of effective theories to the very beginning of physics itself. Just to mention an example, consider Newton's laws, we know today that they are just an effective way to describe the motion of particles in the sense that their regime of applicability breaks down for high speeds and also for small scales. Just like Newton's laws there are plenty of examples of effective theories in classical physics as well as quantum physics.

This notion of breaking of applicability is what characterizes effective theories and is what allows us to define such theories in the following way: An effective theory is a theory which only describes the physics below some scale Λ, as opposed to a fundamental theory which should be valid up to arbitrarily high energies.

In this thesis we are only interested in quantum field theories, so that we particularize the general definition given above for general effective theories to the realm of quantum fields, the result is what we know as effective field theories of EFTs for short. These are going to be the foundations under which all this thesis work is constructed and all the results we are going to present here have to do with EFTs in one way or another.

Physical theories have three fundamental ingredients:

(i) Symmetries
(ii) Degrees of freedom
(iii) Stable quantum vacuum

Naturally, EFTs must have these three ingredients as any other reasonable theory, the only special thing is that the degrees of freedom and symmetries might not be those of the fundamental or "full" theory. It might be the case that some degrees of freedom are not present at the energy scale we are working with. Also the symmetry at the scale of interest might not be the complete symmetry of the full theory, or it can be a combination of both situations. Note that the stable quantum vacuum requirement is not a problem, since it is trivially the same in the full theory and in the EFT. At this point it is natural to ask if one can construct a valid theory with incomplete degrees of freedom and possibly incomplete symmetries. The answer is yes and we have been doing this all the time, sometimes without noticing. There is just one caveat, we can construct such theories but they will only work for energies bounded from above by some scale Λ, where new degrees of freedom and possibly new symmetries might appear. The theoretical basis behind the construction of EFTs can be formulated in terms of a theorem, first stated by S. Weinberg [27]:
"To any given order in perturbation theory, and for a given set of asymptotic states, the most general possible Lagrangian containing all terms allowed by the assumed symmetries will yield the most general S-matrix elements consistent with analyticity, perturbative unitarity, cluster decomposition and assumed symmetry principles."

Having said that, the idea to construct EFTs is very simple, one implements an expansion in a parameter $\lambda = E/\Lambda$ in the form of a Taylor series, where each term in the expansion comes from different pieces of a Lagrangian $\mathcal{L}_{eff}$ called the effective Lagrangian. Note that $\mathcal{L}_{eff}$ must be constructed with the symmetries and degrees of freedom adequate to the energy scale we are working with as it was clear from the Weinberg's theorem stated in the previous paragraph. Conceptually, the idea is to expand $\mathcal{L}_{eff}$ as a string of operators with different energy dimension

$$\mathcal{L}_{eff} = \mathcal{L}_{\leq D} + \mathcal{L}_{\leq D+1} + \mathcal{L}_{\leq D+2} + \dots , \tag{2.1}$$

where D is the dimension of spacetime. From the previous equation we see that while computing amplitudes we can pull out different powers of $\lambda = E/\Lambda$ from each of the terms of the effective Lagrangian. We will explain in detail the energy dimension of operators and their classification in what follows, for now it suffices to say that we will work with $D = 4$.

Note from Weinberg's statement that we can have in principle an infinite number of terms in $\mathcal{L}_{eff}$ if we just follow blindly the three points stated previously: (i), (ii) and (iii), that is, there is an infinite number of terms consistent with fixed degrees of freedom and symmetries and this is really

bad because the theory loses any predictive power. To prevent this problem there is an additional fourth point which is a key concept in EFTs and is unique in this kind of theories:

(iv) Power counting

Power counting allows us to arrange calculations in order to have a finite number of terms and this fundamental point is what makes EFTs possible. Power counting is closely related with renormalizability. Remember that in the SM there are no infinities in the calculations since they can be absorbed in the free parameters of the theory in a systematic way. Although EFTs are not renormalizable in the old sense, power counting saves the day since it organizes our calculations in order to produce finite results at any desired order in the EFT expansion. At the end the required precision is going to be dictated by the experiments, thus, we need to make our power expansion such that the ratio $(E/\Lambda)^n$ is sufficiently small when compared with experimental uncertainties. There is nothing sacred about renormalizability, for all the calculations and for all practical purposes, a non-renormalizable theory is just as good as a renormalizable theory, provided that we are satisfied with a finite accuracy ϵ, and this is of course always the case.

Mathematically this means that our accuracy ϵ must satisfy the following relation:

$$\epsilon \leq \left(\frac{E}{\Lambda}\right)^{D_{max}-4} , \tag{2.2}$$

where D_{max} is the highest dimension needed in our operators to achieve a given precision ϵ.

A natural question that arises now is the following: is all the high energy dependence completely lost in the low energy theory?. The answer is no, the effects of the heavy particles (high energy scale Λ) in the low energy dynamics is only manifest through corrections proportional to a negative power of the high energy scale Λ or through renormalization. This is a manifestation of the famous Appelquist-Carazonne theorem [28] also known as the decoupling theorem. Decoupling is the reason behind the natural separation of physical scales, this is for example why we do not need to know about the bottom quark to describe the hydrogen atom [1], and in general this is why we do not need to know about heavy particles to study low energy phenomena. Just to stress the fundamental character and importance of the decoupling theorem, here I would like to add a beautiful phrase that I read from Cliff Burgess [29]:

[1] Of course m_b affects the $e^- p$ interaction in the hydrogen atom, but this effect is suppressed by the ratio $\left(\frac{m_e}{m_b}\right)^2$, which is negligible in that context.

"Decoupling is a very good thing, since it means that the onion of knowledge can be peeled one layer at a time."

EFTs are very useful in particle physics. In the old days they were used to understand the theoretical foundations of the weak interactions with the famous Fermi Theory, which was the first attempt to describe processes like muon and beta decays. Now we know the Electroweak Theory, which is the corresponding full theory for the electric and weak interactions, but we keep using the Fermi Theory in our calculations of low energy weak processes like muon, tau, or beta decays due to its power and its computational advantages. Another old example is that of the Euler-Heisenberg Lagrangian, which is an EFT of QED that describes photon-photon scattering in a theory with no electrons, that is, integrating out the electron field. This approach is really useful in the calculations and has all the features of QED at low energies. Another good example of a useful EFT is that of Chiral Perturbation Theory (ChPT), in this case the use of ChPT is not just for computational convenience, again, despite we know the fundamental theory of strong interactions (QCD), for tau decays, the power series in the α_s parameter is not convergent since we are in the domain of non-perturbative QCD, thus, we have at least two options: change the nature of the degrees of freedom from quarks and gluons to mesons in order to have a convergent calculation, i.e. work with EFTs; or use numerical methods, i.e. Lattice QCD. Here, as we have stated before, we follow the first approach. There are many other examples, but we would like to mention one more that is going to be ubiquitous in this work, that is the one that treats the SM itself as an EFT, as we will see, this is just an extension of the SM Lagrangian that incorporates operators of higher dimension than four. We will discuss the Fermi Theory, ChPT, and the SMEFT in more detail in what follows.

Note that there is always a fundamental scale for each of the EFTs. For the Fermi Theory it is the mass of the W-boson, for the Euler-Heisenberg EFT it is the mass of the electron, for ChPT we have the mass of the ρ meson, and for the SMEFT we do not have an obvious scale, but it is reasonable to suppose that New Physics is above the Electroweak scale.

Note also that we can distinguish between two different approaches when dealing with EFTs. We have the top-down approach when we start with the fundamental theory and we want to construct an effective theory at low energies, that is, we go from high to low energies. The Euler-Heisenberg EFT

and the Fermi Theory[2] are examples of this top-down approach. On the other hand, we have the bottom-up approach when we do not know the fundamental theory, but we have a reasonable low energy theory that we try to extend by using EFT techniques. The SMEFT is an example of this bottom-up approach. Sometimes the bottom-up approach is also used when we have the full theory but we cannot do the matching for some reason, this occurs for example at low energies in QCD when the theory is non-perturbative. To avoid this last problem we construct ChPT with the low energy degrees of freedom and symmetries, following the bottom-up approach.

For the convenience of the reader, we summarize all the information presented in the previous three paragraphs regarding the specific examples of EFTs we chose, their fundamental scales and the approach they belong to in the following table.

Low Energy EFT	Full Theory	Fundamental Scale	Approach
SM	?	TeVs?	Bottom-Up
Euler-Heisenberg Theory	QED	m_e ∼511 KeV	Top-Down
Fermi Theory	SM	m_W ∼80 GeV	Top-Down
ChPT	QCD	m_ρ ∼1 GeV	Bottom-Up

Table 2.1: Examples of EFTs

The fundamental piece in the study of EFTs is the effective Lagrangian (or the effective Hamiltonian), which contains all the relevant information of our physical systems. We construct the effective Lagrangian $\mathcal{L}_{eff}$ depending on the approach that we are trying to implement, in the top-down approach we have the fundamental theory and from there we integrate out (remove) the heaviest particles and match onto a low energy theory, as a result we will produce new operators and new couplings. This process is expressed mathematically in the following equation

$$\mathcal{L}_{High} \to \mathcal{L}_{Low} = \sum_n \mathcal{L}^{(n)}_{Low} \,. \tag{2.3}$$

The Lagrangians $\mathcal{L}_{High}$ and $\mathcal{L}_{Low}$ will agree in the infrared, but will differ in the ultraviolet. An example of this is the Fermi $V-A$ Theory of Weak interactions, where one starts with the SM Lagrangian and integrates out the W boson ending up with a Lagrangian composed of dimension 6 operators.

[2]Nowadays we treat the Fermi Theory in the top-down approach because we know the EW Theory, but at the beginning it was constructed following the bottom-up approach by Fermi since he did not know the fundamental theory behind.

On the other hand, when we try to explore the UV completion for low-energy theories we can extend our low energy Lagrangian following the bottom-up approach as we show below

$$\mathcal{L}_{eff} = \mathcal{L}_0 + \sum_{i,k} \frac{c_i^{(k)}}{\Lambda^{i-4}} O_i^{(k)}(\phi_L)\,, \tag{2.4}$$

where $\mathcal{L}_0$ is the low energy renormalizable Lagrangian (for example the SM Lagrangian), Λ is the new physics scale, ϕ_L are the low energy degrees of freedom (for instance the SM degrees of freedom), $O_i^{(k)}$ are operators with different dimensions, and $c_i^{(k)}$ are the corresponding couplings known as the Wilson coefficients [3]. Note that the sum is over both indices i and k since we can have several different operators with the same dimension. We will see an explicit example of this in section 2.2 when we discuss the SMEFT. There is another possibility in the bottom-up approach in which we have to change completely the degrees of freedom in our description of our system for some reason. As we have pointed out before, this occurs for example in ChPT, when it is convenient to change the original degrees of freedom (quarks and gluons) to mesons in order to have convergent calculations since the full theory (QCD) is strongly coupled. We will discuss Chiral Perturbation Theory in section 2.3.

From eqs. (2.3) and (2.4) we see that the result of working with EFTs is that at the end we have a string of operators with different dimensions contributing to the physical processes. There is a natural classification for these operators that follows directly from dimensional analysis. Since we are working with natural units and also in four-dimensional space-time, the Lagrangian must have dimension of E^4:

$$[\mathcal{L}] = 4\,, \tag{2.5}$$

therefore, the different operators and couplings will satisfy the following relations

$$[O_i] = d_i \to \alpha_i \sim \frac{1}{\Lambda^{d_i-4}}\,, \tag{2.6}$$

this allows us to classify the operators according to their dimension:

- Relevant ($d_i < 4$)
- Marginal ($d_i = 4$)

[3] The Wilson coefficients $c_i^{(k)}$ are dimensionless, but they could depend logarithmically on the scale Λ.

- Irrelevant ($d_i > 4$)

as we can see from eq. (2.6) the operators O_i behave very differently for each of these three categories, their names are taken from their behaviour at energies lower than the scale Λ, while irrelevant operators are suppressed by the high energy scale Λ, relevant operators are reinforced. Finally, marginal operators are equally important at all energy scales and quantum effects can make them look relevant or irrelevant depending on the particular system.

Finally, before concluding this section, we want to mention that it was mostly based on the reviews [30, 31, 32, 33, 34, 35, 36] and on the books [37, 29].

2.2 Standard Model Effective Field Theory (SMEFT)

2.2.1 Standard Model

Before discussing the SMEFT, it is important and appropriate at this point to discuss the SM first since it is ultimately the root and the basis of this work and the whole area of particle physics.

The SM is the most successful theory in physics along with general relativity, it describes three of the four fundamental forces known in nature: the strong force, the electromagnetic force and the weak force. These last two forces are ultimately unified and together they are known as the electroweak interaction. The remaining force known as gravity is described by general relativity quite remarkably.

The SM is a gauge theory constructed in the framework of Quantum Field Theory with $SU(3)_c \times SU(2)_L \times U(1)_Y$ as the gauge group. The $SU(3)_c$ part of the group describes the strong interaction which is known as Quantum Chromodynamics (QCD) and the remaining $SU(2)_L \times U(1)_Y$ group describes the electroweak force that we mentioned in the previous paragraph. The symmetry group of the SM fixes the interactions, thus, the number and properties of the vector gauge bosons is fixed. We have as many vector bosons as generators in the gauge group, for example, eight vector bosons for $SU(3)_c$ known as gluons and represented by the fields G^i_μ, three for $SU(2)_L$ represented by the fields W^i_μ and one for $U(1)_Y$ represented by B_μ. We will shortly see that the $W^\pm$ bosons are a linear combination of the W^1_μ and W^2_μ bosons and also that the photon and the Z boson are both linear combinations of the W^3_μ and the B_μ fields. As in any gauge theory, the vector bosons are introduced

replacing the normal derivative ∂_μ with the covariant derivative D_μ,

$$D_\mu = \partial_\mu + ig\vec{W}_\mu \cdot \vec{I} + ig' B_\mu \frac{Y}{2}\,, \tag{2.7}$$

where $\vec{I} = (I_1, I_2, I_3)$ is a compact form to write the three generators of the $SU(2)_L$ group and Y is the only generator of the $U(1)_Y$ group and is known as the hypercharge. In this section we only concentrate on the electroweak part of the Lagrangian, we will consider the strong part in the next section when we discuss ChPT. The explicit form for $\vec{I}$ depends on the representation we choose for the matter content, as we will see, it turns out that nature chooses doublets ($I_i = \tau_i/2$ where τ_i are the three Pauli matrices) and singlets ($I_i = 0$). Once we choose the representation for $\vec{I}$, the value of Y is automatically fixed through the Gell-Mann-Nishijima relation,

$$Q = I_3 + \frac{Y}{2}\,. \tag{2.8}$$

The gauge fields are not static entities, they of course have their own dynamics, therefore we have to construct the proper dynamical terms in the Lagrangian, this is trivially done for the case of the B^μ field from the experience with gauge invariance in QED which can be easily extended for the construction of the dynamical terms for the W^i_μ fields following the ideas of Yang-Mills,

$$\mathcal{L}_{gauge} = -\frac{1}{4} W^i_{\mu\nu} W^{\mu\nu i} - \frac{1}{4} B_{\mu\nu} B^{\mu\nu}\,. \tag{2.9}$$

The terms $W^i_{\mu\nu}$, and $B_{\mu\nu}$ are respectively the field strength tensors for $SU(2)_L$, and $U(1)_Y$ and are given by the following equations:

$$W^i_{\mu\nu} = \partial_\mu W^i_\nu - \partial_\nu W^i_\mu - g\epsilon^{ijk} W_{\mu j} W_{\nu k}, \quad i,j,k = 1,2,3, \tag{2.10}$$

$$B_{\mu\nu} = \partial_\mu B_\nu - \partial_\nu B_\mu\,. \tag{2.11}$$

Note from eq. (2.9) that gauge symmetry forbids the construction of mass terms for the gauge bosons, but, on the other hand we know that the $W^\pm$ and the Z bosons do have mass. We will see that this is possible via the Higgs mechanism.

From our previous discussion, we see that at the end we only have three independent parameters coming from $\mathcal{L}_{gauge}$, these are the three independent gauge couplings: g and g' that we saw explicitly before, and g_s that we will see in the next section. Each of these gauge couplings are determined from experiments.

So far we have discussed the electroweak gauge sector, now it is time

to discuss the matter content and the interactions between matter and the gauge bosons. Matter is composed of fundamental particles of spin 1/2, so that, these particles are fermions. These fermions divide into two groups: quarks and leptons.

Quarks participate in all fundamental interactions: they are the only particles that 'feel' the strong force, they also 'feel' the electromagnetic force, the weak force and gravity. These particles are the smallest constituents of hadronic matter, like the atomic nuclei present everywhere or the pions and kaons that we observe in cosmic rays. Quarks accommodate in two different ways: baryons and mesons [4]. Baryons are composed of three quarks and mesons are composed of a quark-antiquark pair, both states are singlets of color or colorless as we like to say it. Baryons and mesons together form what we know as hadrons.

Leptons participate in three of the four fundamental interactions, they are 'blind' to the strong force, so that QCD is the only one absent. Leptons are divided into two categories: the charged ones and the neutral ones. The charged ones 'feel' the electromagnetic force, the weak force and gravity, and the neutral ones are called neutrinos and only 'feel' the weak force and gravity. For each of the charged leptons there is a neutrino partner. For the convenience of the reader we have summarized the matter content of the SM in the following table.

	1^{st} generation	2^{nd} generation	3^{rd} generation
quarks	u (up)	c (charm)	t (top)
	d (down)	s (strange)	b (bottom)
leptons	ν_e (electron neutrino)	ν_μ (muon neutrino)	ν_τ (tau neutrino)
	e (electron)	μ (muon)	τ (tau)

Table 2.2: Matter content of the SM.

Unlike the gauge boson sector where everything was fixed, there is nothing that constraints the number and the properties of fermions, the only requirement for fermions is that they must fulfil a representation of the symmetry group and that these representations comply with the cancellation of quantum anomalies.

The matter content shown in table 2.2 is the one that fulfils the current phenomenology, as we can see, matter accommodates in three different families or generations, where all of them have exactly the same properties

[4]It is believed that quarks could accommodate in more general color-neutral configurations. These are known as exotic hadrons. Examples of these configurations are tetraquarks and pentaquarks.

except for the mass. In principle there is no theoretical argument in the SM that forbids more families of particles, we could just as well have a fourth generation of quarks and leptons that accomplishes with the cancellation of quantum anomalies, but at the end experiment tells us that there are just three families and that is all that matters.

The left-handed components of quarks and leptons accommodate in the $SU(2)_L$ doublets, $q_{mL} = \begin{pmatrix} u_m \\ d_m \end{pmatrix}$, and $l_{mL} = \begin{pmatrix} \nu_m \\ e_m^- \end{pmatrix}$ and the right-handed components accommodate in the $SU(2)_L$ singlets u_{mR}, d_{mR} and e_{mR}^-. The m subscript labels the family, thus $m = 1, 2, 3$. Some authors refer to this arrange as the 'qudle' representation for a useful mnemonic.

Now that we have the fundamental pieces of matter, we can easily construct the Lagrangian corresponding to the fermion sector $\mathcal{L}_f$ as a collection of massless Dirac Lagrangians with the appropriate covariant derivatives,

$$\begin{aligned} \mathcal{L}_f = \sum_{m=1}^{3} \Big[& \bar{q}_{mL} i \not{D} q_{mL} + \bar{l}_{mL} i \not{D} l_{mL} + \bar{u}_{mR} i \not{D} u_{mR} + \bar{d}_{mR} i \not{D} d_{mR} \\ & + \bar{e}_{mR} i \not{D} e_{mR} \Big] , \end{aligned} \tag{2.12}$$

fermion mass terms are forbidden because the weak interaction is chiral since it treats the left and right components of fermions in a different way. As in the case of the gauge bosons, the masses of the fermions are also acquired through the Higgs mechanism.

The covariant derivatives in eq. (2.12) provide the interaction between the fermions and the weak gauge bosons $W^\pm$ and Z and also between the charged fermions and the photon. As we will see these interactions divide in two categories charged-current (CC) and neutral-current (NC) interactions.

For clarity purposes let us discuss the leptonic part of eq. (2.12) first,

$$\mathcal{L}_{f,L} = -\frac{1}{2} (\bar{\nu}_{eL} \bar{e}_L) \begin{pmatrix} g \not{W}_3 - g' \not{B} & g(\not{W}_1 - i \not{W}_2) \\ g(\not{W}_1 + i \not{W}_2) & -g \not{W}_3 - g' \not{B} \end{pmatrix} \begin{pmatrix} \nu_{eL} \\ e_L \end{pmatrix} + g' \bar{e}_R \not{B} e_R \, , \tag{2.13}$$

where we have used the fact that the hypercharge for the lepton doublet and singlet is $Y = -1$ and $Y = -2$, respectively. The off-diagonal terms in eq. (2.13) form the charged-current interaction Lagrangian,

$$\mathcal{L}_{f,L}^{(CC)} = -\frac{g}{2} \left(\bar{\nu}_{eL} (\not{W}_1 - i \not{W}_2) e_L + \bar{e}_L (\not{W}_1 + i \not{W}_2) \nu_{eL} \right) , \tag{2.14}$$

here, it is convenient to define a field W^μ that annihilates W^+ bosons and creates W^- bosons as,

$$W^\mu \equiv \frac{W_1^\mu - i W_2^\mu}{\sqrt{2}} , \tag{2.15}$$

substituting eq. (2.15) in eq. (2.14), we obtain,

$$\begin{aligned}\mathcal{L}_{f,L}^{(CC)} &= -\frac{g}{\sqrt{2}}\left(\bar{\nu}_{eL}\not{W}e_L + \bar{e}_L\not{W}^{\dagger}\nu_{eL}\right) \\ &= -\frac{g}{2\sqrt{2}}\bar{\nu}_e\gamma^{\mu}(1-\gamma^5)eW_{\mu} + h.c \\ &= -\frac{g}{2\sqrt{2}}j_{W,L}^{\mu}W_{\mu} + h.c\,,\end{aligned} \tag{2.16}$$

where the leptonic charged-current $j_{W,L}^{\mu}$ is defined as,

$$j_{W,L}^{\mu} = \bar{\nu}_e\gamma^{\mu}(1-\gamma^5)e\,. \tag{2.17}$$

As we have seen on chapter 1, formula (2.16) plays a central role in this thesis work since tau decays are mediated via the charged-current interaction. We will use the effective realization of the $(V-A)$ interaction shown in eq. (2.16) and its generalization to more complex spin-one currents and also the effective realization of general scalar, pseudoscalar and tensor interactions along this work.

From the diagonal terms in eq. (2.13) we also have a neutral-current interaction given by the Lagrangian,

$$\mathcal{L}_{f,L}^{(NC)} = -\frac{1}{2}\left[\bar{\nu}_{eL}(g\not{W}_3 - g'\not{B})\nu_{eL} - \bar{e}_L(g\not{W}_3 + g'\not{B})e_L - 2g'\bar{e}_R\not{B}e_R\right]\,. \tag{2.18}$$

The electromagnetic force is hidden inside the previous Lagrangian, to decouple it Glashow suggested that the photon field A^{μ} and a new neutral boson field Z^{μ} are a mixture of the W_3^{μ} and B^{μ} bosons as shown in the following equation,

$$\begin{aligned} A^{\mu} &= \sin\theta_W W_3^{\mu} + \cos\theta_W B^{\mu}\,, \\ Z^{\mu} &= \cos\theta_W W_3^{\mu} - \sin\theta_W B^{\mu}\,, \end{aligned} \tag{2.19}$$

the angle θ_W is known as the weak mixing angle, the Glashow angle or the Weinberg angle sometimes. Substituting eq. (2.19) in eq. (2.18) we can write the neutral-current Lagrangian in the form,

$$\begin{aligned}\mathcal{L}_{f,L}^{(NC)} = &-\frac{g}{2\cos\theta_W}\left[\bar{\nu}_{eL}\not{Z}\nu_{eL} - (1-2\sin^2\theta_W)\bar{e}_L\not{Z}e_L + 2\sin^2\theta_W\bar{e}_R\not{Z}e_R\right] \\ &+ g\sin\theta_W\bar{e}\not{A}e\,,\end{aligned} \tag{2.20}$$

where the couplings g and g' satisfy the relation $g\sin\theta_W = g'\cos\theta_W$ in order to cancel the interaction between the photon and the neutrinos. Note that

the last piece of eq. (2.20) is just the QED Lagrangian, so that we can make the identification $g \sin\theta_W = e$.

Finally, the neutral-current Lagrangian can be written as,

$$\mathcal{L}_{f,L}^{(NC)} = \mathcal{L}_{f,L}^{(Z)} + \mathcal{L}_{f,L}^{(\gamma)} \,, \tag{2.21}$$

where $\mathcal{L}_{f,L}^{(\gamma)}$ is the QED Lagrangian and $\mathcal{L}_{f,L}^{(Z)}$ is the part of the neutral-current corresponding to the Z boson which is given by the following expression,

$$\mathcal{L}_{f,L}^{(Z)} = -\frac{g}{2\cos\theta_W} j_{Z,L}^{\mu} Z_{\mu} \,, \tag{2.22}$$

where the explicit form for the leptonic weak neutral current is,

$$j_{Z,L}^{\mu} = 2g_L^{\nu} \bar{\nu}_{eL} \gamma^{\mu} \nu_{eL} + 2g_L^{\ell} \bar{e}_L \gamma^{\mu} e_L + 2g_R^{\ell} \bar{e}_R \gamma^{\mu} e_R \,, \tag{2.23}$$

with $g_L^f = I_3^f - q_f \sin^2\theta_W$ and $g_R^f = -q_f \sin^2\theta_W$.

Sometimes it is also convenient to write the leptonic weak neutral current in the form

$$j_{Z,L}^{\mu} = \bar{\nu}_e \gamma^{\mu} (g_V^{\nu} - g_A^{\nu} \gamma^5) \nu_e + \bar{e} \gamma^{\mu} (g_V^{\ell} - g_A^{\ell} \gamma^5) e \,, \tag{2.24}$$

where $g_V^f = g_L^f + g_R^f = I_3^f - 2q_f \sin^2\theta_W$ and $g_A^f = g_L^f - g_R^f = I_3^f$.

The results can be trivially extended for the case of three generations, we just have to replace eq. (2.17) and eq. (2.23) in the following way,

$$j_{W,L}^{\mu} = 2\bar{\nu}_L \gamma^{\mu} \ell_L = 2 \sum_{\alpha=e,\mu,\tau} \bar{\nu}_{\alpha L} \gamma^{\mu} \ell_{\alpha L} \,, \tag{2.25}$$

$$j_{Z,L}^{\mu} = 2g_L^{\nu} \bar{\nu}_L \gamma^{\mu} \nu_L + 2g_L^{\ell} \bar{\ell}_L \gamma^{\mu} \ell_L + 2g_R^{\ell} \bar{\ell}_R \gamma^{\mu} \ell_R \,, \tag{2.26}$$

where $\ell_L = \begin{pmatrix} e_L \\ \mu_L \\ \tau_L \end{pmatrix}$ and $\nu_L = \begin{pmatrix} \nu_{eL} \\ \nu_{\mu L} \\ \nu_{\tau L} \end{pmatrix}$.

So far, we have discussed the charged and neutral weak interactions of leptons but we can obtain similar expressions for quarks starting again with eq. (2.12) and following exactly the same procedure. In fact, the formulas for the charged and neutral weak interactions for quarks are given exactly by eq. (2.16) and eq. (2.22) respectively. The only difference comes in the currents, here eq. (2.17) and eq. (2.23) are replaced by,

$$j_{W,Q}^{\mu} = 2\bar{q}_L^U \gamma^{\mu} V_{CKM} q_L^D \,, \tag{2.27}$$

$$
\begin{aligned}
j^{\mu}_{Z,Q} =& 2g^U_L \bar{q}^U_L \gamma^\mu q^U_L + 2g^U_R \bar{q}^U_R \gamma^\mu q^U_R \\
&+ 2g^D_L \bar{q}^D_L \gamma^\mu q^D_L + 2g^D_R \bar{q}^D_R \gamma^\mu q^D_R \,,
\end{aligned}
\tag{2.28}
$$

with

$$
\begin{aligned}
q^U_L &= \begin{pmatrix} u_L \\ c_L \\ t_L \end{pmatrix} \,, \quad q^U_R = \begin{pmatrix} u_R \\ c_R \\ t_R \end{pmatrix} \,, \\
q^D_L &= \begin{pmatrix} d_L \\ s_L \\ b_L \end{pmatrix} \,, \quad q^D_R = \begin{pmatrix} d_R \\ s_R \\ b_R \end{pmatrix} \,,
\end{aligned}
\tag{2.29}
$$

where V_{CKM} is known as the Cabibbo-Kobayashi-Maskawa matrix [38, 39], which incorporates the mixing between the different quark flavors. Note that the mixing is only present for the weak charged current in the quark sector, there is no mixing for the leptonic weak charged current nor for the leptonic and quark weak neutral currents.

We write the values for the neutral weak couplings that appear in eqs. (2.23), (2.24), (2.26) and (2.28) in the following table,

Fermions	g_L	g_R	g_V	g_A
ν_e,ν_μ,ν_τ	$g^\nu_L = \frac{1}{2}$	$g^\nu_R = 0$	$g^\nu_V = \frac{1}{2}$	$g^\nu_A = \frac{1}{2}$
e,μ,τ	$g^\ell_L = -\frac{1}{2} + s^2_W$	$g^\ell_R = s^2_W$	$g^\ell_V = -\frac{1}{2} + 2s^2_W$	$g^\ell_A = -\frac{1}{2}$
u,c,t	$g^U_L = \frac{1}{2} - \frac{2}{3}s^2_W$	$g^U_R = -\frac{2}{3}s^2_W$	$g^U_R = \frac{1}{2} - \frac{4}{3}s^2_W$	$g^U_A = \frac{1}{2}$
d,s,b	$g^D_L = -\frac{1}{2} + \frac{1}{3}s^2_W$	$g^D_R = \frac{1}{3}s^2_W$	$g^D_V = -\frac{1}{2} + \frac{2}{3}s^2_W$	$g^D_A = -\frac{1}{2}$

Table 2.3: Values for g_L, g_R, g_V and g_A.

The weak neutral current interactions will not play a major role in this work since tau decays via the weak charged current, but they are fundamental in our understanding of neutrino physics.

Now it is time to discuss the scalar sector. As we pointed out before, in the SM, the masses of the W and Z gauge bosons, as well as those of the fermions, are generated through the Higgs mechanism [40, 41, 42, 43] where one introduces a scalar doublet $\phi = \begin{pmatrix} \phi^+ \\ \phi^0 \end{pmatrix}$ and constructs the following Lagrangian,

$$
\mathcal{L}_\phi = (D^\mu \phi)^\dagger D_\mu \phi - V(\phi) \,,
\tag{2.30}
$$

where,

$$
V(\phi) = \mu^2 \phi^\dagger \phi + \lambda (\phi^\dagger \phi)^2 \,,
\tag{2.31}
$$

the first thing to note from the previous Lagrangian is that λ must be greater than zero since the potential must be bounded from below and also that μ^2

must be less than zero in order to realize the spontaneous symmetry breaking.

It is convenient to write the Higgs potential in eq. (2.31) in the following equivalent form,

$$V(\phi) = \lambda \left(\phi^\dagger \phi - \frac{v^2}{2} \right)^2 , \tag{2.32}$$

where we have defined $v \equiv \sqrt{\frac{-\mu^2}{\lambda}}$ and we have neglected an irrelevant constant term.

Since $\lambda > 0$, we see from eq. (2.32) that the potential has a minimum for

$$\phi^\dagger \phi = \frac{v^2}{2} . \tag{2.33}$$

The vacuum of the theory must be electrically neutral so that the charged part of the doublet ϕ must have a zero value in the vacuum, on the other hand, the neutral part of the doublet ϕ can have a nonzero value in the vacuum, in fact, in order to satisfy eq. (2.33) we must have the following relation for the vacuum expectation value (VEV),

$$\langle \phi \rangle = \frac{1}{\sqrt{2}} \begin{pmatrix} 0 \\ v \end{pmatrix} . \tag{2.34}$$

The Higgs doublet $\phi = \begin{pmatrix} \phi^+ \\ \phi^0 \end{pmatrix}$ can be conveniently written in the unitary gauge as

$$\phi(x) = \frac{1}{\sqrt{2}} \begin{pmatrix} 0 \\ v + H(x) \end{pmatrix} , \tag{2.35}$$

where only the physical degrees of freedom appear explicitly, namely the Higgs boson field $H(x)$.

The dynamics of the Higgs field and the interactions of the Higgs and the gauge bosons can be derived from eq. (2.30). First note that in the unitary gauge the covariant derivative becomes

$$\begin{aligned} D_\mu \phi(x) &= \left[\partial_\mu + \frac{i}{2} g \vec{W}_\mu \cdot \vec{\tau} + \frac{i}{2} g' B_\mu(x) \right] \phi(x) \\ &= \frac{1}{\sqrt{2}} \begin{pmatrix} i \frac{g}{\sqrt{2}} W_\mu(x) [v + H(x)] \\ \partial_\mu - \frac{i}{2} \frac{g}{\cos\theta_W} Z_\mu(x) [v + H(x)] \end{pmatrix} , \end{aligned} \tag{2.36}$$

thus, the Higgs Lagrangian in eq. (2.30) takes the following form

$$\begin{aligned}\mathcal{L}_\phi &= \frac{1}{2}(\partial H)^2 + \frac{g^2}{4}(v+H)^2 W_\mu^\dagger W^\mu + \frac{g^2}{8\cos^2\theta_W}(v+H)^2 Z_\mu Z^\mu - \frac{\lambda}{4}(H^2+2vH)^2 \\ &= \frac{1}{2}(\partial H)^2 - \lambda v^2 H^2 - \lambda v H^3 - \frac{\lambda}{4}H^4 + \frac{g^2 v^2}{4} W_\mu^\dagger W^\mu + \frac{g^2 v^2}{8\cos^2\theta_W} Z_\mu Z^\mu \\ &+ \frac{g^2 v}{2} W_\mu^\dagger W^\mu H + \frac{g^2 v}{4\cos^2\theta_W} Z_\mu Z^\mu H + \frac{g^2}{4} W_\mu^\dagger W^\mu H^2 + \frac{g^2}{8\cos^2\theta_W} Z_\mu Z^\mu H^2 \,,\end{aligned} \tag{2.37}$$

focusing on the second equality we have that the first term is just the kinematical term for the Higgs field, the second term gives the mass for the Higgs boson, the third and fourth terms are cubic and quartic self interactions of the Higgs boson, the fifth and sixth terms are the masses for the W and Z bosons, and the last four terms are cubic and quartic interactions of the Higgs with the W and Z gauge bosons.

The explicit form for the masses of the Higgs, the $W^\pm$ and the Z bosons is given by,

$$\begin{aligned} m_H &= \sqrt{2\lambda v^2} = \sqrt{-2\mu^2}\,, \\ m_W &= \frac{gv}{2}\,, \\ m_Z &= \frac{gv}{2\cos\theta_W}\,, \end{aligned} \tag{2.38}$$

the mass of the Higgs is a free parameter of the SM, so that it has to be fixed by experiment, on the other hand, the masses of the $W^\pm$ and Z bosons are predicted once the SM parameters are fixed.

One of the most useful parameters to test the SM is the ρ parameter defined in the following equation

$$\rho = \frac{m_W^2}{m_Z^2\cos^2\theta_W} = 1\,, \tag{2.39}$$

where we have used eq. (2.38). The relation in (2.39) is only valid at tree level, that value is of course modified by loop corrections.

The last piece in our discussion of the SM Lagrangian is the Yukawa Lagrangian $\mathcal{L}_{Yuk}$ which gives the masses for the fermions

$$\mathcal{L}_{Yuk} = -\sum_{m,n=1}^{3} [\Gamma^u_{mn}\bar{q}_{mL}\tilde{\phi}u_{nR} + \Gamma^d_{mn}\bar{q}_{mL}\phi d_{nR} + \Gamma^e_{mn}\bar{\ell}_{mL}\phi e_{nR}] + h.c\,, \tag{2.40}$$

where $\phi = \begin{pmatrix} \phi^+ \\ \phi^0 \end{pmatrix}$ and $\tilde{\phi} \equiv i\tau^2\phi^\dagger = \begin{pmatrix} \phi^{0\dagger} \\ -\phi^- \end{pmatrix}$.

As we have pointed out before, there are no right-handed neutrinos in the SM so that we do not have neutrino masses in the SM, but we know that neutrinos do have mass from oscillation experiments, to reconcile this fact it is clear that we must extend the SM to include a mechanism for the mass generation of neutrinos. This can be done in several ways, one is the exact analogue of eq. (2.40) in which one just adds right-handed neutrinos by hand as happens with all the other leptons, if that is the case we have Dirac neutrinos, the other possibility is that the mass of the neutrinos is generated with left-handed neutrinos only or with right-handed neutrinos only but not a mixture of both as happens with Dirac neutrinos, for this second possibility we have Majorana neutrinos. This is still an open question in particle physics and is beyond the scope of this thesis work.

Finally, putting all the pieces together we have that the SM is described by the following Lagrangian [5]

$$\mathcal{L} = \mathcal{L}_f + \mathcal{L}_{gauge} + \mathcal{L}_\phi + \mathcal{L}_{Yuk}\,, \tag{2.41}$$

where we have a total of 19 independent parameters:

- 3 gauge couplings (g, g', g_s)
- 6 quark masses
- 3 masses for the charged leptons
- 3 mixing angles from the CKM matrix
- 1 CP phase also from the CKM matrix
- 2 parameters from the scalar sector (μ^2 and λ)
- θ_{QCD}

It is amazing how the previous Lagrangian with its 19 independent parameters describes the electroweak and the strong force with such a level of accuracy. To convince oneself of the predictive power of the SM it is enough to take a look at the PDG [6] and see how well the SM is describing the vast majority of the processes. There are very few exceptions, which we call anomalies, that are in tension with the SM prediction. Those anomalies tend to disappear with time (they were due to statistical fluctuations in the early

[5] Gauge fixing, as well as ghost and the θ_{QCD} terms (in the case of QCD) are omitted.

data and/or coming from underestimated theory/experimental errors). All these facts make the SM the most precise theory in the history of physics.

This section was mostly based on the two amazing books [44, 45] and the famous review [46].

2.2.2 SMEFT

Now that we have introduced the SM, it is time to discuss the Standard Model Effective Field Theory (SMEFT) which is the framework on which this thesis relies. First we suppose that the EW symmetry is linearly realized [6] and that there is no new physics below the electroweak scale, so that all possible new degrees of freedom appear at a scale Λ_{NP} that is above the EW scale. As a consequence of this assumption, new higher-dimensional operators need to be introduced,

$$\mathcal{L} = \mathcal{L}^{(4)}_{SM} + \frac{1}{\Lambda}\sum_k c^{(5)}_k O^{(5)}_k + \frac{1}{\Lambda^2}\sum_k c^{(6)}_k O^{(6)}_k + \mathcal{O}\left(\frac{1}{\Lambda^3}\right), \tag{2.42}$$

where $\mathcal{L}^{(4)}_{SM}$ is the usual renormalizable SM Lagrangian and all these high-dimensional operators $(O^5_k, O^6_k, ...)$ are suppressed by powers of Λ_{NP}. This natural suppression allows us to neglect operators of dimension equal or greater than 7 as a first approximation.

The operators O^5_k and O^6_k are constructed with the symmetries and degrees of freedom of the SM. It turns out that with these requirements we only have one operator of dimension 5 [47], the so called Weinberg operator, and 59 independent operators of dimension 6 (barring flavor structure and hermitian conjugation) [48].

The Lagrangian corresponding to the Weinberg operator is given by

$$\mathcal{L}_5 = \frac{c_5}{\Lambda_{NP}}\epsilon_{ij}\bar{\ell}^{ci}_L\phi^j\epsilon_{kl}\ell^k_L\phi^l\,, \tag{2.43}$$

where $\phi = \begin{pmatrix}\phi^+\\ \phi^0\end{pmatrix}$ and $\ell_L = \begin{pmatrix}\nu_L\\ e_L\end{pmatrix}$. After spontaneous symmetry breaking we obtain a Majorana mass term for the neutrinos

$$\mathcal{L}_5 = \frac{1}{2}m_\nu\epsilon_{ab}\nu^a_L\nu^b_L + h.c\,, \tag{2.44}$$

with $m_\nu = \frac{c_5 v^2}{2\Lambda_{NP}}$. From experimental data $m_\nu \leq 0.5$ eV, so, one expects the energy scale for new physics to be around $\Lambda_{NP} \geq 6\times 10^{14}$ GeV assuming

[6] If the EW symmetry were non-linearly realized, we would need to use chiral Lagrangians as occurs in ChPT.

that $c_5 \sim 1$, which is natural.

For the dimension 6 operators there are a total of 59 independent operators [48] as we can see in figures 2.1 and 2.2. Only eight of these operators will contribute to low-energy charged current processes, namely:
four-fermion operators:

$$\mathcal{O}_{\ell q}^{(3)} = (\bar{\ell}\gamma^{\mu}\tau^{a}\ell)(\bar{q}\gamma_{\mu}\tau^{a}q)\,, \tag{2.45}$$

$$\mathcal{O}_{qde} = (\bar{\ell}e)(\bar{d}q) + h.c.\,, \tag{2.46}$$

$$\mathcal{O}_{\ell q} = (\bar{\ell}_{a}e)\epsilon^{ab}(\bar{q}_{b}u) + h.c.\,, \tag{2.47}$$

$$\mathcal{O}_{\ell q}^{T} = (\bar{\ell}_{a}\sigma^{\mu\nu}e)\epsilon^{ab}(\bar{q}_{b}\sigma_{\mu\nu}u) + h.c.\,, \tag{2.48}$$

vertex corrections:

$$\mathcal{O}_{\phi\phi} = i(\phi^{T}\epsilon D_{\mu}\phi)(\bar{u}\gamma^{\mu}d) + h.c.\,, \tag{2.49}$$

$$\mathcal{O}_{\phi q}^{(3)} = i(\phi^{\dagger}D^{\mu}\tau^{a}\phi)(\bar{q}\gamma_{\mu}\tau^{a}q) + h.c\,, \tag{2.50}$$

and also two more operators that introduce some modifications to the Fermi constant:

$$\mathcal{O}_{\ell\ell}^{(3)} = \frac{1}{2}(\bar{\ell}\gamma^{\mu}\tau^{a}\ell)(\bar{\ell}\gamma_{\mu}\tau^{a}\ell)\,, \tag{2.51}$$

$$\mathcal{O}(3)_{\phi\ell} = i(\phi^{\dagger}D^{\mu}\tau^{a}\phi)(\bar{\ell}\gamma_{\mu}\tau^{a}\ell) + h.c.\,, \tag{2.52}$$

where, as usual, τ^{a} are the three Pauli matrices

$$\tau^{1} = \begin{pmatrix} 0 & 1 \\ 1 & 0 \end{pmatrix}, \quad \tau^{2} = \begin{pmatrix} 0 & -i \\ i & 0 \end{pmatrix}, \quad \tau^{3} = \begin{pmatrix} 1 & 0 \\ 0 & -1 \end{pmatrix}. \tag{2.53}$$

The previous eight operators are the only ones that contribute to semileptonic decays [49], and for this reason they will be extremely useful in chapters 4, 5 and 6, where we will analyze semileptonic tau decays. Our calculations will be given not in terms of SMEFT itself, but with its low energy limit, that sometimes is referred as LEFT (from low-energy EFT). The running of the couplings from a scale of 1 TeV to the scale of the Z mass and from there to the scale of the tau mass has been studied in ref. [50].

It is interesting to point out that the work [48] that obtained the 59 independent dimension 6 operators was part of a masters thesis, in that work they realized that many of the operators first discussed in [51] were dependent on each other through the use of equations of motion.

X^3		φ^6 and $\varphi^4 D^2$		$\psi^2\varphi^3$	
$\mathcal{O}_G$	$f^{ABC}G^{A\nu}_{\mu}G^{B\rho}_{\nu}G^{C\mu}_{\rho}$	$\mathcal{O}_{\varphi}$	$(\varphi^\dagger\varphi)^3$	$\mathcal{O}_{e\varphi}$	$(\varphi^\dagger\varphi)(\bar{l}_p e_r \varphi)$
$\mathcal{O}_{\widetilde{G}}$	$f^{ABC}\widetilde{G}^{A\nu}_{\mu}G^{B\rho}_{\nu}G^{C\mu}_{\rho}$	$\mathcal{O}_{\varphi\Box}$	$(\varphi^\dagger\varphi)\Box(\varphi^\dagger\varphi)$	$\mathcal{O}_{u\varphi}$	$(\varphi^\dagger\varphi)(\bar{q}_p u_r \widetilde{\varphi})$
$\mathcal{O}_W$	$\varepsilon^{IJK}W^{I\nu}_{\mu}W^{J\rho}_{\nu}W^{K\mu}_{\rho}$	$\mathcal{O}_{\varphi D}$	$\left(\varphi^\dagger D^\mu\varphi\right)^\star\left(\varphi^\dagger D_\mu\varphi\right)$	$\mathcal{O}_{d\varphi}$	$(\varphi^\dagger\varphi)(\bar{q}_p d_r \varphi)$
$\mathcal{O}_{\widetilde{W}}$	$\varepsilon^{IJK}\widetilde{W}^{I\nu}_{\mu}W^{J\rho}_{\nu}W^{K\mu}_{\rho}$				

$X^2\varphi^2$		$\psi^2 X\varphi$		$\psi^2\varphi^2 D$	
$\mathcal{O}_{\varphi G}$	$\varphi^\dagger\varphi\, G^A_{\mu\nu}G^{A\mu\nu}$	$\mathcal{O}_{eW}$	$(\bar{l}_p\sigma^{\mu\nu}e_r)\tau^I\varphi W^I_{\mu\nu}$	$\mathcal{O}^{(1)}_{\varphi l}$	$(\varphi^\dagger i\overleftrightarrow{D}_\mu\varphi)(\bar{l}_p\gamma^\mu l_r)$
$\mathcal{O}_{\varphi\widetilde{G}}$	$\varphi^\dagger\varphi\,\widetilde{G}^A_{\mu\nu}G^{A\mu\nu}$	$\mathcal{O}_{eB}$	$(\bar{l}_p\sigma^{\mu\nu}e_r)\varphi B_{\mu\nu}$	$\mathcal{O}^{(3)}_{\varphi l}$	$(\varphi^\dagger i\overleftrightarrow{D}^I_\mu\varphi)(\bar{l}_p\tau^I\gamma^\mu l_r)$
$\mathcal{O}_{\varphi W}$	$\varphi^\dagger\varphi\, W^I_{\mu\nu}W^{I\mu\nu}$	$\mathcal{O}_{uG}$	$(\bar{q}_p\sigma^{\mu\nu}T^A u_r)\widetilde{\varphi}\,G^A_{\mu\nu}$	$\mathcal{O}_{\varphi e}$	$(\varphi^\dagger i\overleftrightarrow{D}_\mu\varphi)(\bar{e}_p\gamma^\mu e_r)$
$\mathcal{O}_{\varphi\widetilde{W}}$	$\varphi^\dagger\varphi\,\widetilde{W}^I_{\mu\nu}W^{I\mu\nu}$	$\mathcal{O}_{uW}$	$(\bar{q}_p\sigma^{\mu\nu}u_r)\tau^I\widetilde{\varphi}\,W^I_{\mu\nu}$	$\mathcal{O}^{(1)}_{\varphi q}$	$(\varphi^\dagger i\overleftrightarrow{D}_\mu\varphi)(\bar{q}_p\gamma^\mu q_r)$
$\mathcal{O}_{\varphi B}$	$\varphi^\dagger\varphi\, B_{\mu\nu}B^{\mu\nu}$	$\mathcal{O}_{uB}$	$(\bar{q}_p\sigma^{\mu\nu}u_r)\widetilde{\varphi}\,B_{\mu\nu}$	$\mathcal{O}^{(3)}_{\varphi q}$	$(\varphi^\dagger i\overleftrightarrow{D}^I_\mu\varphi)(\bar{q}_p\tau^I\gamma^\mu q_r)$
$\mathcal{O}_{\varphi\widetilde{B}}$	$\varphi^\dagger\varphi\,\widetilde{B}_{\mu\nu}B^{\mu\nu}$	$\mathcal{O}_{dG}$	$(\bar{q}_p\sigma^{\mu\nu}T^A d_r)\varphi\, G^A_{\mu\nu}$	$\mathcal{O}_{\varphi u}$	$(\varphi^\dagger i\overleftrightarrow{D}_\mu\varphi)(\bar{u}_p\gamma^\mu u_r)$
$\mathcal{O}_{\varphi WB}$	$\varphi^\dagger\tau^I\varphi\, W^I_{\mu\nu}B^{\mu\nu}$	$\mathcal{O}_{dW}$	$(\bar{q}_p\sigma^{\mu\nu}d_r)\tau^I\varphi\, W^I_{\mu\nu}$	$\mathcal{O}_{\varphi d}$	$(\varphi^\dagger i\overleftrightarrow{D}_\mu\varphi)(\bar{d}_p\gamma^\mu d_r)$
$\mathcal{O}_{\varphi\widetilde{W}B}$	$\varphi^\dagger\tau^I\varphi\,\widetilde{W}^I_{\mu\nu}B^{\mu\nu}$	$\mathcal{O}_{dB}$	$(\bar{q}_p\sigma^{\mu\nu}d_r)\varphi\, B_{\mu\nu}$	$\mathcal{O}_{\varphi ud}$	$i(\widetilde{\varphi}^\dagger D_\mu\varphi)(\bar{u}_p\gamma^\mu d_r)$

Figure 2.1: Dimension-six operators other than the four-fermion ones, from Ref. [48].

2.3 QCD and Chiral Perturbation Theory

2.3.1 Quantum Chromodynamics

So far, we have discussed in detail the electroweak part of the SM, which is contained in the $SU(2)_L \otimes U(1)_Y$ gauge group. Now we will discuss the strong force, which is contained in the $SU(3)_C$ group in order to give a complete and self-contained discussion of the Standard Model.

The gauge group $SU(3)_C$ is left unbroken after spontaneous symmetry breaking, as a consequence of this fact, the gluons remain massless. There are eight gluons, one for each of the generators of $SU(3)_C$ that together with the quarks represent the degrees of freedom of QCD. Besides the $SU(3)_C$ and the Lorentz symmetries, the strong interaction Lagrangian is also invariant under charge conjugation (C), parity (P) and time reversal (T), its explicit form is given by

$$\mathcal{L}_{QCD} = -\frac{1}{4}G^i_{\mu\nu}G^{\mu\nu i} + \sum_{r=1}^{6}\overline{q}_r[i\not{D} - m_r]q_r\,, \tag{2.54}$$

$(\bar{L}L)(\bar{L}L)$		$(\bar{R}R)(\bar{R}R)$		$(\bar{L}L)(\bar{R}R)$	
$\mathcal{O}_{ll}$	$(\bar{l}_p\gamma_\mu l_r)(\bar{l}_s\gamma^\mu l_t)$	$\mathcal{O}_{ee}$	$(\bar{e}_p\gamma_\mu e_r)(\bar{e}_s\gamma^\mu e_t)$	$\mathcal{O}_{le}$	$(\bar{l}_p\gamma_\mu l_r)(\bar{e}_s\gamma^\mu e_t)$
$\mathcal{O}_{qq}^{(1)}$	$(\bar{q}_p\gamma_\mu q_r)(\bar{q}_s\gamma^\mu q_t)$	$\mathcal{O}_{uu}$	$(\bar{u}_p\gamma_\mu u_r)(\bar{u}_s\gamma^\mu u_t)$	$\mathcal{O}_{lu}$	$(\bar{l}_p\gamma_\mu l_r)(\bar{u}_s\gamma^\mu u_t)$
$\mathcal{O}_{qq}^{(3)}$	$(\bar{q}_p\gamma_\mu\tau^I q_r)(\bar{q}_s\gamma^\mu\tau^I q_t)$	$\mathcal{O}_{dd}$	$(\bar{d}_p\gamma_\mu d_r)(\bar{d}_s\gamma^\mu d_t)$	$\mathcal{O}_{ld}$	$(\bar{l}_p\gamma_\mu l_r)(\bar{d}_s\gamma^\mu d_t)$
$\mathcal{O}_{lq}^{(1)}$	$(\bar{l}_p\gamma_\mu l_r)(\bar{q}_s\gamma^\mu q_t)$	$\mathcal{O}_{eu}$	$(\bar{e}_p\gamma_\mu e_r)(\bar{u}_s\gamma^\mu u_t)$	$\mathcal{O}_{qe}$	$(\bar{q}_p\gamma_\mu q_r)(\bar{e}_s\gamma^\mu e_t)$
$\mathcal{O}_{lq}^{(3)}$	$(\bar{l}_p\gamma_\mu\tau^I l_r)(\bar{q}_s\gamma^\mu\tau^I q_t)$	$\mathcal{O}_{ed}$	$(\bar{e}_p\gamma_\mu e_r)(\bar{d}_s\gamma^\mu d_t)$	$\mathcal{O}_{qu}^{(1)}$	$(\bar{q}_p\gamma_\mu q_r)(\bar{u}_s\gamma^\mu u_t)$
		$\mathcal{O}_{ud}^{(1)}$	$(\bar{u}_p\gamma_\mu u_r)(\bar{d}_s\gamma^\mu d_t)$	$\mathcal{O}_{qu}^{(8)}$	$(\bar{q}_p\gamma_\mu T^A q_r)(\bar{u}_s\gamma^\mu T^A u_t)$
		$\mathcal{O}_{ud}^{(8)}$	$(\bar{u}_p\gamma_\mu T^A u_r)(\bar{d}_s\gamma^\mu T^A d_t)$	$\mathcal{O}_{qd}^{(1)}$	$(\bar{q}_p\gamma_\mu q_r)(\bar{d}_s\gamma^\mu d_t)$
				$\mathcal{O}_{qd}^{(8)}$	$(\bar{q}_p\gamma_\mu T^A q_r)(\bar{d}_s\gamma^\mu T^A d_t)$

$(\bar{L}R)(\bar{R}L)$ and $(\bar{L}R)(\bar{L}R)$	
$\mathcal{O}_{ledq}$	$(\bar{l}_p^j e_r)(\bar{d}_s q_t^j)$
$\mathcal{O}_{quqd}^{(1)}$	$(\bar{q}_p^j u_r)\varepsilon_{jk}(\bar{q}_s^k d_t)$
$\mathcal{O}_{quqd}^{(8)}$	$(\bar{q}_p^j T^A u_r)\varepsilon_{jk}(\bar{q}_s^k T^A d_t)$
$\mathcal{O}_{lequ}^{(1)}$	$(\bar{l}_p^j e_r)\varepsilon_{jk}(\bar{q}_s^k u_t)$
$\mathcal{O}_{lequ}^{(3)}$	$(\bar{l}_p^j \sigma_{\mu\nu} e_r)\varepsilon_{jk}(\bar{q}_s^k \sigma^{\mu\nu} u_t)$

59 operators
(1 family & B conservation)

Figure 2.2: Four-fermion operators, from Ref. [48].

with

$$q_r = \begin{pmatrix} q_r^1 \\ q_r^2 \\ q_r^3 \end{pmatrix} \tag{2.55}$$

and

$$G_{\mu\nu}^i = \partial_\mu G_\nu^i - \partial_\nu G_\mu^i - g_s f_{ijk} G_\mu^j G_\nu^k, \quad i,j,k = 1,...,8\,, \tag{2.56}$$

$$D_\mu = \partial_\mu + i\frac{g_s}{2}\lambda^i G_\mu^i\,, \tag{2.57}$$

where λ^i are the eight Gell-Mann matrices and f_{ijk} are the structure constants of $SU(3)$,

$$\begin{aligned}
\lambda_1 &= \begin{pmatrix} 0 & 1 & 0 \\ 1 & 0 & 0 \\ 0 & 0 & 0 \end{pmatrix}, \quad \lambda_2 = \begin{pmatrix} 0 & -i & 0 \\ i & 0 & 0 \\ 0 & 0 & 0 \end{pmatrix}, \quad \lambda_3 = \begin{pmatrix} 1 & 0 & 0 \\ 0 & -1 & 0 \\ 0 & 0 & 0 \end{pmatrix}, \\
\lambda_4 &= \begin{pmatrix} 0 & 0 & 1 \\ 0 & 0 & 0 \\ 1 & 0 & 0 \end{pmatrix}, \quad \lambda_5 = \begin{pmatrix} 0 & 0 & -i \\ 0 & 0 & 0 \\ i & 0 & 0 \end{pmatrix}, \quad \lambda_6 = \begin{pmatrix} 0 & 0 & 0 \\ 0 & 0 & 1 \\ 0 & 1 & 0 \end{pmatrix}, \\
\lambda_7 &= \begin{pmatrix} 0 & 0 & 0 \\ 0 & 0 & -i \\ 0 & i & 0 \end{pmatrix}, \quad \lambda_8 = \frac{1}{\sqrt{3}} \begin{pmatrix} 1 & 0 & 0 \\ 0 & 1 & 0 \\ 0 & 0 & -2 \end{pmatrix}.
\end{aligned} \tag{2.58}$$

abc	123	147	156	246	257	345	367	458	678
f_{abc}	1	$\frac{1}{2}$	$-\frac{1}{2}$	$\frac{1}{2}$	$\frac{1}{2}$	$\frac{1}{2}$	$-\frac{1}{2}$	$\frac{\sqrt{3}}{2}$	$\frac{\sqrt{3}}{2}$

Table 2.4: Totally antisymmetric nonvanishing structure constants of $SU(3)$.

From the previous equations we see that the quarks are in the fundamental representation and the gluons are in the adjoint representation (as any other gauge boson) of the gauge group $SU(3)_C$.

There are many features that make QCD really special, for instance:
(i) The gluons have a color charge, this means that not only quarks interact with other quarks via the exchange of gluons, gluons themselves interact with other gluons. In fact, according to eqs. (2.54) and (2.56), we have trilinear and quadrilinear interactions between the gluons. This is similar to what we saw for the $W^{\pm}$ and the Z gauge bosons. This feature is inherited by the fact that $SU(3)$ is a non-abelian group.
(ii) The strength of the strong interaction reduces as the energy of those interactions increases.
(iii) There is a scale Λ_{QCD} at which hadronization takes place and at which QCD becomes non-perturbative. This means that we cannot do perturbative calculations with quarks and gluons at that scale or below. There is nothing wrong with the theory per se, it is just that we are used to do perturbative calculations and we do not know exactly what to do when we have strongly coupled theories. When we work with tau decays we fall exactly in that regime and to avoid this problem with the QCD Lagrangian we work in an effective field theory framework, this EFT is called chiral perturbation theory (ChPT) and we will discuss it in detail in the following section.
(iv) Quarks are confined inside hadrons, if we try to separate them ever-increasing amounts of energy are required, so that, it becomes energetically favorable to create a quark-antiquark pair, turning the initial hadron into a pair of hadrons.

Point (ii) is called asymptotic freedom and is a well established fact from QCD since 1973 when it was discovered by David Gross and Frank Wilczek [52] and independently by David Politzer [53]. In fig. 2.3 you can see this behavior of QCD; when you go to high energies or equivalently low distance scales, the strong coupling $\alpha_s(s)$ becomes smaller and smaller, and when you go to low energies the $\alpha_s(s)$ coupling becomes bigger and bigger.

Points (iii) and (iv) are part of what is known as color confinement. Color confinement is not yet analytically proven and is one of the millenium prize problems, but otherwise is really well established by experiments and by lattice QCD calculations.

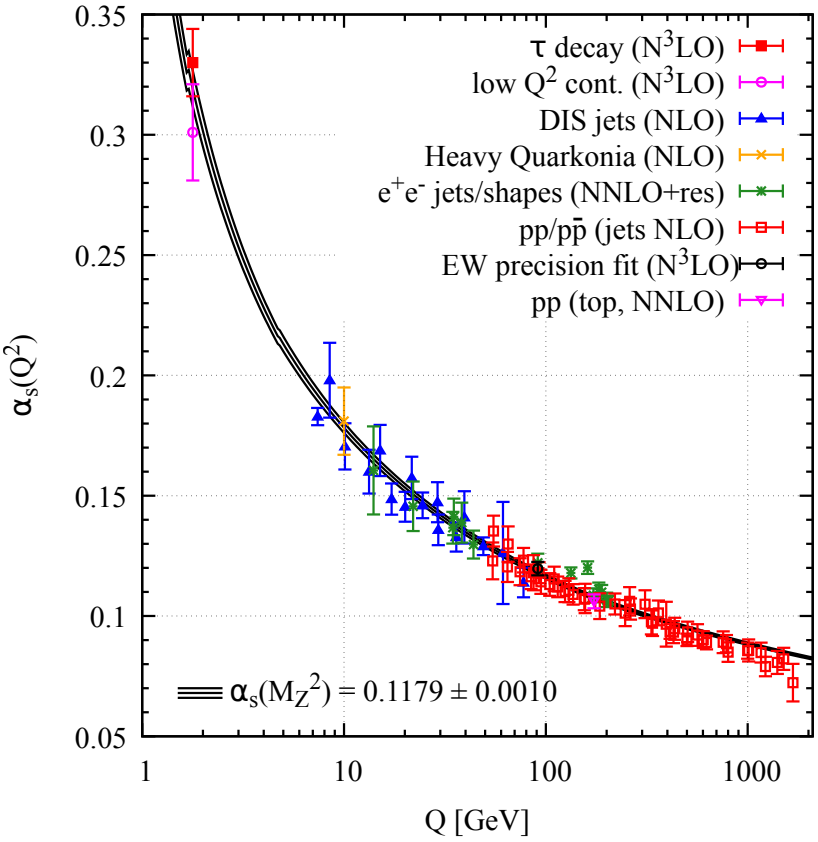

Figure 2.3: Measurements of the α_s coupling as a function of energy Q (experimental dots) compared with QCD prediction (solid lines), from Ref. [6].

From the QCD Lagrangian (2.54) we see that QCD is a vector theory, that is, it treats right-handed and left-handed spinors in the same manner. The fact that QCD is a vector theory enables one to construct mass terms as you can see in eq. (2.54). In table 2.5 you can see the masses for the six quarks, the quarks u, d and s are known as light quarks and the quarks c, b and t are known as heavy quarks ('light' and 'heavy' compared to Λ_{QCD}). Note that the errors for the light quark masses are big compared with the corresponding errors for the heavy quark masses, this is due to the fact that non-perturbative QCD effects are dominant for the light quarks. If one works with the light quarks only (as we will), one obtains several accidental symmetries.

From table 2.5 we see that the masses for the up and down quarks are really close. If we set $m_u = m_d$ in a first approximation, the Lagrangian in eq. (2.54) acquires a new symmetry called Isospin symmetry. With this assumption the theory is invariant under the continuous group of isospin

Flavor	Mass	Charge
u	$2.2^{+0.5}_{-0.4}\,\mathrm{MeV}$	$2/3$
d	$4.7^{+0.5}_{-0.3}\,\mathrm{MeV}$	$-1/3$
s	$95^{+9}_{-3}\,\mathrm{MeV}$	$-1/3$
c	$1.275^{+0.025}_{-0.035}\,\mathrm{GeV}$	$2/3$
b	$4.18^{+0.04}_{-0.03}\,\mathrm{GeV}$	$-1/3$
t	$173.0 \pm 0.4\,\mathrm{GeV}$	$2/3$

Table 2.5: Mass and charge of quarks [6]. The u-, d-, and s-quark masses are estimates of the so-called "current-quark masses" in the $\overline{MS}$ scheme at a scale $\mu = 2$ GeV. The c- and b- quark masses are the "running" masses in the $\overline{MS}$ scheme, while for the t mass, we report the PDG "direct measurements" result. The charge is given in units of the elementary charge e.

rotations

$$\psi_i \to (e^{i\vec{\alpha}\cdot\frac{\vec{\tau}}{2}})_{ij}\psi_j\,, \tag{2.59}$$

where i, j run over the values u, d and $\vec{\tau} = (\tau_1, \tau_2, \tau_3)$ is a vector arrange with the three Pauli matrices. The associated Noether current is given by,

$$j^{\mu a} = \bar{\psi}\gamma^\mu \frac{\tau^a}{2}\psi\,, \tag{2.60}$$

this is the $SU(2)$ isospin symmetry, although it is broken since the up and down quark masses are not exactly the same, we can always assume the symmetry as a first approximation and if needed, take isospin breaking effects, which will always be very small (proportional to $m_d - m_u$).

The same ideas can be extended to include the s quark, that is, we can go from the $SU(2)$ to the $SU(3)$ isospin group, although in this last case the assumption that $m_u = m_d = m_s$ is not as strong as the previous one $m_u = m_d$, due to the fact that the mass of the strange quark is not that close to the mass of the other light quarks, in any case, the $SU(3)$ accidental quasi-symmetry turns out to be really useful when analyzing the hadronic spectra.

As a consequence of the $SU(2)$ and $SU(3)$ flavor symmetries we see that mesons and baryons form multiplets which are representations of those groups.

Note that this new $SU(3)$ isospin symmetry is very different to the previous $SU(3)_C$ gauge symmetry, the isospin is an accidental flavor symmetry while the other is an exact gauge symmetry. There is at least one more area in the context of strong interactions in which the $SU(3)$ group plays a fundamental role. This is the chiral symmetry group of QCD for vanishing u, d,

and s quark masses, which is given by the direct product $SU(3)_L \times SU(3)_R$. We will study chiral symmetry in great detail in the following section when we review chiral perturbation theory.

It is important to mention at this point that the QCD Lagrangian given in eq. (2.54) is not the most general Lagrangian that one can construct, there is one additional term consistent with the Lorentz and the $SU(3)_C$ gauge symmetries that can be included in (2.54) that has the following form,

$$\mathcal{L}_\theta = \frac{\theta}{16\pi^2} Tr\tilde{\mathbf{G}}_{\mu\nu}\mathbf{G}^{\mu\nu}\,, \tag{2.61}$$

where $\mathbf{G}_{\mu\nu} = G^a_{\mu\nu}T^a$ is the gluon field strength tensor and $\tilde{\mathbf{G}}_{\mu\nu} = \frac{1}{2}\epsilon_{\mu\nu\alpha\beta}\mathbf{G}^{\alpha\beta}$ is the dual of the gluon field strength tensor. Note that although this term can be written as a total derivative, or surface term, it cannot be ignored since the gauge fields do not necessarily vanish at infinity.

This is the famous θ_{QCD} parameter that we mentioned in section 2.2.1, which is one of the 19 parameters that conform the SM. This parameter is very special in the sense that it is very suppressed and we do not have a fundamental theoretical reason that explains why this is the case, that is why some authors sometimes exclude this parameter and speak about 18 free parameters in the SM. Although we do not have a deep theoretical reason, we know from phenomenology that this parameter theta is almost zero. In fact from the upper limit on the neutron's electric dipole moment at 90% CL [54, 55],

$$|d_n| \leq 2.9 \times 10^{-26}\, e\, cm\,, \tag{2.62}$$

we have that the parameter θ [7] must be extraordinarily small:

$$|\theta_{QCD}| \leq 10^{-10}\,. \tag{2.63}$$

It is important to note that the θ_{QCD} term given in eq. (2.61) violates CP. Actually, it is the only term that can violate CP in the strong sector, however, due to the suppression of θ_{QCD}, CP is conserved for all practical purposes in QCD. The fact that we do not have a fundamental theoretical argument to impose CP conservation in QCD could be perceived as a fine tuning problem. This is an open question in physics and is known as the strong CP problem. A possible solution to this problem is the Peccei-Quinn theory [56], which proposes a new pseudoscalar particle known as the axion. In this thesis work, we will not deal with the strong CP problem in any of the subsequent chapters. Given that QED satisfies the CP symmetry trivially,

[7] In fact, this applies to a linear combination of θ with the argument of the determinant of the mass matrix, which is called θ_{QCD}.

one expects that measurable violations of the CP symmetry come only from the weak force.

While writing this section on QCD, the books [57] and [58] were extremely helpful. The review [59] is also a very clear exposition of the subject.

2.3.2 Chiral Perturbation Theory (ChPT)

Previously, we saw that if we set $m_u = m_d = m_s$ we obtain an accidental $SU(3)$ flavor symmetry, if we go further and set the masses to zero, the group of symmetries is enlarged. To see this, let us write the QCD Lagrangian in eq. (2.54) for the light quarks in the massless approximation

$$\mathcal{L}_{QCD} = -\frac{1}{4} G^i_{\mu\nu} G^{\mu\nu i} + \sum_{f=u,d,s} \left(\overline{q}_{fL} i \not{D} q_{fL} + \overline{q}_{fR} i \not{D} q_{fR} \right), \tag{2.64}$$

where $q_f = \begin{pmatrix} q_{fL} \\ q_{fR} \end{pmatrix}$. Note from eq. (2.64) that the left- and right-handed components of the quarks decouple in the massless limit. This means that we can make independent $U(3)$ transformations on the left- and right-handed components of the quark spinors

$$\begin{aligned} \psi^i_L &\rightarrow L^i_j \psi^j_L \,, \\ \psi^i_R &\rightarrow R^i_j \psi^j_R \,, \end{aligned} \tag{2.65}$$

where $L^i_j \in U(3)_L$ and $R^i_j \in U(3)_R$, so that the new group of symmetries is $U(3)_L \otimes U(3)_R$.

This new symmetry group can be conveniently decomposed in the following way: $U(3)_L \otimes U(3)_R \sim SU(3)_L \otimes SU(3)_R \otimes U(1)_V \otimes U(1)_A$, where we now have the special unitary groups, baryon symmetry and axial symmetry. As we will see $SU(3)_L \otimes SU(3)_R$ is spontaneously broken, $U(1)_V$ is realized and $U(1)_A$ is anomalous.

$U(1)_V$ refers just to a global rephasing of the left- and right-handed fields, that is,

$$\begin{aligned} \psi^i_L &\rightarrow e^{i\alpha} \psi^i_L \,, \\ \psi^i_R &\rightarrow e^{i\alpha} \psi^j_R \,, \end{aligned} \tag{2.66}$$

this symmetry known as baryon number is realized in nature, but note that is completely different to gauge symmetries in the sense that baryon number is an accidental symmetry, it was not required from first principles.

$U(1)_A$ refers to opposite rephasings for the left- and right-handed fields

$$\begin{aligned} \psi^i_L &\rightarrow e^{i\beta} \psi^i_L \,, \\ \psi^i_R &\rightarrow e^{-i\beta} \psi^j_R \,, \end{aligned} \tag{2.67}$$

the axial symmetry $U(1)_A$ is exact in the classical theory, but it is broken by quantum effects in QCD [60, 61].

The chiral symmetry $SU(3)_L \otimes SU(3)_R$ refers to transformations of the type in eq. (2.65) with the additional condition that L^i_j and R^i_j must have a determinant equal to one (that is, L^i_j and R^i_j must be unitary, unimodular 3×3 matrices). This symmetry is spontaneously broken by the presence of the operator $\langle \bar{\psi}^i_R \psi^j_L \rangle$ as we see in the following equation

$$\langle \bar{\psi}^i_R \psi^j_L \rangle = v^3 \delta^{ij} \,, \tag{2.68}$$

so that, the vacuum of QCD is not symmetric under general $SU(3)_L \otimes SU(3)_R$ transformations. However, the QCD vacuum is invariant under a subgroup of the chiral group, namely $SU(3)_V$, that is, for the case of equal left- and right-handed transformations we have the symmetry breaking pattern

$$SU(3)_L \otimes SU(3)_R \to SU(3)_V \,. \tag{2.69}$$

According to Goldstone's theorem, we have eight Nambu-Goldstone bosons as a consequence of this spontaneous breaking of the chiral symmetry, that is, one Nambu-Goldstone boson for each generator of the symmetry that is broken. These eight Nambu-Goldstone bosons correspond to the meson octet; pions, kaons and the eta.

The spontaneous breaking of the chiral symmetry is responsible for the fact that we only see one meson octet and not two, if the QCD vacuum were symmetric under the full $SU(3)_L \otimes SU(3)_R$ group, we would observe two meson octets with opposite parity, but since this group breaks to $SU(3)_V$, only the pseudoscalar octet is allowed, and that is indeed what we see in nature.

Strictly speaking the mesons in the octet are not exactly Nambu-Goldstone bosons since they do have a mass, however their masses are very light compared with the masses of all the other hadrons, this is specially true for the pions, which are much lighter than the ρ meson, which is the next hadron with the same flavor quantum numbers in the mass spectrum. Due to this fact, these mesons are known as pseudo Nambu-Goldstone particles. This mass gap rapidly suggests the idea of using an effective field theory, and this is precisely what is done. The effective field theory that describes the strong interactions between the light mesons is known as Chiral Perturbation Theory (ChPT) [62, 63].

Also note that there is one more apparent symmetry in the Lagrangian (2.64), this symmetry, known as conformal symmetry, is related to the fact that there is no apparent scale when we have massless quarks, however, the hadronization process introduces one scale to the problem, this scale is denoted as Λ_{QCD}, and has an approximate value of $\Lambda_{QCD} \sim 300\,\text{MeV}$. Hence,

at the end conformal symmetry is anomalous.

For the convenience of the reader we write a summary of the realized and broken symmetries of the Lagrangian in eq. (2.64) in what follows,

Symmetries:

- Conformal Symmetry: anomalous
- $U(3)_L \otimes U(3)_R \sim SU(3)_L \otimes SU(3)_R \otimes U(1)_V \otimes U(1)_A$
  - $SU(3)_L \otimes SU(3)_R \to SU(3)_V$: spontaneously broken
  - $U(1)_V$: realized
  - $U(1)_A$: anomalous

Having understood all the symmetries of the massless QCD Lagrangian in eq. (2.64) and particularly the chiral symmetry breaking pattern, now it is time to discuss the Chiral Perturbation Theory Lagrangian [27, 62, 63]. Note that since QCD is not perturbative in this regime, it is impossible to do a matching between QCD and ChPT, therefore ChPT must be constructed entirely with the Nambu-Goldstone fields as the degrees of freedom, following the bottom-up approach.

The Lagrangian is constructed according to the Callan, Coleman, Wess, and Zumino (CCWZ) prescription [64, 65] [8] where the Nambu-Goldstone fields are parametrized in the following way

$$U(\phi) = u(\phi)^2 = exp\left[i\frac{\sqrt{2}\Phi}{f}\right], \tag{2.70}$$

with,

$$\Phi(x) \equiv \frac{\lambda^a \phi^a}{\sqrt{2}} = \begin{pmatrix} \frac{1}{\sqrt{2}}\pi^0 + \frac{1}{\sqrt{6}}\eta_8 & \pi^+ & K^+ \\ \pi^- & -\frac{1}{\sqrt{2}}\pi^0 + \frac{1}{\sqrt{6}}\eta_8 & K^0 \\ K^- & \bar{K^0} & -\frac{2}{\sqrt{6}}\eta_8 \end{pmatrix}, \tag{2.71}$$

for the moment, the f in eq. (2.70) is just a constant with dimensions of energy in order to have a dimensionless argument for the exponential. As we will see in what follows, f will turn out to be the decay constant for the

[8] The CCWZ formalism is discussed in appendix A.

pion.

In this prescription, $U(\phi)$ transforms as

$$U(\phi) \to LU(\phi)R^\dagger\,, \tag{2.72}$$

so, the Lagrangian for ChPT must be constructed with terms with products of the form $UU^\dagger$. But $UU^\dagger = 1$, so that the lowest order Lagrangian must contain derivatives in order to have dynamics for the Goldstones

$$\mathcal{L}_2 = \frac{f^2}{4}\langle \partial_\mu U^\dagger \partial^\mu U\rangle\,, \tag{2.73}$$

where $\langle U\rangle$ stands for the trace of the matrix U and the 4 in the denominator is chosen so that we have a canonical normalization for the kinematic terms of the Goldstones. Note that the effective Lagrangian describes a theory of weakly interacting Goldstone bosons at low energy. The Goldstone boson couplings are proportional to their momentum, and so vanish at low-energies.

Also note from eq. (2.72) that while U transforms linearly, the Goldstone fields ϕ^a transform non-linearly. This is an example of a non-linear realization of a symmetry.

Expanding $U(\phi)$ to fourth order in Φ we arrive to the following expression for $\mathcal{L}_2$

$$\mathcal{L}_2 = \frac{1}{2}\langle \partial_\mu \Phi \partial^\mu \Phi\rangle + \frac{1}{12f^2}\langle (\Phi \overleftrightarrow{\partial}_\mu \Phi)(\Phi \overleftrightarrow{\partial}^\mu \Phi)\rangle + \mathcal{O}\left(\Phi^6/f^4\right)\,, \tag{2.74}$$

where $(\Phi \overleftrightarrow{\partial}_\mu \Phi) \equiv \Phi(\partial_\mu \Phi) - (\partial_\mu \Phi)\Phi$. The first term is the usual kinetic term canonically normalized and the second term is a four-boson interaction between two fields with two derivatives of the field. The only important parameter here is the constant f, once it is fixed (through pion decay, for example) every other pion-pion process is predicted.

From the lowest order Lagrangian in eq. (2.73) we already see some general features that must be satisfied by higher order Lagrangians, for example the pair of derivatives in (2.73). In general the Lagrangian will be given in a power series of momentum or, equivalently, in a power series of derivatives, and the number of these derivatives must be even in order to accomplish the parity conservation of the strong force.

$$\mathcal{L}_{eff}(U) = \sum_n \mathcal{L}_{2n}\,. \tag{2.75}$$

The Lagrangian in eq. (2.73) and more generally, any Lagrangian of the form shown in eq. (2.75) describes processes of the form $\pi\pi \to \pi\pi$, 4π, 6π,

etc, but does not describe electromagnetic or weak processes for pions and does not even take into account the pion masses. If we want to introduce all those effects we need to extend our lowest order Lagrangian $\mathcal{L}_2$ via the introduction of external fields, that is, via the introduction of sources. With that in mind, one starts again with the QCD Lagrangian for the light quarks in the chiral limit (2.64) and introduce external fields v_μ, a_μ, s, p, and $\bar{t}^{\mu\nu}$, such that they couple to the quarks in the following way [62, 63, 66]

$$\mathcal{L}_{QCD} = \mathcal{L}^0_{QCD} + \bar{q}\gamma^\mu(v_\mu + \gamma^5 a_\mu)q - \bar{q}(s - i\gamma^5 p)q + \bar{q}\sigma_{\mu\nu}\bar{t}^{\mu\nu}q\,, \tag{2.76}$$

with $\bar{t}^{\mu\nu}$ defined in the following way

$$\bar{t}^{\mu\nu} = \sum_{a=0}^{8} \frac{\lambda^a}{2}\bar{t}^{\mu\nu}_a\,, \tag{2.77}$$

where λ^a are the eight Gell-Mann matrices that we have introduced before and $\lambda^0 = \sqrt{\frac{2}{n_f}} I_{n_f\times n_f}$ [9].

Quark masses, and electromagnetic and semileptonic weak interactions can be incorporated if we make the following identifications in eq. (2.76):

$$\begin{aligned} r_\mu &\equiv v_\mu + a_\mu = eQA_\mu + \dots\,, \\ \ell_\mu &\equiv v_\mu - a_\mu = eQA_\mu + \frac{e}{\sqrt{2}\sin\theta_W}(W^\dagger_\mu T_+ + h.c.) + \dots\,, \\ s &= \mathcal{M} + \dots\,, \end{aligned} \tag{2.78}$$

where Q and $\mathcal{M}$ denote the quark-charge and quark-mass matrices respectively, and T_+ is a 3×3 matrix with the appropriate CKM parameters,

$$Q = \begin{pmatrix} \frac{2}{3} & 0 & 0 \\ 0 & -\frac{1}{3} & 0 \\ 0 & 0 & -\frac{1}{3} \end{pmatrix}\,,\ \mathcal{M} = \begin{pmatrix} m_u & 0 & 0 \\ 0 & m_d & 0 \\ 0 & 0 & m_s \end{pmatrix}\,,\ T_+ = \begin{pmatrix} 0 & V_{ud} & V_{us} \\ 0 & 0 & 0 \\ 0 & 0 & 0 \end{pmatrix}\,. \tag{2.79}$$

The tensor part in eq. (2.76) is specially important in this work since it is involved in an interesting CP violating observable that we will study in detail in chapter 4. This structure will also lead to the study of the tensor form factors for the different decay channels that we will analyze in this thesis.

Due to the inclusion of these external fields, the original global chiral symmetry $SU(3)_L \otimes SU(3)_R$ in $\mathcal{L}^0_{QCD}$ is now promoted to a local one for the

[9] This ninth matrix λ^0 together with the eight Gell-Mann matrices forms a basis of the Lie algebra for $U(3)$.

new $\mathcal{L}_{QCD}$ in eq. (2.76)

$$\begin{aligned} q &\to Rq_R + Lq_L\,, \\ s+ip &\to R(s+ip)L^\dagger\,, \\ \ell_\mu &\to L\ell_\mu L^\dagger + iL\partial_\mu L^\dagger\,, \\ r_\mu &\to Rr\mu R^\dagger + iR\partial_\mu R^\dagger\,, \\ t_{\mu\nu} &\to Rt_{\mu\nu}L^\dagger\,, \end{aligned} \tag{2.80}$$

where the tensor source $\bar{t}^{\mu\nu}$ in eq. (2.76) and the tensor source $t^{\mu\nu}$ in eq. (2.80) are related by a change of basis,

$$\bar{\psi}\sigma_{\mu\nu}\bar{t}^{\mu\nu}\psi = \bar{\psi}_L\sigma^{\mu\nu}t^\dagger_{\mu\nu}\psi_R + \bar{\psi}_R\sigma^{\mu\nu}t_{\mu\nu}\psi_L\,, \tag{2.81}$$

so that, the only difference is that $t_{\mu\nu}$ and $t^\dagger_{\mu\nu}$ are expressed in the chiral basis

$$\begin{aligned} \bar{t}^{\mu\nu} &= P_L^{\mu\nu\lambda\rho}t_{\lambda\rho} + P_R^{\mu\nu\lambda\rho}t^\dagger_{\lambda\rho}\,, \\ t^{\mu\nu} &= P_L^{\mu\nu\lambda\rho}\bar{t}_{\lambda\rho}\,, \end{aligned} \tag{2.82}$$

where the explicit form for the chiral projectors is given by

$$\begin{aligned} P_R^{\mu\nu\lambda\rho} &= \frac{1}{4}(g^{\mu\lambda}g^{\nu\rho} - g^{\nu\lambda}g^{\mu\rho} + i\epsilon^{\mu\nu\lambda\rho})\,, \\ P_L^{\mu\nu\lambda\rho} &= (P_R^{\mu\nu\lambda\rho})^\dagger\,. \end{aligned} \tag{2.83}$$

Finally, with the transformation properties for the external fields given in (2.80) we can easily construct the lowest order effective Lagrangian analogous to the one in eq. (2.73). As basic ingredients we have the covariant derivatives

$$\begin{aligned} D_\mu U &= \partial_\mu U - ir_\mu U + iU\ell_\mu\,, \\ D_\mu U^\dagger &= \partial_\mu U^\dagger + iU^\dagger r_\mu - i\ell_\mu U^\dagger\,, \end{aligned} \tag{2.84}$$

and the field strength tensors

$$F_x^{\mu\nu} = \partial^\mu x^\nu - \partial^\nu x^\mu - i[x^\mu, x^\nu]\,,\ x = r, \ell\,. \tag{2.85}$$

The lowest order effective Lagrangian invariant under local chiral symmetry has the form [62, 63]

$$\mathcal{L}_2 = \frac{f^2}{4}\langle D_\mu U^\dagger D^\mu U + U^\dagger\chi + \chi^\dagger U\rangle\,, \tag{2.86}$$

where $\chi = 2B_0(s+ip)$. Note that at this point we have only encountered two free parameters: f and B_0. The first, as we have pointed out before, is just

the pion decay constant and the second is related to the quark condensate, both in the chiral limit. Let us see this explicitly by computing the chiral currents from the effective action. First note that

$$exp(iZ) = \int DqD\bar{q}DG_\mu exp\left[i\int d^4x\mathcal{L}_{QCD}\right] = \int DU exp\left[i\int d^4x\mathcal{L}_{eff}\right] . \tag{2.87}$$

At lowest order in momenta, Z reduces to $S_2 = \int d^4x\mathcal{L}_2$. Therefore, we have the following relations:

$$\begin{aligned} J_L^\mu &= \frac{\delta S_2}{\delta \ell_\mu} = \frac{i}{2}f^2 D_\mu U^\dagger U = \frac{f}{\sqrt{2}}D_\mu\Phi - \frac{i}{2}(\Phi \overleftrightarrow{D}^\mu \Phi) + \mathcal{O}\left(\Phi^3/f\right) , \\ J_R^\mu &= \frac{\delta S_2}{\delta r_\mu} = \frac{i}{2}f^2 D_\mu U U^\dagger = -\frac{f}{\sqrt{2}}D_\mu\Phi - \frac{i}{2}(\Phi \overleftrightarrow{D}^\mu \Phi) + \mathcal{O}\left(\Phi^3/f\right) \end{aligned} \tag{2.88}$$

Thus, the physical interpretation of the chiral coupling f is clear, f is the pion decay constant, defined as

$$\langle 0|(J_A^\mu)^{12}|\pi^+\rangle \equiv i\sqrt{2}fp^\mu . \tag{2.89}$$

Similarly, for the B_0 constant we have,

$$\begin{aligned} \bar{q}_L^j q_R^i &= -\frac{\delta S_2}{\delta(s-ip)^{ji}} = -\frac{f^2}{2}B_0 U(\phi)^{ij} , \\ \bar{q}_R^j q_L^i &= -\frac{\delta S_2}{\delta(s+ip)^{ji}} = -\frac{f^2}{2}B_0 U(\phi)^{\dagger ij} , \end{aligned} \tag{2.90}$$

thus, B_0 is related to the quark condensate

$$\langle 0|\bar{q}^j q^i|0\rangle = -f^2 B_0 \delta^{ij} . \tag{2.91}$$

These two constants characterize completely ChPT at $\mathcal{O}(p^2)$.

Following the same logic, we can construct the next-to-leading order (NLO) effective Lagrangian, which appears at $\mathcal{O}(p^4)$. Note that this is precisely the order at which the tensor source appears for the first time (there was no tensor interaction for $\mathcal{L}_2$ in eq. (2.86)). So, it is convenient to analyze the NLO Lagrangian $\mathcal{L}_4$ with and without tensor sources in order to isolate the modifications introduced by them. First, turning off the tensor source $\bar{t}_{\mu\nu}$, we have

$$\begin{aligned} \mathcal{L}_4 =& L_1\langle D_\mu U^\dagger D^\mu U\rangle^2 + L_2\langle D_\mu U^\dagger D_\nu U\rangle\langle D^\mu U^\dagger D^\nu U\rangle \\ &+ L_3\langle D_\mu U^\dagger D^\mu U D_\nu U^\dagger D^\nu U\rangle + L_4\langle D_\mu U^\dagger D^\mu U\rangle\langle U^\dagger\chi + \chi^\dagger U\rangle \\ &+ L_5\langle D_\mu U^\dagger D^\mu U(U^\dagger\chi + \chi^\dagger U)\rangle + L_6\langle U^\dagger\chi + \chi^\dagger U\rangle^2 \\ &+ L_7\langle U^\dagger\chi - \chi^\dagger U\rangle^2 + L_8\langle\chi^\dagger U\chi^\dagger U + U^\dagger\chi U^\dagger\chi\rangle \\ &- iL_9\langle F_R^{\mu\nu}D_\mu U D_\nu U^\dagger + F_L^{\mu\nu}D_\mu U^\dagger D_\nu U\rangle + L_{10}\langle U^\dagger F_R^{\mu\nu}U F_{L\mu\nu}\rangle \\ &+ H_1\langle F_{R\mu\nu}F_R^{\mu\nu} + F_{L\mu\nu}F_L^{\mu\nu}\rangle + H_2\langle\chi^\dagger\chi\rangle . \end{aligned} \tag{2.92}$$

From eq. (2.85) we see that at $\mathcal{O}(p^4)$ we have ten additional parameters L_i with $i = 1, ..., 10$. The parameters H_1 and H_2 do not contain Goldstone bosons, so that they are not phenomenologically relevant in this thesis work.

Now let us go back to the general tensor case. In this case it is not convenient to work directly with the set $(U, F^{\mu\nu}_{L,R}, \chi, t_{\mu\nu})$ since these building blocks transform differently under a chiral transformation (see eq. (2.80) and this can complicate things as the order in the EFT expansion increases. For this reason we introduce the following redefinitions [67]

$$\begin{aligned} u_\mu &= i[u^\dagger(\partial_\mu - ir_\mu)u - u(\partial_\mu - il_\mu)u^\dagger]\,, \\ h_{\mu\nu} &= \nabla_\mu u_\nu + \nabla_\nu u_\mu\,, \\ f^{\mu\nu}_\pm &= uF^{\mu\nu}_L u^\dagger \pm u^\dagger F^{\mu\nu}_R u\,, \\ t^{\mu\nu}_\pm &= u^\dagger t^{\mu\nu} u^\dagger \pm u t^{\mu\nu\dagger} u\,, \\ \chi_\pm &= u^\dagger \chi u^\dagger \pm u \chi^\dagger u\,, \end{aligned} \tag{2.93}$$

where signs are correlated. With these convenient redefinitions, all the operators in eq. (2.93) transform in the same way

$$hXh^\dagger\,, \quad X = u_\mu, f^{\mu\nu}_\pm, t^{\mu\nu}_\pm, ... \tag{2.94}$$

where $h \in SU(3)_V$. This allows us to define a unique covariant derivative for all the terms in eq. (2.94)

$$\nabla_\mu X + [\Gamma_\mu, X]\,, \qquad \Gamma_\mu = \frac{1}{2}\left[u^\dagger(\partial_\mu - ir_\mu)u + u(\partial_\mu - il_\mu)u^\dagger\right]\,. \tag{2.95}$$

The field strength tensor comes naturally from the covariant derivative in the following way

$$[\nabla_\mu, \nabla_\nu]X = [\Gamma_{\mu\nu}, X]\,, \tag{2.96}$$

where,

$$\Gamma_{\mu\nu} = \partial_\mu\Gamma_\nu - \partial_\nu\Gamma_\mu + [\Gamma_\mu, \Gamma_\nu] = \frac{1}{4}[u_\mu, u_\nu] - \frac{i}{2}f_{+\mu\nu}\,. \tag{2.97}$$

The conclusion is that the sets $\{U^{(\dagger)}, F^{\mu\nu}_{L,R}, \chi^{(\dagger)}, t^{(\dagger)}_{\mu\nu}\}$ and $\{u_\mu, h_{\mu\nu}, f^{\mu\nu}_\pm, t^{\mu\nu}_\pm, \chi_\pm\}$ are completely equivalent.

Now that we have finally introduced all the basic ingredients for chiral Lagrangians, it is easy to see that the addition of the tensor source will modify our previous Lagrangian at $\mathcal{O}(p^4)$ in eq. (2.92), amazingly this modification is introduced by four new terms only, in fact, the new chiral Lagrangian $\mathcal{L}_4$ is given by [66]

$$\mathcal{L}_4 = \Lambda_1\langle t^{\mu\nu}_+ f_{+\mu\nu}\rangle - i\Lambda_2\langle t^{\mu\nu}_+ u_\mu u_\nu\rangle + \Lambda_3\langle t^{\mu\nu}_+ t^+_{\mu\nu}\rangle + \Lambda_4\langle t^{\mu\nu}_+\rangle^2\,. \tag{2.98}$$

From these four additional terms, only the one with Λ_2 is phenomenologically relevant for our analyses since it is the only one involving two derivatives for the Goldstones. This part of the discussion is of fundamental importance in this thesis, since tensor interactions play a main role, specially in chapter 4.

This section is heavily based on the amazing reviews [68, 69] and on the book [70]. Refs. [32, 33] were also very helpful, specially in the understanding of the CCWZ formalism, which is a key ingredient in ChPT and which is discussed in detail in appendix A.

2.3.3 Resonance Chiral Theory

In the previous section, we have made clear the necessity of introducing ChPT in the study of hadronic tau decays. We saw that a description in terms of quarks and gluons as degrees of freedom is meaningless for these decays. For this reason we changed from quarks and gluons to mesons as the relevant degrees of freedom.

Resonance Chiral Theory (RChT) [74, 75, 76, 77] is a phenomenological Lagrangian framework with pseudoGoldstone bosons and resonances as active fields, which is driven by chiral and unitary symmetries. The large-N_C limit of QCD [78, 79] is a useful expansion parameter for RChT.

The chiral symmetry for the pseudoGoldstones and the unitary symmetry for the resonances (together with the discrete symmetries of QCD and general symmetries of QFT) determine the possible operators in the Lagrangian of RChT.

Still, these symmetries (as in ChPT) cannot tell us the values of the coefficients of the different operators. In ChPT, couplings of operators with the same chiral counting should share order of magnitude (a similar reasoning is more difficult in RChT as it may depend on the order in $1/N_C$, the number of resonance fields, the chiral counting -for its IR limit- itself, etc.).

It is good -for RChT's predictivity- that the known short-distance behaviour of QCD [71, 72, 73] imposes constraints on Green functions and related form factors that relate some of the resonance couplings. This procedure, which has been carried out systematically [74, 75, 76, 77, 80, 81, 82, 83, 84], is also supported phenomenologically [85, 86, 87, 88, 89, 90, 91, 92, 181, 94, 95, 96, 97, 98, 99]. In fact, UV QCD provides a good argument for disregarding operators which are subleading in the chiral counting within RChT. This limits, in practice, the number of operators to be included for a

given calculation.

The Lagrangian of RChT includes kinetic terms for the resonances, operators akin to those in ChPT (but with different values for the corresponding LECs, as those in ChPT include the effect of the integrated-out resonances) and operators with resonance fields. The latter can also include pseudoGoldstones and couplings to external sources.

We will give, for definiteness, the Lagrangian corresponding to the interactions of the lightest vector mesons in case there is only one resonance field. This is [74]

$$\mathcal{L} = \frac{F_V}{2\sqrt{2}} \langle V_{\mu\nu} f_+^{\mu\nu} \rangle + i \frac{G_V}{\sqrt{2}} \langle V_{\mu\nu} u^\mu u^\nu \rangle \ , \tag{2.99}$$

where the chiral tensors $f_+^{\mu\nu}$ and u^μ were defined in the previous section, for ChPT, and $V_{\mu\nu}$ is an antisymmetric tensor field whose flavor structure is the same as that of Φ for the pseudoGoldstone bosons (i. e., $\pi \leftrightarrow \rho$, $K \leftrightarrow K^*$, $\eta_{8,1} \leftrightarrow \omega_{8,1}$); being F_V and G_V real couplings with dimensions of energy.

With this minimal Lagrangian it is possible to compute the two-meson form factors that are the seed of the phaseshift in the dispersive approach employed throughout this work (see appendix C for more details). Ref. [100] gives a concise introduction to RChT. More detailed accounts are given in Refs. [23, 24, 26].

Chapter 3

Effective-field theory analysis of the $\tau^- \to (K\pi)^-\nu_\tau$ decays

3.1 Summary

So far, we have presented all the tools that we need in the previous chapters. Now it is time to apply them to the study of the different hadronic tau decays that we promised at the beginning of this thesis. In this chapter we start studying the $\tau^- \to (K\pi)^-\nu_\tau$ decays in the framework of the Standard Model Effective Field Theory (SMEFT) which was discussed in chapter 2. We include the leading dimension six operators and work at linear order in the effective couplings. Here is a brief summary of what you are going to encounter along this chapter:
i) we study in detail the CP violation induced by heavy New Physics in the $\tau \to \pi K_S \nu_\tau$ channel, following the approach in ref. [101], where it was proved unambiguously that it is impossible to understand within this framework the corresponding anomaly in the CP asymmetry [1] measured by BaBar [102]. We confirmed this result, and as a novelty, we allow for reasonable variations of the hadronic input involved and study the associated uncertainty;
ii) among other things, we have studied the spectrum of the decay $\tau^- \to \pi^- K_S \nu_\tau$ as a function of the invariant mass of the di-meson system. In this respect, we are the first to show that the anomalous bump present in the published Belle data for the $K_S\pi^-$ invariant mass distribution [103] close to threshold cannot be due to heavy NP;
iii) we also study the constraints imposed in the effective couplings of the theory. In fact we are the first to constrain the heavy NP effective couplings using $\tau^- \to (K\pi)^-\nu_\tau$ decays and we show that they are competitive

[1] This CP asymmetry will be defined in the following section.

with other traditional low-energy probes like those found in hyperon semileptonic decays and those obtained in the effective tensor interactions of Kaon (semi)leptonic decays [2];
iv) moreover, we compare the SM predictions with the possible deviations caused by heavy NP in a couple of Dalitz plot distributions, in the forward-backward asymmetry and in the di-meson invariant mass distribution. Finally we discuss the most interesting measurements to be performed at Belle-II using these decays data.

3.2 Introduction

In chapter 1, we have made clear the importance of Tau physics as a powerful tool for precision electroweak studies and also as a clean low energy QCD laboratory. There, we also had the opportunity to mention briefly other interesting ways in which Tau physics can be very useful, for example in the searches for: lepton flavor and lepton number violations, CP violation, and potential new interactions due to heavy NP. In this chapter we discuss precisely, how Tau physics is important in two of these topics, namely: CP violation and new physics interactions.

As can be inferred from the four points stated in the summary, at the beginning of the chapter, we were motivated to do this study basically by the following reasons,

- Check the results in ref. [101], which disprove earlier claims [104, 105, 106] that tensor interactions could explain the BaBar CP anomaly in $\tau \to K_S \pi \nu_\tau$ decays [102]. This corresponds to the measurement of A_{CP}, defined in the following way:

$$A_{CP} = \frac{\Gamma(\tau^+ \to \pi^+ K_S \bar{\nu}_\tau) - \Gamma(\tau^- \to \pi^- K_S \nu_\tau)}{\Gamma(\tau^+ \to \pi^+ K_S \bar{\nu}_\tau) + \Gamma(\tau^- \to \pi^- K_S \nu_\tau)} = -3.6(2.3)(1.1)\times 10^{-3}\,, \tag{3.1}$$

  which disagrees remarkably with the SM prediction $A_{CP} = 3.32(6) \times 10^{-3}$, driven by neutral kaon mixing [107, 108], probed with high accuracy in semileptonic kaon decays [6]. In fact, the SM prediction is slightly modified by the experimental conditions corresponding to the reconstruction of the K_S at the B-factory, yielding $A_{CP} = 3.6(1) \times 10^{-3}$ [109], which increases the discrepancy at the 2.8 σ level. As a novelty of our treatment, we will discuss the uncertainty induced on A_{CP} by the

[2] As we will see in section 5, our effective couplings are not competitive with those coming from effective scalar interactions in semileptonic Kaon decays, they are only competitive if we only restrict to the tensor couplings.

error of the tensor form factor modulus, while for its phase uncertainty we will follow ref. [101]. This point is extremely important because the CP violation present in the SM [39] is clearly insufficient to understand the baryon asymmetry of the universe [110, 111, 112] so that any hint of NP involving CP violation becomes a candidate for providing with a clue to understand the enormous matter-antimatter imbalance. With respect to this BaBar anomaly, however, the related Belle measurement [113] of a binned CP asymmetry in the same decay channel analyzing the decay angular distributions is compatible with zero, as expected in the SM with a permille level precision. An explanation of this discrepancy is needed, and this is precisely one of the goals of this work.

- Three data points at the beginning of the $K_S\pi^-$ spectra measured by Belle [103] have been excluded from the reference fits or signalled as controversial in the dedicated analyses [114, 115, 116, 117, 118, 119, 120, 121] and are at variance with the prediction [122]. To our knowledge, only Ref. [123] was able to describe these data points due to the effect on the scalar form factor of the longitudinal correction to the $K^*(892)$ propagator induced by flavor symmetry breaking [3]. We will study if it is possible to explain these conflicting data points by the most general description of heavy NP contributions modifying the $\tau^- \to \bar{u}s\nu_\tau$ decays in the SM.

- Within an effective field theory analysis of possible non-standard charged current interactions, semileptonic tau decays [126, 127, 128] have been proved competitive with the traditional semileptonic decays involving light quarks [49, 129, 130, 131, 132, 133, 134, 135, 136, 50, 137], like nuclear beta or leptonic and radiative pion decays. In this context, for the Cabibbo-suppressed sector, hyperon semileptonic decays [132, 135] cannot compete with (semi)leptonic Kaon decays [134], given the (very accurately measured) dominant branching fractions of the latter and the suppressed ones (at most at the permille level) of the former. This intuitive reasoning suggests that strangeness-changing tau decays can also give non-trivial bounds on non-standard charged current interactions, although it is not likely that at a competitive level with $K_{\ell(2,3)}$ decays (however, if we restrict to tensor interactions only, we will see

[3] As we will recall in section 3.5, the scalar form factor contribution that we employ [124] was obtained as a result of analyzing strangeness-changing meson-meson scattering [125] within Chiral Perturbation Theory [62, 63] with resonances [74, 75], accounting for the leading flavor symmetry breaking.

that our couplings are competitive with the ones coming from $K_{\ell(2,3)}$ decays). The present work will make these statements precise.

We published the results that we are going to present in this chapter in ref. [138] and a shorter discussion can be found in the proceedings [139].

3.3 Effective theory analysis of $\tau^- \to \nu_\tau \bar{u} s$

The lepton number conserving effective Lagrangian density constructed with dimension six operators and invariant under the local $SU(3)_C \otimes SU(2)_L \otimes U(1)_Y$ SM gauge group has the following form [48, 51],

$$\mathcal{L}^{(eff)} = \mathcal{L}_{SM} + \frac{1}{\Lambda^2}\sum_i \alpha_i O_i \longrightarrow \mathcal{L}_{SM} + \frac{1}{v^2}\sum_i \hat{\alpha}_i O_i \,, \tag{3.2}$$

with $\hat{\alpha}_i = (v^2/\Lambda^2)\alpha_i$ the dimensionless couplings encoding NP at a scale of some TeV. Note that we have not included the Weinberg operator which has dimension five since it does not contribute to our processes. The Weinberg operator changes the lepton number in two units ($\Delta L = 2$) and lepton number violation is not present in our decays.

In this framework we can explicitly construct the leading low-scale $\mathcal{O}(1$ GeV) effective Lagrangian (which has $SU(3)_C \otimes U(1)_{em}$ local gauge symmetry) for the strangeness-changing semi-leptonic transitions upon integrating out the heavy degrees of freedom [49, 129],

$$\begin{aligned}\mathcal{L}_{cc} =& \frac{-4G_F}{\sqrt{2}} V_{us} \Big[(1 + [v_L]_{\ell\ell}) \bar{\ell}_L \gamma_\mu \nu_{\ell L} \bar{u}_L \gamma^\mu s_L + [v_R]_{\ell\ell} \bar{\ell}_L \gamma_\mu \nu_{\ell L} \bar{u}_R \gamma^\mu s_R \\ &+ [s_L]_{\ell\ell} \bar{\ell}_R \nu_{\ell L} \bar{u}_R s_L + [s_R]_{\ell\ell} \bar{\ell}_R \nu_{\ell L} \bar{u}_L s_R \\ &+ [t_L]_{\ell\ell} \bar{\ell}_R \sigma_{\mu\nu} \nu_{\ell L} \bar{u}_R \sigma^{\mu\nu} s_L \Big] + \text{h.c.}\,,\end{aligned} \tag{3.3}$$

where G_F is the tree-level definition of the Fermi constant, $L(R)$ stand for left(right)-handed chiral projections and $\sigma^{\mu\nu} = i\left[\gamma^\mu, \gamma^\nu\right]/2$. Note that if we set $v_L = v_R = s_L = s_R = t_L = 0$, we recover the SM Lagrangian for the strangeness-changing semileptonic tau decays, with momentum transfer much smaller than the M_W scale. Right-handed and wrong-flavor neutrino contributions were neglected in equation (3.3) since they do not interfere with the SM amplitudes and do not contribute at leading order in the NP effective coefficients. The couplings v_L, v_R, s_L, s_R, t_L are of course related to the α_i couplings of eq. (3.2). From the 59 independent operators with

dimension six present in the SMEFT (see figures 2.1 and 2.2) only a handful of them contribute to the charged-current processes that we are interested in [129]. In fact only eight of these operators will contribute to the semileptonic decays we are analyzing, namely:

- Four-fermion operators:

$$\mathcal{O}_{\ell q}^{(3)} = (\bar{\ell}\gamma^\mu \tau^a \ell)(\bar{q}\gamma_\mu \tau^a q)\,, \tag{3.4}$$

$$\mathcal{O}_{qde} = (\bar{\ell} e)(\bar{d} q) + h.c.\,, \tag{3.5}$$

$$\mathcal{O}_{\ell q} = (\bar{\ell}_a e)\epsilon^{ab}(\bar{q}_b u) + h.c.\,, \tag{3.6}$$

$$\mathcal{O}_{\ell q}^{T} = (\bar{\ell}_a \sigma^{\mu\nu} e)\epsilon^{ab}(\bar{q}_b \sigma_{\mu\nu} u) + h.c.\,, \tag{3.7}$$

- Vertex corrections:

$$\mathcal{O}_{\phi\phi} = i(\phi^T \epsilon D_\mu \phi)(\bar{u}\gamma^\mu d) + h.c.\,, \tag{3.8}$$

$$\mathcal{O}_{\phi q}^{(3)} = i(\phi^\dagger D^\mu \tau^a \phi)(\bar{q}\gamma_\mu \tau^a q) + h.c\,, \tag{3.9}$$

- Two more operators that modify the Fermi constant:

$$\mathcal{O}_{\ell\ell}^{(3)} = \frac{1}{2}(\bar{\ell}\gamma^\mu \tau^a \ell)(\bar{\ell}\gamma_\mu \tau^a \ell)\,, \tag{3.10}$$

$$\mathcal{O}(3)_{\phi\ell} = i(\phi^\dagger D^\mu \tau^a \phi)(\bar{\ell}\gamma_\mu \tau^a \ell) + h.c.\,. \tag{3.11}$$

The relation between the α_i couplings in eq. (3.2) and the effective couplings in eq. (3.3) is given by (assuming a weakly coupled scenario at the few-TeV scale)

$$\begin{aligned}
V_{ij}[v_L]_{\ell\ell ij} &= 2V_{ij}[\hat{\alpha}_{\phi l}^{(3)}]_{\ell\ell} + 2V_{im}[\hat{\alpha}_{\phi q}^{(3)}]^*_{jm} - 2V_{im}[\hat{\alpha}_{lq}^{(3)}]_{\ell\ell mj}\,,\\
V_{ij}[v_R]_{\ell\ell ij} &= -[\hat{\alpha}_{\phi\phi}]_{ij}\,,\\
V_{ij}[s_L]_{\ell\ell ij} &= -[\hat{\alpha}_{lq}]^*_{\ell\ell ji}\,,\\
V_{ij}[s_R]_{\ell\ell ij} &= -V_{im}[\hat{\alpha}_{qde}]^*_{\ell\ell jm}\,,\\
V_{ij}[t_L]_{\ell\ell ij} &= -[\hat{\alpha}^t_{lq}]^*_{\ell\ell ji}\,.
\end{aligned} \tag{3.12}$$

Besides Lorentz invariance, the only assumptions behind eq. (3.3) are the local gauge symmetries at low-energies ($U(1)_{em}$ and $SU(3)_C$ of electrodynamics and chromodynamics, respectively) and the absence of light non-SM particles.

It is convenient to recast the spin-zero contributions in terms of currents with defined parity (scalar and pseudoscalar) in the following way

$$\begin{aligned}
\mathcal{L}_{cc} = -\frac{G_F V_{us}}{\sqrt{2}}(1+\epsilon_L+\epsilon_R)\Big[&\bar{\tau}\gamma_\mu(1-\gamma_5)\nu_\ell \cdot \bar{u}[\gamma^\mu - (1-2\hat{\epsilon}_R)\gamma^\mu\gamma_5]s\\
&+ \bar{\tau}(1-\gamma_5)\nu_\ell \cdot \bar{u}[\hat{\epsilon}_s - \hat{\epsilon}_p\gamma_5]s + 2\hat{\epsilon}_T \bar{\tau}\sigma_{\mu\nu}(1-\gamma_5)\nu_\ell \cdot \bar{u}\sigma^{\mu\nu}s\Big] + \text{h.c.}\,,
\end{aligned} \tag{3.13}$$

where: $\epsilon_{L,R} = v_{L,R}$, $\epsilon_s = s_L + s_R$, $\epsilon_p = s_L - s_R$, and $\epsilon_T = t_L$. In eq. (3.13) we have particularized the Lagrangian for the tau lepton case ($\ell = \tau$), and we have also introduced the convenient notation $\hat{\epsilon}_i = \epsilon_i/(1 + \epsilon_L + \epsilon_R)$ [126] for $i = R, S, P, T$ [4]. In this way, our Lagrangian in eq. (3.13) is equivalent to the one in eq. (9) of Ref. [101] working at linear order in the epsilon Wilson coefficients.

3.4 Semileptonic τ decay amplitude

In this section we calculate the decay amplitudes corresponding to the $\tau^- \to \bar{K}^0\pi^-\nu_\tau$ and the $\tau^- \to K^-\pi^0\nu_\tau$ decays. The first thing to note is that due to the parity of pseudoscalar mesons, only the vector, scalar and tensor currents give a non-zero contribution to the decay amplitude (see appendix B for a general discussion of hadronic matrix elements), as shown in the following equation [5] [6]

$$\begin{aligned}\mathcal{M} =& \mathcal{M}_V + \mathcal{M}_S + \mathcal{M}_T \\ =& \frac{G_F V_{us}\sqrt{S_{EW}}}{\sqrt{2}}(1 + \epsilon_L + \epsilon_R)[L_\mu H^\mu + \hat{\epsilon}_S L H + 2\hat{\epsilon_T} L_{\mu\nu} H^{\mu\nu}]\,,\end{aligned} \tag{3.14}$$

where the leptonic currents have the following structure (p and p' are the momenta of the tau lepton and its neutrino, respectively),

$$\begin{aligned} L_\mu &= \bar{u}(p^{'})\gamma_\mu(1 - \gamma_5)u(p)\,, \\ L &= \bar{u}(p^{'})(1 + \gamma_5)u(p)\,, \\ L_{\mu\nu} &= \bar{u}(p^{'})\sigma_{\mu\nu}(1 + \gamma_5)u(p)\,, \end{aligned} \tag{3.15}$$

and the vector, scalar and tensor hadronic matrix elements for the case of the $\tau^- \to \bar{K}^0\pi^-\nu_\tau$ decay, are defined as follows

$$H^\mu = \langle \pi^- \bar{K}^0 | \bar{s}\gamma^\mu u | 0\rangle = Q^\mu F_+(s) + \frac{\Delta_{K\pi}}{s} q^\mu F_0(s)\,, \tag{3.16}$$

[4] We note that this reshuffling is not convenient when comparing neutral and charged current processes and also when analyzing different semileptonic tau decays with an odd and an even number of pseudoscalar mesons, respectively [128]. Since $\epsilon_i = \hat{\epsilon}_i$ at linear order in these coefficients, we may use ϵ_i instead of $\hat{\epsilon}_i$ when comparing to works which use the former instead of the latter.

[5] Eq.(3.14) displays clearly that the renormalization scale dependence of the Wilson coefficients $\hat{\epsilon}_i$ needs to be cancelled by the one of the hadron matrix elements. As it is conventional, both are defined in the $\overline{MS}$ scheme at $\mu = 2$ GeV.

[6] For convenience, the short-distance electroweak correction factor S_{EW} [7, 8, 9, 10, 11, 12, 13, 14] is written as an overall constant, although it only affects the SM contribution. The error of this simplification is negligible working at leading order in the $\hat{\epsilon}_i$ coefficients [126, 127].

$$H = \langle \pi^- \bar{K}^0 | \bar{s} u | 0 \rangle = F_S(s)\,, \tag{3.17}$$

$$H^{\mu\nu} = \langle \pi^- \bar{K}^0 | \bar{s} \sigma^{\mu\nu} u | 0 \rangle = i F_T(s) (p_K^\mu p_\pi^\nu - p_\pi^\mu p_K^\nu)\,, \tag{3.18}$$

where $q^\mu = (p_\pi + p_K)^\mu$, $Q^\mu = (p_K - p_\pi)^\mu - \frac{\Delta_{K\pi}}{s} q^\mu$, $s = q^2$, and $\Delta_{ij} = m_i^2 - m_j^2$.

The hadron matrix elements H, H^μ and $H^{\mu\nu}$ were decomposed in terms of the allowed Lorentz structures, taking into account the discrete symmetries of the strong interactions, and a number of scalar functions of the invariant mass of the $K\pi$ system: the $F_S(s)$, $F_+(s)$, $F_0(s)$ and $F_T(s)$ form factors; which encode the details of the hadronization process.

The $\tau^- \to K^- \pi^0 \nu_\tau$ decay is completely analogous. Neglecting (tiny) isospin corrections, the only difference is given by the Clebsch-Gordan flavor symmetry factor of $\sqrt{2}$ between both decay channels, that is $\sqrt{2} F_{0,+,T}^{K^-\pi^0}(s) = F_{0,+,T}^{\bar{K}^0\pi^-}(s)$.

From equations (3.15) one can easily see that the vector and the scalar currents are related through the Dirac equation, to see this, let us multiply the leptonic vector current by q^μ

$$\begin{aligned} q^\mu L_\mu &= q^\mu \bar{u}(p') \gamma_\mu (1 - \gamma^5) u(p) \\ &= (p_\tau - p_\nu) \bar{u}(p') \gamma_\mu (1 - \gamma^5) u(p) \\ &= \bar{u}(p') (\not{p}_\tau - \not{p}_\nu)(1 - \gamma^5) u(p) \\ &= \bar{u}(p') (1 + \gamma^5) M_\tau u(p)\,, \end{aligned} \tag{3.19}$$

therefore, we find the following relation

$$L = \frac{L_\mu q^\mu}{M_\tau}\,. \tag{3.20}$$

Similarly, one can find a relation between the vector and the scalar hadronic matrix elements by taking the four-divergence of equation (3.16). This yields

$$F_S(s) = \frac{\Delta_{K\pi}}{m_s - m_u} F_0(s)\,. \tag{3.21}$$

Taking into account the previous two equations, we conclude that the scalar and vector contributions in eq. (3.14) can be treated jointly by doing the convenient replacement

$$\frac{\Delta_{K\pi}}{s} \to \frac{\Delta_{K\pi}}{s} \left[1 + \frac{s \hat{\epsilon}_s}{M_\tau (m_s - m_u)} \right]\,. \tag{3.22}$$

Obtaining the three independent form factors ($F_0(s)$, $F_+(s)$ and $F_T(s)$) using as much experimental and theoretical knowledge as possible is the subject of the next section.

3.5 Hadronization of the scalar, vector and tensor currents

In this section we study in detail the scalar, vector and tensor form factors. These are crucial in this work since they are needed SM inputs for binding the non-standard interactions. Therefore, it is fundamental to obtain them reliably (including associated errors) in order to have precise NP limits. We calculate the form factors using chiral perturbation theory, dispersion relations and lattice data. For the scalar and vector form factors this approach is discussed in refs. [116, 117, 121, 124]. We construct the tensor form factor following ref. [127] where an analogue work for the $\tau^- \to \pi^-\pi^0\nu_\tau$ channel was done. This tensor form factor is very special in this work, as we will see, it is connected with the A_{CP} observable that we introduced in section 4.2 and that we will study in much more detail in section 4.6. In appendix C you can find more information about all the form factors that we will discuss in the text.

We will start our discussion with a brief reminder of the approach employed for the scalar form factor, $F_0(s)$. In a series of papers [125, 124, 140, 141, 142] an analysis for meson-meson scattering within Chiral Perturbation Theory with resonances for strangeness-changing coupled-channels was carried out and very precise information on the corresponding scalar form factors, light quark masses and related chiral low-energy constants was obtained. We benefit from that analysis here [7]. In particular, we employ the update presented in Ref. [142] for the dispersive representation of the $K\pi$ channel, together with its corresponding uncertainties [8].

Now we will discuss the vector form factor $F_+(s)$. In refs. [116, 117, 121], a dispersion relation for $F_+(s)$ was formulated and it was seen that a thrice-subtracted dispersion relation was optimal:

$$F_+(s) = \exp\left[\alpha_1 s + \frac{\alpha_2}{2}s^2 + \int_{s_{\pi K}}^{\infty} ds' \frac{\delta_1^{1/2}(s)}{(s')^3(s'-s-i\epsilon)}\right], \tag{3.23}$$

where α_1, α_2, and the one to set $F_+(0) = 1$ are the three subtraction constants, and $s_{\pi K} = (m_{\bar{K}^0} + m_{\pi^-})^2$. Eq. (3.23) shows that each additional subtraction in the dispersion relation gives rise to a further suppression fac-

[7] We thank Matthias Jamin for providing us with these data.

[8] For the analysis of the $K\pi$ spectra near threshold it is particularly important to employ a scalar form factor that is consistent with the information coming from S-wave $K\pi$ scattering (including the coupled channels $K\eta$ and $K\eta'$). The scalar form factor obtained in Ref. [142] is included in the RChL version of TAUOLA [90], but not in other releases.

tor $1/s^{'}$ in the integrand, enhancing the relative importance of the low-energy input.

In eq. (3.23) Watson's final-state interactions theorem [143] was used. It states that below inelasticities the phase of the form factor equals the scattering phase of the Kπ system ($\delta_1^{1/2}(s)$ in this case, as it has spin one and isospin one half). For this decay channel, departures are expected above $(m_K + m_\eta)^2 \sim 1.022$ GeV^2. These are accounted for in the analyses cited above and are included in our study. We consider as reference input the results obtained in section 3 of Ref. [117] (without using constraints from Kaon decays [117, 118] or information from $\tau^- \to K^-\eta\nu_\tau$ decays [144, 121]). The corresponding systematic and statistical errors of $F_+(s)$ that we use can be traced back to the results in Table 1 of Ref. [117]: the (correlated) statistical errors of the fitted parameters characterizing $F_+(s)$ are those coming from the fit and given in this table and the systematic errors are estimated from the differences induced by changing s_{cut} between the different columns of that table for a given $F_0(s)$. The phase $\delta_1^{1/2}(s)$ is confronted to data in Fig. 2 of Ref. [117]. The fine agreement of $|F_+(s)|$ with the corresponding measurements can be appreciated in various plots of the papers quoted above.

To finish this section, we study the hadronization of the tensor current, which was presented in equation (3.18). We will start with the calculation of this matrix element using Chiral Perturbation Theory. This will give us its normalization at zero-momentum transfer (equivalently, it will fix the first –and only in this case– subtraction constant). The energy dependence will be obtained solving numerically the dispersion relation, where the input phase corresponds to the one of the vector form factor in the elastic region [101].

The appropriate effective Lagrangian according to Ref. [66] is shown in the following equation,

$$\mathcal{L} = \Lambda_1 \langle t_+^{\mu\nu} f_{+\mu\nu} \rangle - i\Lambda_2 \langle t_+^{\mu\nu} u_\mu u_\nu \rangle + \dots , \tag{3.24}$$

where $t_+^{\mu\nu} = u^\dagger t^{\mu\nu} u^\dagger + u t^{\mu\nu\dagger} u$, and $u_\mu = i[u^\dagger(\partial_\mu - ir_\mu)u - u(\partial_\mu - i\ell_\mu)u^\dagger]$. The non-linear representation of the pseudo-Goldstone bosons is $u = \exp\left(\frac{i}{\sqrt{2}F}\phi\right)$ where F is the pion decay constant in the chiral limit, and ℓ_μ and r_μ are left- and right-handed sources (also appearing in the operator with coefficient Λ_1 through $f_+^{\mu\nu} = u F_L^{\mu\nu} u^\dagger + u^\dagger F_R^{\mu\nu} u$ via the familiar field-strength tensors $F_{L,R}^{\mu\nu}$). The symbol $\langle ... \rangle$ denotes a trace in flavour space. The Λ_i are (real) low-energy constants which cannot be fixed by symmetries alone.
The explicit form of ϕ is given as follows:

$$\phi = \begin{pmatrix} \frac{\pi^0+\eta_q}{\sqrt{2}} & \pi^+ & K^+ \\ \pi^- & \frac{-\pi^0+\eta_q}{\sqrt{2}} & K^0 \\ K^- & \bar{K}^0 & \eta_s \end{pmatrix} , \tag{3.25}$$

where η_q and η_s are the non-strange and strange components of the $\eta - \eta'$ mesons (see e. g. eqs. (9) and (10) in ref. [96] and related discussion, we have used the excellent approximation $\pi^3 \sim \pi^0$ which comes from neglecting the isospin-suppressed mixing of the neutral pion with the $\eta - \eta'$ mesons [145]). At the quark level (with corresponding field ψ), the tensor current has the form $\bar{\psi}\sigma_{\mu\nu}\bar{t}^{\mu\nu}\psi$, where according to Ref. [66] and as we have discussed in chapter 2, the tensor source ($\bar{t}^{\mu\nu}$) is related to its chiral projections ($t^{\mu\nu}$ and $t^{\mu\nu\,\dagger}$) by means of

$$t^{\mu\nu} = P_L^{\mu\nu\lambda\rho}\bar{t}_{\lambda\rho}, \quad 4P_L^{\mu\nu\lambda\rho} = (g^{\mu\lambda}g^{\nu\rho} - g^{\mu\rho}g^{\nu\lambda} + i\epsilon^{\mu\nu\lambda\rho}) . \tag{3.26}$$

Now let us compute the functional derivative of eq. (3.24) with respect to $\bar{t}_{\alpha\beta}$. The first thing to note is that only the operator with coefficient Λ_2 contributes to the decays we are analyzing,

$$\frac{\delta\mathcal{L}}{\delta\bar{t}_{\alpha\beta}} = -i\Lambda_2\frac{\delta}{\delta\bar{t}_{\alpha\beta}}\langle t_+^{\mu\nu}u_\mu u_\nu\rangle . \tag{3.27}$$

Putting the left and right sources to zero, expanding u in powers of ϕ and using the first of eqs. (3.26) we obtain,

$$\frac{\delta\mathcal{L}}{\delta\bar{t}_{\alpha\beta}} = \frac{-2i\Lambda_2}{F^2}\frac{\delta}{\delta\bar{t}_{\alpha\beta}}\left[\left(P_L^{\mu\nu\lambda\rho}\bar{t}_{\lambda\rho} + \bar{t}_{\lambda\rho}P_R^{\mu\nu\lambda\rho}\right)\partial_\mu\phi\partial_\nu\phi\right] = -\frac{i\Lambda_2}{F^2}[\partial^\alpha\phi, \partial^\beta\phi] . \tag{3.28}$$

In the calculation of the matrix element $i\langle\pi^0K^-|\frac{\partial\mathcal{L}}{\partial\bar{t}_{\alpha\beta}}|0\rangle$ we need the element $(1,3)$ of the previous matrix, which yields:

$$i\left\langle\pi^0K^-\left|\frac{\delta\mathcal{L}}{\delta\bar{t}_{\alpha\beta}}\right|0\right\rangle = \frac{\Lambda_2}{\sqrt{2}F^2}\left(p_K^\alpha p_0^\beta - p_0^\alpha p_K^\beta\right) . \tag{3.29}$$

From the same matrix element we obtain:

$$i\left\langle\pi^-\bar{K}^0\left|\frac{\delta\mathcal{L}}{\delta\bar{t}_{\alpha\beta}}\right|0\right\rangle = \frac{\Lambda_2}{F^2}\left(p_K^\alpha p_-^\beta - p_-^\alpha p_K^\beta\right) , \tag{3.30}$$

which checks explicitly the relative factor of $\frac{1}{\sqrt{2}}$ between the matrix elements for both decay channels.

As anticipated earlier, the value of Λ_2 is not restricted by symmetry requirements and cannot be fixed from phenomenology. Fortunately, the lattice

QCD evaluation of Ref. [146] found $f_T^{\bar{K}^0\pi^-}(0) = 0.417(15)$. This, together with the fact that $F_T^{\bar{K}^0\pi^-}(0) = \frac{\Lambda_2}{F^2}$ implies that $\Lambda_2 = (11.1 \pm 0.4)$ MeV, that we will use in our numerical analysis. This value is consistent within one sigma with the one employed in Ref. [127] for the $\pi\pi$ channel.
Unlike the vector and scalar form factor cases, there is no experimental data that can help us constructing $F_T(s)$ so that we must rely only on theory.
We calculate the energy-dependence of the tensor form factor $F_T(s)$ using again a phase dispersive representation as it is shown in refs. [101] and [127];

$$\frac{F_T(s)}{F_T(0)} = \exp\left[\frac{s}{\pi}\int_{s_{\pi K}}^{\infty} ds^{'}\,\frac{\delta_T(s^{'})}{s^{'}(s^{'}-s-i\epsilon)}\right]\,, \tag{3.31}$$

where $F_T^{\bar{K}^0\pi^-}(0) = \Lambda_2/F^2$ was calculated previously at leading order in the χPT framework (see eq. (4.17)), and $s_{\pi K} = (m_{\bar{K}^0} + m_{\pi^-})^2$. As in the scalar case we have included one subtraction. In this case it is clear, that lacking precise low-energy information, we cannot increase the number of subtractions of $F_T(s)$. This, in turn, implies a sizable sensitivity to the upper limit of the integral that is used numerically (s_{cut}), which is illustrated in our figure 3.1, where we consider the cases $s_{cut} = M_\tau^2, 4, 9$ GeV^2 [127] [9]. We take the differences between these curves as an estimate of our systematic theoretical error on $F_T(s)/F_T(0)$. In the right panel of figure 3.1 we show the tensor form factor phase corresponding to $\delta_T(s) = \delta_+(s)$, with $\delta_+(s)$ from the fits in table 1 of Ref. [117]. In the inelastic region, our curve plotted for $\delta_T(s)$ lies within the error band shown in figure 2 of Ref. [101] [10]. It is, however, important to note –for computing the CP asymmetry later on– that our phase $\delta_+(s)$ does not have a monotonous energy-dependence in this region, as opposed to the curve in the middle of the uncertainty band for $\delta_T(s)$ plotted in figure 2 of Ref. [101]. This oscillation of the phase is unambiguous theoretically (as indicated, e. g., by the error band in figure 2 of Ref. [116]) and is supported by LASS data [148] (although the corresponding errors are quite large). The data from Estabrooks *et al.* [149] are not conclusive in this respect, as there are only a couple of points in the region of interest.

The phases of $F_T(s)$ and $F_+(s)$ can be related as shown in Ref. [101]. We will not repeat their argument here, but only quote their main result: in the elastic region, $\delta_T(s) = \delta_+(s) = \delta_1^{1/2}(s)$. We will also estimate violations of this equation in the inelastic region (with their corresponding uncertainties) following again Ref. [101] (see figure 2 in that reference).

[9] In principle, one could try to reduce this sensitivity following the strategies employed in Ref. [147], but the procedure will again be limited in this case by the absence of measurements sensitive to $F_T(s)$.

[10] Our phase is given in degrees while theirs is in radians.

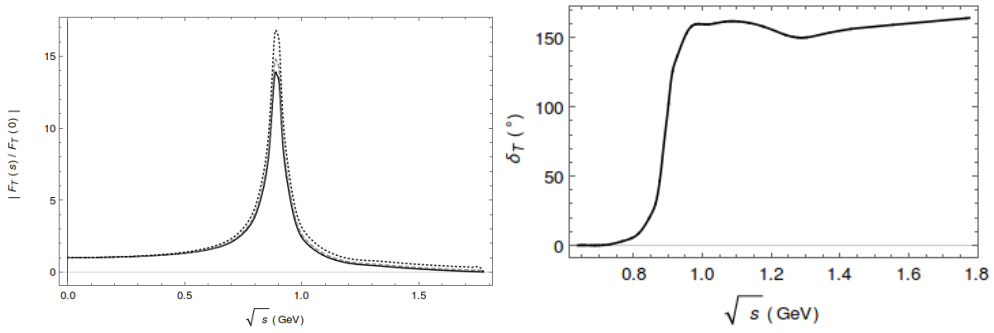

Figure 3.1: Modulus and phase, $|F_T(s)|$ (left) and $\delta_T(s) = \delta_+(s)$ (right), of the tensor form factor, $F_T(s)$. On the left plot, the dotted line corresponds to $s_{cut} = 9$ GeV^2, the dashed one to $s_{cut} = 4$ GeV^2, and the solid one to $s_{cut} = M_\tau^2$.

3.6 Decay observables

In the rest frame of the τ lepton, the doubly differential decay width for the $\tau^- \to K_S\pi^-\nu_\tau$ process is

$$\frac{d^2\Gamma}{dsdt} = \frac{1}{32(2\pi)^3 M_\tau^3}\overline{|\mathcal{M}|^2}\,, \tag{3.32}$$

where $\overline{|\mathcal{M}|^2}$ is given by eq. (3.43), s is the invariant mass of the $\pi^- K_S$ system taking values in the $(m_{K^0} + m_{\pi^-})^2 \leq s \leq M_\tau^2$ interval, and

$$\begin{aligned} t^{\pm}(s) =& \frac{1}{2s}\Big[2s(M_\tau^2 + m_{K^0}^2 - s) - \left(M_\tau^2 - s\right)\left(s + m_{\pi^-}^2 - m_{K^0}^2\right) \\ & \pm \left(M_\tau^2 - s\right)\sqrt{\lambda(s, m_{\pi^-}^2, m_{K^0}^2)}\Big]\,, \end{aligned} \tag{3.33}$$

with $\lambda(x,y,z) = x^2 + y^2 + z^2 - 2xy - 2xz - 2yz$ being the usual Källen function and $t = (P_\tau - p_\pi)^2$.

3.6.1 Dalitz plots

By combining the equations of section 3.4, we obtain the following form for the amplitude (we will omit from now on the indices identifying the $K_S\pi^-$

charge channel)

$$\begin{aligned}\mathcal{M} =&\frac{G_F}{\sqrt{2}}V_{us}\sqrt{S_{EW}}(1+\epsilon_L+\epsilon_R)\Bigg[\left((p_K-p_\pi)^\mu+\frac{\Delta_{\pi K}}{s}(p_\pi+p_K)^\mu\right)L_\mu F_+(s)\\&+\frac{\Delta_{K\pi}}{s}\left(1+\frac{s\hat{\epsilon}_s}{M_\tau(m_s-m_u)}\right)(p_\pi+p_K)^\mu L_\mu F_0(s)\\&+2i\hat{\epsilon}_T(p_K^\mu p_\pi^\nu-p_\pi^\mu p_K^\nu)L_{\mu\nu}F_T(s)\Bigg]\,.\end{aligned} \tag{3.34}$$

The previous equation can be written as follows:

$$\mathcal{M}=\frac{G_F}{\sqrt{2}}V_{us}\sqrt{S_{EW}}(1+\epsilon_L+\epsilon_R)(M_0+M_++M_T)\,, \tag{3.35}$$

where,

$$\begin{aligned}M_+ &= \left((p_K-p_\pi)^\mu+\frac{\Delta_{\pi K}}{s}(p_\pi+p_K)^\mu\right)L_\mu F_+(s)\,,\\ M_0 &= \frac{\Delta_{K\pi}}{s}\left(1+\frac{s\hat{\epsilon}_s}{M_\tau(m_s-m_u)}\right)(p_\pi+p_K)^\mu L_\mu F_0(s)\,,\\ M_T &= 2i\hat{\epsilon}_T(p_K^\mu p_\pi^\nu-p_\pi^\mu p_K^\nu)L_{\mu\nu}F_T(s)\,.\end{aligned} \tag{3.36}$$

The squared of the amplitude, computed from eq. (3.35), has six (all non-vanishing) contributions: three of them coming from scalar-scalar (M_{00}), vector-vector (M_{++}), and tensor-tensor (M_{TT}) contributions, and the remaining three from interference terms (M_{0+}, M_{0T}, and M_{+T}). Their expressions are

$$\begin{aligned}M_{0+} =&\Big[-2M_\tau^2 Re[F_+(s)F_0^*(s)]\Delta_{K\pi}\left(1+\frac{s\hat{\epsilon}_s}{M_\tau(m_s-m_u)}\right)\\&\times\Big(s(M_\tau^2-s+\Sigma_{K\pi}-2t)+M_\tau^2\Delta_{K\pi}\Big)\Big]\,,\end{aligned} \tag{3.37}$$

$$M_{T+}=-4\hat{\epsilon}_T M_\tau^3 s Re[F_T(s)F_+^*(s)]\left(1-\frac{s}{M_\tau^2}\right)\lambda(s,m_\pi^2,m_K^2)\,, \tag{3.38}$$

$$\begin{aligned}M_{T0} =&4\Delta_{K\pi}\hat{\epsilon}_T M_\tau s Re[F_T(s)F_0^*(s)]\left(1+\frac{s\epsilon_s}{M_\tau(m_s-m_u)}\right)\\&\times\Big[s(M_\tau^2-s+\Sigma_{K\pi}-2t)+M_\tau^2\Delta_{K\pi}\Big]\,,\end{aligned} \tag{3.39}$$

$$M_{00}=(\Delta_{K\pi})^2M_\tau^4\left(1-\frac{s}{M_\tau^2}\right)|F_0(s)|^2\left(1+\frac{s\hat{\epsilon}_s}{M_\tau(m_s-m_u)}\right)^2\,, \tag{3.40}$$

$$M_{++} = |F_+(s)|^2 \Big[M_\tau^4 (s+\Delta_{K\pi})^2 - M_\tau^2 s \big(2\Delta_{K\pi}(-m_K^2 + s + 2t - m_\pi^2) - \Delta_{K\pi}^2 + s(s+4t) \big) + 4m_K^2 s^2 (m_\pi^2 - t) + 4s^2 t (s + t - m_\pi^2) \Big] , \tag{3.41}$$

$$M_{TT} = 4\hat{\epsilon}_T^2 F_T^2 s^2 \Big[m_\pi^4 (M_\tau^2 - s) - 2m_\pi^2 (M_\tau^2 - s)(s + 2t - m_K^2) - m_K^4 (3M_\tau^2 + s) + 2m_K^2 \left((s + M_\tau^2)(s + 2t) - 2M_\tau^4 \right) - s \left((s+2t)^2 - M_\tau^2 (s+4t) \right) \Big] , \tag{3.42}$$

where we have introduced $\Sigma_{K\pi} = m_\pi^2 + m_K^2$.

Taking into account all previous contributions we can finally write the unpolarized spin-averaged squared amplitude as follows

$$\overline{|\mathcal{M}|^2} = G_F^2 |V_{us}|^2 S_{EW} (1 + \epsilon_L + \epsilon_R)^2 (M_{0+} + M_{T+} + M_{T0} + M_{00} + M_{++} + M_{TT}) . \tag{3.43}$$

It is convenient in the study of the Dalitz plots to define the following observable introduced in Ref. [127]

$$\tilde{\Delta}(\hat{\epsilon}_S, \hat{\epsilon}_T) = \frac{\left| \overline{|\mathcal{M}(\hat{\epsilon}_S, \hat{\epsilon}_T)|^2} - \overline{|\mathcal{M}(0,0)|^2} \right|}{\overline{|\mathcal{M}(0,0)|^2}} , \tag{3.44}$$

which is sensitive to the relative difference between the squared matrix element in presence/absence of NP contributions (the SM case corresponds to $\mathcal{M}(0,0)$).

In the left panel of figure 3.2 we show the Dalitz plot for the SM case in the (s,t) variables, and in the left part of figures 3.3 and 3.4 we show the corresponding plots for the values $(\hat{\epsilon}_S = -0.5, \hat{\epsilon}_T = 0)$ and $(\hat{\epsilon}_S = 0, \hat{\epsilon}_T = 0.6)$, respectively. The election of these particular values of the $\hat{\epsilon}_{S,T}$ is discussed in section 5.5.

In the SM plots (figure 3.2) it is clearly appreciated that the dynamics is dominated by the $K^*(892)$ vector resonance but the effect of its excitation $K^*(1410)$ and of the dynamically generated $K_0^*(700)$ [150], of the $K_0^*(1430)$ and heavier states cannot be appreciated from the figure, although it is visible both in $F_+(s)$ and the decay spectrum [116] and in $F_0(s)$ [142], respectively. The left panel of figures 3.3 and 3.4 shows the relative modification of the squared matrix element for non-zero reasonable values of $\hat{\epsilon}_S$ and $\hat{\epsilon}_T$ in the (s,t) plane. Although large variations are seen in a couple of regions close to the border of the Dalitz plot in figure 3.3 (left), these correspond to zones with very suppressed probability, as can be seen in figure 3.2 (left). On the contrary, the regions with larger probability have a small relative change, according to figure 3.3 (left). In figure 3.4 (left) the region with the most

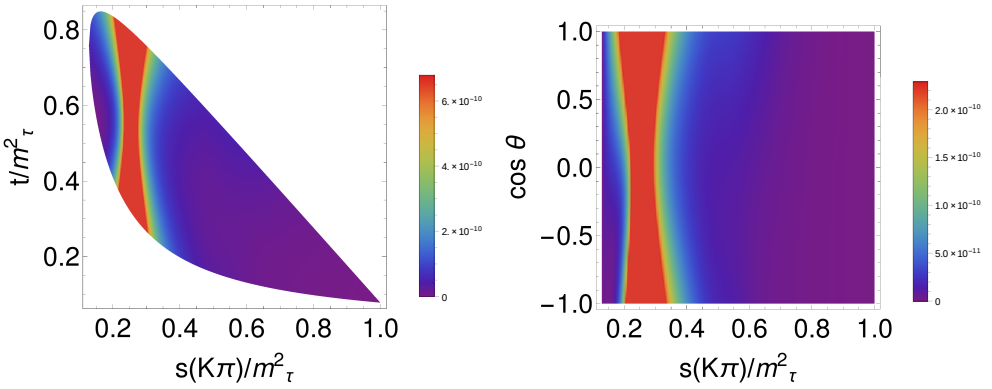

Figure 3.2: Dalitz plot distribution $\overline{|\mathcal{M}|^2}_{00}$ in the SM, eq. (3.43): Differential decay distribution for $\tau^- \to K_S\pi^-\nu_\tau$ in the (s,t) variables (left). The right-hand figure shows the differential decay distribution in the $(s,\cos\theta)$ variables, eq. (3.45). The Mandelstam variables, s and t, are normalized to M_τ^2.

noticeable change (though still smaller than those seen in figure 3.3) is located very close to the s minimum of the Dalitz plot, which has very small probability density in figure 3.2 (left). This region quite overlaps with one of the two mentioned for the fig. 3.3 left plot. Because of this feature, observing a deviation from the SM result in this region could be due to both tensor and non-standard scalar interactions. On the contrary, a deviation in the region of small t values would be signalling spin-zero NP contribution. In any case, changes are very small in the region most densely populated by measured events in both left plots of figs. 3.3 and 3.4. Due to this, we conclude that it will be extremely challenging to identify NP contributions in the (s,t) Dalitz plot even with the large data samples accumulated by the end of operation of Belle-II [18].

3.6.2 Angular distribution

In this section we are going to study the angular dependence of the decay distribution. It is convenient to work in the rest frame of the hadronic system, in which we have $\vec{p}_\pi + \vec{p}_K = \vec{p}_\tau - \vec{p}_\nu = \vec{0}$, consequently the tau lepton and the pion energies are given by $E_\tau = (s + M_\tau^2)/(2\sqrt{s})$ and $E_\pi = (s + m_\pi^2 - m_K^2)/(2\sqrt{s})$.
We will study the decay distribution in terms of the $(s,\cos\theta)$ variables, where θ is the angle between the three-momenta of the pion and the three-momenta of the tau lepton, this angle is related to the invariant t variable by $t = M_\tau^2 + m_\pi^2 - 2E_\tau E_\pi + 2|\vec{p}_\pi||\vec{p}_\tau|\cos\theta$, where $|\vec{p}_\pi| = \sqrt{E_\pi^2 - m_\pi^2}$ and $|\vec{p}_\tau| =$

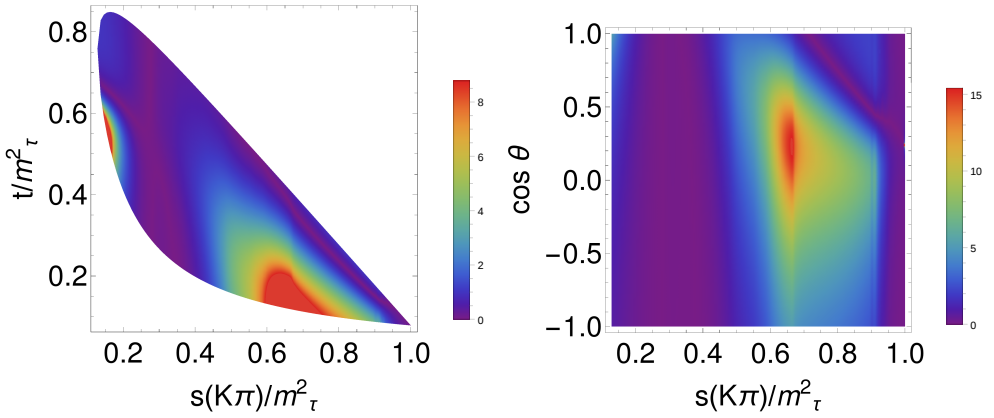

Figure 3.3: Dalitz plot distribution $\tilde{\Delta}(\hat{\epsilon}_S, \hat{\epsilon}_T)$, eq. (3.44), in the $\tau^- \to K_S\pi^-\nu_\tau$ decays: left-hand side corresponds to eq. (3.43) and the right-hand side corresponds to the differential decay distribution in the $(s, \cos\theta)$ variables, eq. (3.45), both with $(\hat{\epsilon}_S = -0.5, \hat{\epsilon}_T = 0)$. The Mandelstam variables, s and t, are normalized to M_τ^2.

$\sqrt{E_\tau^2 - M_\tau^2}$ [11].
Changing variables to $(s, \cos\theta)$ in eq. (3.32) we obtain the following:

$$\frac{d^2\Gamma}{d\sqrt{s}d\cos\theta} = \frac{G_F^2|V_{us}|^2 S_{EW}}{128\pi^3 M_\tau}(1+\epsilon_L+\epsilon_R)^2\left(\frac{M_\tau^2}{s}-1\right)^2|\vec{p}_{\pi^-}|\Bigg\{\Delta_{\pi K}^2|F_0(s)|^2$$

$$\times\left(1+\frac{s\hat{\epsilon}_S}{M_\tau(m_s-m_u)}\right)^2 + 16|\vec{p}_{\pi^-}|^2 s^2\left|-\frac{F_+(s)}{2M_\tau}+\hat{\epsilon}_T F_T(s)\right|^2$$

$$+4|\vec{p}_{\pi^-}|^2 s\left(1-\frac{s}{M_\tau^2}\right)\cos^2\theta\left[|F_+(s)|^2 - 4s\hat{\epsilon}_T^2|F_T(s)|^2\right] + 4\Delta_{\pi K}|\vec{p}_{\pi^-}|\sqrt{s}\cos\theta$$

$$\times\left(1+\frac{s\hat{\epsilon}_S}{M_\tau(m_s-m_u)}\right)\left[-Re\left[F_0(s)F_+^*(s)\right]+\frac{2s\hat{\epsilon}_T}{M_\tau}Re\left[F_T(s)F_0^*(s)\right]\right]\Bigg\}. \tag{3.45}$$

The Dalitz plots for the $(s, \cos\theta)$ variables are shown on the right panels of figures 3.2, 3.3 and 3.4 (in these last two the observable $\tilde{\Delta}(\hat{\epsilon}_S, \hat{\epsilon}_T)$ is plotted).

[11] The tau lifetime and decay width (τ_τ and Γ_τ, respectively) are defined in the τ rest frame. Consequently, their values are boosted in the reference frame considered in this subsection.

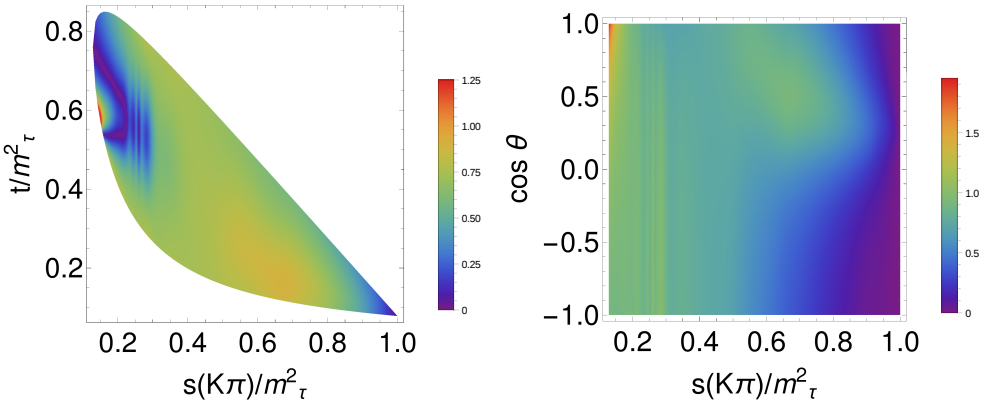

Figure 3.4: Dalitz plot distribution $\tilde{\Delta}(\hat{\epsilon}_S, \hat{\epsilon}_T)$, eq. (3.44), in the $\tau^- \to K_S\pi^-\nu_\tau$ decays: left-hand side corresponds to eq. (3.43) and the right-hand side corresponds to the differential decay distribution in the $(s, \cos\theta)$ variables, eq. (3.45), both with $(\hat{\epsilon}_S = 0, \hat{\epsilon}_T = 0.6)$. The Mandelstam variables, s and t, are normalized to M_τ^2.

On figure 3.2 we plot the SM case, and in figures 3.3 and 3.4 we show Dalitz plots for the values $(\hat{\epsilon}_S = -0.5, \hat{\epsilon}_T = 0)$ and $(\hat{\epsilon}_S = 0, \hat{\epsilon}_T = 0.6)$, respectively. The SM plot gives equivalent information in the $(s, \cos\theta)$ variables as the one seen in the (s, t) variables (right versus left plot of figure 3.2). Comparing both panels of figs. 3.3 one can see that one of the enhanced regions in the (s, t) plot (the one at very low s values) is washed away in the $(s, \cos\theta)$ diagram, while the other is slightly further enhanced in a limited region $(0 \leq \cos\theta \leq 0.5)$. The comparison of the left and right plots of figure 3.4 shows that the enhanced area for large t values is a bit more prominent in the $(s, \cos\theta)$ distribution (for nearly maximal $\cos\theta$) although again it will be very hard to disentangle these possible deviations from the SM patterns in near future data.
Assuming approximate lepton universality, using the bounds from Ref. [134] (obtained analyzing Kaon (semi)leptonic decays) $\hat{\epsilon}_S \sim -8 \times 10^{-4}$, $\hat{\epsilon}_T \sim 6 \times 10^{-3}$ (maximum allowed absolute values at one standard deviation) minimizes the deviations from the SM to unobservable level both in the (s, t) and $(s, \cos\theta)$ Dalitz plots.

3.6.3 Decay rate

Integrating eq. (3.32) upon the t variable we obtain the invariant mass distribution as follows

$$\begin{aligned}\frac{d\Gamma}{ds} =& \frac{G_F^2|V_{us}|^2 M_\tau^3 S_{EW}}{384\pi^3 s}(1+\epsilon_L+\epsilon_R)^2\left(1-\frac{s}{M_\tau^2}\right)^2 \lambda^{1/2}(s,m_\pi^2,m_K^2) \\ &\times\left[X_{VA}+\hat{\epsilon}_S X_S+\hat{\epsilon}_T X_T+\hat{\epsilon}_S^2 X_{S^2}+\hat{\epsilon}_T^2 X_{T^2}\right],\end{aligned} \tag{3.46}$$

where

$$X_{VA} = \frac{1}{2s^2}\left[3|F_0(s)|^2\Delta_{K\pi}^2 + |F_+(s)|^2\left(1+\frac{2s}{M_\tau^2}\right)\lambda(s,m_\pi^2,m_K^2)\right], \tag{3.47a}$$

$$X_S = \frac{3}{sM_\tau}|F_0(s)|^2\frac{\Delta_{K\pi}^2}{m_s-m_d}, \tag{3.47b}$$

$$X_T = \frac{6}{sM_\tau}Re[F_T(s)F_+^*(s)]\lambda(s,m_\pi^2,m_K^2), \tag{3.47c}$$

$$X_{S^2} = \frac{3}{2M_\tau^2}|F_0(s)|^2\frac{\Delta_{K\pi}^2}{(m_s-m_u)^2}, \tag{3.47d}$$

$$X_{T^2} = \frac{4}{s}|F_T(s)|^2\left(1+\frac{s}{2M_\tau^2}\right)\lambda(s,m_\pi^2,m_K^2). \tag{3.47e}$$

Note from the previous equations that the only possible source of CP violation coming from the hadronic part is due to the Vector-Tensor interference, we will comment about this in section 3.7.
In figure 3.5, we plot the invariant mass distribution of the $K\pi$ system for $\tau^- \to K_S\pi^-\nu_\tau$ decays for the SM case and for ($\hat{\epsilon}_S = -0.5$, $\hat{\epsilon}_T = 0$) and ($\hat{\epsilon}_S = 0$, $\hat{\epsilon}_T = 0.6$) which would be realistic values for these couplings, according to their impact on the decay width. Despite the logarithmic scale of the plot, the deviations from the SM curve shown in figure 3.5 are too large when they are confronted with the Belle measurements of this spectrum, as we will see in the fits of section 5.5. This will allow us to set better bounds on $\hat{\epsilon}_{S,T}$ than those used in this subsection.

3.6.4 Forward-backward asymmetry

Now we turn to the study of the forward-backward asymmetry, which is defined in the following way

$$\mathcal{A}_{K\pi}(s) = \frac{\int_0^1 d\cos\theta\frac{d^2\Gamma}{ds d\cos\theta} - \int_{-1}^0 d\cos\theta\frac{d^2\Gamma}{ds d\cos\theta}}{\int_0^1 d\cos\theta\frac{d^2\Gamma}{ds d\cos\theta} + \int_{-1}^0 d\cos\theta\frac{d^2\Gamma}{ds d\cos\theta}}. \tag{3.48}$$

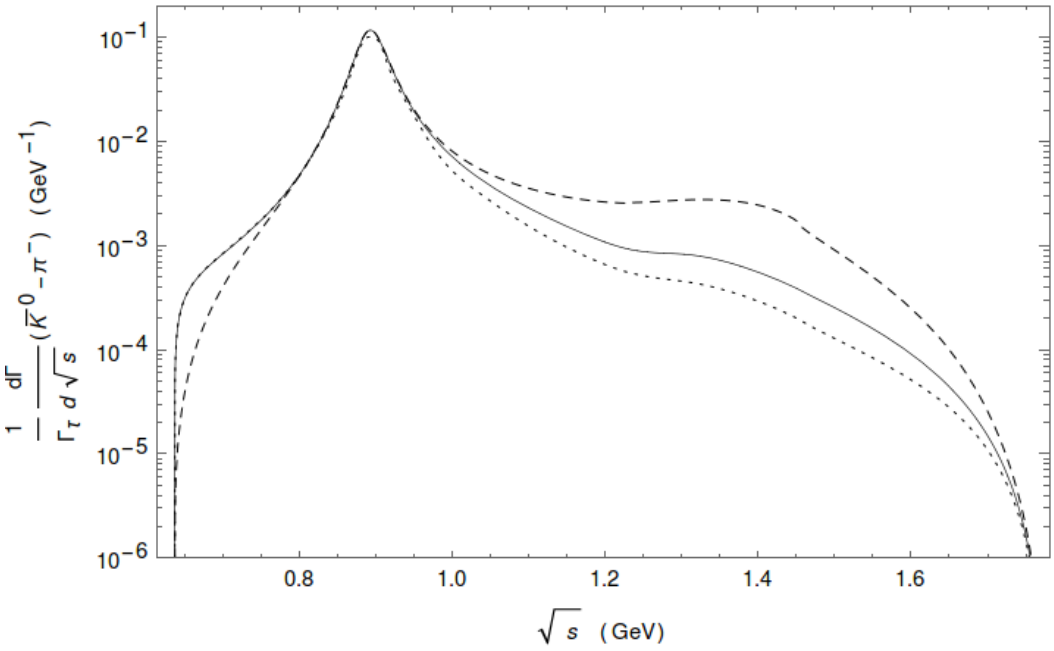

Figure 3.5: The $\bar{K}^0\pi^-$ hadronic invariant mass distribution for the SM (solid line) and $\hat{\epsilon}_S = -0.5$, $\hat{\epsilon}_T = 0$ (dashed line) and $\hat{\epsilon}_S = 0$, $\hat{\epsilon}_T = 0.6$ (dotted line). The decay distributions are normalized to the tau decay width.

We find the analytical expression for this observable substituting eq. (3.45) into eq. (3.48) and integrating upon the cosθ variable with the following result [12]

$$\mathcal{A}_{K\pi} = \frac{3\sqrt{\lambda(s,m_\pi^2,m_K^2)}}{2s^2[X_{VA}+\hat{\epsilon}_S X_S+\hat{\epsilon}_T X_T+\hat{\epsilon}_S^2 X_{S^2}+\hat{\epsilon}_T^2 X_{T^2}]}\left(1+\frac{s\hat{\epsilon}_S}{M_\tau(m_s-m_u)}\right)\Delta_{\pi K} \times\left[-Re[F_0(s)F_+^*(s)]+\frac{2s\hat{\epsilon}_T}{M_\tau}Re[F_T(s)F_0^*(s)]\right]. \tag{3.49}$$

Before studying the forward-backward asymmetry in the general case, it is important to study its behaviour in the standard model case. If we set $\epsilon_R = \epsilon_L = \hat{\epsilon}_S = \hat{\epsilon}_T = 0$ we get the SM forward-backward asymmetry, which is plotted in the solid line of figure 3.6.

The important thing to note from the SM result in figure 3.6 (solid line) is that the graph is peaked around $\sqrt{s} \sim 0.6$ GeV so that this is an important region to analyze and pay special attention. It was already emphasized

[12] In eq. (3.49) we use $\mathcal{A}_{K\pi}$ to emphasize the decay channel under consideration to distinguish it to the other two-meson decay modes. Otherwise we will also be using the most common notation A_{FB} for this observable.

long ago that a measurement of the forward-backward asymmetry in this decay channel would be crucial in improving our knowledge of both vector and scalar form factors [151] [13].

For the more general case where we include NP interactions, we have figure 3.6, where we plot $\mathcal{A}_{K\pi}$ for the values ($\hat{\epsilon}_S = -0.5$, $\hat{\epsilon}_T = 0$) and ($\hat{\epsilon}_S = 0$, $\hat{\epsilon}_T = 0.6$) [14], and we compare those plots with the SM case. There we can see that for quite large $\hat{\epsilon}_T$ values some difference is appreciated for the tensor case; otherwise it may not be possible to disentangle it from the standard contribution. Conversely, for non-standard scalar interactions the changes are more noticeable since $A_{K\pi}$ flips sign with respect to the SM. Note also that for scalar interactions the value of $A_{K\pi}$ gets smaller in magnitude as s increases. If it is possible to measure $A_{K\pi}$ in a low-energy bin, this would ease the identification of this type of NP in $A_{K\pi}$.

If we make the comparison with more realistic limits for the NP values [134] (under the assumption of approximate lepton universality), it is impossible to identify any departures from the SM prediction in this observable. For this reason, we make use of the following convenient definition introduced in Ref. [127]

$$\Delta\mathcal{A}_{K\pi} = \mathcal{A}_{K\pi}(s, \hat{\epsilon}_S, \hat{\epsilon}_T) - \mathcal{A}_{K\pi}(s, 0, 0)\,. \tag{3.50}$$

The corresponding (unmeasurably small) deviations from the SM result are plotted in figure 3.7.

3.6.5 Limits on $\hat{\epsilon}_S$ and $\hat{\epsilon}_T$

Our purpose in this section is to set bounds on the effective couplings $\hat{\epsilon}_S$ and $\hat{\epsilon}_T$. We achieve this by comparing the total width Γ (which depends explicitly on the NP couplings $\hat{\epsilon}_S$ and $\hat{\epsilon}_T$) with the SM width Γ^0 (obtained by neglecting NP interactions which we get by setting $\hat{\epsilon}_S = \hat{\epsilon}_T = 0$). This comparison is conveniently implemented with the introduction of the observable Δ which we define as follows

$$\Delta \equiv \frac{\Gamma - \Gamma^0}{\Gamma^0} = \alpha\hat{\epsilon}_S + \beta\hat{\epsilon}_T + \gamma\hat{\epsilon}_S^2 + \delta\hat{\epsilon}_T^2\,, \tag{3.51}$$

where we obtained the following results for the coefficients: $\alpha \in [0.30, 0.34]$, $\beta \in [-2.92, -2.35]$, $\gamma \in [0.95, 1.13]$ and $\delta \in [3.57, 5.45]$.

[13] We note that in this reference, and also later on in Refs. [152, 119], the angle θ used to compute A_{FB} is defined between the three-momenta of the tau lepton and the K_S in the di-meson rest frame. Taking into account the different sign conventions, it can be checked there is reasonable agreement with these works in the elastic region.

[14] Again, as we mentioned when we discussed the Dalitz plots, we will justify the use of these particular values in the next section.

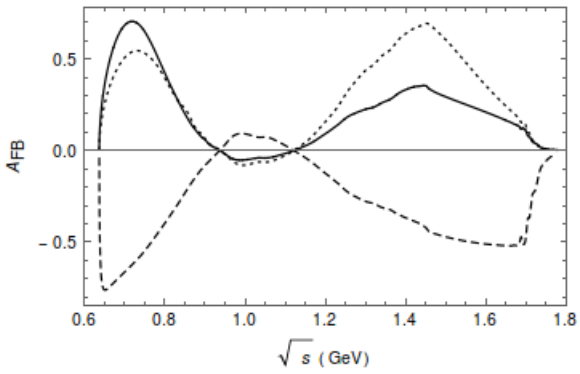

Figure 3.6: Forward-backward asymmetry in $\tau^- \to K_S\pi^-\nu_\tau$ decays compared with the SM prediction (solid line). The dashed line corresponds to $\hat{\epsilon}_S = -0.5$, $\hat{\epsilon}_T = 0$, and the dotted line corresponds to $\hat{\epsilon}_S = 0$, $\hat{\epsilon}_T = 0.6$.

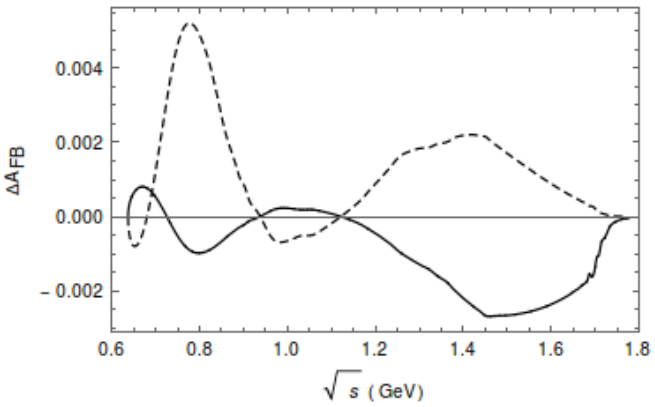

Figure 3.7: Deviations from the SM forward-backward asymmetry, $\Delta\mathcal{A}_{K\pi}$, in $\tau^- \to K_S\pi^-\nu_\tau$ decays using the bounds from Ref. [134]. The solid line corresponds to $\hat{\epsilon}_S = -8 \times 10^{-4}$, $\hat{\epsilon}_T = 0$ and the dashed line to $\hat{\epsilon}_S = 0$, $\hat{\epsilon}_T = 6 \times 10^{-3}$.

With the help of the Δ observable we obtain our limits for the $\hat{\epsilon}_S$ and $\hat{\epsilon}_T$ couplings in two different ways. First, we set one of the couplings to zero and obtain bounds for the other, and viceversa. This process gives us the two parabolas shown in figure 3.8.

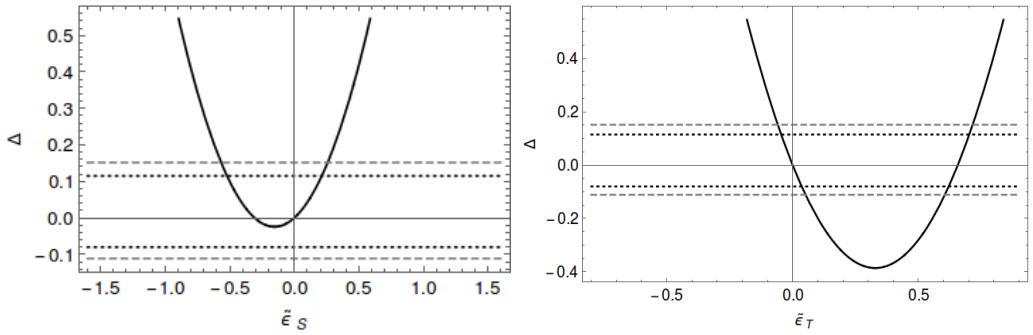

Figure 3.8: Δ as a function of $\hat{\epsilon}_S$ for $\hat{\epsilon}_T = 0$ (left hand) and of $\hat{\epsilon}_T$ for $\hat{\epsilon}_S = 0$ (right hand) for $\tau^- \to K_S\pi^-\nu_\tau$ decays. Horizontal lines represent the values of Δ according to the current measurement and theory errors (at three standard deviations) of the branching ratio (dashed line) and in the hypothetical case where the measured branching ratio at Belle-II has a three times reduced uncertainty (dotted line).

The second way in which we set constraints is again using Eq. (3.51), but now taking the general case where both couplings are non-vanishing. In this case we obtain the ellipse shown in figure 3.9.

For the convenience of the reader we summarize our findings for the constraints in the following table.

Δ limits	$\hat{\epsilon}_S(\hat{\epsilon}_T = 0)$	$\hat{\epsilon}_T(\hat{\epsilon}_S = 0)$	$\hat{\epsilon}_S$	$\hat{\epsilon}_T$
Current bounds	$[-0.57, 0.27]$	$[-0.059, 0.052] \cup [0.60, 0.72]$	$[-0.89, 0.58]$	$[-0.07, 0.72]$
Future bounds	$[-0.52, 0.22]$	$[-0.047, 0.036] \cup [0.62, 0.71]$	$[-0.87, 0.56]$	$[-0.06, 0.71]$

Table 3.1: Constraints on the scalar and tensor couplings obtained through the limits on the current branching ratio at three standard deviations using the current theory and experimental errors and assuming the latter be reduced to a third ('Future bounds'). This last case should be taken only as illustrative of the improvement that can be achieved thanks to higher-statistics measurements, even in absence of any progress on the theory side. It is clear that the knowledge of $\hat{\epsilon}_{S,T}$ using $\tau^- \to K_S\pi^-\nu_\tau$ decays data is limited by theory uncertainties.

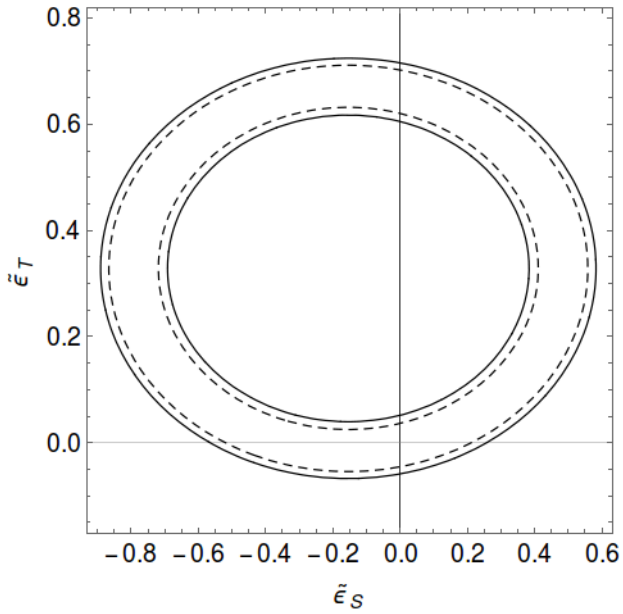

Figure 3.9: Constraints on the scalar and tensor couplings obtained from $\Delta(\tau^- \to K_S\pi^-\nu_\tau)$ using theory and the measured value reported in the PDG, with their corresponding uncertainties at three standard deviations (solid line). The dashed line ellipse corresponds to the case where the measurements error was reduced to a third of the current uncertainty.

Next we will consider fits to the branching ratio and decay spectrum [15] of the $\tau^- \to K_S\pi^-\nu_\tau$ decays as measured by Belle [103]. We will pay special attention to the possible explanation of the conflicting data points (bins 5, 6 and 7) by the non-standard interactions. Therefore, we will consider fits with and without these data points. In all our fits, as explained e. g. in Ref. [121], we will not consider the first data point (as it lies below the threshold for physical K_S and π^- masses) and will disregard the data from the last 10 bins, as suggested by the Belle collaboration.
The χ^2 function minimized in our fits is

$$\sum_i \left(\frac{\mathcal{N}_i^{exp} - \mathcal{N}_i^{th}}{\sigma_{\mathcal{N}_i}}\right)^2 + \left(\frac{BR^{exp} - BR^{th}}{\sigma_{BR}^{exp}}\right)^2 , \tag{3.52}$$

where the sum over the i bins may or may not include the $i = 5, 6, 7$ bins. We will consider the measurement of BR^{exp} reported in the Belle paper [103] (and not the PDG [6] or the HFLAV [153] values), as discussed in Ref. [121]. Along our fits we float the meson form factors within their estimated uncertainty

[15] We thank Denis Epifanov for providing us with these data.

bands and our quoted results take these errors into account. We present our results in table 3.2

Best fit values	$\hat{\epsilon}_S$	$\hat{\epsilon}_T$	χ^2	χ^2 in the SM
Excluding $i = 5, 6, 7$ bins	$(1.3 \pm 0.9) \times 10^{-2}$	$(0.7 \pm 1.0) \times 10^{-2}$	[72, 73]	[74, 77]
Including $i = 5, 6, 7$ bins	$(0.9 \pm 1.0) \times 10^{-2}$	$(1.7 \pm 1.7) \times 10^{-2}$	[83, 86]	[91, 95]

Table 3.2: Best fit values to the Belle spectrum and branching ratio of the $\tau^- \to K_S\pi^-\nu_\tau$ decays [103]. The cases where the $i = 5, 6, 7$ bins are excluded/included are considered. We display the reference results obtained floating $\hat{\epsilon}_S$ and $\hat{\epsilon}_T$ simultaneously. In the last two columns the χ^2 of these fits is compared to the SM result.

3.7 CP violation

The observable A_{CP}, measured by BaBar [102] has the right magnitude but the wrong sign compared with the SM prediction (tiny corrections from direct CP violation are neglected along this section). It is defined as

$$A_{CP} = \frac{\Gamma(\tau^+ \to \pi^+ K_S \bar{\nu}_\tau) - \Gamma(\tau^- \to \pi^- K_S \nu_\tau)}{\Gamma(\tau^+ \to \pi^+ K_S \bar{\nu}_\tau) + \Gamma(\tau^- \to \pi^- K_S \nu_\tau)} \,. \tag{3.53}$$

In the SM, A_{CP} is given by the neutral kaon mixing contribution. Thus, it comes from the analogous asymmetry measured in semileptonic kaon decays [101] ($\ell = e,\, \mu$)

$$\frac{\Gamma(K_L \to \pi^- \ell^+ \nu_\ell) - \Gamma(K_L \to \pi^+ \ell^- \bar{\nu}_\ell)}{\Gamma(K_L \to \pi^- \ell^+ \nu_\ell) + \Gamma(K_L \to \pi^+ \ell^- \bar{\nu}_\ell)} = 3.32(6) \times 10^{-3} \,, \tag{3.54}$$

up to small corrections caused by the fact that the K_S is reconstructed at the B-factories through its $\pi^+\pi^-$ decay mode with a decay time of the order of the K_S lifetime. This changes the previous value to $A_{CP}^{SM} = 3.6(1) \times 10^{-3}$ [109], that is 2.8 σ away from the BaBar measurement, $A_{CP} = -3.6(2.3)(1.1) \times 10^{-3}$.
Ref. [104] shows that beyond the SM (BSM) interactions modify A_{CP} to

$$A_{CP} = \frac{A_{CP}^{SM} + A_{CP}^{BSM}}{1 + A_{CP}^{SM} \times A_{CP}^{BSM}} \,, \tag{3.55}$$

where [101] [16]

$$A_{CP}^{BSM} = \frac{2\sin\delta_T^W |\hat{\epsilon}_T| G_F^2 |V_{us}|^2 S_{EW}}{256\pi^3 M_\tau^2 \Gamma(\tau \to K_S \pi \nu_\tau)} \int_{s_{\pi K}}^{M_\tau^2} \mathrm{d}s |f_+(s)||F_T(s)| \sin\left(\delta_+(s) - \delta_T(s)\right) \frac{\lambda^{3/2}(s, m_\pi^2, m_K^2)(M_\tau^2 - s)^2}{s^2}\,, \quad (3.56)$$

where δ_T^W corresponds to the relative weak phase between the SM (V-A) and the tensor contributions. Ref. [101] uses $SU(2)_L$ invariance of the weak interactions within the EFT to find stringent constraints on $\Im m[\hat{\epsilon}_T]$, using the $D - \bar{D}$ mixing measurements and the upper limit on the electric dipole moment of the neutron. This yields the bound $2\Im m[\hat{\epsilon}_T] < 10^{-5}$, that we will use. To see that δ_T^W is a small parameter, we remind the limits from the global EFT analysis of NP in Kaon (semi)leptonic decays [134], according to which $|\epsilon_T| = (0.5 \pm 5.2) \times 10^{-3}$. Considering this, $\sin\delta_T^W |\hat{\epsilon}_T| \sim \Im m[\hat{\epsilon}_T]$ and the numerical evaluation of eq. (3.56) is straightforward with the inputs at hand.

We have computed eq. (3.56) using $|F_T(s)|$ obtained with $s_{cut} = M_\tau^2, 4, 9$ GeV^2 (shown in the left panel of fig. 1) and with $\delta_T(s)$ varying (smoothly) within the band shown in fig. 2 of Ref. [101], as we agree with the estimation of this uncertainty [17]. The errors on $|F_+(s)|$ and $\delta_+(s)$ are negligible compared to the uncertainties on $F_T(s)$. Among these two uncertainties, the error on $\delta_T(s)$ dominates: changing s_{cut} for a given $\delta_T(s)$ can modify A_{CP}^{BSM} by a factor three, at most; while, with a fixed s_{cut}, A_{CP}^{BSM} can be vanishing for $\delta_T(s) \to \delta_+(s)$ also in the inelastic region. In this way, we find

$$A_{CP}^{BSM} < 8 \cdot 10^{-7}\,, \quad (3.57)$$

which is slightly weaker bound than the one reported in Ref. [101]: $A_{CP}^{BSM} < 3 \cdot 10^{-7}$. This small difference comes mainly from our accounting for the variation in s_{cut} and also for the slightly different phase $\delta_+(s)$ in both analyses. In any case, it is clear that heavy BSM interactions can only modify A_{CP} at the 10^{-6} level at most, which is at least three orders of magnitude smaller than the theoretical uncertainty in its prediction (which is, in turn, some 25 times smaller than the error of the BaBar measurement). Therefore, any conclusive anomaly in A_{CP} must be explained outside the framework considered in this paper (and in Ref. [101]); for instance, by BSM effects of very light particles.

[16] We remind that c_T in this reference equals $2\hat{\epsilon}_T$ in our notation.

[17] See also Ref. [154], where NP bounds obtained from $\tau^- \to K^- \nu_\tau$ decays are first discussed.

Chapter 4

Effective-field theory analysis of the $\tau^- \to K^-(\eta^{(\prime)}, K^0)\nu_\tau$ decays

4.1 Summary of the chapter

In this chapter we continue with our studies of semileptonic decays of the Tau lepton into two mesons. We have already studied in detail the strangeness-changing decays $\tau^- \to (K\pi)^-\nu_\tau$ in the previous chapter and we have published those results in Ref. [138]. In chapter 3 we have also mentioned the analogue work for the strangeness-conserving decay $\tau^- \to \pi^-\pi^0\nu_\tau$, which was studied in Ref. [127], and the work [126] where the decays $\tau^- \to \eta^{(\prime)}\pi^-\nu_\tau$ were studied. Here we want to close the circle for these kind of studies into two-meson decays by presenting similar analyses for the decay channels $\tau^- \to K^-(\eta^{(\prime)}, K^0)\nu_\tau$. For this task, we follow the logic of chapter 3, that is, we propose an effective Lagrangian constructed with dimension six operators with the SM degrees of freedom. In particular, we examine different interesting phenomenological observables i.e. decay spectra and branching ratio, Dalitz plot distributions and the forward-backward asymmetry, to explore the sensitivity of the corresponding decays to the effects of non-standard interactions. We also put constraints on the NP effective couplings from each of the decay modes. This has only been possible thanks to the study of the corresponding form factors, which serve as necessary theoretical input for the SM. As in chapter 3, the form factors are constructed based on chiral symmetry, dispersion relations, data and asymptotic QCD properties. Special attention is paid to the tensor form factors. The results of this chapter were published in Ref. [155].

In chapter 5 we will put together all the information of the previous and the present chapters in order to perform a global analysis of exclusive hadronic decays of the tau lepton into two-mesons so that the information presented here will turn out fundamental in what follows.

4.2 Introduction

From our experience with chapter 3 we have learned that tau physics is not only a powerful tool to study QCD at low energies but also an interesting laboratory to study non-standard interactions. This opens a new window that complements other low-energy semileptonic probes considered before, such as nuclear beta decays, semileptonic pion and kaon decays, or hyperon decays, see for example Refs. [49, 129, 130, 131, 132, 133, 134, 135, 50, 136, 137].

We should start by saying that in general we have a good knowledge of tau decays into a pair of pseudoscalar mesons. As we have pointed out in chapter 1, half of the process is purely electroweak, therefore that part is very clean and under good theoretical control. For the other part, which involves the hadronization process, the Standard Model (SM) input is encoded in terms of hadronic form factors. These form factors are obtained with the help of dispersion relations, which incorporate both theoretical calculations and experimental data. For example, the analyses of the decays $\pi^-\pi^0$ [167, 168, 169, 147] and $K_S\pi^-$ [122, 115, 116, 117, 121], carried out by exploiting the synergy between Resonance Chiral Theory [74] and dispersion theory, are found to be in a nice agreement with the rich data provided by the experiments. On the other hand, accord with experimental measurements is also found for the K^-K_S [147] and $K^-\eta$ [144, 121] decay modes, although higher-quality data on these processes is required to constrain the corresponding theories or models.

In contrast to chapters 3 and 5, in this chapter we will not attempt to extract new physics bounds from the corresponding experimental data as competitive as those coming from other low-energy probes, like the ones mentioned before, but rather explore the size of the deviations from the SM predictions that one could expect in these decay channels. We will explore these potential deviations by making use of several observables like Dalitz plots, decay spectra, and forward-backward asymmetries. Having said that, we hope that our paper strengths the case for a (re)analysis, with a larger data sample, of the K^-K^0, K^-K_S and $K^-\eta$ decay spectra and encourage experimental groups to measure the $K^-\eta'$ decay mode. All this should be well within the reach of Belle-II [18], and of other future Z, tau-charm and B-factories where new measurements should be possible.

This chapter is organized in the following way: we first discuss the theoretical framework in section 4.3 where we introduce the effective Lagrangian and discuss the different effective weak currents contributing to the decays. The hadronic matrix elements and form factors are also defined in this section. The latter are the matter subject of section 4.4, where we pay special attention to the tensor form factor. Then, in section 4.5, we discuss different interesting phenomenological observables like Dalitz plot distributions, decay spectra and forward-backward asymmetries. In this section we also find limits for the scalar and tensor NP effective couplings (see section 4.5.5). We will state our conclusions in chapter 6.

4.3 Effective field theory analysis and decay amplitude of $\tau^- \to \nu_\tau \bar{u} D$ $(D = d, s)$

As always, we start with the appropriate effective Lagrangian. The charged-current transitions $\tau^- \to \nu_\tau \bar{u} D$ for strangeness-conserving $(D = d)$ and for strangeness-changing $(D = s)$ modes are mediated by the following effective Lagrangian [126, 127, 138]

$$\begin{aligned}
\mathcal{L}_{CC} &= -\frac{G_F}{\sqrt{2}} V_{uD} (1 + \epsilon_L + \epsilon_R) \big[\bar{\tau} \gamma_\mu (1 - \gamma^5) \nu_\tau \\
&\quad \cdot \bar{u} \big[\gamma^\mu - (1 - 2\hat{\epsilon}_R) \gamma^\mu \gamma^5 \big] D \\
&\quad + \bar{\tau} (1 - \gamma^5) \nu_\tau \, \bar{u} (\hat{\epsilon}_S - \hat{\epsilon}_P \gamma^5) D \\
&\quad + 2\hat{\epsilon}_T \bar{\tau} \sigma_{\mu\nu} (1 - \gamma^5) \nu_\tau \, \bar{u} \sigma^{\mu\nu} D \big] + h.c. \,, \qquad (4.1)
\end{aligned}$$

where G_F is the tree-level definition of the Fermi constant. In eq. (4.1) we have again made use of the convenient definition $\hat{\epsilon}_i = \epsilon_i / (1 + \epsilon_L + \epsilon_R)$ for $i = R, S, P, T$ (see chapter 3). In this chapter we are only interested in CP conserving quantities so that the effective couplings ϵ_i can be taken real.

Now we proceed with the calculation of the amplitude for the process $\tau^- (P) \to K^- (p_K) K^0 (p_{K^0}) \nu_\tau (P')$. As was discussed before, due to the parity of pseudoscalar mesons, only the vector, scalar and tensor currents give a non-zero contribution to the decay amplitude:

$$\begin{aligned}
\mathcal{M} &= \mathcal{M}_V + \mathcal{M}_S + \mathcal{M}_T \\
&= \frac{G_F V_{ud} \sqrt{S_{EW}}}{\sqrt{2}} (1 + \epsilon_L + \epsilon_R) \\
&\quad \times \big[L_\mu H^\mu + \hat{\epsilon}_S L H + 2\hat{\epsilon}_T L_{\mu\nu} H^{\mu\nu} \big] \,, \qquad (4.2)
\end{aligned}$$

where the leptonic currents have the following form

$$L_\mu = \bar{u}(P')\gamma_\mu(1-\gamma^5)u(P)\,, \tag{4.3}$$

$$L = \bar{u}(P')(1+\gamma^5)u(P)\,, \tag{4.4}$$

$$L_{\mu\nu} = \bar{u}(P')\sigma_{\mu\nu}(1+\gamma^5)u(P)\,, \tag{4.5}$$

and where the hadronic matrix elements are given by

$$H = \langle K^-K^0|\bar{d}u|0\rangle = F_S^{K^-K^0}(s)\,, \tag{4.6}$$

$$H^\mu = \langle K^-K^0|\bar{d}\gamma^\mu u|0\rangle = C^V_{K^-K^0}Q^\mu F_+^{K^-K^0}(s) + C^S_{K^-K^0}\left(\frac{\Delta_{KK}}{s}\right)q^\mu F_0^{K^-K^0}(s)\,, \tag{4.7}$$

$$H^{\mu\nu} = \langle K^-K^0|\bar{d}\sigma^{\mu\nu}u|0\rangle = iF_T^{K^-K^0}(s)(p^\mu_{K^0}p^\nu_K - p^\mu_K p^\nu_{K^0})\,, \tag{4.8}$$

in which we have made use of the following definitions:
$q^\mu = (p_K + p_{K^0})^\mu$, $Q^\mu = (p_{K^0} - p_K)^\mu + (\Delta_{KK}/s)q^\mu$, $s = q^2$ and $\Delta_{ij} = m_i^2 - m_j^2$, and with the Clebsch-Gordan coefficients: $C^V_{KK} = -1$ and $C^S_{KK} = -1$.

As it has been pointed out in chapter 3, the hadron matrix elements H, H^μ and $H^{\mu\nu}$ are decomposed in terms of the allowed Lorentz structures and also taking into account the discrete symmetries of the strong interactions. These matrix elements are parametrized in terms of the form factors $F_S^{K^-K^0}(s)$, $F_+^{K^-K^0}(s)$, $F_0^{K^-K^0}(s)$ and $F_T^{K^-K^0}(s)$ which we will discuss in the next section.

Here it is also convenient to use the relation between the form factors $F_S(s)$ and $F_0(s)$ that we have found previously in chapter 3 [1]

$$F_S^{K^-K^0}(s) = \frac{C^S_{KK^0}\Delta_{KK}}{m_d - m_u}F_0^{K^-K^0}(s)\,. \tag{4.9}$$

As in [126, 127, 138], the scalar and vector contributions in Eqs. (4.6) and (4.7), respectively, can be treated jointly by doing the following replacement

$$C^S_{KK^0}\frac{\Delta_{KK}}{s} \to C^S_{KK^0}\frac{\Delta_{KK}}{s}\left(1 + \frac{s\,\hat{\epsilon}_S}{m_\tau(m_d - m_u)}\right)\,, \tag{4.10}$$

in Eq. (4.7).

For the decays $\tau^- \to K^-\eta^{(\prime)}\nu_\tau$, the associated amplitude is that of Eq. (4.2)

[1] Remember that this relation was found by taking the divergence of the vector current Eq. (4.7).

but replacing; $p_{K^0} \to p_{\eta^{(\prime)}}$, $\Delta_{K^-K^0} \to \Delta_{K^-\eta^{(\prime)}}$, $V_{ud} \to V_{us}$ and $m_d \to m_s$ along the lines of the previous equations, and with the Clebsch-Gordan coefficients $C^V_{K\eta^{(\prime)}} = -\sqrt{\frac{3}{2}}$, $C^S_{K\eta} = -\frac{1}{\sqrt{6}}$ and $C^S_{K\eta'} = \frac{2}{\sqrt{3}}$. In this chapter we will not go into much detail in these two strangeness-changing decay modes since I will focus in the strangeness-conserving decay $\tau^- \to K^-K^0\nu_\tau$, but I will present some results for them that we have derived in [155] [2].

4.4 Hadronization of the scalar, vector and tensor currents

In this section we comment very briefly about the vector and the scalar form factors involved in the decay $\tau^- \to K^-K^0\nu_\tau$ and we explain in detail how the corresponding tensor form factor is obtained. We start with the the kaon vector form factor for which we will follow Ref. [147], where a three-times dispersion relation was found to be optimal

$$F_+^{KK}(s) = \exp\left[\tilde{\alpha}_1 s + \frac{\tilde{\alpha}_2}{2}s^2 + \frac{s^3}{\pi}\int_{4m_\pi^2}^{s_{\rm cut}} ds' \frac{\delta_+^{KK}(s)}{(s')^3(s'-s-i0)}\right], \qquad (4.11)$$

where $\tilde{\alpha}_1$ and $\tilde{\alpha}_2$, are two subtraction constants related to the slope and curvature appearing in the low-energy expansion of the form factor of the kaon and $F_+^{KK}(0) = 1$ is the third subtraction constant. To get a model for the form factor phase, $\delta_+^{KK}(s)$ in Eq. (4.11), we adopt the so-called exponential Omnès representation of the form factor [147]:

$$\begin{aligned} f_+^{KK}(s) \;=\; & \frac{M_\rho^2 + s\left(\tilde{\gamma}e^{i\tilde{\phi}_1} + \tilde{\delta}e^{i\tilde{\phi}_2}\right)}{M_\rho^2 - s - iM_\rho\Gamma_\rho(s)} \exp\left\{\mathrm{Re}\left[-\frac{s}{96\pi^2F_\pi^2}\left(A_\pi(s) + \frac{1}{2}A_K(s)\right)\right]\right\} \\ & - \frac{\tilde{\gamma}\, s\, e^{i\tilde{\phi}_1}}{M_{\rho'}^2 - s - iM_{\rho'}\Gamma_{\rho'}(s)} \exp\left\{-\frac{s\Gamma_{\rho'}(M_{\rho'}^2)}{\pi M_{\rho'}^3\sigma_\pi^3(M_{\rho'}^2)}\mathrm{Re}A_\pi(s)\right\} \\ & - \frac{\tilde{\delta}\, s\, e^{i\tilde{\phi}_2}}{M_{\rho''}^2 - s - iM_{\rho''}\Gamma_{\rho''}(s)} \exp\left\{-\frac{s\Gamma_{\rho''}(M_{\rho''}^2)}{\pi M_{\rho''}^3\sigma_\pi^3(M_{\rho''}^2)}\mathrm{Re}A_\pi(s)\right\}. \end{aligned} \qquad (4.12)$$

In Eq. (4.12), the mixing between resonances is taken with respect to the ρ with relative strengths $1, \tilde{\gamma}, \tilde{\delta}$. These parameters are in general complex thus

[2] The decays $\tau^- \to K^-\eta^{(\prime)}\nu_\tau$ are going to be discussed in much more detail in a future thesis presented by Alejandro Miranda.

carrying a phase that is denoted by $\tilde{\phi}_1$ and $\tilde{\phi}_2$, respectively. Taking $\tilde{\gamma}$ and $\tilde{\delta}$ real would demand a perfect knowledge of the amplitudes of the ρ' and ρ'' contributions and, as this is not the case, we consider a more flexible scenario and add a phase that can absorb part of the associated shortcomings. The ρ-meson resonance width is accounted for through [170]

$$\begin{aligned}\Gamma_\rho(s) &= -\frac{M_\rho s}{96\pi^2 F_\pi^2}\mathrm{Im}\left[A_\pi(s)+\frac{1}{2}A_K(s)\right] \\ &= \frac{M_\rho s}{96\pi F_\pi^2}\left[\sigma_\pi^3(s)\theta(s-4m_\pi^2)+\frac{1}{2}\sigma_K^3(s)\theta(s-4m_K^2)\right] ,\end{aligned} \tag{4.13}$$

while for the energy-dependent width of the ρ' and ρ'' we do not take intermediate states other than $\pi\pi$

$$\Gamma_{\rho',\rho''}(s) = \Gamma_{\rho',\rho''}\frac{s}{M_{\rho',\rho''}^2}\frac{\sigma_\pi^3(s)}{\sigma_\pi^3(M_{\rho',\rho''}^2)}\theta(s-4m_\pi^2)\,. \tag{4.14}$$

From Eq. (4.12) we extract its phase through

$$\tan\delta_+^{KK}(s) = \frac{\mathrm{Im}f_+^{KK}(s)}{\mathrm{Re}f_+^{KK}(s)}\,. \tag{4.15}$$

In fact, we only use the phase thus extracted to describe the energy region that goes from 1 GeV^2 to m_τ^2. From $4m_\pi^2$ to 1 GeV^2 we employ the P-wave phase shift of the pion-pion scattering solution of the Roy equations [172] that we match to the phase in Eq. (4.15) at 1 GeV^2, while for the region $m_\tau^2 \leq s$ we guide smoothly the phase to π such that the correct $1/s$ high-energy behavior of the form factor is ensured (see Ref. [147] for more details). For our analysis, we employ the numerical values given under the label of Fit i) of Table 7 of Ref. [147] for the corresponding parameters.

For the K^-K^0 scalar form factor, we use the results of Ref. [173, 174, 175][3]. These were obtained after the unitarization, based on the method of N/D, of the complete one-loop calculation of the strangeness conserving scalar form factors within $U(3)$ ChPT.

Finally, the tensor form factor is obtained exactly as in chapter 3. The appropriate Lagrangian from ChPT with tensor sources reads [66]

$$\mathcal{L} = \Lambda_1\left\langle t_+^{\mu\nu}f_{+\mu\nu}\right\rangle - i\Lambda_2\left\langle t_+^{\mu\nu}u_\mu u_\nu\right\rangle + \Lambda_3\left\langle t_+^{\mu\nu}t_{+\mu\nu}^{+}\right\rangle + \Lambda_4\left\langle f_+^{\mu\nu}\right\rangle^2 , \tag{4.16}$$

[3]We thank very much Zhi-Hui Guo for providing us tables with the unitarized $\pi\eta$, $\pi\eta'$ and $K^0\bar{K}^0$ scalar form factors. We translate the result of $K^0\bar{K}^0$ to the K^-K^0 concerning us through the relation $F_0^{K^-K^0}(s) = -F_0^{K^0\bar{K}^0}(s)/\sqrt{2}$.

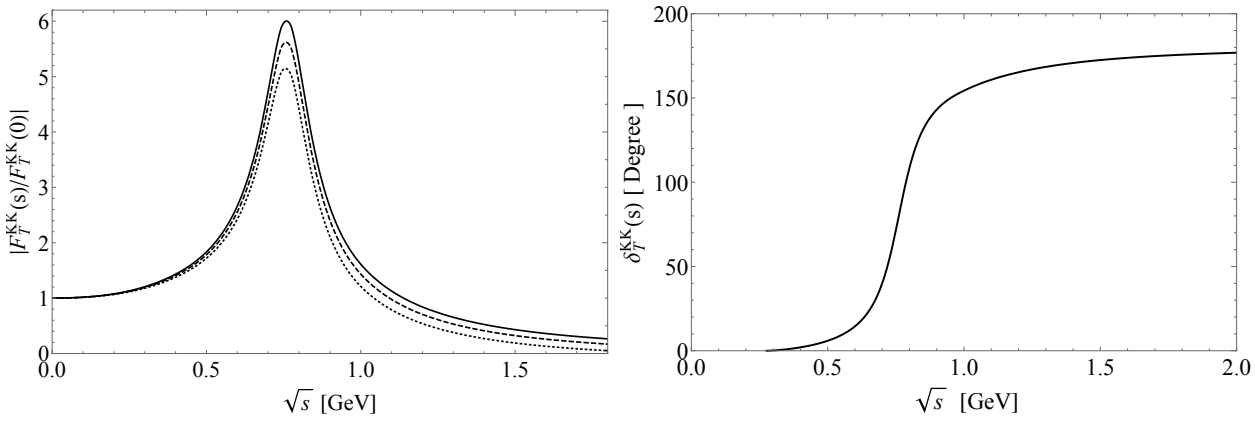

Figure 4.1: Normalized absolute value of the tensor form factor $F_T^{KK}(s)$ given in Eq. (4.18) (left), for $s_{\rm cut} = 4$ GeV^2 (dotted line), 9 GeV^2 (dashed line) and $s_{\rm cut} \to \infty$ GeV^2 (solid line), and tensor form factor phase $\delta_T^{KK}(s)$ (right).

where $t_+^{\mu\nu} = u^\dagger t^{\mu\nu} u^\dagger + u t^{\mu\nu\dagger} u$ includes the tensor source and its adjoint, and $\langle \cdots \rangle$ stands for a flavor space trace. Again, only terms proportional to Λ_2 contribute to the decays we are considering. From the previous Lagrangian we obtain

$$i\left\langle K^- K^0 \right| \frac{\delta \mathcal{L}}{\delta \bar{t}_{\alpha\beta}} \left| 0 \right\rangle = \frac{\Lambda_2}{F_\pi^2} \left(p_{K^0}^\alpha p_{K^-}^\beta - p_{K^-}^\alpha p_{K^0}^\beta \right) , \tag{4.17}$$

so that $F_T^{K^-K^0}(0) = \frac{\Lambda_2}{F_\pi^2}$, with $\Lambda_2 = (11.1 \pm 0.4)\,\text{MeV}$ as we have derived in chapter 3.

As usual, the energy-dependence of the tensor form factor $F_T^{K^-K^0}(s)$ is calculated with the following dispersion relation

$$F_T^{K^-K^0}(s) = F_T^{K^-K^0}(0) \exp\left[\frac{s}{\pi} \int_{4m_\pi^2}^{s_{\rm cut}} ds' \frac{\delta_T^{KK}(s')}{s'(s' - s - i\epsilon)} \right] , \tag{4.18}$$

where we take $\delta_T^{KK}(s) = \delta_+^{\pi\pi}(s)$ in the elastic region i.e. until 1 GeV^2, with $\delta_+^{\pi\pi}(s)$ being the P-wave $\pi\pi$ scattering phase (see text below Eq. (4.15)).

In Fig. 4.1, we show the tensor phase $\delta_T^{KK}(s)$ (right panel) and the (normalized) absolute value $|F_T^{KK}(s)|$ for the cases $s_{\rm cut} = 4, 9$ GeV^2 and $s_{\rm cut} \to \infty$, which is taken as the baseline hypothesis. As before, the variations due to $s_{\rm cut}$ will be taken into account as a source of systematic uncertainty in section 4.5.5.

4.5 Decay observables

Now we proceed to the study of the decay observables. We analyze particularly Dalitz plots, angular and decay distributions, and the forward-backward asymmetry. As in chapter 3, we start by noting that in the rest frame of the τ lepton, the doubly differential decay width for $\tau^- \to K^- K^0 \nu_\tau$ decay is given by

$$\frac{d^2\Gamma}{ds\,dt} = \frac{1}{32\,(2\pi)^3\,m_\tau^3}\overline{|\mathcal{M}|^2}\,, \tag{4.19}$$

where $\overline{|\mathcal{M}|^2}$ is the unpolarized spin-averaged squared matrix element, s is the invariant mass of the K^-K^0 system, limited in the interval $(m_{K^0}+m_K)^2 \leq s \leq m_\tau^2$, and $t = (P' + p_{K^0})^2 = (P - p_K)^2$ with kinematic boundaries given by $t^-(s) \leq t \leq t^+(s)$, with

$$\begin{aligned} t^\pm(s) &= \frac{1}{2s}\Big[2s\,m_{K^0}^2 + (m_\tau^2 - s)(s + m_{K^0}^2 - m_K^2) \\ &\pm (m_\tau^2 - s)\sqrt{\lambda(s, m_{K^0}^2, m_K^2)}\Big]\,, \end{aligned} \tag{4.20}$$

and where $\lambda(x,y,z) = x^2 + y^2 + z^2 - 2xy - 2xz - 2yz$ is the usual Kallen function. The kinematic limits in s and t for the decay channels $\tau^- \to K^-\eta^{(\prime)}\nu_\tau$ are obtained by replacing $m_{K^0} \to m_{\eta^{(\prime)}}$ above.

4.5.1 Dalitz plot

Putting all the pieces of the previous section together, we see that the amplitude for the process $\tau^- \to K^- K^0 \nu_\tau$ can be written as follows

$$\begin{aligned} \mathcal{M} =& \frac{G_F}{\sqrt{2}} V_{ud}\sqrt{S_{EW}}(1 + \epsilon_L + \epsilon_R)\times \\ & \Bigg[C_{KK^0}^V \left((p_{K^0} - p_K)^\mu + \frac{\Delta_{KK}}{s}(p_{K^0} + p_K)^\mu \right) L_\mu F_+^{KK^0}(s) \\ & + C_{KK^0}^S \frac{\Delta_{KK}}{s}\left(1 + \frac{s\hat{\epsilon}_s}{M_\tau(m_d - m_u)}\right)(p_{K^0} + p_K)^\mu L_\mu F_0^{KK^0}(s) \\ & + 2i\hat{\epsilon}_T(p_{K^0}^\mu p_K^\nu - p_K^\mu p_{K^0}^\nu) L_{\mu\nu} F_T^{KK^0}(s) \Bigg]\,, \end{aligned} \tag{4.21}$$

which can also be conveniently written as

$$\mathcal{M} = \frac{G_F}{\sqrt{2}} V_{ud}\sqrt{S_{EW}}(1 + \epsilon_L + \epsilon_R)(M_0 + M_+ + M_T)\,, \tag{4.22}$$

where,

$$
\begin{aligned}
M_+ &= C^V_{KK^0}\left((p_{K^0}-p_K)^\mu+\frac{\Delta_{KK}}{s}(p_{K^0}+p_K)^\mu\right)L_\mu F_+^{KK^0}(s)\,,\\
M_0 &= C^S_{KK^0}\frac{\Delta_{KK}}{s}\left(1+\frac{s\hat{\epsilon}_s}{M_\tau(m_d-m_u)}\right)(p_{K^0}+p_K)^\mu L_\mu F_0^{KK^0}(s)\,,\\
M_T &= 2i\hat{\epsilon}_T(p^\mu_{K^0}p^\nu_K-p^\mu_K p^\nu_{K^0})L_{\mu\nu}F_T^{KK^0}(s)\,. \qquad (4.23)
\end{aligned}
$$

Therefore, the unpolarized spin-averaged squared amplitude yields

$$
\begin{aligned}
\overline{|\mathcal{M}|^2} &= \frac{G_F^2|V_{ud}|^2S_{EW}}{s^2}\left(1+\epsilon_L+\epsilon_R\right)^2\\
&\times\ \left[M_{00}+M_{++}+M_{0+}+M_{T+}+M_{T0}+M_{TT}\right], \qquad (4.24)
\end{aligned}
$$

where M_{00}, M_{++} and M_{TT} are, respectively, the scalar, vector and tensor amplitudes, whereas M_{0+}, M_{T+} and M_{T0} are their corresponding interferences. The explicit form for each of these terms reads

$$
\begin{aligned}
M_{0+} &= -2C^S_{KK^0}C^V_{KK^0}m_\tau^2\mathrm{Re}[F_+^{KK^0}(s)(F_0^{KK^0}(s))^*]\\
&\quad\times\Delta_{KK}\left(1+\tfrac{s\,\hat{\epsilon}_S}{m_\tau(m_d-m_u)}\right)\left(s(m_\tau^2-s-2t+\Sigma_{KK^0})-m_\tau^2\Delta_{KK^0}\right),\\
M_{T+} &= -4C^V_{KK^0}\hat{\epsilon}_T m_\tau^3 s\mathrm{Re}[F_T^{KK^0}(s)(F_+^{KK^0}(s))^*]\left(1-\tfrac{s}{m_\tau^2}\right)\lambda(s,m^2_{K^0},m^2_K)\,,\\
M_{T0} &= 4C^S_{KK^0}\hat{\epsilon}_T\Delta_{KK}m_\tau s\mathrm{Re}[F_T^{KK^0}(s)(F_0^{KK^0}(s))^*]\\
&\quad\times\left(1+\tfrac{s\,\hat{\epsilon}_S}{m_\tau(m_d-m_u)}\right)\left(s(m_\tau^2-s-2t+\Sigma_{KK^0})-m_\tau^2\Delta_{KK^0}\right),\\
M_{00} &= (C^S_{KK^0})^2\Delta^2_{KK}m_\tau^4\left(1-\tfrac{s}{m_\tau^2}\right)|F_0^{KK^0}(s)|^2\left(1+\tfrac{s\,\hat{\epsilon}_S}{m_\tau(m_d-m_u)}\right)^2,\\
M_{++} &= (C^V_{KK^0})^2|F_+^{KK^0}(s)|^2\left\{m_\tau^4(s-\Delta_{KK^0})^2+4m_k^2s^2(m^2_{K^0}-t)+4s^2t(s+t-m^2_{K^0})\right.\\
&\quad\left.-m_\tau^2s\left(s\,(s+4t)-2\Delta_{KK^0}(s+2t-2m^2_{K^0})+\Delta^2_{KK^0}\right)\right\},\\
M_{TT} &= 4\hat{\epsilon}_T^2|F_T^{KK^0}(s)|^2s^2\left\{m_K^4(m_\tau^2-s)-m^4_{K^0}(3m_\tau^2+s)-s\left((s+2t)^2-m_\tau^2(s+4t)\right)\right.\\
&\quad\left.+2m^2_{K^0}\left((s+2t)(s+m_\tau^2)-2m_\tau^4\right)-2m_K^2(m_\tau^2-s)(s+2t-m^2_{K^0})\right\},
\end{aligned}
\qquad (4.25)
$$

where as usual, we have used the notation $\Delta_{PQ}=m_P^2-m_Q^2$ and $\Sigma_{PQ}=m_P^2+m_Q^2$.

The analogue expressions for $\tau^- \to K^-\eta^{(\prime)}\nu_\tau$ are obtained by replacing $V_{ud} \to V_{us}$ in Eq. (4.24), and $m_{K^0} \to m_{\eta^{(\prime)}}$, $m_d \to m_s$ and $C_{KK}^{S,V} \to C_{K\eta^{(\prime)}}^{S,V}$ in Eq. (4.25).

As we have pointed out in chapter 3, it is convenient to define the following observable in our studies of Dalitz plots

$$\widetilde{\Delta}\left(\hat{\epsilon}_S, \hat{\epsilon}_T\right) = \frac{\left|\overline{|\mathcal{M}\left(\hat{\epsilon}_S, \hat{\epsilon}_T\right)|^2} - \overline{|\mathcal{M}\left(0,0\right)|^2}\right|}{\overline{|\mathcal{M}\left(0,0\right)|^2}}\,, \tag{4.26}$$

where $\mathcal{M}(0,0)$ corresponds to the SM case.

In the left panel of figure 4.2 we show the Dalitz plot for the SM case in the (s,t) variables.

4.5.2 Angular distribution

Now we turn to the study of the angular dependence of the decay distribution. For this task we work in the rest frame of the hadronic system, that is, a frame in which we have $\vec{p}_K + \vec{p}_{K^0} = \vec{p}_\tau - \vec{p}_\nu = \vec{0}$. In this frame, the tau lepton and the charged kaon energies are given by $E_\tau = (s + m_\tau^2)/2\sqrt{s}$ and $E_K = (s+m_K^2-m_{K^0}^2)/2\sqrt{s}$, and the angle θ between these two particles can be found from the invariant t variable through $t = m_\tau^2 + m_K^2 - 2E_\tau E_K + 2|\vec{p}_K||\vec{p}_\tau|\cos\theta$, where $|\vec{p}_K| = \sqrt{E_K^2 - m_K^2}$ and $|\vec{p}_\tau| = \sqrt{E_\tau^2 - m_\tau^2}$.
The form of the decay distribution in the (s,θ) variables has the form

$$\begin{aligned}
\frac{d^2\Gamma}{d\sqrt{s}d\cos\theta} &= \frac{G_F^2|V_{ud}|^2 S_{EW}}{128\pi^3 m_\tau}(1+\epsilon_L+\epsilon_R)^2\left(\frac{m_\tau^2}{s}-1\right)^2|\vec{p}_K|\Bigg\{(C_{KK^0}^S)^2(\Delta_{KK})^2|F_0^{KK^0}(s)|^2 \\
&\times \left(1+\frac{s\hat{\epsilon}_S}{m_\tau(m_d-m_u)}\right)^2 + 16|\vec{p}_K|^2 s^2\left|\frac{C_{KK^0}^V}{2m_\tau}F_+^{KK^0}(s) - \hat{\epsilon}_T F_T^{KK^0}(s)\right|^2 \\
&+ 4|\vec{p}_K|^2 s\left(1-\frac{s}{m_\tau^2}\right)\cos^2\theta\left[(C_{KK^0}^V)^2|F_+^{KK^0}(s)|^2 - 4s\hat{\epsilon}_T^2|F_T^{KK^0}(s)|^2\right] \\
&+ 4C_{KK^0}^S\Delta_{KK}|\vec{p}_K|\sqrt{s}\cos\theta\left(1+\frac{s\hat{\epsilon}_S}{m_\tau(m_d-m_u)}\right) \\
&\times \left[C_{KK^0}^V \mathrm{Re}[F_0^{KK^0}(s)F_+^{*KK^0}(s)] - \frac{2s\hat{\epsilon}_T}{m_\tau}\mathrm{Re}[F_T^{KK^0}(s)F_0^{*KK^0}(s)]\right]\Bigg\}\,,
\end{aligned} \tag{4.27}$$

Again, the corresponding expressions for the decays $\tau^- \to K^-\eta^{(\prime)}\nu_\tau$ are obtained by replacing $V_{ud} \to V_{us}$, $m_{K^0} \to m_{\eta^{(\prime)}}$, $m_d \to m_s$ and $C_{KK}^{S,V} \to C_{K\eta^{(\prime)}}^{S,V}$ in Eq. (4.27).

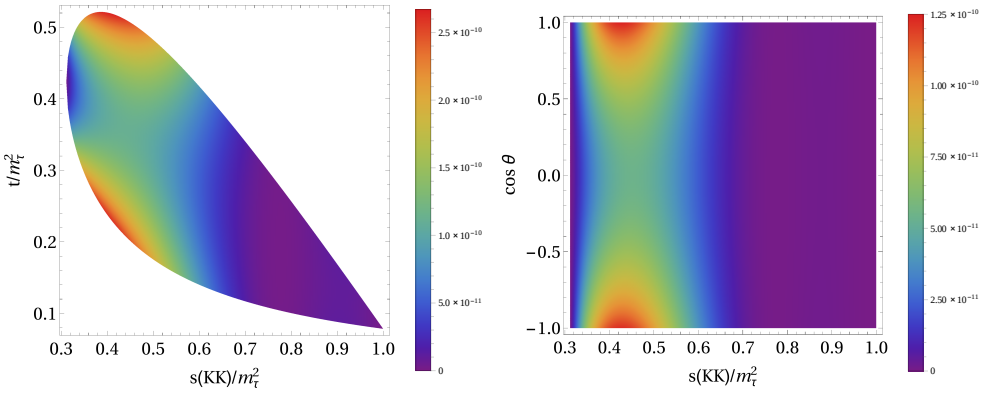

Figure 4.2: Dalitz plot distribution in the SM, $\overline{|\mathcal{M}(0,0)|^2}$ in Eq. (4.24), for $\tau^- \to K^- K^0 \nu_\tau$ in the (s,t) variables (left). The figure shown on the right corresponds to the differential decay distribution in the $(s, \cos\theta)$ variables, Eq. (4.27). The s and t variables are normalized to m_τ^2.

The Dalitz plots for the (s,θ) variables are shown in the right panel of figure 4.2 and in the lower row of figure 4.3.

4.5.3 Decay rate

We find the decay rate for the process $\tau^- \to K^- K^0 \nu_\tau$ by integrating Eq. (4.19) in the t variable so that the $K^- K^0$ invariant mass distribution yields

$$\begin{aligned} \frac{d\Gamma}{d\sqrt{s}} &= \frac{G_F^2 |V_{ud}|^2 m_\tau^3 S_{EW}}{192\pi^3\sqrt{s}}(1+\epsilon_L+\epsilon_R)^2 \left(1-\frac{s}{m_\tau^2}\right)^2 \lambda^{1/2}(s, m_{K^0}^2, m_K^2) \\ &\times \left[X_{VA} + \hat{\epsilon}_S X_S + \hat{\epsilon}_T X_T + \hat{\epsilon}_S^2 X_{S^2} + \hat{\epsilon}_T^2 X_{T^2}\right], \end{aligned} \tag{4.28}$$

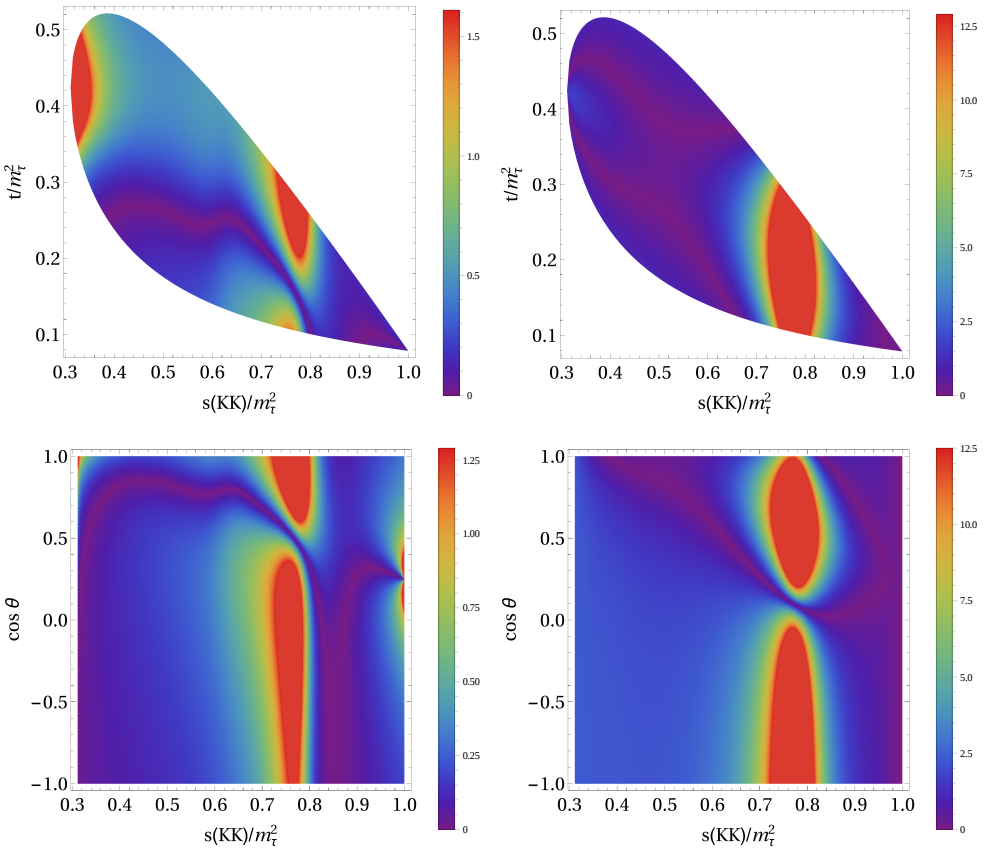

Figure 4.3: Dalitz plot distribution of $\widetilde{\Delta}(\hat{\epsilon}_S, \hat{\epsilon}_T)$ in Eq. (4.26) for $\tau^- \to K^- K^0 \nu_\tau$ with $(\hat{\epsilon}_S = 0.10, \hat{\epsilon}_T = 0)$ (left panels) and $(\hat{\epsilon}_S = 0, \hat{\epsilon}_T = 0.9)$ (right panels). The lower row show the differential decay distribution in the $(s, \cos\theta)$ variables, Eq. (4.27). The s and t variables are normalized to m_τ^2.

where each of the terms is given by

$$X_{VA} = \frac{(C^V_{KK^0})^2}{2s^2}\Big[3|F_0^{KK^0}(s)|^2\Delta^2_{KK^0} + |F_+^{KK^0}(s)|^2\left(1+\frac{2s}{m_\tau^2}\right)\lambda(s,m^2_{K^0},m^2_K)\Big]\,, \tag{4.29}$$

$$X_S = \frac{3}{s\,m_\tau}(C^V_{KK^0})^2|F_0^{KK^0}(s)|^2\frac{\Delta^2_{KK^0}}{m_d-m_u}\,, \tag{4.30}$$

$$X_T = -\frac{6}{s\,m_\tau}C^V_{KK^0}\mathrm{Re}[F_T^{KK^0}(s)F_+^{*KK^0}(s)]\lambda(s,m^2_{K^0},m^2_K)\,, \tag{4.31}$$

$$X_{S^2} = \frac{3}{2\,m_\tau^2}(C^V_{KK^0})^2|F_0^{KK^0}(s)|^2\frac{\Delta^2_{KK^0}}{(m_d-m_u)^2}\,, \tag{4.32}$$

$$X_{T^2} = \frac{4}{s}|F_T^{KK^0}(s)|^2\left(1+\frac{s}{2\,m_\tau^2}\right)\lambda(s,m^2_{K^0},m^2_K)\,. \tag{4.33}$$

In figure 4.4, we plot the invariant mass distribution of the K^-K^0 system for the $\tau^-\to K^-K^0\nu_\tau$ decays. There, we show three different scenarios: first the SM case (solid line), and then the representative values $\{\hat{\epsilon}_S=0.1,\ \hat{\epsilon}_T=0\}$ (dashed line) and $\{\hat{\epsilon}_S=0,\ \hat{\epsilon}_T=0.9\}$ (dotted line). As we have mentioned on previous sections these values are used just for illustration. We will discuss more about their magnitudes in section 4.4.5 where we set bounds on these effective couplings.

From figure 4.4 we see that while the (small) effects of non-SM scalar interactions are mostly seen in the first half of the decay spectrum, and in the interference region of the $\rho(1450)$ and $\rho(1700)$ resonances to some extent, the departure from the SM due to tensor interactions is seen on the second half of the spectrum.

4.5.4 Forward-backward asymmetry

As we saw in chapter 3, the forward-backward asymmetry is defined as [126, 127, 138]

$$\mathcal{A}_{K\eta^{(\prime)}}(s) = \frac{\int_0^1 d\cos\theta\frac{d^2\Gamma}{ds\,d\cos\theta} - \int_{-1}^0 d\cos\theta\frac{d^2\Gamma}{ds\,d\cos\theta}}{\int_0^1 d\cos\theta\frac{d^2\Gamma}{ds\,d\cos\theta} + \int_{-1}^0 d\cos\theta\frac{d^2\Gamma}{ds\,d\cos\theta}}\,. \tag{4.34}$$

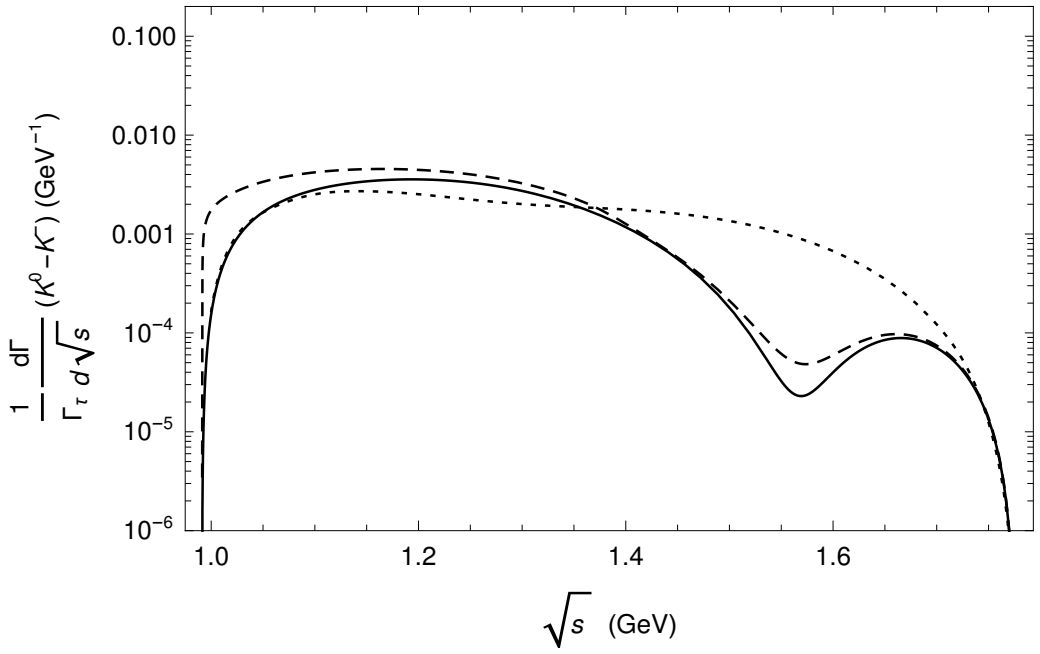

Figure 4.4: Invariant mass distribution for the decay $\tau^- \to K^- K^0 \nu_\tau$ in the SM (solid line), and for $\hat{\epsilon}_S = 0.1$, $\hat{\epsilon}_T = 0$ (dashed line) and $\hat{\epsilon}_S = 0$, $\hat{\epsilon}_T = 0.9$ (dotted line). The decay distribution is normalized to the tau decay width.

The analytical expression for this observable is obtained substituting Eq. (4.27) into Eq. (4.34). After integrating upon the $\cos\theta$ variable we find

$$\begin{aligned}\mathcal{A}_{KK}(s) &= \frac{3C^S_{KK^0}\Delta_{KK}\sqrt{\lambda(s,m^2_{K^0},m^2_K)}}{2s^2[X_{VA}+\hat{\epsilon}_S X_S+\hat{\epsilon}_T X_T+\hat{\epsilon}^2_S X_{S^2}+\hat{\epsilon}^2_T X_{T^2}]}\\ &\times \left(1+\frac{s\hat{\epsilon}_S}{m_\tau(m_d-m_u)}\right)\Big\{C^V_{KK^0}\mathrm{Re}[F_0^{KK^0}(s)F_+^{*KK^0}(s)]\\ &- \frac{2s\,\hat{\epsilon}_T}{m_\tau}\mathrm{Re}[F_T^{KK^0}(s)F_0^{*KK^0}(s)]\Big\}\,. \qquad (4.35)\end{aligned}$$

By making $\epsilon_R=\epsilon_L=\hat{\epsilon}_S=\hat{\epsilon}_T=0$ we get the SM forward-backward asymmetry, which is plotted in figure 4.5 (solid line). For the more general case where we include NP interactions we also have figure 4.5, there, we plot the cases $\{\hat{\epsilon}_S=0.1,\,\hat{\epsilon}_T=0\}$ (dashed line) and $\{\hat{\epsilon}_S=0,\,\hat{\epsilon}_T=0.9\}$ (dotted line).

The important thing to note for the K^-K^0 decay channel is that the SM $\mathcal{A}_{KK}$ is in general small with a signature right before 1 GeV and a small bump at around 1.55 GeV. On the other hand, when we turn on the effective couplings we see that clear non-zero values for the NP coupling of the scalar contributions will unambiguously dominate over the tensor ones. Therefore, the $\mathcal{A}_{KK}$ would be a good observable for searching non-standard scalar interactions: despite its numerator in Eq. (4.35) is suppressed by the small value of $\Delta_{K^-K^0}$; its denominator is further suppressed by the dependence of the X_{S^2} on $\Delta_{K^-K^0}$.

4.5.5 Limits on $\hat{\epsilon}_S$ and $\hat{\epsilon}_T$

Our purpose in this section is to set bounds on the effective couplings $\hat{\epsilon}_S$ and $\hat{\epsilon}_T$. We achieve this by comparing the total width Γ (which depends explicitly on the NP couplings $\hat{\epsilon}_S$ and $\hat{\epsilon}_T$) with the SM width Γ^0 (obtained by neglecting NP interactions which we get by setting $\hat{\epsilon}_S=\hat{\epsilon}_T=0$). This comparison is conveniently implemented with the introduction of the observable Δ which we define as follows

$$\Delta \equiv \frac{\Gamma-\Gamma^0}{\Gamma^0} = \alpha\hat{\epsilon}_S+\beta\hat{\epsilon}_T+\gamma\hat{\epsilon}^2_S+\delta\hat{\epsilon}^2_T\,. \qquad (4.36)$$

After integrating the invariant mass distribution Eq. (4.28) upon the s variable we find Γ and Γ^0, and with them we find Δ. The numerical values of the coefficients α,β,γ and δ are found to be:
$\alpha=0.24\pm0.01$, $\beta=-3.66^{+0.16}_{-1.74}$, $\gamma=34.4^{+1.3}_{-1.4}$ and $\delta=9.2^{+1.0}_{-5.2}$ for the K^-K^0

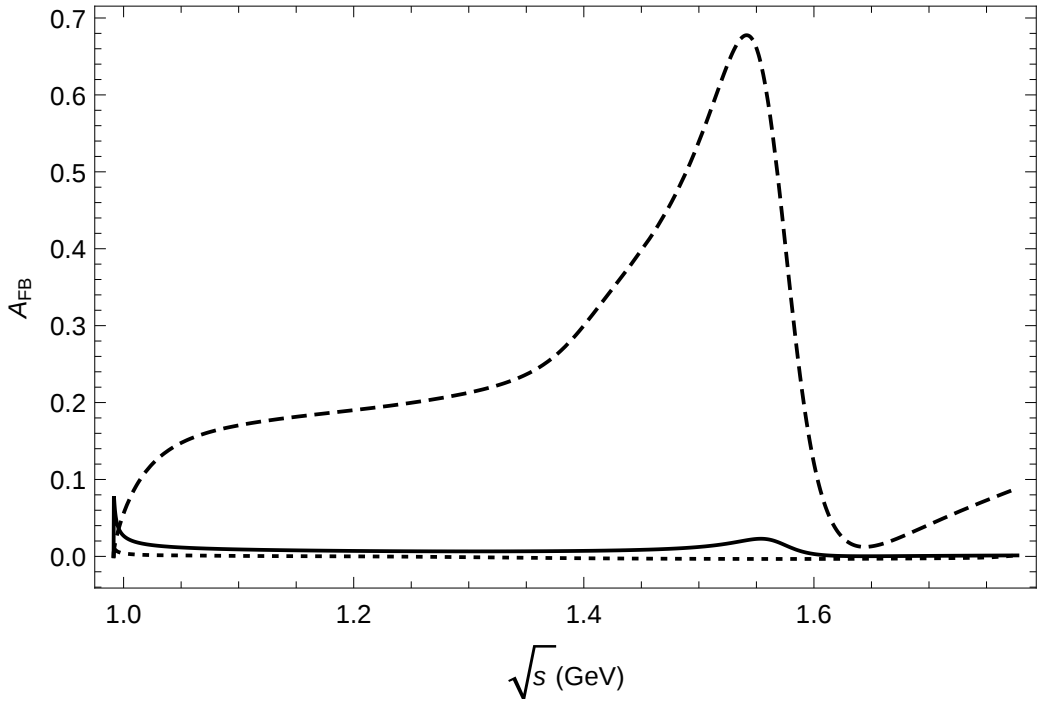

Figure 4.5: Forward-backward asymmetry for the decay $\tau^- \to K^- K^0 \nu_\tau$ in the SM (solid line), and for $\hat{\epsilon}_S = 0.1$, $\hat{\epsilon}_T = 0$ (dashed line), and $\hat{\epsilon}_T = 0.9$, $\hat{\epsilon}_S = 0$ (dotted line).

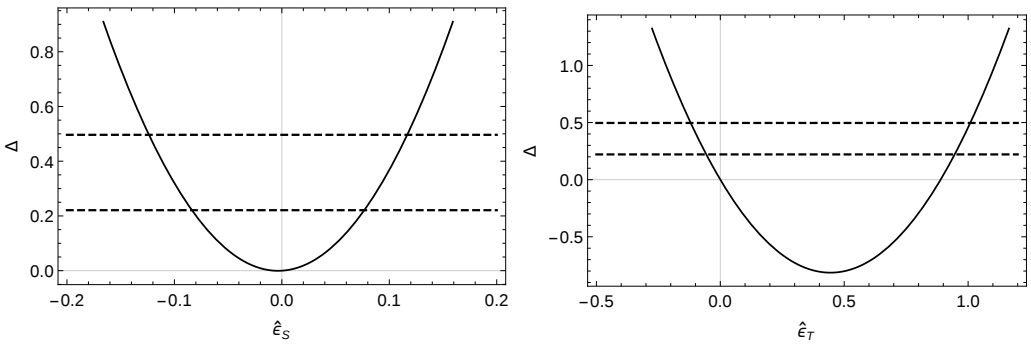

Figure 4.6: Δ as a function of $\hat{\epsilon}_S$ for $\hat{\epsilon}_T = 0$ (left plot) and $\hat{\epsilon}_T$ for $\hat{\epsilon}_S = 0$ (right plot) for the decay $\tau^- \to K^- K^0 \nu_\tau$. Horizontal lines represent the values of Δ according to the current measurement and theory errors (at three standard deviations) of the branching ratio (dashed line).

transition. The errors carried by the previous coefficients come from the uncertainty associated to the corresponding form factors (see section 4.4).

With the help of the Δ observable we obtain our limits for $\hat{\epsilon}_S$ and $\hat{\epsilon}_T$ couplings in two different ways. First, we set one of the couplings to zero and obtain bounds for the other, and vice versa. This process gives us the two parabolas shown in figure 4.6. We can summarize that information as follows:

$$\hat{\epsilon}_S = [-0.12, -0.08] \cup [0.08, 0.12]\,, \quad \hat{\epsilon}_T = 0\,, \tag{4.37}$$

$$\hat{\epsilon}_S = 0\,, \quad \hat{\epsilon}_T = [-0.12, -0.06] \cup [0.92, 0.99]\,, \tag{4.38}$$

from $\tau^- \to K^- K^0 \nu_\tau$ ($BR_{\text{exp}} = 1.486(34) \times 10^{-3}$ [6]). Had we used the BaBar measurement of $\tau^- \to K^- K_S \nu_\tau$ ($BR_{\text{exp}} = 0.739(11)(20) \times 10^{-3}$ [156]), we would have obtained instead

$$\hat{\epsilon}_S = [-0.12, -0.09] \cup [0.08, 0.11]\,, \quad \hat{\epsilon}_T = 0\,, \tag{4.39}$$

$$\hat{\epsilon}_S = 0\,, \quad \hat{\epsilon}_T = [-0.12, -0.06] \cup [0.93, 0.99]\,. \tag{4.40}$$

The second way in which we set constraints is again using Eq. (4.36), but now taking the general case where both couplings are non-vanishing. In this case we obtain the ellipse shown in figure 4.7.

For the convenience of the reader we summarize all our findings for our constraints into two-meson decay modes in table 4.1. The first three rows of this table show the constraints we have obtained for the channels we have mentioned in this chapter ($\tau^- \to K^-(\eta^{(\prime)}, K^0)\nu_\tau$) and the last four rows show our contraints from previous works for the other two-meson modes [127, 138, 126].

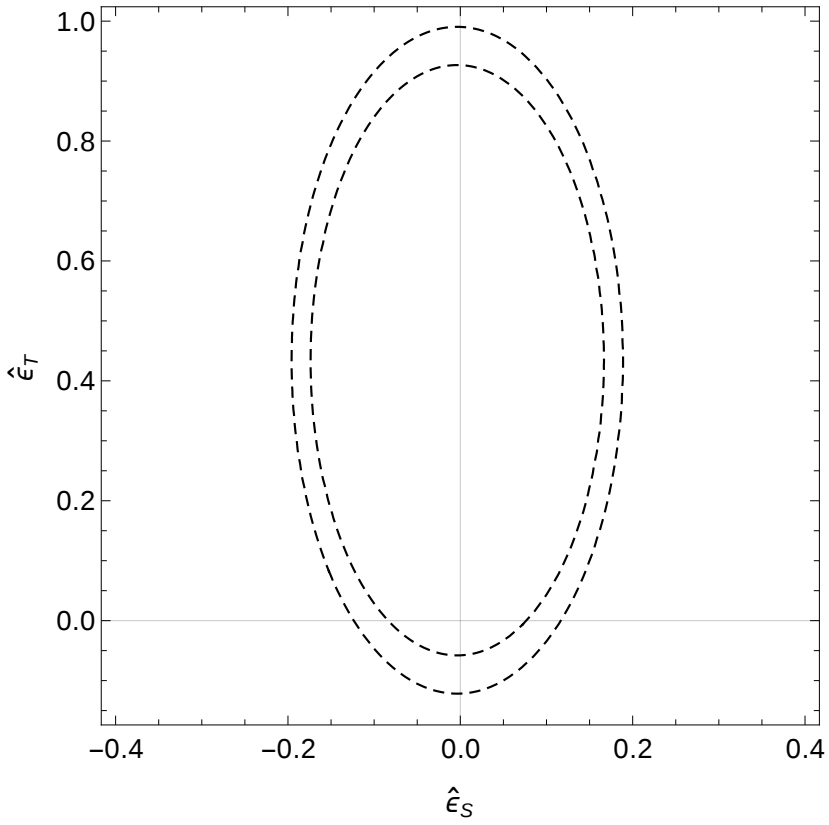

Figure 4.7: Constraints on the scalar and tensor couplings obtained from $\Delta(\tau^- \to K^- K^0 \nu_\tau)$ using the measured branching ratio (at three standard deviations).

Decay channel	$\hat{\epsilon}_S$ ($\hat{\epsilon}_T = 0$)	$\hat{\epsilon}_T$ ($\hat{\epsilon}_S = 0$)	$\hat{\epsilon}_S$	$\hat{\epsilon}_T$
$\tau^- \to K^- \eta \nu_\tau$	$[-0.38, 0.16]$	$[-1.4, -0.7] \cup [-4.7, 8.5] \cdot 10^{-2}$	$[-0.7, 0.5]$	$[-1.5, 0.1]$
$\tau^- \to K^- \eta' \nu_\tau$	$[-0.20, 0.05]$	$[-7.6, 14.9]$	$[-0.21, 0.05]$	$[-10.4, 17.7]$
$\tau^- \to K^- K^0 \nu_\tau$	$[-0.12, -0.08] \cup [0.08, 0.12]$	$[-0.12, -0.06] \cup [0.92, 0.99]$	$[-0.2, 0.2]$	$[-0.12, 0.98]$
$\tau^- \to \pi^- \pi^0 \nu_\tau$ [127]	$[-1.33, 1.31]$	$[-0.79, -0.57] \cup [-1.4, 1.3] \cdot 10^{-2}$	$[-5.2, 5.2]$	$[-0.79, 0.013]$
$\tau^- \to (K\pi)^- \nu_\tau$ [138]	$[-0.57, 0.27]$	$[-0.059, 0.052] \cup [0.60, 0.72]$	$[-0.89, 0.58]$	$[-0.07, 0.72]$
$\tau^- \to \pi^- \eta \nu_\tau$ [126]	$[-8.3, 3.9] \cdot 10^{-3}$	$[-0.43, 0.39]$	$[-0.83, 0.37] \cdot 10^{-2}$	$[-0.55, 0.50]$
$\tau^- \to \pi^- \eta' \nu_\tau$ [126]	$[-1.13, 0.68] \cdot 10^{-2}$	$\lvert\hat{\epsilon}_T\rvert < 11.4$	$[-1.13, 0.67] \cdot 10^{-2}$	$[-11.9, 11.9]$

Table 4.1: Constraints on the scalar and tensor couplings obtained (at three standard deviations) through the limits on the current branching ratio measurements. Theory errors are included.

Chapter 5

Global analysis of exclusive hadronic tau decays

5.1 Introduction

In chapters 3 and 4, we have studied separately several hadronic decays of the tau lepton into two mesons. We can divide these decays into two categories: strangeness-changing decays and strangeness-conserving decays. The decays $\tau^- \to (K\pi)^-\nu_\tau$ that we studied extensively in chapter 3 and the decays $\tau^- \to K^-\eta^{(\prime)}\nu_\tau$ that we mentioned briefly in chapter 4 belong to the first category, and the decays $\tau^- \to K^-K^0\nu_\tau$ that we studied in detail in chapter 4 belong to the second category. Each of these studies was very important on its own way since we have learned different things from all of them by treating them individually.

Our purpose in this chapter, based in [205], is a little bit different, we want to learn in this case what can we gain by studying all these channels (and others that we will add) [1] in a global way. For this task we will take advantage from many of the results of our previous chapters, for example, form factors, amplitudes, spectra, etc.

We organize this chapter as follows: we discuss the theoretical framework in section 5.2, where we present the effective Lagrangian that we use and calculate the analytical expressions for several interesting observables, namely, the decay rates for the one-meson processes $\tau^- \to P^-\nu_\tau$ with $P = \pi, K$, and the partial decay widths for the two-meson decays $\tau^- \to (PP')^-\nu_\tau$. Next, in sections 5.3 and 5.4, we study the bounds on the New Physics effective cou-

[1] To the two-meson decay modes of the tau lepton that we have mentioned, we will add the one-meson decay modes $\tau^- \to P^-\nu_\tau$, where $P = \pi, K$.

plings for the strangeness-conserving ($\Delta S = 0$) and the strangeness-changing ($|\Delta S| = 1$) transitions, respectively. Then, a global fit to both sectors i.e. ($\Delta S = 0$ and $|\Delta S| = 1$), is studied in section 5.5. We will state our conclusions in chapter 6.

We will not discuss the relevant form factors in this chapter since we have already done it in chapters 3 and 4, and in appendix C. So, every time we need that input, we will refer the reader to previous chapters or to the relevant appendix.

5.2 SMEFT Lagrangian and decay rate

As usual, we start by writing the proper effective Lagrangian for our problem. We will describe semileptonic charged-current decays of the form $\tau^- \to \nu_\tau \bar{u} D$, where $D = d$ for strangeness-conserving and $D = s$ for strangeness-changing transitions. The low-energy limit of the Standard Model Effective Field Theory Lagrangian including dimension six operators with left-handed neutrinos has the form [49, 129].

$$\begin{aligned}\mathcal{L}_{CC} \;=\; & -\frac{G_F V_{uD}}{\sqrt{2}}\Big[(1+\epsilon_L^\tau)\bar{\tau}\gamma_\mu(1-\gamma^5)\nu_\tau \cdot \bar{u}\gamma^\mu(1-\gamma^5)D \\ & +\epsilon_R^\tau \bar{\tau}\gamma_\mu(1-\gamma^5)\nu_\tau \cdot \bar{u}\gamma^\mu(1+\gamma^5)D \\ & +\bar{\tau}(1-\gamma^5)\nu_\tau \cdot \bar{u}(\epsilon_S^\tau - \epsilon_P^\tau\gamma^5)D \\ & +\epsilon_T^\tau \bar{\tau}\sigma_{\mu\nu}(1-\gamma^5)\nu_\tau\, \bar{u}\sigma^{\mu\nu}(1-\gamma^5)D\Big] + h.c.\,, \end{aligned} \tag{5.1}$$

where $\sigma^{\mu\nu} = i[\gamma^\mu, \gamma^\nu]/2$, G_F is the tree-level definition of the Fermi constant and ϵ_i ($i = L, R, S, P, T$) are effective couplings encoding NP. It is important to note at this point that the product $G_F V_{uD}$ in Eq. (5.1) will carry a dependence on ϵ_L^e and ϵ_R^e since it is determined from superallowed nuclear Fermi β decays, this dependence is given by [134]

$$G_F \tilde{V}_{uD}^e = G_F\,(1 + \epsilon_L^e + \epsilon_R^e)\,V_{uD}\,, \tag{5.2}$$

if we set the coefficients $\epsilon_i = 0$ in eqs. (5.1) and (5.2), we recover the SM Lagrangian.

We start our analysis with the one-meson decay modes $\tau^- \to P^- \nu_\tau$ ($P = \pi, K$) since these are the simplest semileptonic decays that can be calculated with the low-energy effective Lagrangian of Eq. (5.1). This simplicity arises from the fact that these are two-body decays so that the kinematics is fixed

and the form factors become decay constants. The expression for the decay rate for the process $\tau^- \to \pi^- \nu_\tau$ takes the form

$$\begin{aligned}\Gamma(\tau^- \to \pi^- \nu_\tau) &= \frac{G_F^2 |\tilde{V}_{ud}^e|^2 f_\pi^2 m_\tau^3 S_{EW}}{16\pi} \left(1 - \frac{m_\pi^2}{m_\tau^2}\right)^2 \\ &\times \left(1 + \delta_{\rm em}^{\tau\pi} + 2\Delta^{\tau\pi} + \mathcal{O}(\epsilon_i^\tau)^2 + \mathcal{O}(\delta_{\rm em}^{\tau\pi}\epsilon_i^\tau)\right),\end{aligned} \tag{5.3}$$

where f_π is the pion decay constant [2], S_{EW} resums the short-distance electroweak corrections, the quantity $\delta_{\rm em}^{\tau\pi}$ accounts for the electromagnetic radiative corrections and the term $\Delta^{\tau\pi}$ contains the tree-level NP corrections that arise from the Lagrangian in Eq. (5.1)[3] that are not absorbed in $\tilde{V}_{ud}^e$. For the channel $\tau^- \to K^- \nu_\tau$, the decay rate is that of Eq. (5.3) but replacing $\tilde{V}_{ud}^e \to \tilde{V}_{us}^e$, $f_\pi \to f_K$, $m_\pi \to m_K$, and $\delta_{\rm em}^{\tau\pi}$ and $\Delta^{\tau\pi}$ by $\delta_{\rm em}^{\tau K}$ and $\Delta^{\tau K}$, respectively.

As we will see, the inclusion of the one-meson decay modes in the analysis will be very useful since it helps constraining some combinations of Wilson coefficients involving the couplings ϵ_L and ϵ_R.

Now we continue our discussion with the two-meson decay modes $\tau^- \to (PP')^- \nu_\tau$. The resulting partial decay width for these decays is given by (the variable s is the invariant mass of the corresponding two-meson system):

$$\begin{aligned}\frac{d\Gamma}{ds} &= \frac{G_F^2 |\tilde{V}_{uD}^e|^2 m_\tau^3 S_{EW}}{384\pi^3 s} \left(1 - \frac{s}{m_\tau^2}\right)^2 \lambda^{1/2}(s, m_P^2, m_{P'}^2) \\ &\times \Big[\left(1 + 2(\epsilon_L^\tau - \epsilon_L^e + \epsilon_R^\tau - \epsilon_R^e)\right) X_{VA} \\ &+ \epsilon_S^\tau X_S + \epsilon_T^\tau X_T + (\epsilon_S^\tau)^2 X_{S^2} + (\epsilon_T^\tau)^2 X_{T^2} \Big],\end{aligned} \tag{5.4}$$

[2] We use here, for convenience, the 'electroweak' decays constant, ~ 130 MeV, which is $\sqrt{2}$ times larger than its chiral counterpart ~ 92 MeV.

[3] In Eq. (5.3) we have expanded up to linear order on the effective couplings ϵ_i^τ.

with

$$
\begin{aligned}
X_{VA} &= \frac{1}{2s^2}\Big\{3\left(C^S_{PP'}\right)^2|F_0^{PP'}(s)|^2\Delta^2_{PP'} \\
&\quad + \left(C^V_{PP'}\right)^2|F_+^{PP'}(s)|^2\left(1+\frac{2s}{m_\tau^2}\right)\lambda(s,m_P^2,m_{P'}^2)\Big\}\,, \\
X_S &= \frac{3}{s\,m_\tau}\left(C^S_{PP'}\right)^2|F_0^{PP'}(s)|^2\frac{\Delta^2_{PP'}}{m_d-m_u}\,, \\
X_T &= \frac{6}{s\,m_\tau}C^V_{PP'}\,\mathrm{Re}\big[F_T^{PP'}(s)\big(F_+^{PP'}(s)\big)^*\big]\lambda(s,m_P^2,m_{P'}^2)\,, \\
X_{S^2} &= \frac{3}{2\,m_\tau^2}\left(C^S_{PP'}\right)^2|F_0^{PP'}(s)|^2\frac{\Delta^2_{PP'}}{(m_d-m_u)^2}\,, \\
X_{T^2} &= \frac{4}{s}|F_T^{PP'}(s)|^2\left(1+\frac{s}{2\,m_\tau^2}\right)\lambda(s,m_P^2,m_{P'}^2)\,,
\end{aligned}
\tag{5.5}
$$

where $C^V_{PP'}$ and $C^S_{PP'}$ are the corresponding Clebsch-Gordan coefficients that we mentioned in chapter 1, $\lambda(x,y,z) = x^2+y^2+z^2-2xy-2xz-2yz$ is the usual Kallen function, and $\Delta_{PP'} = m_P^2 - m_{P'}^2$.

5.3 New Physics bounds from $\Delta S = 0$ decays

Before discussing the global analysis for $\Delta S = 0$ decays, which is the main goal for this section, we will see first what we can learn from the individual decay mode $\tau^- \to \pi^-\nu_\tau$. From the decay rate given in Eq. (5.3) and using as input [4] $f_\pi = 130.2(8)$ MeV from the lattice[5] [15] together with $\delta^{\tau\pi}_{\rm em} = 1.92(24)\%$ [160, 161, 162] and the PDG reported values [6] for: $|\tilde{V}^e_{ud}| = 0.97420(21)$ from nuclear β decays, the measured branching ratio $BR(\tau^- \to \pi^-\nu_\tau) = 10.82(5)\%$, $m_\pi = 0.13957061(24)$ GeV, $m_\tau = 1.77686(12)$ GeV, $\Gamma_\tau = 2.265\times10^{-12}$ GeV and $G_F = 1.16637(1)\times10^{-5}$ GeV^{-2}, we obtain the constraint:

$$
\epsilon^\tau_L - \epsilon^e_L - \epsilon^\tau_R - \epsilon^e_R - \frac{m_\pi^2}{m_\tau(m_u+m_d)}\epsilon^\tau_P = (-0.12\pm0.68)\times10^{-2}\,, \tag{5.6}
$$

[4] These radiative corrections have recently been updated in [157], using the results for the real photon emission in [158]. Employing also the updated V_{ud} value [159] ($|V_{ud}| = 0.97373\pm0.00031$), this results in the limit $\epsilon^\tau_L - \epsilon^e_L - \epsilon^\tau_R - \epsilon^e_R - \frac{m_\pi^2}{m_\tau(m_u+m_d)}\epsilon^\tau_P = (-0.15\pm0.72)\times10^{-2}$.

[5] The pion decay constant determined from data cannot be employed as it may be contaminated of NP effects.

where the uncertainty is dominated by f_π, followed by the error of branching ratio and the radiative corrections uncertainty.

Now we turn to the global analysis for $\Delta S = 0$ decays. For this task we perform a simultaneous fit to one and two meson strangeness-conserving exclusive hadronic decays of the tau lepton taking into account the following observables:

- the high-statistics $\tau^- \to \pi^-\pi^0\nu_\tau$ experimental data reported by the Belle collaboration [163], including both the normalized unfolded spectrum and the branching ratio.
- the branching ratio for the decay $\tau^- \to K^-K^0\nu_\tau$.
- the branching ratio for $\tau^- \to \pi^-\nu_\tau$.

The χ^2 function that is minimized in our fits is

$$\begin{aligned}\chi^2 \;=\; & \sum_k \left(\frac{\bar{N}_k^{\rm th} - \bar{N}_k^{\rm exp}}{\sigma_{\bar{N}_k^{\rm exp}}}\right)^2 + \left(\frac{BR_{\pi\pi}^{\rm th} - BR_{\pi\pi}^{\rm exp}}{\sigma_{BR_{\pi\pi}^{\rm exp}}}\right)^2 \\ & + \left(\frac{BR_{KK}^{\rm th} - BR_{KK}^{\rm exp}}{\sigma_{BR_{KK}^{\rm exp}}}\right)^2 + \left(\frac{BR_{\tau\pi}^{\rm th} - BR_{\tau\pi}^{\rm exp}}{\sigma_{BR_{\tau\pi}^{\rm exp}}}\right)^2 ,\end{aligned} \tag{5.7}$$

where $\bar{N}_k^{\rm th}$ relates the decay rate of Eq. (5.4) for $\tau^- \to \pi^-\pi^0\nu_\tau$ to the normalized distribution of the measured number of events through

$$\frac{1}{N_{\rm events}}\frac{dN_{\rm events}}{ds} = \frac{1}{\Gamma(\epsilon_i^\tau, \epsilon_j^e)}\frac{d\Gamma(s, \epsilon_i^\tau, \epsilon_j^e)}{ds}\Delta^{\rm bin} , \tag{5.8}$$

where $N_{\rm events}$ is the total number of measured events and $\Delta^{\rm bin}$ is the bin width. Additionally, $\bar{N}_k^{\rm exp}$ and $\sigma_{\bar{N}_k^{\rm exp}}$ in Eq. (5.7) are, respectively, the experimental number of events and the corresponding uncertainties in the k-th bin.

The bounds for the effective couplings characterizing the NP that result from our global fit are found to be (in the $\overline{MS}$ at a scale $\mu = 2$GeV)

$$\begin{pmatrix} \epsilon_L^\tau - \epsilon_L^e + \epsilon_R^\tau - \epsilon_R^e \\ \epsilon_R^\tau + \frac{m_\pi^2}{2m_\tau(m_u+m_d)}\epsilon_P^\tau \\ \epsilon_S^\tau \\ \epsilon_T^\tau \end{pmatrix} = \begin{pmatrix} 0.5 \pm 0.6^{+2.3\,+0.2}_{-1.8\,-0.1} \pm 0.4 \\ 0.3 \pm 0.5^{+1.1\,+0.1}_{-0.9\,-0.0} \pm 0.2 \\ 9.7^{+0.5}_{-0.6} \pm 21.5^{\,+0.0}_{-0.1} \pm 0.2 \\ -0.1 \pm 0.2^{+1.1\,+0.0}_{-1.4\,-0.1} \pm 0.2 \end{pmatrix} \times 10^{-2}, \tag{5.9}$$

where the first error is the statistical fit uncertainty, the second error –which is the dominant one– comes from the theoretical uncertainty associated to the pion vector form factor, while the third and fourth ones are systematic uncertainties coming, respectively, from the error of the quark masses and from the uncertainty associated to the corresponding tensor form factors.

The correlation matrix (ρ_{ij}) associated to the results of Eq. (5.9) is

$$\rho_{ij} = \begin{pmatrix} 1 & 0.684 & -0.493 & -0.545 \\ & 1 & -0.337 & -0.372 \\ & & 1 & 0.463 \\ & & & 1 \end{pmatrix}, \tag{5.10}$$

with $\chi^2/\text{d.o.f.} \sim 0.6$.

5.4 New Physics bounds from $|\Delta S| = 1$ decays

In this section we will perform a global analysis for $|\Delta S| = 1$ decays, but before we do so, following the ideas of the previous section, we will first discuss what we can learn from the individual decay mode $\tau^- \to K^- \nu_\tau$. As we have pointed out before, this strangeness-changing decay rate has the same form that the one in Eq. (5.3), thus, using that formula with the appropriate replacements and using the lattice calculation of $f_K = 155.7(7)$ MeV [15], the radiative corrections $\delta_{\text{em}}^{\tau K} = 1.98(31)\%$ [160, 161, 162] and $|\tilde{V}_{us}^e| = 0.2231(7)$, $BR(\tau^- \to K^- \nu_\tau) = 6.96(10) \times 10^{-3}$ and $m_K = 0.493677(16)$ GeV from the PDG [6] as numerical inputs, we obtain the constraint:

$$\epsilon_L^\tau - \epsilon_L^e - \epsilon_R^\tau - \epsilon_R^e - \frac{m_K^2}{m_\tau(m_u + m_s)}\epsilon_P^\tau = (-0.41 \pm 0.93) \times 10^{-2}\,. \tag{5.11}$$

where the error is dominated by f_K and $|V_{us}|$ followed by the branching ratio and the radiative corrections uncertainty [6].

Now for the global analysis for $|\Delta S| = 1$ decays, we proceed exactly as we did for the $\Delta S = 0$ case, that is, we perform a simultaneous fit to one and two meson strangeness-changing exclusive hadronic decays of the tau lepton taking into account the following observables:

- the $\tau^- \to K_S \pi^- \nu_\tau$ Belle spectrum [103] together with the measured branching ratio, $BR_{K\pi}^{\text{exp}} = 0.404(2)(13)\%$.

[6] These radiative corrections have recently been updated in [157], using the results for the real photon emission in [158], yielding $\epsilon_L^\tau - \epsilon_L^e - \epsilon_R^\tau - \epsilon_R^e - \frac{m_K^2}{m_\tau(m_u+m_s)}\epsilon_P^\tau = (-0.36 \pm 1.18) \times 10^{-2}$.

- the branching ratio of the decay $\tau^- \to K^-\eta\nu_\tau$ ($BR^{\rm exp}_{K\eta} = 1.55(8)\times 10^{-4}$) [6] [7] [8].
- the branching ratio of the decay $\tau^- \to K^-\nu_\tau$ ($BR^{\rm exp}_{\tau K} = 6.96(10)\times 10^{-3}$) [6].

In this case the χ^2 function that is minimized in our fits is given by

$$\begin{aligned}\chi^2 &= \sum_k \left(\frac{\bar{N}_k^{\rm th} - \bar{N}_k^{\rm exp}}{\sigma_{\bar{N}_k^{\rm exp}}}\right)^2 + \left(\frac{BR^{\rm th}_{K\pi} - BR^{\rm exp}_{K\pi}}{\sigma_{BR^{\rm exp}_{K\pi}}}\right)^2 \\ &+ \left(\frac{BR^{\rm th}_{K\eta} - BR^{\rm exp}_{K\eta}}{\sigma_{BR^{\rm exp}_{K\eta}}}\right)^2 + \left(\frac{BR^{\rm th}_{\tau K} - BR^{\rm exp}_{\tau K}}{\sigma_{BR^{\rm exp}_{\tau K}}}\right)^2 ,\end{aligned} \tag{5.12}$$

where now $\bar{N}_k^{\rm th}$ refers to the $K_S\pi^-$ decay mode and its expression is given by

$$\frac{dN_{\rm events}}{d\sqrt{s}} = \frac{N_{\rm events}}{\Gamma(\epsilon_i^\tau, \epsilon_j^e)} \frac{d\Gamma(\sqrt{s}, \epsilon_i^\tau, \epsilon_j^e)}{d\sqrt{s}} \Delta^{\rm bin} . \tag{5.13}$$

The bounds coming from the global fit to the $|\Delta S| = 1$ decays are given by [9]

$$\begin{pmatrix} \epsilon_L^\tau - \epsilon_L^e + \epsilon_R^\tau - \epsilon_R^e \\ \epsilon_R^\tau + \frac{m_K^2}{2m_\tau(m_u+m_s)}\epsilon_P^\tau \\ \epsilon_S^\tau \\ \epsilon_T^\tau \end{pmatrix} = \begin{pmatrix} 0.5 \pm 1.5 \pm 0.3 \\ 0.4 \pm 0.9 \pm 0.2 \\ 0.8^{+0.8}_{-0.9} \pm 0.3 \\ 0.9 \pm 0.7 \pm 0.4 \end{pmatrix} \times 10^{-2}, \tag{5.14}$$

where the first error is the statistical fit uncertainty while the second one is the systematic uncertainty coming from the tensor form factor. In contrast with the $\Delta S = 0$ case which is given in Eq. (5.14), the uncertainty associated

[7] While the $\tau^- \to K^-\eta\nu_\tau$ decay spectrum has been measured by Belle [164], unfolding detector effects has not been performed and we therefore have decided to include only the branching ratio in our study.

[8] The decay $\tau^- \to K^-\eta'\nu_\tau$ has not been detected yet, there is only an upper limit at the 90% confidence level placed by BaBar [165] and we therefore have decided to not include it in our analysis.

[9] The bounds are obtained in the $\overline{MS}$ at a scale $\mu = 2$GeV just as was done for the $\Delta S = 0$ case.

to the kaon vector form factor and to the quark masses is negligible.

The correlation matrix associated to the results of Eq. (5.14) is

$$\rho_{ij} = \begin{pmatrix} 1 & 0.854 & -0.147 & 0.437 \\ & 1 & -0.125 & 0.373 \\ & & 1 & -0.055 \\ & & & 1 \end{pmatrix}, \tag{5.15}$$

with $\chi^2/\text{d.o.f.} \sim 0.9$.

There are two important points to note from Eqs. (5.14) and (5.15), one is that the element ρ_{12} in Eq. (5.15) is large (it was also the largest element in Eq. (5.10)). This is a result of the strong correlation between the couplings ϵ_R^τ and ϵ_P^τ. The other point is that the ϵ_S^τ coupling is more competitive by an order of magnitude than the corresponding one for the $\Delta S = 0$ sector shown in Eq. (5.9). However the ϵ_T^τ coupling has now increased by about one order of magnitude and has changed sign which makes it a little less restrictive than in the $\Delta S = 0$ case. In the next section we will see that if we combine both ($\Delta S = 0$ and $|\Delta S| = 1$) kind of decays we take the advantages of each sector.

5.5 New Physics bounds from a global fit to both $\Delta S = 0$ and $|\Delta S| = 1$ sectors

In this section we take advantage of the previous two and perform a global fit to both $\Delta S = 0$ and $|\Delta S| = 1$ sectors simultaneously. This can only be done under the assumption of $d \leftrightarrow s$ universality (apart from the CKM mixing), which is quite reasonable as a realization of the celebrated Minimal Flavor Violation hypothesis [166]. The reason to do this is that, on the one hand, we will be able to disentangle the ϵ_R^τ and the ϵ_P^τ couplings, and on the other hand, we will benefit in our bounds for ϵ_T^τ and ϵ_S^τ from the strangeness-conserving sector and the strangeness-changing sector, respectively.

Since the correlation of parameters is important, we will take the $|V_{ud}|$ and $|V_{us}|$ elements of the CKM matrix to be used in this case correlated according to [15]

$$\frac{|V_{us}|}{|V_{ud}|} = 0.2313(5)\,. \tag{5.16}$$

For our analysis, we take $|V_{us}| = 0.2231(7)$ [6] and extract $|V_{ud}|$ through Eq. (5.16).

For our global fit the χ^2 function to be minimized includes all the quantities that we used for the separate analyses in Eqs. (5.7) and (5.12). In this case

the NP effective couplings are found to be (again in the $\overline{\text{MS}}$ scheme at scale $\mu = 2$ GeV)

$$\begin{pmatrix} \epsilon_L^\tau - \epsilon_L^e + \epsilon_R^\tau - \epsilon_R^e \\ \epsilon_R^\tau \\ \epsilon_P^\tau \\ \epsilon_S^\tau \\ \epsilon_T^\tau \end{pmatrix} =$$

$$\begin{pmatrix} 2.9 & \pm 0.6 & {}^{+1.0}_{-0.9} & \pm 0.6 & \pm 0.0 & \pm 0.4 & {}^{+0.2}_{-0.3} \\ 7.1 & \pm 4.9 & {}^{+0.5}_{-0.4} & {}^{+1.3}_{-1.5} & {}^{+1.2}_{-1.3} & \pm 0.2 & {}^{+40.9}_{-14.1} \\ -7.6 & \pm 6.3 & \pm 0.0 & {}^{+1.9}_{-1.6} & {}^{+1.7}_{-1.6} & \pm 0.0 & {}^{+19.0}_{-53.6} \\ 5.0 & {}^{+0.7}_{-0.8} & {}^{+0.8}_{-1.3} & {}^{+0.2}_{-0.1} & \pm 0.0 & \pm 0.2 & {}^{+1.1}_{-0.6} \\ -0.5 & \pm 0.2 & {}^{+0.8}_{-1.0} & \pm 0.0 & \pm 0.0 & \pm 0.6 & \pm 0.1 \end{pmatrix} \times 10^{-2} \,, \tag{5.17}$$

where the first error is the statistical error resulting from the fit, the second one comes from the uncertainty on the pion vector form factor, the third error corresponds to the CKM elements $|V_{ud}|$ and $|V_{us}|$, the fourth one is due to the radiative corrections $\delta_{\text{em}}^{\tau\pi}$ and $\delta_{\text{em}}^{\tau K}$, the fifth estimates the (uncontrolled) systematic uncertainty associated to the tensor form factor, while the last, is due to the errors of the quark masses.

The correlation matrix associated with Eq. (5.17) is given by

$$\mathcal{A} = \begin{pmatrix} 1 & 0.055 & 0.000 & -0.279 & -0.394 \\ & 1 & -0.997 & -0.015 & -0.022 \\ & & 1 & 0.000 & 0.000 \\ & & & 1 & 0.243 \\ & & & & 1 \end{pmatrix} , \tag{5.18}$$

with $\chi^2/\text{d.o.f.} \sim 1.38$.

As we see from Eq. (5.18) the price that we pay for disentangling the effective couplings ϵ_R^τ and ϵ_P^τ is that they are strongly correlated, but otherwise we gain in our capacity to constrain at the same time ϵ_T^τ and ϵ_S^τ.

As we have pointed out in chapters 3 and 4, the limits on the NP effective couplings can be translated into bounds for the corresponding NP scale in the following way

$$\Lambda \sim v \left(V_{uD} \epsilon_i \right)^{-1/2} , \tag{5.19}$$

where $v = (\sqrt{2} G_F)^{-1/2} \sim 246$ GeV. In this chapter we repeat this process for our present results which are shown in Eq. (5.17) and we find that our bounds can probe scales of $\mathcal{O}(5)$ TeV, which are quite restricted compared to the energy scale probed in semileptonic kaon decays i.e. $\mathcal{O}(500)$ TeV [134].

Chapter 6

Summary and conclusions

We have finally arrived at the conclusions of this thesis work. We divide our conclusions in three parts, which correspond to each of the central chapters of this work, namely: chapters 3, 4 and 5. There are of course some generalities that repeat for these three chapters, but we have decided to divide the conclusions in three because each chapter is important in its own way and also because some of our conclusions refer to very specific topics belonging to a very particular chapter.

6.1 Conclusions for chapter 3

In this chapter we focused on the $\tau^- \to (K\pi)^-\nu_\tau$ decays. Here we have studied the effect of NP in several interesting observables like Dalitz plots, decay spectrum and forward-backward asymmetry. The effect of this NP was encoded in the effective couplings $\hat{\epsilon}_S$ and $\hat{\epsilon}_T$ for which we have also set constraints. All these observables were calculated in the SM case as well, in order to be able to compare the way in which NP could manifest. Apart from that, we have three main conclusions for this chapter:

- In agreement with Ref. [101], we confirm that it is not possible to understand within the low-energy limit of the SMEFT framework the BaBar measurement [102] of the CP asymmetry, which disagrees at 2.8σ with the SM prediction [109]. As a consequence of our dedicated treatment of the uncertainties on the tensor form factor, we find an slightly weaker bound than in Ref. [101], $A_{CP}^{BSM} \leq 8 \cdot 10^{-7}$, which is anyway some three (five) orders of magnitude smaller than the theoretical uncertainty in its prediction (the error of the BaBar measurement). If the BaBar anomaly is confirmed, its explanation must be due to light

NP. A determination of this quantity with Belle-I data, together with the future measurement at Belle-II [18], will shed light on this puzzle.

- The bins number 5, 6 and 7 of the Belle measurement [103] of the $K_S\pi^-$ mass spectrum in $\tau^- \to K_S\pi^-\nu_\tau$ decays could not find an explanation using a scalar form factor obtained from the corresponding partial-wave of a meson-meson scattering coupled channels analysis [125, 115] [1]. We have shown here, for the first time, that non-standard scalar or tensor interactions produced by heavy NP are not capable of explaining these data points either. Again a caveat remains with respect to light NP effects, which are beyond the scope of this work.

- Current branching ratio and spectrum measurements of the $\tau^- \to K_S\pi^-\nu_\tau$ decays restrict the NP effective couplings, $\hat{\epsilon}_S$ and $\hat{\epsilon}_T$, as we have studied in this work for the first time. Our results are consistent with naive expectations: while the considered decays set bounds similar to those coming from hyperon semileptonic decays (which are at the level of a few TeV NP energy scale under reasonable assumptions), they are not competitive with (semi)leptonic Kaon decays, that could probe NP at a scale of order $\mathcal{O}(500)$ TeV for the case of scalar interactions. However, we must say that tensor interactions in $\tau^- \to (K\pi)^-\nu_\tau$ decays are probed with similar NP energy reach than in (semi)leptonic Kaon and hyperon decays. Therefore, the corresponding comparisons for $\hat{\epsilon}_T$ are meaningful tests of lepton universality and under this assumption tau decays can complement Kaon and hyperon physics in restricting tensor interactions.

6.2 Conclusions for chapter 4

In chapter 4 we have focused on the decay channel $\tau^- \to K^-K^0\nu_\tau$, but we have also mentioned very briefly some results about the decay channels $\tau^- \to K^-\eta^{(\prime)}\nu_\tau$ [2]. Similar to what we did in chapter 3, in chapter 4 we have studied the effect of NP in several interesting observables like Dalitz plots, decay spectrum and forward-backward asymmetry. We calculated the SM result for all those observables as well. This was in order to have a comparison that could shed some light disentangling the potential effects introduced

[1] The effect of the otherwise dominant vector form factor is kinematically suppressed in this region and can never give such a strong enhancement as observed in these data points.

[2] As we have pointed out in chapter 4 the decays $\tau^- \to K^-\eta^{(\prime)}\nu_\tau$ are going to be discussed in much more detail in a future thesis presented by Alejandro Miranda.

by non-standard interactions (NSI).

We have focused our analysis on setting bounds on the corresponding New Physics couplings from the current experimental measurements of these decays. This has been possible due to the satisfactory knowledge we have on the necessary Standard Model hadronic input, the form factors. For the description of the participating vector and scalar form factors, we have employed previous results based on constraints from Chiral Perturbation Theory supplemented by dispersion relations and experimental data. On the contrary, there are no experimental data to help us constructing the required tensor form factor and, therefore, it has been described under theoretical arguments solely.

Our main results for this chapter can be found in table 4.1, where we show limits for the NP effective couplings $\hat{\epsilon}_S$ and $\hat{\epsilon}_T$ coming from different decays of the tau lepton into two mesons.

Despite our bounds on the NP couplings coming only from the BR constraints are not as precise as those placed, for example, from semileptonic kaon decays [134], we see that when we introduce fits including spectra we gain a lot in our constraining power. This has been possible in chapter 3 and 5, where we have high-quality data for some of the decay channels, however it has not been possible in chapter 4, where more data is required. In this respect we hope our works can serve as a motivation for the experimental tau physics groups at Belle-II to measure the different observables we have discussed.

6.3 Conclusions for chapter 5

In this chapter we took advantage from many of the previous results of chapters 3 and 4 in which we have discussed extensively tau decays into two mesons. Here we have changed directions and instead of performing particular analyses for each of the decay modes as we did before, we have performed a global analysis for all of them at the same time, we have also included tau decays into one meson in this analysis.

Our work divides naturally in three sections: an analysis for strangeness-conserving decays ($\Delta S = 0$), an analysis for strangeness-changing decays ($|\Delta S| = 1$) and finally a global analysis for both sectors simultaneously.

Our main results here are found in Eqs. (5.9), (5.14) and (5.17), which represent our bounds for the NP effective couplings for the strangeness-conserving sector, the strangeness-changing sector, and the global case, respectively. In general, our bounds on the NP couplings, are competitive. This is specially the case for the combination of couplings $\epsilon_L^\tau - \epsilon_L^e + \epsilon_R^\tau - \epsilon_R^e$,

which is found to be in accord with the constraints placed from a combination of inclusive and exclusive (strangeness-conserving) tau decays [128], and for ϵ_T^τ, that can even compete with the constraints set by the theoretically cleaner $K_{\ell 3}$ decays (for the comparison, lepton flavor universality is assumed as mentioned in chapter 5). Our separate fits to both $\Delta S = 0$ and $|\Delta S| = 1$ decays reflect that we are not sensitive to the coefficients ϵ_P^τ and ϵ_R^τ individually but rather to a combination of them. It is still possible to fit them separately performing a global fit to both $\Delta S = 0$ and $|\Delta S| = 1$ sectors simultaneously (relying on the well-motivated and experimentally supported hypothesis of minimal flavor violation). However, they carry large error bars whose origin stems from the very strong correlation between them. As for ϵ_S^τ, it is impossible to compete with the limits coming from $K_{\ell 3}$ decays. Our limit, however, is found to be much weaker than previous constraints from tau decays. This is due to the fact that, for lack of experimental data, the decay $\tau^- \to \pi^- \eta \nu_\tau$ has not been taken into account in our analysis. This different bounds on ϵ_S^τ obtained with and without the $\pi\eta$ mode thus increase the interest of its measurement and demands refined theoretical descriptions accordingly.

Appendices

Appendix A

The CCWZ Formalism

In this appendix we present in some detail the CCWZ formalism which has been used in chapter 2 for the construction of ChPT and which is used more generally in the construction of effective Lagrangians with SSB.

This general formalism was worked out by Callan, Coleman, Wess and Zumino (CCWZ) [64, 65]. As we will see in what follows the most important part in the construction of an effective Lagrangian is the spontaneous symmetry breaking pattern, that is, given a group of symmetries G for a theory and a subgroup H of those symmetries respected by the vacuum, a general effective Lagrangian can be constructed following some simple arguments.

For convenience and to illustrate some points, take the global symmetry group $G = O(N)$ and the subgroup $H = O(N-1)$. Let us consider $\Xi(x) \in G$. We can parametrize any vector ϕ in terms of the Ξ matrix as is shown in the following equation

$$\phi(x) = \Xi(x) \begin{pmatrix} 0 \\ 0 \\ . \\ . \\ . \\ 0 \\ v \end{pmatrix} , \tag{A.1}$$

the matrix Ξ is not unique since Ξh, where $h \in H$ gives the same field configuration due to the invariance of the vacuum under H transformations. This means that $\phi(x)$ can also be described by $\Xi(x)h(x)$, where $h(x)$ has the form:

$$h(x) = \begin{pmatrix} h'(x) & 0 \\ 0 & 1 \end{pmatrix} , \tag{A.2}$$

with $h'(x)$ an arbitrary $O(N-1)$ matrix. You can see this explicitly in the following equation

$$\begin{pmatrix} h'(x) & 0 \\ 0 & 1 \end{pmatrix} \begin{pmatrix} 0 \\ 0 \\ . \\ . \\ . \\ 0 \\ v \end{pmatrix} = \begin{pmatrix} 0 \\ 0 \\ . \\ . \\ . \\ 0 \\ v \end{pmatrix} . \tag{A.3}$$

The CCWZ prescription consists in choosing a set of broken generators X and taking

$$\Xi(x) = e^{iX\cdot\pi(x)} . \tag{A.4}$$

For the case $N = 3$, our symmetry group is $G = O(3)$ and the subgroup that leaves the vacuum invariant is $O(2)$. In this simple case the generators of G are J_1, J_2 and J_3. If we choose J_3 as the unbroken generator, then $\Xi(x)$ takes the following form

$$\Xi(x) = e^{i[J_1\pi_1(x)+J_2\pi_2(x)]} . \tag{A.5}$$

Under a global symmetry transformation g, the matrix $\Xi(x)$ is transformed to $g\Xi(x)$. This new matrix $g\Xi(x)$ is no longer in standard form (see eq. (A.4)), but can be written as

$$g\Xi = \Xi' h , \tag{A.6}$$

where we have used the fact that two matrices $g\Xi$ and Ξ' differ only by an H transformation.

We can rewrite eq. (A.6) in the following way

$$\Xi(x) \to g\Xi(x)h^{-1}(g, \Xi(x)) . \tag{A.7}$$

Eqs. (A.4) and (A.7) give the CCWZ choice for the Goldstone boson fields, and its transformation law. These two formulas are the basic ingredients that we used in chapter 2 when we discussed ChPT.

A.1 Application of the formalism to the QCD Chiral Lagrangian

As we have pointed out, the important thing in the formulation is the symmetry breaking pattern. In this case we have

$$G \equiv SU(3)_L \times SU(3)_R \to H \equiv SU(3)_V . \tag{A.8}$$

The generators of G are T_L^a and T_R^a and those of H are $T^a = T_L^a + T_R^a$.

There are two important basis that we want to discuss: the ξ-basis and the Σ-basis.

1. ξ-basis:

In this case the broken generators are chosen as $X^a = T_L^a - T_R^a$. The $SU(3)_L \times SU(3)_R$ transformation can be represented as

$$g = \begin{pmatrix} L & 0 \\ 0 & R \end{pmatrix} , \tag{A.9}$$

where L and R are $SU(3)_L$ and $SU(3)_R$ transformations, respectively. For the case of the unbroken symmetry transformations we have the same form that in eq. (A.9), except that in this case $L = R = U$,

$$h = \begin{pmatrix} U & 0 \\ 0 & U \end{pmatrix} . \tag{A.10}$$

Then, with our choice of broken generators, the CCWZ prescription which is shown in eq. (A.4) takes the form

$$\Xi(x) = e^{iX\cdot\pi(x)} = \exp i \begin{pmatrix} T\cdot\pi & 0 \\ 0 & -T\cdot\pi \end{pmatrix} = \begin{pmatrix} \xi(x) & 0 \\ 0 & \xi^\dagger(x) \end{pmatrix} , \tag{A.11}$$

where $\xi = e^{iT\cdot\pi}$. Similarly, the transformation rule shown in eq. (A.7), for this case takes the form

$$\begin{pmatrix} \xi(x) & 0 \\ 0 & \xi^\dagger(x) \end{pmatrix} \to \begin{pmatrix} L & 0 \\ 0 & R \end{pmatrix} \begin{pmatrix} \xi(x) & 0 \\ 0 & \xi^\dagger(x) \end{pmatrix} \begin{pmatrix} U^{-1} & 0 \\ 0 & U^{-1} \end{pmatrix} , \tag{A.12}$$

therefore, ξ transforms in the following way

$$\xi(x) \to L\xi(x)U^{-1} = U(x)\xi(x)R^\dagger . \tag{A.13}$$

2. Σ-basis:

In this case we choose $X^a = T_L^a$ as the broken generators, then the CCWZ prescription takes the form

$$\Xi(x) = e^{iX\cdot\pi(x)} = \exp i \begin{pmatrix} T\cdot\pi & 0 \\ 0 & 0 \end{pmatrix} = \begin{pmatrix} \Sigma(x) & 0 \\ 0 & 1 \end{pmatrix} , \tag{A.14}$$

where $\Sigma = e^{iT\cdot\pi}$. Now the transformation law in eq. (A.7) takes the form

$$\begin{pmatrix} \Sigma(x) & 0 \\ 0 & 1 \end{pmatrix} \to \begin{pmatrix} L & 0 \\ 0 & R \end{pmatrix} \begin{pmatrix} \Sigma(x) & 0 \\ 0 & 1 \end{pmatrix} \begin{pmatrix} U^{-1} & 0 \\ 0 & U^{-1} \end{pmatrix} , \tag{A.15}$$

thus, $U = R$, and

$$\Sigma(x) \to L\Sigma(x)R^\dagger \,. \tag{A.16}$$

From eq. (A.13) and eq. (A.16), we see that ξ and Σ are related by

$$\Sigma(x) = \xi^2(x) \,. \tag{A.17}$$

In chapter 2, when we discussed ChPT, we used the notation $U(X)$ and $u(x)$ instead of $\Sigma(x)$ and $\xi(x)$, respectively. Our conclusion there was that we can parametrize the Goldstone boson fields in the following way

$$U(\Phi) = u(\Phi)^2 = \exp\left(i\frac{\sqrt{2}\Phi}{f}\right) , \tag{A.18}$$

where

$$\Phi(x) \equiv \sqrt{2}T^a\phi^q(x) = \frac{\lambda^a\phi^a}{\sqrt{2}} = \begin{pmatrix} \frac{1}{\sqrt{2}}\pi^0 + \frac{1}{\sqrt{6}}\eta_8 & \pi^+ & K^+ \\ \pi^- & -\frac{1}{\sqrt{2}}\pi^0 + \frac{1}{\sqrt{6}}\eta_8 & K^0 \\ K^- & \bar{K^0} & -\frac{2}{\sqrt{6}}\eta_8 \end{pmatrix} . \tag{A.19}$$

Appendix B

Spin and parity of hadronic currents

Since we have discussed a lot about the structure of hadronic currents along this thesis work, specially in chapters 4, 5 and 6, it might be worthwhile to have a general discussion of hadronic matrix elements in this appendix. The form of the hadronic matrix elements, or more importantly, their vanishing, depends only on their symmetry properties under parity (P). So, let us first remember the transformation of Dirac bilinears under parity:

F	1	γ^0	γ^i	σ^{0i}	σ^{ij}	$\gamma^0\gamma^5$	γ^5
F_P	1	γ^0	$-\gamma^i$	$-\sigma^{0i}$	σ^{ij}	$-\gamma^0\gamma^5$	$-\gamma^5$

Table B.1: Transformation of Dirac bilinears under P

where F stands for the different choices of Dirac bilinears and F_P stands for their corresponding transformations under parity. Recall that the mesons like pions, kaons and the etas are pseudoscalar particles so that they have quantum numbers $J^P = 0^-$, recall also that the vacuum has quantum numbers $J^P = 0^+$. This is basically all we need to determine the general form of the hadronic matrix elements. Let us start with the elements with only one pseudoscalar meson as an initial or as final state, that is, matrix elements of the form $\langle 0|\mathcal{V}^\mu(0)|M(p)\rangle$ and $\langle 0|\mathcal{A}^\mu(0)|M(p)\rangle$, where M represents any meson in the 0^- octet and $\mathcal{V}^\mu$ and $\mathcal{A}^\mu$ represent vector and axial vector currents, respectively (the tensor structure is not needed in this simple case). These structures are fundamental in the study of $\pi_{\ell 2}$, $K_{\ell 2}$ and $\tau^- \to P^-\nu_\tau$ ($P = \pi, K$) decays.

The spin and parity properties of vector and axial vector currents are

summarized in the following equation:

$$\begin{aligned} J^P(\mathcal{V}^0) = 0^+, \quad J^P(\mathcal{V}) = 1^-\,, \\ J^P(\mathcal{A}^0) = 0^-, \quad J^p(\mathcal{A}) = 1^+\,, \end{aligned} \tag{B.1}$$

therefore, the time component of the matrix element $\langle 0|\mathcal{V}^\mu|M(p)\rangle$ should have $J^P = 0^-$ and the spatial component should have $J^P = 1^+$. On the other hand, this matrix element can depend only on the four-momentum p^μ, but p^μ has spin and parity quantum numbers $J^P = (0^+, 1^-)$. The conclusion of this analysis is that one cannot construct any quantity that depends only on one four-vector and transforms like $J^P = (0^-, 1^+)$. Hence this matrix element must be zero.

For the axial-vector current a similar analysis shows that $\langle 0|\mathcal{A}^\mu|M(p)\rangle$ should have spin and parity quantum numbers $J^P = (0^+, 1^-)$, but these are precisely the spin-parity quantum numbers of p^μ. Then, this matrix element is proportional to the four-momentum p^μ.

We summarize the previous two results in the following equation,

$$\begin{aligned} \langle 0|\mathcal{V}^\mu(0)|M(p)\rangle = 0\,, \\ \langle 0|\mathcal{A}^\mu(0)|M(p)\rangle = \sqrt{2} i f_M p^\mu\,, \end{aligned} \tag{B.2}$$

where f_M is the decay constant of the meson M. Note that the proportionality with respect to p^μ could just have been obtained by Lorentz invariance, in this case this is trivial, but when we have more mesons things complicate a little bit, as we will see next.

When we have two pseudoscalar mesons in the initial (final) state and the vacuum in the final (initial) state, or equivalently, one meson in the initial state and one meson in the final state, the structures that we obtain for the hadronic matrix elements become richer. These structures are fundamental in the understanding of $\pi_{\ell 3}$, $K_{\ell 3}$ and $\tau \to (PP')^- \nu_\tau$ decays. An argument analogue to the one in the previous paragraph shows that for the spin-parity quantum numbers of the matrix element $\langle M_b(k)|\mathcal{V}^\mu|M_a(p)\rangle$ we have $J^P = (0^+, 1^-)$, which is the way four-momentum vectors transform. Thus, we can write these elements as the more general combination of all the four-momentum available, as we show in the following equation:

$$\langle M_b(k)|\mathcal{V}^\mu(0)|M_a(p)\rangle = f_1 p^\mu + f_2 k^\mu\,, \tag{B.3}$$

where f_1 and f_2 are form factors. There are of course different parametrizations for the previous expression, one that it is used frequently is the following,

$$\langle M_b(k)|\mathcal{V}^\mu(0)|M_a(p)\rangle = f_+(p+k)^\mu + f_-(p-k)^\mu\,. \tag{B.4}$$

There is an important difference between the objects f_1 and f_2 (or f_+ and f_-) that appear in the two-meson case and the object f_M that we have defined in the one meson case. All these objects must be Lorentz scalars. For the case of f_M the only scalar that can be constructed from the parameters of the problem is p^2, which is equal to the mass of the meson m_M, that is, a constant. As a consequence f_M is also a constant. On the other hand, for the matrix element involving two mesons, we can define three Lorentz invariants, i.e., p^2, k^2 and $k \cdot p$. The first two are constants, related to the masses of the two mesons. The third one, which comes from $q^2 = (p-k)^2$, is a dynamical variable. So, the form factors f_1 and f_2 will depend on the momentum transfer q^2 between the two mesons.

On the other hand, the matrix element $\langle M_b(k)|\mathcal{A}^\mu|M_a(p)\rangle$ has spin-parity quantum numbers $J^P = (0^-, 1^+)$ so that there is no way to construct this quantum numbers with the four-momentum vectors p^μ and k^μ. Therefore, we have:

$$\langle M_b(k)|\mathcal{A}^\mu(0)|M_a(p)\rangle = 0\,. \tag{B.5}$$

Finally, let us discuss the tensor structure. As we mentioned previously, this structure does not appear in the one meson case, but it becomes important when we have two or more mesons. It has the general form $\langle M_b(k)|\mathcal{T}^{\mu\nu}|M_a(p)\rangle$, where $\mathcal{T}^{\mu\nu}$ is a tensor current that is proportional to $\sigma^{\mu\nu} = i[\gamma^\mu, \gamma^\nu]/2$. Note that $\sigma^{\mu\nu}$ is antisymmetric, thus, the matrix element must be proportional to an antisymmetric combination of the two four-momentum vectors involved. This leads naturally to the following expression

$$\langle M_b(k)|\mathcal{T}^{\mu\nu}(0)|M_a(p)\rangle = i f_T(p^\mu k^\nu - p^\nu k^\mu)\,, \tag{B.6}$$

where f_T is the tensor form factor, which, again, is a function of q^2 just like f_1 and f_2 (or f_+ and f_-).

Appendix C

Form Factors

In this appendix, for the convenience of the reader, we discuss in more depth the form factors presented along this work. Here we pay special attention to the scalar and vector form factors since the tensor form factors for the different decay channels have been discussed in great detail in the text.

As we have explained before, all form factors are calculated using chiral perturbation theory and dispersion relations [1].

We start our discussion with the vector form factor for the decay into a pair of pions since it was the first one to be studied following this formalism.

The vector form factor for the $\pi\pi$ case was first analyzed using ChPT with resonances in [167] and has later been revisited, within a dispersive framework, in refs. [168, 169, 147]. It is defined as

$$\langle \pi^0\pi^-|\bar{d}\gamma^\mu u|0\rangle = \sqrt{2}F_+(s)(p_{\pi^-}-p_{\pi^0})^\mu\,, \tag{C.1}$$

where $s \equiv q^2 \equiv (p_{\pi^-}+p_{\pi^0})^2$. At $s>0$, $F_+(s)$ is experimentally known from the decay $\tau^- \to \pi^-\pi^0\nu_\tau$ and (through an isospin rotation) from $e^+e^- \to \pi^+\pi^-$, while the elastic $e^-\pi^+$ scattering provides information at $s<0$.

Near threshold, the vector form factor $F_+^{\pi\pi}(s)$ is well described by ChPT. At one loop, it is given by [63]

$$F_+^{\pi\pi}(s) = 1+\frac{2L_9^r(\mu)}{f_\pi^2}s-\frac{s}{96\pi^2 f_\pi^2}\left[A\left(\frac{m_\pi^2}{s},\frac{m_\pi^2}{\mu^2}\right)+\frac{1}{2}A\left(\frac{m_K^2}{s},\frac{m_K^2}{\mu^2}\right)\right]\,, \tag{C.2}$$

where

$$A\left(\frac{m_P^2}{s},\frac{m_P^2}{\mu^2}\right) = \ln\left(\frac{m_P^2}{\mu^2}\right)+\frac{8m_P^2}{s}-\frac{5}{3}+\sigma_P^3\ln\left(\frac{\sigma_P+1}{\sigma_P-1}\right) \tag{C.3}$$

[1] In three-meson tau decays, dispersive formulations have been followed for the $KK\pi$ mode in ref. [114] but the results obtained in Resonance Chiral Theory are not dispersive [88, 89, 90, 92].

contain the loop contributions. The phase-space factor σ_P is given by

$$\sigma_P = \sqrt{1 - \frac{4m_P^2}{s}}\,, \tag{C.4}$$

and the $L_9^r(\mu)$ term is an $O(p^4)$ chiral counterterm renormalized at the scale μ, which is of the order of the $\rho(770)$ meson mass.

The previous result for $F_+^{\pi\pi}(s)$ is of course valid for very low energies (near threshold), where ChPT is good enough. For higher energies, we need to incorporate the new (heavier) degrees of freedom in the calculation. These are the different resonances that emerge in the energies under consideration and the formalism to incorporate them explicitly is Resonance Chiral Theory, RChT [74, 75].

For the $\pi\pi$ channel, the $\rho(770)$ resonance dominates the vector form factor. At leading order in powers of $1/N_C$, which is $O(p^4)$ in the chiral expansion, we have:

$$F_+^{\pi\pi}(s) = 1 + \frac{F_V G_V}{f_\pi^2}\frac{s}{M_\rho^2 - s}\,, \tag{C.5}$$

where the couplings F_V and G_V measure the strength of the $\rho\gamma$ and $\rho\pi\pi$ couplings, respectively. Assuming that the form factor vanishes when $s \to \infty$ we obtain the following condition

$$F_V G_V = f_\pi^2\,, \tag{C.6}$$

that implies the Vector Meson Dominance (VMD) result in the vanishing width approximation:

$$F_+^{\pi\pi}(s) = \frac{M_\rho^2}{M_\rho^2 - s}\,. \tag{C.7}$$

Taylor-expanding the previous equation allows to estimate the next-to-leading order chiral coupling L_9^r

$$L_9^r(M_\rho) = \frac{F_V G_V}{2M_\rho^2} = \frac{f_\pi^2}{2M_\rho^2} \sim 7.2 \cdot 10^{-3}\,, \tag{C.8}$$

in good agreement with its phenomenological determination. This accord shows neatly the the dominant physical effect in the pion vector form factor is given by the $\rho(770)$ meson exchange.

The combination of the ChPT and VMD results yields an improved description of this form factor

$$f_+^{\pi\pi}(s) = \frac{M_\rho^2}{M_\rho^2 - s} - \frac{s}{96\pi^2 f_\pi^2}\left[A_\pi(s,\mu^2) + \frac{1}{2}A_K(s,\mu^2)\right]\,. \tag{C.9}$$

The VMD result dominates in the large number of colours limit and resums an infinite tower of local interactions in ChPT to all orders. The second term includes loop contributions, which are subleading in that expansion.

The $\pi\pi$ and KK final-state interactions can be resummed to all orders using unitarity and analyticity, leading to the famous Omnès exponentiation of the loop functions

$$f_+^{\pi\pi}(s) = \frac{M_\rho^2}{M_\rho^2 - s} \exp\left\{ -\frac{s}{96\pi^2 f_\pi^2} \left[A_\pi(s,\mu^2) + \frac{1}{2} A_K(s,\mu^2) \right] \right\} . \tag{C.10}$$

Still, another subleading effect in $1/N_C$ is fundamental to understand phenomenology, and that is the finite ρ meson width. This energy-dependent function is given in terms of the imaginary part of the A_P loop functions [170]

$$\begin{aligned} \Gamma_\rho(s) &= -\frac{M_\rho s}{96\pi^2 f_\pi^2} \mathrm{Im} \left[A_\pi(s, M_\rho^2) + \frac{1}{2} A_K(s, M_\rho^2) \right] \\ &= \frac{M_\rho s}{96\pi f_\pi^2} \left[\sigma_\pi^3(s)\theta(s - 4m_\pi^2) + \frac{1}{2}\sigma_K^3(s)\theta(s - 4m_K^2) \right] . \end{aligned} \tag{C.11}$$

Then, the Omnès-resummed form factor will be

$$f_+^{\pi\pi}(s) = \frac{M_\rho^2}{M_\rho^2 - s - i M_\rho \Gamma_\rho(s)} \exp\left\{ -\frac{s}{96\pi^2 f_\pi^2} \mathrm{Re} \left[A_\pi(s,\mu^2) + \frac{1}{2} A_K(s,\mu^2) \right] \right\} , \tag{C.12}$$

where only the real part of the loop function was exponentiated in order to avoid double counting its imaginary part (already present in the width) [2].

The previous form factor can be extended to include ρ excitations in a straightforward way (see [147] and references therein).

In the more refined dispersive description, the previous form factor would act as seed, giving the input phase. This dispersive representation will be introduced in the following.

The key observation is Watson's final-state interactions theorem [143], stating that the form factor phase, in the elastic region, equals that of the $\pi\pi$ scattering. Thus, the form factor can be solved analytically in terms of the corresponding phase shift. Explicitly, the Omnès equation [171] does the job

$$f_+^{\pi\pi}(s) = \Omega(s) = \exp\left(\frac{s}{\pi} \int_{4m_\pi^2}^{\infty} ds' \frac{\delta_1^1(s')}{s'(s' - s)} \right) , \tag{C.13}$$

[2] It is certainly possible to resum in the propagator also the real part of the loop function (as strict unitarity and analyticity demand). The difference between both approaches is numerically negligible.

where $\delta_1^1(s)$ is the isovector spin-one $\pi\pi$ scattering phaseshift, which encapsulates the ρ meson physics.

This phase can be written $\tan\delta_1^1(s) = \frac{\mathrm{Im} f_+^{\pi\pi}(s)}{\mathrm{Re} f_+^{\pi\pi}(s)}$, and the resonances' parameters determining $f_+^{\pi\pi}(s)$ (and $\delta_1^1(s)$, subsequently) can be fitted to data.

Noteworthy, the dispersion relation determines the form factor at a given energy provided its phase is known everywhere. While the known asymptotic behaviour of the form factor is required in the UV, its experimental knowledge beyond $\sim$ 2 GeV is not sufficient to support an Omnés solution. Being this the case (always), it is extremely convenient to subtract the dispersion relation. This enhances the weight of the middle- and low-energy regions (with both good experimental and theoretical knowledge) and reduces the impact of the multi-GeV realm. Specifically, a thrice-subtracted form factor is ideal (nothing is gained with an extra subtraction and two of them are not accurate enough)

$$f_+^{\pi\pi}(s) = \exp\left[\alpha_1 s + \frac{\alpha_2}{2}s^2 + \frac{s^3}{\pi}\int_{4m_\pi^2}^{\infty} ds' \frac{\delta_1^1(s')}{(s')^3(s'-s-i0)}\right], \qquad \text{(C.14)}$$

where $\alpha_{1,2}$ are subtraction constants (determining low-energy observables: the pion radius and slope parameters) and the first subtraction ensures $f_+^{\pi\pi}(0) = 1$, corresponding to the conservation of the vector current.

Fig. C.1 shows the modulus and phase of the dispersive $\pi\pi$ vector form factor [169], compared to the Guerrero-Pich parametrization [167].

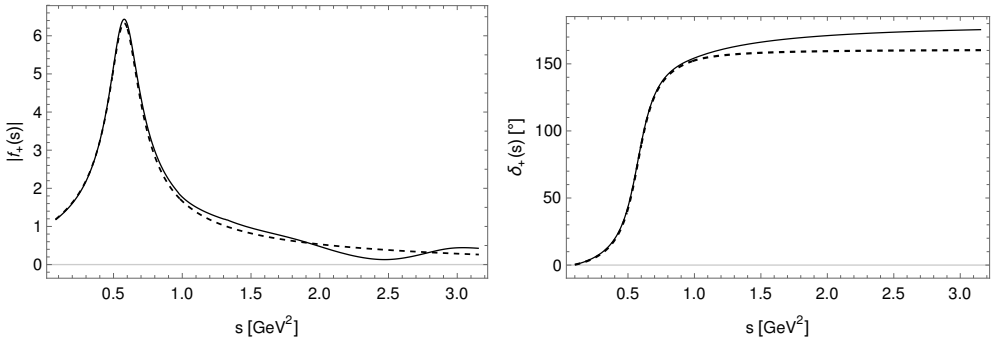

Figure C.1: Modulus and phase of the pion vector form factor, $f_+^{\pi\pi}(s)$. The solid line corresponds to the dispersive representation used in ref. [169] while the dashed line corresponds to the Guerrero-Pich parametrization [167].

The corresponding form factor for the $K\pi$ case was shown in Fig. 3.1. The vector form factors for the $\pi\pi$ and $K\pi$ channels are the basis to build the corresponding ones for the $\eta\pi$, $K\bar{K}$ and $\eta'\pi$ systems [145, 147], and the $K\eta$ and $K\eta'$ channels [144], respectively.

In the case of the scalar form factors, coupled-channel effects cannot be neglected, which makes these studies much more complicated. For the strangeness-changing case these form factors $(K\pi, K\eta, K\eta')$ were obtained in [124], as application of the corresponding results for the S-wave meson-meson scattering amplitudes [125]. For the strangeness-conserving cases $(\pi\pi, \eta\pi, \eta'\pi, K\bar{K})$ we have used the results in refs. [174, 176], obtained by an analogous procedure [3]. The form factors discussed in this appendix have also been used in another type of new physics searches in tau lepton decays, in those violating lepton flavor [177, 178, 179].

[3] As we recalled previously, the tensor form factors were treated in detail along the main text and we will know dwell further into them here.

Appendix D

Polarization effects in the decay $\tau^- \to \pi^-\ell^+\ell^-\nu_\tau$

This appendix is based on work started during my master thesis [180]. The purpose of such work was to study the effects of the polarization of the initial Tau lepton in the decay $\tau^- \to \pi^-\ell^+\ell^-\nu_\tau$. The unpolarized case has been studied in Ref. [181].

The calculation of the branching ratio for the $\tau^- \to \pi^-\ell^+\ell^-\nu_\tau$ decay and its measurement are important for the following reasons:

- Clean enviroment for the study of low energy hadronic interactions.
- Important for the study of $\tau \to \pi\gamma\nu$, which is notable background for $\tau \to \mu\gamma$ (due to mis-ID of $\pi \to \mu$). $\tau \to \pi\gamma\nu$ is also important in the search of $\tau \to \pi\eta\nu$ because the η can be detected in its desintegration to two photons, so that one can confuse the photon in $\tau \to \pi\gamma\nu$ together with another photon with the signal of a η particle. I must say that there are mexican physicist working in the search of $\tau \to \pi\eta\nu$, so the work done here is an important background for them.
- $\tau \to \ell^+\ell^-\pi\nu_\tau$ is also background for $\tau \to \ell^-\ell^-\ell^+$ (again due to mis-ID of $\pi \to \mu$).
- Search for long lived Sterile neutrino [182, 183].

The conclusion of the previous comments is that it is important to study this decay because it is background for several processes in the search for new physics (lepton flavor violation, sterile neutrinos and genuine second class currents, for example). Adding polarization effects just enriches the process and complements previous studies.

There are five Feynmann diagrams contributing to the amplitude in this

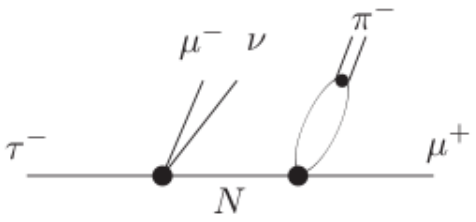

Figure D.1: Possible sterile neutrino interaction.

process as can be seen in figure D.2: the first three are model independent, and together they contribute to the so called inner bremsstralhung (IB) amplitude, the other two diagrams depend on the model we use for describing the vertex $\gamma^* W \pi^-$, and for this reason the amplitude corresponding to those is called model dependent (also called structure dependent, because it corresponds to the non point-like part of the interaction) amplitude.

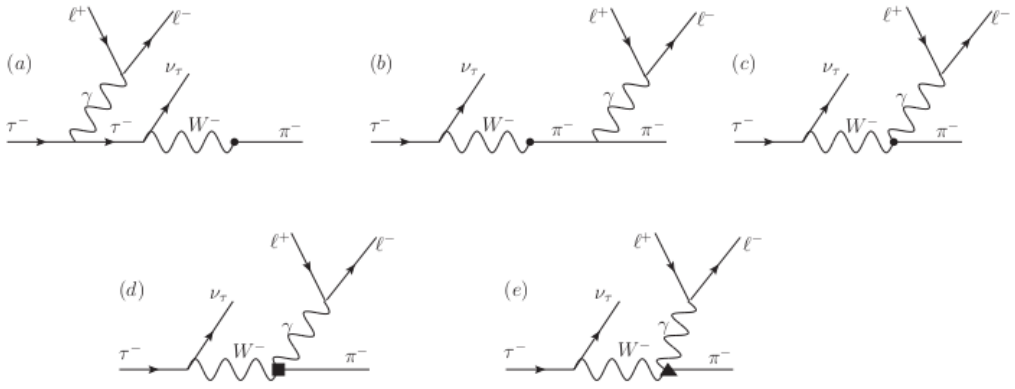

Figure D.2: Feynman diagrams for the $\tau^- \to \pi^- \ell^+ \ell^- \nu_\tau$ decay

The amplitude for diagram (a) in figure D.2 is,

$$\mathcal{M}_{IB\tau} = -iG_F V_{ud}^* e^2 F_\pi p_\mu \frac{\ell_\nu}{k^2} \overline{u}(q)\gamma^\mu(1-\gamma^5)\Big(\frac{p\!\!\!/_t u - k\!\!\!/ + M_\tau}{(p_\tau - k)^2 - M_\tau^2}\Big)\gamma^\nu u_(p_\tau)\,. \quad \text{(D.1)}$$

The amplitude for diagrams (b) and (c) in figure D.2 is,

$$\mathcal{M}_{IB\pi} = -iG_F V_{ud}^* e^2 F_\pi \frac{\ell^\nu}{k^2}\Big(\frac{2p_\nu(p\!\!\!/ + k\!\!\!/)}{(p+k)^2 - m_\pi^2} - g_{\mu\nu}\Big)\overline{u}(q)(1+\gamma^5)\gamma^\mu u(p_\tau)\,. \quad \text{(D.2)}$$

We can check gauge invariance in the case of the real photon by substituting $\frac{\ell^\nu}{k^2} \to \epsilon^\nu$ in the total inner bremsstrahlung amplitude, this must vanish when $\epsilon \to k$,

$$\lim_{\epsilon \to k}(\mathcal{M}_{IB\tau} + \mathcal{M}_{IB\pi}) = 0\,. \tag{D.3}$$

The model dependent amplitudes are given by the following equations,

$$\mathcal{M}_V = -G_F V_{ud}^* \frac{e^2}{k^2} F_V(p\cdot k, k^2)\epsilon_{\mu\nu\rho\sigma}k^\rho p^\sigma \ell^\nu \tau^\mu\,, \tag{D.4}$$

$$\begin{aligned}\mathcal{M}_A =& iG_F V_{ud}^* \frac{2e^2}{k^2}\ell_\nu \Bigg(F_A(p\cdot k, k^2)\left[(k^2 + p\cdot k)g^{\mu\nu} - k^\mu p^\nu\right] \\ &+ B(k^2)k^2\left[g^{\mu\nu} - \frac{(p+k)^\mu p^\nu}{k^2 + 2p\cdot k}\right]\Bigg)\tau_\mu\,,\end{aligned} \tag{D.5}$$

where we have used $\ell_\mu := \bar{u}(p_-)\gamma_\mu v(p_+)$ and $\tau_\mu := \bar{u}(q)\gamma_\mu(1-\gamma_5)u(p_\tau)$ as short for the electromagnetic and weak spinor currents.

The total amplitude for the process is the sum of the amplitudes corresponding to the inner bremmstrahlung and the structure dependent contributions, including the vector and axial vector form factors, which is shown in the next equation:

$$\mathcal{M} = \mathcal{M}_{IB} + \mathcal{M}_V + \mathcal{M}_A\,, \tag{D.6}$$

where each of the contributions is given by the following equations:

$$\mathcal{M}_{IB} = -iG_F V_{ud}^* \frac{e^2}{k^2} F_\pi M_\tau \ell_\mu \bar{u}(q)(1+\gamma_5)\left[\frac{2p^\mu}{2p\cdot k + k^2} + \frac{2p_\tau^\mu - \not{k}\gamma^\mu}{k^2 - 2p_\tau\cdot k}\right]u(p_\tau)\,, \tag{D.7}$$

$$\mathcal{M}_V = -G_F V_{ud}^* \frac{e^2}{k^2} F_V(p\cdot k, k^2)\epsilon_{\mu\nu\rho\sigma}k^\rho p^\sigma \ell^\nu \tau^\mu\,, \tag{D.8}$$

$$\begin{aligned}\mathcal{M}_A =& iG_F V_{ud}^* \frac{2e^2}{k^2}\ell_\nu \Bigg(F_A(p\cdot k, k^2)\left[(k^2 + p\cdot k)g^{\mu\nu} - k^\mu p^\nu\right] \\ &+ B(k^2)k^2\left[g^{\mu\nu} - \frac{(p+k)^\mu p^\nu}{k^2 + 2p\cdot k}\right]\Bigg)\tau_\mu\,.\end{aligned} \tag{D.9}$$

Therefore, the square of the amplitude in equation (D.6) is given by

$$|\mathcal{M}|^2 = |\mathcal{M}_{IB}|^2 + |\mathcal{M}_V|^2 + |\mathcal{M}_A|^2 + 2\Re e(\mathcal{M}_{IB}\mathcal{M}_V^\dagger) + 2\Re e(\mathcal{M}_{IB}\mathcal{M}_A^\dagger) + 2\Re e(\mathcal{M}_V\mathcal{M}_A^\dagger)\,. \tag{D.10}$$

The explicit form for each of the previous terms reads (for more details of the derivation of these formulas see [180])

$$\begin{aligned}\overline{|\mathcal{M}_{IB}|^2} = 16{G_F}^2{V_{ud}}^2\frac{e^4}{k^4}{F_\pi}^2{M_\tau}^2\ell_{\mu\nu}\Big[&-\frac{\tau^{\mu\nu}k^2}{(k^2-2p_\tau\cdot k)^2}+\frac{4p^\mu q^\nu(p_\tau\cdot k)}{(k^2-2p_\tau\cdot k)(k^2+2p\cdot k)}\\ &+\frac{4p_\tau^\mu q^\nu(p_\tau\cdot k)}{(k^2-2p_\tau\cdot k)^2}-\frac{2g^{\mu\nu}(p_\tau\cdot k)(k\cdot q)}{(k^2-2p_\tau\cdot k)^2}-\frac{4p^\mu p_\tau^\nu(k\cdot q)}{(k^2+2p\cdot k)(k^2-2p_\tau\cdot k)}\\ &-\frac{4p_\tau^\mu p_\tau^\nu(k\cdot q)}{(k^2-2p_\tau\cdot k)^2}+\frac{8p^\mu p_\tau^\nu(p_\tau\cdot q)}{(k^2+2p\cdot k)(k^2-2p_\tau\cdot k)}\\ &+\frac{4p^\mu p^\nu(p_\tau\cdot q)}{(k^2+2p\cdot k)^2}+\frac{4p_\tau^\mu p_\tau^\nu(p_\tau\cdot q)}{(k^2-2p_\tau\cdot k)^2}\\ +M_\tau\Big(&-\frac{\Omega^{\mu\nu}k^2}{(k^2-2p_\tau\cdot k)^2}+\frac{4p^\mu q^\nu(k\cdot s)}{(k^2-2p_\tau\cdot k)(k^2+2p\cdot k)}\\ &+\frac{4p_\tau^\mu q^\nu(k\cdot s)}{(k^2-2p_\tau\cdot k)^2}-\frac{2g^{\mu\nu}(k\cdot s)(k\cdot q)}{(k^2-2p_\tau\cdot k)^2}-\frac{4p^\mu s^\nu(k\cdot q)}{(k^2+2p\cdot k)(k^2-2p_\tau\cdot k)}\\ &-\frac{4p_\tau^\mu s^\nu(k\cdot q)}{(k^2-2p_\tau\cdot k)^2}+\frac{8p^\mu p_\tau^\nu(s\cdot q)}{(k^2+2p\cdot k)(k^2-2p_\tau\cdot k)}\\ &+\frac{4p^\mu p^\nu(s\cdot q)}{(k^2+2p\cdot k)^2}+\frac{4p_\tau^\mu p_\tau^\nu(s\cdot q)}{(k^2-2p_\tau\cdot k)^2}\Big)\Big]\,,\end{aligned} \tag{D.11}$$

where

$$\ell_{\mu\nu} = [p_{+\mu}p_{-\nu} + p_{+\nu}p_{-\mu} - g_{\mu\nu}({m_\ell}^2 + p_-\cdot p_+)]\,. \tag{D.12}$$

$$\tau^{\mu\nu} = p_\tau^\mu q^\nu + p_\tau^\nu q^\mu - g^{\mu\nu}p_\tau\cdot q\,. \tag{D.13}$$

$$\Omega^{\mu\nu} = s^\mu q^\nu + s^\nu q^\mu - g^{\mu\nu}s\cdot q\,. \tag{D.14}$$

$$\begin{aligned}\sum_{s_\nu,s_{\ell+},s_{\ell-}}|\mathcal{M}_V|^2 =& 16{G_F}^2|V_{ud}|^2\frac{e^4}{k^4}|F_V(p\cdot k,k^2)|^2\epsilon_{\mu'\nu'\rho'\sigma'}\epsilon_{\mu\nu\rho\sigma}k^\rho p^\sigma k^{\rho'}p^{\sigma'}\ell^{\nu\nu'}\times\\ &[\tau^{\mu\mu'} - M_\tau\Omega^{\mu\mu'}]\,.\end{aligned} \tag{D.15}$$

$$\sum_{s_\nu,s_{\ell+},s_{\ell-}} \left|\mathcal{M}_A\right|^2 = 64{G_F}^2|V_{ud}|^2\frac{e^4}{k^4}\ell_{\nu\nu'}\times$$
$$(\tau_{\mu\mu'} + ip_\tau^a q^b\epsilon_{\mu\mu' ab} - M_\tau\Omega_{\mu\mu'} - iM_\tau s^a q^b\epsilon_{\mu\mu' ab})\mathcal{A}^{\mu\nu}\mathcal{A}^{\mu'\nu'*}\,, \tag{D.16}$$

where:

$$\mathcal{A}^{\mu\nu} = F_A(p\cdot k, k^2)\left[(k^2 + p\cdot k)g^{\mu\nu} - k^\mu p^\nu\right] + B(k^2)k^2\left[g^{\mu\nu} - \frac{(p+k)^\mu p^\nu}{k^2+2p\cdot k}\right]. \tag{D.17}$$

$$\sum_{s_\nu,s_{\ell+},s_{\ell-}} 2\Re e(\mathcal{M}_{IB}{\mathcal{M}_V}^\dagger) = -32{G_F}^2|{V_{ud}}^2|\frac{e^4}{k^4}F_\pi M_\tau\times$$
$$\Im m\left[{F_V}^*(p\cdot k, k^2)\ell^\mu{}_{\nu'}\epsilon^{\mu'\nu'\rho'\sigma'}k_{\rho'}p_{\sigma'}\mathcal{V}_{\mu\mu'}\right], \tag{D.18}$$

where:

$$\begin{aligned}\mathcal{V}^{\mu\mu'} = \frac{1}{ab}\Big[&(q\cdot s)\left(p_\tau{}^{\mu'}(2bp^\mu - ak^\mu) + ag^{\mu\mu'}(k\cdot p_\tau) - ap_\tau{}^\mu\left(k^{\mu'} - 2p_\tau{}^{\mu'}\right) - ia\epsilon^{\mu\mu' kp_\tau}\right)\\
&+ i\epsilon^{\mu' p_\tau qs}\left(ak^\mu - 2\left(ap_\tau^\mu + bp^\mu\right)\right) - aMg^{\mu\mu'}(k\cdot q) - ag^{\mu\mu'}(k\cdot s)(p_\tau\cdot q)\\
&+ ag^{\mu\mu'}(k\cdot q)(p_\tau\cdot s) + aMk^{\mu'}q^\mu - aMk^\mu q^{\mu'} + iaM\epsilon^{\mu\mu' kq} - aq^{\mu'}s^\mu(k\cdot p_\tau)\\
&- aq^\mu s^{\mu'}(k\cdot p_\tau) - ap_\tau^{\mu'}s^\mu(k\cdot q) + ap_\tau^\mu s^{\mu'}(k\cdot q) + ap_\tau^{\mu'}q^\mu(k\cdot s) + ap_\tau^\mu q^{\mu'}(k\cdot s)\\
&+ ak^{\mu'}s^\mu(p_\tau\cdot q) + ak^\mu s^{\mu'}(p_\tau\cdot q) - ak^{\mu'}q^\mu(p_\tau\cdot s) + ak^\mu q^{\mu'}(p_\tau\cdot s) + iap_\tau^\mu\epsilon^{\mu' kqs}\\
&+ iaq^{\mu'}\epsilon^{\mu kp_\tau s} + ias^{\mu'}\epsilon^{\mu kp_\tau q} + ia(k\cdot p_\tau)\epsilon^{\mu\mu' qs} + 2aMp_\tau^\mu q^{\mu'} - 2ap_\tau^\mu s^{\mu'}(p_\tau\cdot q)\\
&- 2ap_\tau{}^\mu q^{\mu'}(p_\tau\cdot s) + 2bMp^\mu q^{\mu'} - 2bp^\mu s^{\mu'}(p_\tau\cdot q) - 2bp^\mu q^{\mu'}(p_\tau\cdot s)\Big].\end{aligned} \tag{D.19}$$

In the previous equation, we introduced the following short-hand notation:

$$a = k^2 + 2p\cdot k\,, \tag{D.20}$$
$$b = k^2 - 2p_\tau\cdot k\,. \tag{D.21}$$

$$\sum_{s_\nu,s_{\ell+},s_{\ell-}} 2\Re e(\mathcal{M}_{IB}{\mathcal{M}_A}^\dagger) = -64{G_F}^2|{V_{ud}}^2|\frac{e^4}{k^4}F_\pi M_\tau\ell_\mu{}^{\nu'}\Re e[\mathcal{A}^*{}_{\mu'\nu'}\mathcal{V}^{\mu\mu'}]\,, \tag{D.22}$$

$$\Rightarrow \sum_{s_\nu, s_{\ell+}, s_{\ell-}} 2\Re e(\mathcal{M}_V \mathcal{M}_A{}^\dagger) = -\,64 G_F^2 |V_{ud}|^2 \frac{e^4}{k^4} \ell^\nu_{\nu'} \Im m \Big[F_V(p\cdot k, k^2) \epsilon_{\mu\nu\rho\sigma} k^\rho p^\sigma$$
$$[\tau^{\mu\mu'} + i p_{\tau a} q_b \epsilon^{\mu\mu' ab} - M_\tau(\Omega^{\mu\mu'} + i s_a q_b \epsilon^{\mu\mu' ab})] \mathcal{A}^{\nu'*}_{\mu'} \Big] . \tag{D.23}$$

The important point to note from the previous formulas is the symmetry between the part that depends on polarization and the part that is independent of the polarization. They have the same structures.

As usual the form factors are the hard part in the calculation. The effective lagrangian is [181, 184, 185],

$$\mathcal{L}_{R\chi T} = \mathcal{L}_{WZW} + \mathcal{L}^V_{Kin} + \frac{F_\pi^2}{4}\langle u_\mu u^\mu + \chi_+\rangle + \frac{F_V}{2\sqrt{2}}\langle V_{\mu\nu} f_+^{\mu\nu}\rangle + \frac{F_A}{2\sqrt{2}}\langle A_{\mu\nu} f_-^{\mu\nu}\rangle$$
$$+ i\frac{G_V}{\sqrt{2}}\langle V_{\mu\nu} u^\mu u^\nu\rangle + \sum_{i=1}^{7} \frac{c_i}{M_V}\mathcal{O}^i_{VJP} + \sum_{i=1}^{4} d_i \mathcal{O}^i_{VVP} + \sum_{i=1}^{5} \lambda_i \mathcal{O}^i_{VAP} , \tag{D.24}$$

where $f_\pm^{\mu\nu} = u F_L^{\mu\nu} u^\dagger \pm u^\dagger F_R^{\mu\nu} u$ and $F_{R,L}^{\mu\nu}$ are the field strenght tensors associated with the external right and left handed auxiliary fields. All coupling constants are real, and M_V is the mass of the lightest vector meson resonance nonet.

The parameters introduced in the previous equation are defined as follows,

$$u_\mu = i\left[u^\dagger(\partial_\mu - i r_\mu) u - u(\partial_\mu - i\ell_\mu)u^\dagger\right] , \tag{D.25}$$
$$\chi_\pm = u^\dagger \chi u^\dagger \pm u \chi^\dagger u , \tag{D.26}$$
$$\chi = 2B_0(s + ip) , \tag{D.27}$$
$$\Phi(x) = \begin{pmatrix} \frac{1}{\sqrt{2}}\pi^0 & \pi^+ & K^+ \\ \pi^- & -\frac{1}{\sqrt{2}}\pi^0 + \frac{1}{\sqrt{6}}\eta_8 & K^0 \\ K^- & \overline{K}^0 & -\frac{2}{\sqrt{6}}\eta_8 \end{pmatrix} \tag{D.28}$$
$$u(\phi) = exp\left[\frac{i}{\sqrt{2}F_\pi}\Phi(x)\right] \tag{D.29}$$

where r_μ, ℓ_μ, s, and p are external fields that promote the global $SU(3)_L \times SU(3)_R$ symmetry to a local one.
The explicit forms of the $\mathcal{O}$ operators is shown in the following equations,

$$\mathcal{O}^1_{VJP} = \epsilon_{\mu\nu\rho\sigma}\langle \{V^{\mu\nu}, f_+^{\rho\alpha}\} \nabla_\alpha u^\sigma\rangle , \tag{D.30}$$

$$\mathcal{O}^2_{VJP} = \epsilon_{\mu\nu\rho\sigma}\langle\{V^{\mu\alpha}, f_+^{\rho\sigma}\}\nabla_\alpha u^\nu\rangle\,, \tag{D.31}$$

$$\mathcal{O}^3_{VJP} = i\epsilon_{\mu\nu\rho\sigma}\langle\{V^{\mu\nu}, f_+^{\rho\sigma}\}\chi_-\rangle\,, \tag{D.32}$$

$$\mathcal{O}^4_{VJP} = i\epsilon_{\mu\nu\rho\sigma}\langle V^{\mu\nu}\,[f_-^{\rho\sigma}, \chi_+]\rangle\,, \tag{D.33}$$

$$\mathcal{O}^5_{VJP} = \epsilon_{\mu\nu\rho\sigma}\langle\{\nabla_\alpha V^{\mu\nu}, f_+^{\rho\alpha}\}u^\sigma\rangle\,, \tag{D.34}$$

$$\mathcal{O}^6_{VJP} = \epsilon_{\mu\nu\rho\sigma}\langle\{\nabla_\alpha V^{\mu\alpha}, f_+^{\rho\sigma}\}u^\nu\rangle\,, \tag{D.35}$$

$$\mathcal{O}^7_{VJP} = \epsilon_{\mu\nu\rho\sigma}\langle\{\nabla^\sigma V^{\mu\nu}, f_+^{\rho\alpha}\}u_\alpha\rangle\,. \tag{D.36}$$

$$\mathcal{O}^1_{VAP} = \langle[V^{\mu\nu}, A_{\mu\nu}]\,\chi_-\rangle\,, \tag{D.37}$$

$$\mathcal{O}^2_{VAP} = i\langle[V^{\mu\nu}, A_{\nu\alpha}]\,h^\alpha_\mu\rangle\,, \tag{D.38}$$

$$\mathcal{O}^3_{VAP} = i\langle[\nabla^\mu V_{\mu\nu}, A^{\nu\alpha}]\,u_\alpha\rangle\,, \tag{D.39}$$

$$\mathcal{O}^4_{VAP} = i\langle[\nabla^\alpha V_{\mu\nu}, A^\nu_\alpha]\,u^\mu\rangle\,, \tag{D.40}$$

$$\mathcal{O}^5_{VAP} = i\langle[\nabla^\alpha V_{\mu\nu}, A^{\nu\nu}]\,u_\alpha\rangle\,, \tag{D.41}$$

where $h_{\mu\nu} = \nabla_\mu u_\nu + \nabla_\nu u_\mu$.

$$\mathcal{O}^1_{VVP} = \epsilon_{\mu\nu\rho\sigma}\langle\{V^{\mu\nu}, V^{\rho\alpha}\}\nabla_\alpha u^\sigma\rangle\,, \tag{D.42}$$

$$\mathcal{O}^2_{VVP} = i\epsilon_{\mu\nu\rho\sigma}\langle\{V^{\mu\nu}, V^{\rho\sigma}\}\chi_-\rangle\,, \tag{D.43}$$

$$\mathcal{O}^3_{VVP} = \epsilon_{\mu\nu\rho\sigma}\langle\{\nabla_\alpha V^{\mu\nu}, V^{\rho\alpha}\}u^\sigma\rangle \tag{D.44}$$

$$\mathcal{O}^4_{VVP} = \epsilon_{\mu\nu\rho\sigma}\langle\{\nabla^\sigma V^{\mu\nu}, V^{\rho\alpha}\}u_\alpha\rangle \tag{D.45}$$

The structure-dependent form factors that appear in the amplitudes in equations (D.8) and (D.9) can be obtained from the Feynman diagrams shown in figure D.3 and figure D.4.

Figure D.3: Vector current contributions to the $W^{-*} \to \pi^-\gamma^*$ vertex.

Figure D.4: Axial-Vector current contributions to the $W^{-*} \to \pi^- \gamma^*$

The vector form factor $F_V(t, k^2)$ is given by the following equation,

$$\begin{aligned} F_V(t,k^2) = &-\frac{N_c}{24\pi^2 F_\pi} + \frac{2\sqrt{2}F_V}{3F_\pi M_V}\Big[(c_2 - c_1 - c_5)t + (c_5 - c_1 - c_2 - 8c_3)m_\pi^2 + 2(c_6 - c_5)k^2\Big] \\ &\Big[\frac{\cos^2\theta}{M_\phi^2 - k^2 - iM_\phi\Gamma_\phi}(1 - \sqrt{2}\mathrm{tg}\theta) + \frac{\sin^2\theta}{M_\omega^2 - k^2 - iM_\omega\Gamma_\omega}(1 + \sqrt{2}\mathrm{cotg}\theta)\Big] \\ &+ \frac{2\sqrt{2}F_V}{3F_{\pi M_V}} D_\rho(t)\Big[(c_1 - c_2 - c_5 + 2c_6)t + (c_5 - c_1 - c_2 - 8c_3)m_\pi^2 + (c_2 - c_1 - c_5)k^2\Big] \\ &+ \frac{4F_V^2}{3F_\pi} D_\rho(t)\Big[d_3(t + 4k^2) + (d_1 + 8d_2 - d_3)m_\pi^2\Big] \\ &\Big[\frac{\cos^2\theta}{M_\phi^2 - k^2 - iM_\phi\Gamma_\phi}(1 - \sqrt{2}\mathrm{tg}\theta) + \frac{\sin^2\theta}{M_\omega^2 - k^2 - iM_\omega\Gamma_\omega}(1 - \sqrt{2}\mathrm{cotg}\theta)\Big]\,, \end{aligned} \tag{D.46}$$

where,

$$D_\rho(t) = \frac{1}{M_\rho^2 - t - iM_\rho\Gamma_\rho(t)}\,, \tag{D.47}$$

and

$$\Gamma_\rho(s) = \frac{sM_\rho}{96\pi F_\pi^2}\left[\sigma_\pi^3(s)(s - 4m_\pi^2) + \frac{1}{2}\sigma_k^3(s)\theta(s - 4m_k^2)\right]\,, \tag{D.48}$$

is the decay width of the $\rho(770)$ resonance with $\sigma_p(s) = \sqrt{1 - \frac{4m_p^2}{s}}$ (ref. [170]).
We will assume the ideal mixing case for the vector resonances ω and ϕ in any numerical application:

$$\omega_1 = \cos\theta\omega - \sin\theta\phi \sim \sqrt{\frac{2}{3}}\omega - \sqrt{\frac{1}{3}}\phi \tag{D.49}$$

$$\omega_8 = \sin\theta\omega + \cos\theta\phi \sim \sqrt{\frac{2}{3}}\phi + \sqrt{\frac{1}{3}}\omega \tag{D.50}$$

Similarly, the axial-vector form factor $F_A(t, k^2)$ is given by,

$$\begin{aligned} F_A(t,k^2) =& \frac{F_V^2}{F_\pi}\left(1 - 2\frac{G_V}{F_V}\right) D_\rho(k^2) - \frac{F_A^2}{F_\pi} D_{a_1}(t) \\ &+ \frac{F_A F_V}{\sqrt{2}F_\pi} D_\rho(k^2) D_{a_1}(t)(-\lambda'' t + \lambda_0 m_\pi^2)\,, \end{aligned} \tag{D.51}$$

where,

$$\sqrt{2}\lambda_0 = -4\lambda_1 - \lambda_2 - \frac{\lambda_4}{2} - \lambda_5\,, \tag{D.52}$$

and

$$\sqrt{2}\lambda'' = \lambda_2 - \frac{\lambda_4}{2} - \lambda_5\,. \tag{D.53}$$

Finally for the $B(k^2)$ form factor we have [169],

$$B(k^2) = \frac{F_\pi F_V^{\pi^+\pi^-}|_\rho(k^2) - 1}{k^2}\,, \tag{D.54}$$

where $F_V^{\pi^+\pi^-}|_\rho$ is the $I = 1$ part of the $\pi^+\pi^-$ vector form factor, and has the following form

$$\langle \pi^+(p_+)\pi^-(p_-)|\overline{u}\gamma^\mu u + \overline{d}\gamma^\mu d|0\rangle = (p_+ - p_-)^\mu F_V^{\pi^+\pi^-}(k^2)\,. \tag{D.55}$$

The arguments in the form factors are $t := (p + k)^2$ and $k^2 = (p_+ + p_-)^2$.

Finally, we discuss the kinematics. The decay we are analyzing is an example of a one to four body decay. In these kind of decays it can be shown [186] that the square of the amplitude $|\mathcal{M}|^2$ can be written as a function of five independent variables. The choice of these variables is not unique, so we are free to choose a convenient way we find. We follow the convention used in [184, 186], which states the following:

- $s_{12} = p_{12}^2 = (p + q)^2$, The invariant mass of the pion-neutrino system
- $s_{34} = p_{34}^2 = (p_- + p_+)^2 = k^2$, The invariant mass of the lepton pair $\ell^+\ell^-$.
- θ_1, the angle between the neutrino trajectory and the 3-momentum vector $\vec{k'} = \vec{p} + \vec{q}$.
- θ_3, the angle between the trajectory of the ℓ^+ lepton and the 3-momentum vector $\vec{k}$ in the rest frame of the center of mass of the lepton pair.
- ϕ, The angle between the planes of the pion-neutrino and the lepton pair systems.

The kinematic limits for these variables were calculated in [186] and are given by the following expressions:

$$(2m_\ell)^2 \leq s_{34} \leq (M_\tau - m_\pi)^2 \tag{D.56}$$

$$(m_\pi)^2 \leq s_{12} \leq (M_\tau - \sqrt{s_{34}})^2 \tag{D.57}$$

$$-1 \leq \cos\theta_{1,3} \leq 1 \tag{D.58}$$

$$0 \leq \phi \leq 2\pi \tag{D.59}$$

Finally the branching ratio can be written in terms of the five variables defined before as is shown in the following equation [184, 186]:

$$d\Gamma = \frac{X\beta_{12}\beta_{34}}{4(4\pi)^6 M_\tau^3}\overline{|\mathcal{M}|^2} ds_{12} ds_{34} \sin(\theta_1) d\theta_1 \sin(\theta_3) d\theta_3 d\phi\,, \tag{D.60}$$

where:

$$\beta_{12} = \frac{\sqrt{s_{12}^2 + m_\pi^4 - 2s_{12}m_\pi^2}}{s_{12}}\,, \tag{D.61}$$

$$\beta_{34} = \frac{\sqrt{s_{34}^2 - 4s_{34}m_\ell^2}}{s_{34}}\,, \tag{D.62}$$

$$X = \frac{\sqrt{s_{12}^2 + s_{34}^2 + M_\tau^4 - 2s_{12}s_{34} - 2s_{12}M_\tau^2 - 2s_{34}M_\tau^2}}{2}\,. \tag{D.63}$$

From conservation of energy and momentum we have that

$$p_\tau = p + p_+ + p_- + q\,. \tag{4.59}$$

When the decaying particle has a definite polarization (as is our case with the tau lepton) $|\mathcal{M}|^2$ depends on the polarization four vector (s) of the decaying particle, in addition to be a function of the invariants formed with all the four independent momenta available (among p_τ, p, p_+, p_- and q in our case). Then $|\mathcal{M}|^2$ will also be a function of products like: $p\cdot s$, $p_+\cdot s$, $p_-\cdot s$, and $q\cdot s$, this can be seen in all the expressions that we found for the different contributions to $|\mathcal{M}|^2$ previously.

With the purpose of calculating $p\cdot s$, $p_+\cdot s$, $p_-\cdot s$, and $q\cdot s$, it will be convenient to construct a specific reference frame in which I will find definite expressions for the four momenta p_τ, p, p_+, p_-, and q, I will follow the technique used in [187].

To simplify things I will do the following substitutions:

$p_\tau \to P$, $p_- \to p_1$, $p_+ \to p_2$, $p \to p_3$, and $q \to p_4$, $M_\tau \to M$.
First, I will choose the reference frame as the rest frame of the decaying particle, then I will choose the z-axis along the direction of $\vec{p_1}$ (the three momentum of the particle with p_1), and finally I will choose the x-axis in such a way that $\vec{p_2}$ lies on the x-z plane. The four momentum p_3, and p_4 will be found using the previous ones.
With the conventions stated before we get the following expressions for the four momentum,

$$P = (M, 0, 0, 0)\,, \tag{D.64}$$

$$p_1 = (E_1, \vec{p_1}) = (E_1, 0, 0, |\vec{p_1}|)\,, \tag{D.65}$$

$$p_2 = (E_2, \vec{p_2}) = (E_2, |\vec{p_2}|\sin\theta, 0, |\vec{p_2}|\cos\theta)\,, \tag{D.66}$$

$$p_3 = (E_3, \vec{p_3}) = (E_3, a_3, b_3, c_3)\,, \tag{D.67}$$

$$p_4 = (E_4, \vec{p_4}) = (E_4, a_4, b_4, c_4)\,, \tag{D.68}$$

$$s = (0, a_5, b_5, c_5)\,, \tag{D.69}$$

where M is the mass of the decaying particle, θ is the angle between the z-axis and the $\vec{p_2}$ direction. The components a_i, b_i, and c_i, $i = 3, 4$ will be calculated using the energy and momentum conservation.
s is a polarization vector, so we have the following constraint ($s^2 = -1 \Rightarrow |\vec{s}| = 1$),

$$(a_5)^2 + (b_5)^2 + (c_5)^2 = 1\,. \tag{D.70}$$

The energies E_k, $k = 1, 2, 3, 4$ can be calculated as follows,

$$E_k = \frac{P \cdot p_k}{M}, \quad k = 1, 2, 3\,. \tag{D.71}$$

And $E_4 = M - E_1 - E_2 - E_3$. For $|\vec{p_1}|$, $|\vec{p_1}|$, cosθ, and sinθ we have,

$$|\vec{p_1}| = \left[\frac{(P \cdot p_1)^2}{M^2} - m_1^2\right]^{\frac{1}{2}}, \tag{D.72}$$

$$|\vec{p_2}| = \left[\frac{(P \cdot p_2)^2}{M^2} - m_2^2\right]^{\frac{1}{2}}, \tag{D.73}$$

$$\cos\theta = \frac{E_1 E_2 - p_1 \cdot p_2}{|\vec{p_1}||\vec{p_2}|} = \frac{(P \cdot p_1)(P \cdot p_2) - M^2 p_1 \cdot p_2}{\left[\left((P \cdot p_1)^2 - M^2 m_1^2\right)\left((P \cdot p_2)^2 - M^2 m_2^2\right)\right]^{\frac{1}{2}}}, \tag{D.74}$$

$$\sin\theta = [1 - \cos^2\theta]^{\frac{1}{2}}\,. \tag{D.75}$$

For c_3 and c_4 we have,

$$c_3 = \frac{E_1 E_3 - p_1 \cdot p_3}{|\vec{p_1}|}\,, \tag{D.76}$$

$$c_4 = \frac{E_1 E_4 - p_1 \cdot p_4}{|\vec{p_1}|} = \frac{E_1(M - E_1 - E_2 - E_3) - P \cdot p_1 + m_1^2 + p_1 \cdot p_2 + p_1 \cdot p_3}{|\vec{p_1}|}\,. \tag{D.77}$$

For a_3 and a_4 we have,

$$a_3 = \frac{E_2 E_3 - p_2 \cdot p_3 - c_3|\vec{p_2}|\cos\theta}{|\vec{p_2}|\sin\theta}\,, \tag{D.78}$$

$$\begin{aligned} a_4 =& \frac{E_2 E_4 - p_2 \cdot p_4 - c_4|\vec{p_2}|\cos\theta}{|\vec{p_2}|\sin\theta} \\ =& \frac{E_2(M - E_1 - E_2 - E_3) - p_2 \cdot P + p_1 \cdot p_2 + m_2^2 + p_2 \cdot p_3 - c_4|\vec{p_2}|\cos\theta}{|\vec{p_2}|\sin\theta}\,. \end{aligned} \tag{D.79}$$

Finally for b_3, and b_4 we have the following expressions,

$$b_3 = [E_3^2 - a_3^2 - c_3^2 - m_3^2]^{\frac{1}{2}}\,, \tag{D.80}$$

$$b_4 = [E_4^2 - a_4^2 - c_4^2 - m_4^2]^{\frac{1}{2}} = [(M - E_1 - E_2 - E_3)^2 - a_4^2 - c_4^2 - m_4^2]^{\frac{1}{2}}\,. \tag{D.81}$$

Now we have everything we need, the four momenta P, p_1, p_2, p_3, and p_4 can be written in terms of the Lorentz invariant quantities that we found previosly, as it is shown in the following equations,

$$P = (M, 0, 0, 0)\,, \tag{D.82}$$

$$p_1 = \left(\frac{P \cdot p_1}{M}, 0, 0, \left[-\frac{\begin{bmatrix} M^2 & P \cdot p_1 \\ P \cdot p_1 & m_1^2 \end{bmatrix}}{M^2} \right]^{\frac{1}{2}} \right)\,, \tag{D.83}$$

$$p_2 = \left(\frac{P \cdot p_2}{M}, \left(-\frac{\begin{bmatrix} M^2 & P \cdot p_1 & P \cdot p_2 \\ P \cdot p_1 & m_1^2 & p_1 \cdot p_2 \\ P \cdot p_2 & p_1 \cdot p_2 & m_2^2 \end{bmatrix}}{\begin{bmatrix} M^2 & P \cdot p_1 \\ P \cdot p_1 & m_1^2 \end{bmatrix}} \right)^{\frac{1}{2}}, 0, -\frac{\begin{bmatrix} M^2 & P \cdot p_2 \\ P \cdot p_1 & p_1 \cdot p_2 \end{bmatrix}}{\left(-m_1^2 \begin{bmatrix} M^2 & P \cdot p_1 \\ P \cdot p_1 & m_1^2 \end{bmatrix} \right)^{\frac{1}{2}}} \right)\,, \tag{D.84}$$

$$p_3 = \left(\frac{P \cdot p_3}{M}, a_3, b_3, c_3 \right) , \tag{D.85}$$

where a_3, b_3, and c_3 can be written in the compact form,

$$a_3 = \frac{\begin{vmatrix} M^2 & P\cdot p_1 & P\cdot p_3 \\ P\cdot p_1 & m_1^2 & p_1\cdot p_3 \\ P\cdot p_2 & p_1\cdot p_2 & p_2\cdot p_3 \end{vmatrix}}{\left(- \begin{vmatrix} M^2 & P\cdot p_1 \\ P\cdot p_1 & m_1^2 \end{vmatrix} \begin{vmatrix} M^2 & P\cdot p_1 & P\cdot p_2 \\ P\cdot p_1 & m_1^2 & p_1\cdot p_2 \\ P\cdot p_2 & p_1\cdot p_2 & m_2^2 \end{vmatrix} \right)^{\frac{1}{2}}} , \tag{D.86}$$

$$b_3 = \left(- \frac{\begin{vmatrix} M^2 & P\cdot p_1 & P\cdot p_2 & P\cdot p_3 \\ P\cdot p_1 & m_1^2 & p_1\cdot p_2 & p_1\cdot p_3 \\ P\cdot p_2 & p_1\cdot p_2 & m_2^2 & p_2\cdot p_3 \\ P\cdot p_3 & p_1\cdot p_3 & p_2\cdot p_3 & m_3^2 \end{vmatrix}}{\begin{vmatrix} M^2 & P\cdot p_1 & P\cdot p_2 \\ P\cdot p_1 & m_1^2 & p_1\cdot p_2 \\ P\cdot p_2 & p_1\cdot p_2 & m_2^2 \end{vmatrix}} \right)^{\frac{1}{2}} , \tag{D.87}$$

$$c_3 = - \frac{\begin{vmatrix} M^2 & P\cdot p_3 \\ P\cdot p_1 & p_1\cdot p_3 \end{vmatrix}}{\left(-m_1^2 \begin{vmatrix} M^2 & P\cdot p_1 \\ P\cdot p_1 & m_1^2 \end{vmatrix} \right)^{\frac{1}{2}}} . \tag{D.88}$$

The term p_4 has the same form as p_3, we just need to replace $3 \to 4$.

The previous expressions can be further simplified noticing that $m_1 = m_2 = m_\ell$, and $m_4^2 = 0$.

I have to calculate polarization effects, these will be given in terms of $p \cdot s$, $p_- \cdot s$, $p_+ \cdot s$, and $q \cdot s$, these terms can be easily calculated using the expressions obtained previously, once I define a direction for the polarization vector. I will simplify things by choosing this polarization vector orthogonal to $\vec{p_-}$, and $\vec{p_+}$, so that $p_- \cdot s = 0$, and $p_+ \cdot s = 0$, then the explicit form of the vector s is, $s = (0, 0, 1, 0)$, given this form, the products $p \cdot s$, and $q \cdot s$ are given by the following equations:

$$p \cdot s = b_3 \, . \tag{D.89}$$

Equation (4.59) fixes the value of $q \cdot s$ according to,

$$q \cdot s = -p \cdot s = -b_3 \, . \tag{D.90}$$

At this point we have succeeded in finding all the products between the polarization four vector and the available momenta in terms of invariants. Now

it is time to write those invariants as fuctions of the variables we chose at the beginning of this section, that is s_{12}, s_{34}, θ_1, θ_3, and ϕ. Here I will follow the conventions used in [186]:

$$p_{12}^2 := s_{12}\,, \tag{D.91}$$

$$p_{34}^2 := s_{34}\,, \tag{D.92}$$

$$q_{12}^2 = 2(m_1^2 + m_2^2) - s_{12}\,, \tag{D.93}$$

$$q_{34}^2 = 2(m_3^2 + m_4^2) - s_{34}\,, \tag{D.94}$$

$$p_{12}\cdot q_{12} = m_2^2 - m_1^2\,, \tag{D.95}$$

$$p_{34}\cdot q_{34} = m_4^2 - m_3^2\,, \tag{D.96}$$

$$p_{12}\cdot p_{34} = \frac{1}{2}(M^2 - s_{12} - s_{34})\,, \tag{D.97}$$

$$p_{12}\cdot q_{34} = -X\beta_{34}\cos\theta_3 + \frac{m_4^2 - m_3^2}{s_{34}} p_{12}\cdot p_{34}\,, \tag{D.98}$$

$$p_{34}\cdot q_{12} = X\beta_{12}\cos\theta_1 + \frac{m_2^2 - m_1^2}{s_{12}} p_{12}\cdot p_{34}\,, \tag{D.99}$$

$$\begin{aligned} q_{12}\cdot q_{34} =& \frac{m_1^2 - m_2^2}{s_{12}}\frac{m_3^2 - m_4^2}{s_{34}} + \frac{m_1^2 - m_2^2}{s_{12}} X\beta_{34}\cos\theta_3 \\ &+ \beta_{12}\beta_{34}[p_{12}p_{34}\cos\theta_1\cos\theta_3 - \sqrt{s_{12}s_{34}}\sin\theta_1\sin\theta_3\cos\phi] \\ &\frac{m_3^2 - m_4^2}{s_{34}} X\beta_{12}\cos\theta_1\,, \end{aligned} \tag{D.100}$$

$$\epsilon_{\alpha\beta\gamma\delta} p_{12}^\alpha p_{34}^\beta q_{12}^\gamma q_{34}^\delta = -\sqrt{s_{12}s_{34}}\beta_{12}\beta_{34}\sin\theta_1\sin\theta_3\sin\phi\,, \tag{D.101}$$

where,

$$p_{12} = p_1 + p_2\,, \tag{D.102}$$

$$p_{34} = p_3 + p_4\,, \tag{D.103}$$

$$q_{12} = p_1 - p_2\,, \tag{D.104}$$

$$q_{34} = p_3 - p_4\,. \tag{D.105}$$

At this point we have calculated the square of the amplitude, we have taken advantage of the calculation of the relevant form factors and we have defined and calculated the kinematics, so that we have all the necessary tools. To complete this work that I started in my masters thesis we need to define several appropriate asymmetry observables (see [180] for a discussion.)

Appendix E

Global constraints on neutral-current generalized neutrino interactions

This appendix is based on a collaboration that I did with Dr. Omar Miranda, Dr. Luis Flores and Dr. Francisco Escrihuela. Together we produced the paper [188]. In this work we have studied generalized neutrino interactions (GNI) by making a global analysis for different neutrino processes. We have included neutrinos from electron-positron collisions, neutrino-electron scattering, and neutrino deep inelastic scattering. We have found constrains for scalar, pseudoscalar, and tensor new physics effective couplings, based on the standard model effective field theory at low energies.

Here I will mention very briefly the most importat results that we found and some details about the formalism. For more information, we will refer the reader to [188].

As usual we start with an effective Lagrangian. We will follow the standard model effective field theory (SMEFT) [48, 51] at low energies. The explicit form for our Lagrangian reads

$$\mathcal{L}_{eff}^{NC} = -\frac{G_F}{\sqrt{2}} \sum_j \epsilon_{\alpha\beta}^{f,j} (\bar{\nu}_\alpha \mathcal{O}_j \nu_\beta)(\bar{f} \mathcal{O}'_j f)\,, \tag{E.1}$$

where G_F is the Fermi coupling constant, f represents a fermion with a given flavor, and ν_α a neutrino with flavor α. The operators $\mathcal{O}_j$ and $\mathcal{O}'_j$ characterize the generalized interactions and they are explicitly shown in table E.1. These operators have an effective strength given by the couplings $\epsilon_{\alpha\beta}^{f,j}$.

We have found our constraints using the following processes:

- Cross-section for $e^+e^- \to \nu\bar{\nu}\gamma$.

ϵ	$\mathcal{O}_j$	$\mathcal{O}'_j$
$\epsilon^{f,L}$	$\gamma_\mu(1-\gamma^5)$	$\gamma^\mu(1-\gamma^5)$
$\epsilon^{f,R}$	$\gamma_\mu(1-\gamma^5)$	$\gamma^\mu(1+\gamma^5)$
$\epsilon^{f,S}$	$(1-\gamma^5)$	1
$-\epsilon^{f,P}$	$(1-\gamma^5)$	γ^5
$\epsilon^{f,T}$	$\sigma_{\mu\nu}(1-\gamma^5)$	$\sigma^{\mu\nu}(1-\gamma^5)$

Table E.1: Effective operators and effective couplings in eq. (E.1) studied in this work.

- Differential cross-section for the process $\nu_\alpha + e^- \to \nu_\beta + e^-$.
- Neutrino-quark scattering.

With the help of these processes we derived limits for the scalar, pseudoscalar, and tensor couplings following two different approaches. First, we considered each of the experiments shown in the tables below separately. These results are presented in Tables E.2 and E.3; next, we performed a global fit considering several of those experiments simultaneously to constrain the relevant parameters. The results for this global analysis are shown in Table E.4. For this second analysis we also show in Figure E.1 the χ^2 profile for the different scalar and tensor GNI parameters for the case of neutrino-electron interactions. We do the same for neutrino-quark interactions in Figure E.2, where we have decided to present the results with and without NuTeV due to its discrepancy with the SM prediction [204].

Experiment	Observable	Parameters	Limit
ALEPH [189, 190, 191]			< 0.535
DELPHI [192]	$\lvert\epsilon^{e,X}_{all}\rvert$	$\lvert\epsilon^{e,X}_{ee}\rvert$, $\lvert\epsilon^{e,X}_{\mu\mu}\rvert$, $\lvert\epsilon^{e,X}_{\tau\tau}\rvert$, $\lvert\epsilon^{e,X}_{e\mu}\rvert$, $\lvert\epsilon^{e,X}_{e\tau}\rvert$, $\lvert\epsilon^{e,X}_{\mu\tau}\rvert$	< 0.830
L3 [193, 194, 195]			< 0.745
OPAL [196, 197, 198]			< 0.637
CHARM-II [199]	$\lvert\epsilon^{e,X}_{\mu}\rvert$	$\lvert\epsilon^{e,X}_{e\mu}\rvert$, $\lvert\epsilon^{e,X}_{\mu\mu}\rvert$, $\lvert\epsilon^{e,X}_{\mu\tau}\rvert$	< 0.401
TEXONO [200]	$\lvert\epsilon^{e,X}_{e}\rvert$	$\lvert\epsilon^{e,X}_{ee}\rvert$, $\lvert\epsilon^{e,X}_{e\mu}\rvert$, $\lvert\epsilon^{e,X}_{e\tau}\rvert$	$\lvert\epsilon^{e,S}_{e}\rvert < 0.56$, $\lvert\epsilon^{e,P}_{e}\rvert < 0.64$
CHARM [201] (ν_{-e} beam)	$\lvert\epsilon^{q,X}_{e}\rvert$	$\lvert\epsilon^{q,X}_{ee}\rvert$, $\lvert\epsilon^{q,X}_{e\mu}\rvert$, $\lvert\epsilon^{q,X}_{e\tau}\rvert$	< 1.9
CHARM [202] ($\bar{\nu}_\mu$ beam)			< 0.205
CDHS [203]	$\lvert\epsilon^{q,X}_{\mu}\rvert$	$\lvert\epsilon^{q,X}_{e\mu}\rvert$, $\lvert\epsilon^{q,X}_{\mu\mu}\rvert$, $\lvert\epsilon^{q,X}_{\mu\tau}\rvert$	< 0.198
NuTeV [204]			< 0.11

Table E.2: Exclusion 90% C.L. limits on the observable scalar and pseudoscalar neutrino interaction parameter for different experiments, with $X = S, P$. Both scalar and pseudoscalar limits are the same for all experiments except for TEXONO.

Experiment	Observable	Parameters	Limit
ALEPH [189, 190, 191]	$\lvert\epsilon^{e,T}_{all}\rvert$	$\lvert\epsilon^{e,T}_{ee}\rvert$, $\lvert\epsilon^{e,T}_{\mu\mu}\rvert$, $\lvert\epsilon^{e,T}_{\tau\tau}\rvert$, $\lvert\epsilon^{e,T}_{e\mu}\rvert$, $\lvert\epsilon^{e,T}_{e\tau}\rvert$, $\lvert\epsilon^{e,T}_{\mu\tau}\rvert$	< 0.163
DELPHI [192]			< 0.254
L3 [193, 194, 195]			< 0.228
OPAL [196, 197, 198]			< 0.194
CHARM-II [199]	$\lvert\epsilon^{e,T}_{\mu}\rvert$	$\lvert\epsilon^{e,T}_{e\mu}\rvert$, $\lvert\epsilon^{e,T}_{\mu\mu}\rvert$, $\lvert\epsilon^{e,T}_{\mu\tau}\rvert$	< 0.036
TEXONO [200]	$\lvert\epsilon^{e,T}_{e}\rvert$	$\lvert\epsilon^{e,T}_{ee}\rvert$, $\lvert\epsilon^{e,T}_{e\mu}\rvert$, $\lvert\epsilon^{e,T}_{e\tau}\rvert$	< 0.073
CHARM [201] (ν_{-e} beam)	$\lvert\epsilon^{q,T}_{e}\rvert$	$\lvert\epsilon^{q,T}_{ee}\rvert$, $\lvert\epsilon^{q,T}_{e\mu}\rvert$, $\lvert\epsilon^{q,T}_{e\tau}\rvert$	< 0.127
CHARM [202] ($\nu_{-\mu}$ beam)	$\lvert\epsilon^{q,T}_{\mu}\rvert$	$\lvert\epsilon^{q,T}_{e\mu}\rvert$, $\lvert\epsilon^{q,T}_{\mu\mu}\rvert$, $\lvert\epsilon^{q,T}_{\mu\tau}\rvert$	< 0.0137
CDHS [203]			< 0.0130
NuTeV [204]			< 0.00754

Table E.3: Exclusion 90% C.L. limits on the observable tensor neutrino interaction parameter for different experiments.

Experiments	Scalar	Pseudoscalar	Tensor
e^-e^+ + TEXONO	$\lvert\epsilon^{e,S}_{ee}\rvert < 0.38$	$\lvert\epsilon^{e,P}_{ee}\rvert < 0.40$	$\lvert\epsilon^{e,T}_{ee}\rvert < 0.07$
e^-e^+ + CHARM-II	$\lvert\epsilon^{e,X}_{\mu\mu}\rvert < 0.31$		$\lvert\epsilon^{e,T}_{\mu\mu}\rvert < 0.03$
e^-e^+	$\lvert\epsilon^{e,X}_{\tau\tau}\rvert < 0.40$		$\lvert\epsilon^{e,T}_{\tau\tau}\rvert < 0.12$
e^-e^+ + TEXONO + CHARM-II	$\lvert\epsilon^{e,S}_{e\mu}\rvert < 0.25$	$\lvert\epsilon^{e,P}_{e\mu}\rvert < 0.25$	$\lvert\epsilon^{e,T}_{e\mu}\rvert < 0.03$
e^-e^+ + TEXONO	$\lvert\epsilon^{e,S}_{e\tau}\rvert < 0.28$	$\lvert\epsilon^{e,P}_{e\tau}\rvert < 0.29$	$\lvert\epsilon^{e,T}_{e\tau}\rvert < 0.07$
e^-e^+ + CHARM-II	$\lvert\epsilon^{e,X}_{\mu\tau}\rvert < 0.25$		$\lvert\epsilon^{e,T}_{\mu\tau}\rvert < 0.03$
CHARM$-e$	$\lvert\epsilon^{q,X}_{ee}\rvert < 1.9$		$\lvert\epsilon^{q,T}_{ee}\rvert < 0.13$
CHARM + CDHS (+ NuTeV)	$\lvert\epsilon^{q,X}_{\mu\mu}\rvert < 0.15\,(0.1)$		$\lvert\epsilon^{q,T}_{\mu\mu}\rvert < 0.01\,(0.006)$
CHARM$-e$ + CHARM + CDHS (+ NuTeV)	$\lvert\epsilon^{q,X}_{e\mu}\rvert < 0.15\,(0.1)$		$\lvert\epsilon^{q,T}_{e\mu}\rvert < 0.01\,(0.006)$
CHARM$-e$	$\lvert\epsilon^{q,X}_{e\tau}\rvert < 1.9$		$\lvert\epsilon^{q,T}_{e\tau}\rvert < 0.13$
CHARM + CDHS (+ NuTeV)	$\lvert\epsilon^{q,X}_{\mu\tau}\rvert < 0.15\,(0.1)$		$\lvert\epsilon^{q,T}_{\mu\tau}\rvert < 0.01\,(0.006)$

Table E.4: Combined 90% C.L. limits on the different scalar, pseudoscalar, and tensor neutrino interaction parameters, with $X = S, P$. For each suitable parameter, we also show in brackets the corresponding limits including the NuTeV measurements.

There are several points that we must highlight in this work. First, some of these constraints are new, such as those coming from the electron-positron collision to a neutrino-antineutrino pair plus photon signal, the CDHS experiment, and the TEXONO experiment. Secondly, we have also re-analyzed the NuTeV anomaly considering the recent results on the systematic uncertainties and provided new restrictive constraints for the GNI parameters. Moreover, from our results we can see that the bounds coming from muon-neutrino experiments are more restrictive than those from electron-neutrino, given their higher statistics, and finally, we see that in general, the interactions with quarks are more constrained than the ones with electrons.

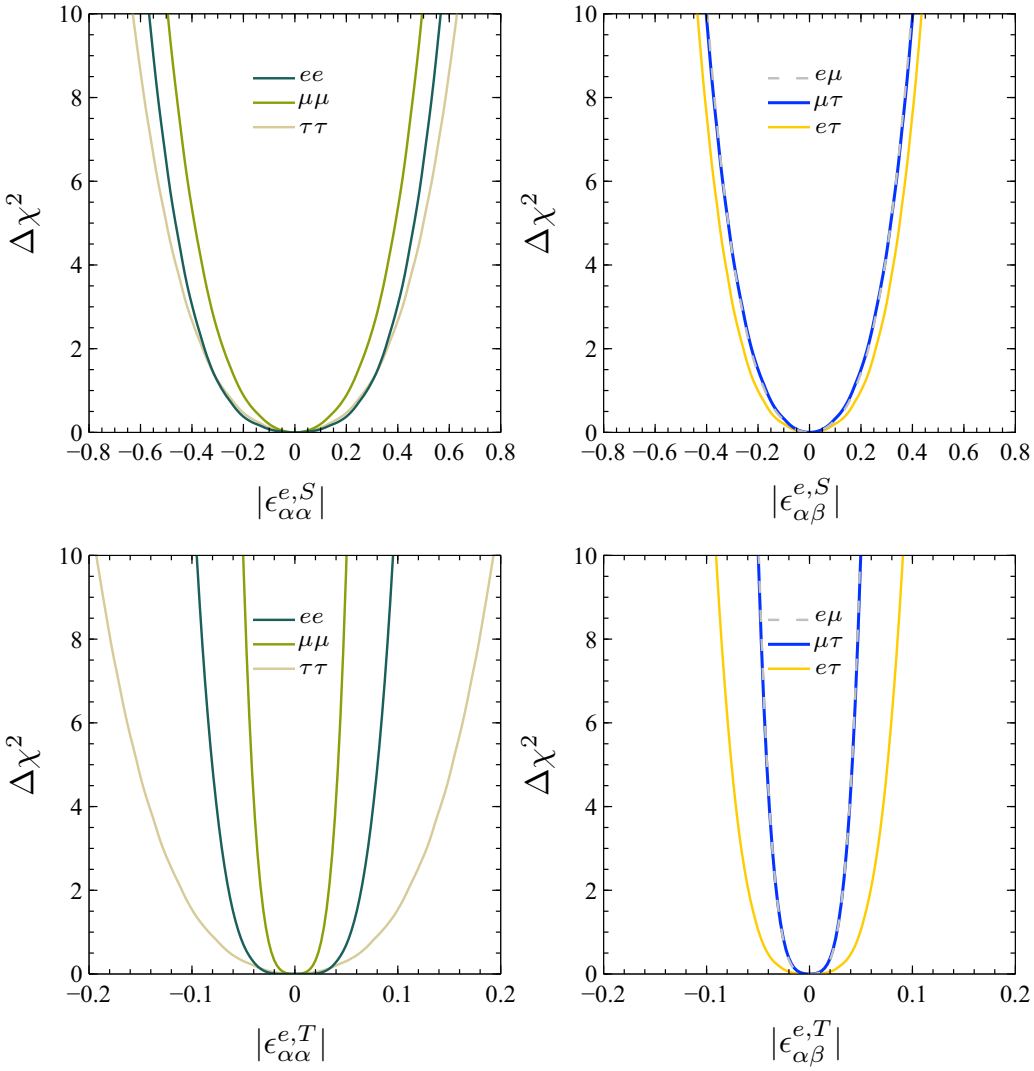

Figure E.1: Global constraints on the neutrino-electron interaction parameters from different experiments. The upper (lower) panels correspond to the scalar (tensor) parameters. In the left (right) panels we present limits for the flavor-diagonal (changing) parameters.

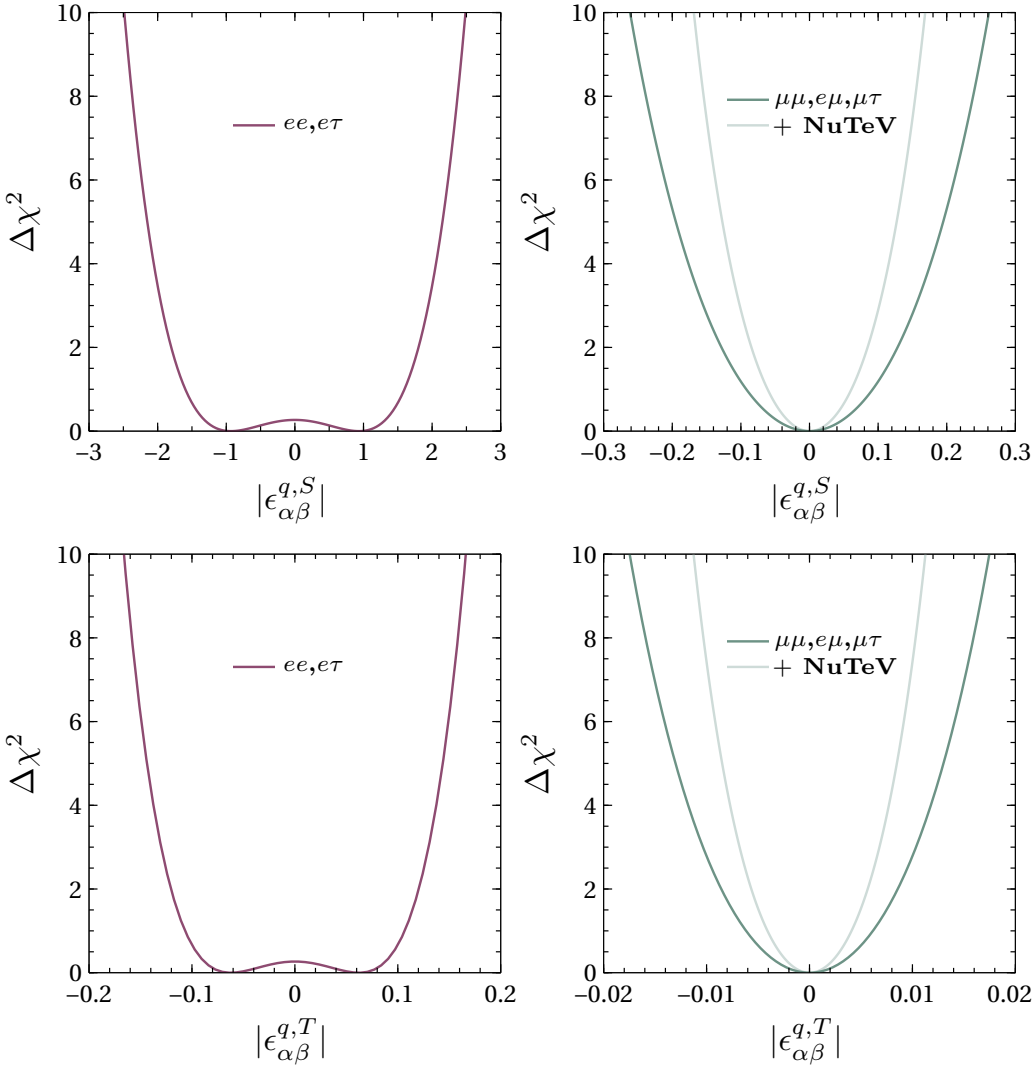

Figure E.2: Global constraints on the neutrino-quark interaction parameters from different experiments. The upper (lower) panels correspond to the scalar (tensor) parameters. In the right panels we present the resulting limits without the NuTeV measurement (solid green line) and including it (solid gray line).

Bibliography

[1] S. L. Glashow, "Partial Symmetries of Weak Interactions," Nucl. Phys. **22**, 579-588 (1961).

[2] S. Weinberg, "A Model of Leptons," Phys. Rev. Lett. **19**, 1264-1266 (1967).

[3] A. Salam, "Weak and Electromagnetic Interactions," Conf. Proc. C **680519**, 367-377 (1968).

[4] M. L. Perl *et al.*, "Evidence for Anomalous Lepton Production in e+ - e- Annihilation," Phys. Rev. Lett. **35**, 1489-1492 (1975).

[5] M. L. Perl *et al.*, "Properties of Anomalous e mu Events Produced in e+ e- Annihilation," Phys. Lett. B **63**, 466 (1976).

[6] M. Tanabashi *et al.* [Particle Data Group], "Review of Particle Physics," Phys. Rev. D **98**, no. 3, 030001 (2018).

[7] A. Sirlin, "Radiative corrections to g(v)/g(mu) in simple extensions of the su(2) x u(1) gauge model," Nucl. Phys. B **71** (1974) 29.

[8] A. Sirlin, "Current Algebra Formulation of Radiative Corrections in Gauge Theories and the Universality of the Weak Interactions," Rev. Mod. Phys. **50** (1978) 573 Erratum: [Rev. Mod. Phys. **50** (1978) 905].

[9] A. Sirlin, "Large m(W), m(Z) Behavior of the O(alpha) Corrections to Semileptonic Processes Mediated by W," Nucl. Phys. B **196** (1982) 83.

[10] W. J. Marciano and A. Sirlin, "Radiative Corrections to beta Decay and the Possibility of a Fourth Generation," Phys. Rev. Lett. **56** (1986) 22.

[11] W. J. Marciano and A. Sirlin, "Electroweak Radiative Corrections to tau Decay," Phys. Rev. Lett. **61** (1988) 1815.

[12] W. J. Marciano and A. Sirlin, "Radiative corrections to pi(lepton 2) decays," Phys. Rev. Lett. **71** (1993) 3629.

[13] E. Braaten and C. S. Li, "Electroweak radiative corrections to the semihadronic decay rate of the tau lepton," Phys. Rev. D **42** (1990) 3888.

[14] J. Erler, "Electroweak radiative corrections to semileptonic tau decays," Rev. Mex. Fis. **50** (2004) 200.

[15] S. Aoki *et al.* [Flavour Lattice Averaging Group], "FLAG Review 2019: Flavour Lattice Averaging Group (FLAG)," Eur. Phys. J. C **80**, no.2, 113 (2020).

[16] S. Schael *et al.* [ALEPH], "Branching ratios and spectral functions of tau decays: Final ALEPH measurements and physics implications," Phys. Rept. **421**, 191-284 (2005).

[17] A. J. Bevan *et al.* [BaBar and Belle], "The Physics of the B Factories," Eur. Phys. J. C **74**, 3026 (2014).

[18] E. Kou *et al.* [Belle-II], "The Belle II Physics Book," PTEP **2019**, no.12, 123C01 (2019) [erratum: PTEP **2020**, no.2, 029201 (2020)].

[19] A. Pich, "Precision Tau Physics," Prog. Part. Nucl. Phys. **75**, 41-85 (2014).

[20] A. Stahl, "Physics with tau leptons," Springer Tracts Mod. Phys. **160**, 1-316 (2000).

[21] S. Gonzàlez-Solís, "Tau decays into two mesons: an overview," EPJ Web Conf. **212**, 08003 (2019).

[22] A. Buras, "Gauge Theory of Weak Decays. The Standard Model and the Expedition to New Physics Summits", C. U. P., June 2020.

[23] P. Roig, "Hadronic and radiative decays of the tau lepton," [arXiv:1301.7626 [hep-ph]]. Ph. D. Thesis, Univ. de València, Spain.

[24] A. Guevara, "Low-energy meson phenomenology with Resonance Chiral Lagrangians," [arXiv:1708.00554 [hep-ph]]. Ph. D. Thesis, Cinvestav, Mexico.

[25] M. González-Alonso, "Low-energy tests of the Standard Model." Ph. D. Thesis, Univ. de València, Spain.

[26] I. Rosell, "Quantum corrections in the resonance chiral theory," [arXiv:hep-ph/0701248 [hep-ph]]. Ph. D. Thesis, Univ. de València, Spain.

[27] S. Weinberg, "Phenomenological Lagrangians," Physica A **96**, no.1-2, 327-340 (1979).

[28] T. Appelquist and J. Carazzone, "Infrared Singularities and Massive Fields," Phys. Rev. D **11**, 2856 (1975).

[29] C. P. Burgess, "Introduction to Effective Field Theory." C. U. P., December 2020.

[30] A. Pich, "Effective field theory: Course," [arXiv:hep-ph/9806303 [hep-ph]].

[31] A. Pich, "Effective Field Theory with Nambu-Goldstone Modes," Les Houches Lect. Notes **108** (2020).

[32] R. Penco, "An Introduction to Effective Field Theories," [arXiv:2006.16285 [hep-th]].

[33] A. V. Manohar, "Effective field theories," [arXiv:hep-ph/9508245 [hep-ph]].

[34] A. V. Manohar, "Introduction to Effective Field Theories," Les Houches Lect. Notes **108** (2020).

[35] D. B. Kaplan, "Effective field theories," [arXiv:nucl-th/9506035 [nucl-th]].

[36] D. B. Kaplan, "Five lectures on effective field theory," [arXiv:nucl-th/0510023 [nucl-th]].

[37] A. A. Petrov and A. E. Blechman, "Effective Field Theories."

[38] N. Cabibbo, "Unitary Symmetry and Leptonic Decays," Phys. Rev. Lett. **10** (1963), 531-533.

[39] M. Kobayashi and T. Maskawa, "CP Violation in the Renormalizable Theory of Weak Interaction," Prog. Theor. Phys. **49** (1973), 652-657.

[40] P. W. Higgs, "Broken symmetries, massless particles and gauge fields," Phys. Lett. **12** (1964), 132-133.

[41] P. W. Higgs, "Broken Symmetries and the Masses of Gauge Bosons," Phys. Rev. Lett. **13** (1964), 508-509.

[42] F. Englert and R. Brout, "Broken Symmetry and the Mass of Gauge Vector Mesons," Phys. Rev. Lett. **13** (1964), 321-323.

[43] G. S. Guralnik, C. R. Hagen and T. W. B. Kibble, "Global Conservation Laws and Massless Particles," Phys. Rev. Lett. **13** (1964), 585-587.

[44] P. Langacker, "The standard model and beyond." CRC Press 2009.

[45] C. Giunti and C. W. Kim, "Fundamentals of Neutrino Physics and Astrophysics." Oxford Univ. Press, 2010.

[46] A. Pich, "The Standard Model of Electroweak Interactions," [arXiv:1201.0537 [hep-ph]].

[47] S. Weinberg, "Baryon and Lepton Nonconserving Processes," Phys. Rev. Lett. **43**, 1566-1570 (1979).

[48] B. Grzadkowski, M. Iskrzynski, M. Misiak and J. Rosiek, "Dimension-Six Terms in the Standard Model Lagrangian," JHEP **10**, 085 (2010).

[49] V. Cirigliano, J. Jenkins and M. González-Alonso, "Semileptonic decays of light quarks beyond the Standard Model," Nucl. Phys. B **830** (2010), 95-115.

[50] M. González-Alonso, J. Martín Camalich and K. Mimouni, "Renormalization-group evolution of new physics contributions to (semi)leptonic meson decays," Phys. Lett. B **772** (2017), 777-785.

[51] W. Buchmuller and D. Wyler, "Effective Lagrangian Analysis of New Interactions and Flavor Conservation," Nucl. Phys. B **268**, 621-653 (1986).

[52] D. J. Gross and F. Wilczek, "Ultraviolet Behavior of Nonabelian Gauge Theories," Phys. Rev. Lett. **30**, 1343-1346 (1973).

[53] H. D. Politzer, "Reliable Perturbative Results for Strong Interactions?," Phys. Rev. Lett. **30**, 1346-1349 (1973).

[54] C. A. Baker, D. D. Doyle, P. Geltenbort, K. Green, M. G. D. van der Grinten, P. G. Harris, P. Iaydjiev, S. N. Ivanov, D. J. R. May and J. M. Pendlebury, *et al.* "An Improved experimental limit on the electric dipole moment of the neutron," Phys. Rev. Lett. **97**, 131801 (2006).

[55] J. M. Pendlebury, S. Afach, N. J. Ayres, C. A. Baker, G. Ban, G. Bison, K. Bodek, M. Burghoff, P. Geltenbort and K. Green, *et al.* "Revised experimental upper limit on the electric dipole moment of the neutron," Phys. Rev. D **92**, no.9, 092003 (2015).

[56] R. D. Peccei and H. R. Quinn, "CP Conservation in the Presence of Instantons," Phys. Rev. Lett. **38**, 1440-1443 (1977).

[57] I. J. R. Aitchison and A. J. G. Hey, "Gauge theories in particle physics: A practical introduction. Vol. 2: Non-Abelian gauge theories: QCD and the electroweak theory." CRC Press, 2012.

[58] M. E. Peskin, "Concepts of Elementary Particle Physics." CRC Press, 1995.

[59] A. Pich, "Quantum chromodynamics," [arXiv:hep-ph/9505231 [hep-ph]].

[60] S. L. Adler, "Axial vector vertex in spinor electrodynamics," Phys. Rev. **177** (1969), 2426-2438.

[61] J. S. Bell and R. Jackiw, "A PCAC puzzle: $\pi^0 \to \gamma\gamma$ in the σ model," Nuovo Cim. A **60** (1969), 47-61.

[62] J. Gasser and H. Leutwyler, "Chiral Perturbation Theory to One Loop," Annals Phys. **158**, 142 (1984).

[63] J. Gasser and H. Leutwyler, "Chiral Perturbation Theory: Expansions in the Mass of the Strange Quark," Nucl. Phys. B **250**, 465-516 (1985).

[64] S. R. Coleman, J. Wess and B. Zumino, "Structure of phenomenological Lagrangians. 1," Phys. Rev. **177**, 2239-2247 (1969).

[65] C. G. Callan, Jr., S. R. Coleman, J. Wess and B. Zumino, "Structure of phenomenological Lagrangians. 2," Phys. Rev. **177**, 2247-2250 (1969).

[66] O. Catà and V. Mateu, "Chiral perturbation theory with tensor sources," JHEP **09**, 078 (2007).

[67] J. Bijnens, G. Colangelo and G. Ecker, "The Mesonic chiral Lagrangian of order p^6," JHEP **02** (1999), 020.

[68] A. Pich, "Chiral perturbation theory," Rept. Prog. Phys. **58**, 563-610 (1995).

[69] S. Scherer, "Introduction to chiral perturbation theory," Adv. Nucl. Phys. **27**, 277 (2003).

[70] S. Scherer and M. R. Schindler, "A Primer for Chiral Perturbation Theory," Lect. Notes Phys. **830**, pp.1-338 (2012).

[71] S. Weinberg, Phys. Rev. Lett. **18** (1967), 507-509 doi:10.1103/PhysRevLett.18.507

[72] S. J. Brodsky and G. R. Farrar, "Scaling Laws at Large Transverse Momentum," Phys. Rev. Lett. **31** (1973) 1153.

[73] G. P. Lepage and S. J. Brodsky, "Exclusive Processes in Perturbative Quantum Chromodynamics," Phys. Rev. D **22** (1980) 2157.

[74] G. Ecker, J. Gasser, A. Pich and E. de Rafael, "The Role of Resonances in Chiral Perturbation Theory," Nucl. Phys. B **321**, 311-342 (1989).

[75] G. Ecker, J. Gasser, H. Leutwyler, A. Pich and E. de Rafael, "Chiral Lagrangians for Massive Spin 1 Fields," Phys. Lett. B **223**, 425-432 (1989).

[76] V. Cirigliano, G. Ecker, M. Eidemüller, R. Kaiser, A. Pich and J. Portolés, "Towards a consistent estimate of the chiral low-energy constants," Nucl. Phys. B **753** (2006), 139-177.

[77] K. Kampf and J. Novotny, "Resonance saturation in the odd-intrinsic parity sector of low-energy QCD," Phys. Rev. D **84** (2011), 014036.

[78] G. 't Hooft, "A Planar Diagram Theory for Strong Interactions," Nucl. Phys. B **72** (1974) 461.

[79] G. 't Hooft, "A Two-Dimensional Model for Mesons," Nucl. Phys. B **75** (1974) 461.

[80] P. D. Ruiz-Femenía, A. Pich and J. Portolés, "Odd intrinsic parity processes within the resonance effective theory of QCD," JHEP **07** (2003), 003.

[81] V. Cirigliano, G. Ecker, M. Eidemüller, A. Pich and J. Portolés, "The $< VAP >$ Green function in the resonance region," Phys. Lett. B **596** (2004), 96-106.

[82] V. Cirigliano, G. Ecker, M. Eidemüller, R. Kaiser, A. Pich and J. Portolés, "The $< SPP >$ Green function and SU(3) breaking in K(l3) decays," JHEP **04** (2005), 006.

[83] P. Roig and J. J. Sanz Cillero, "Consistent high-energy constraints in the anomalous QCD sector," Phys. Lett. B **733** (2014), 158-163.

[84] L. Y. Dai, J. Fuentes-Martín and J. Portolés, "Scalar-involved three-point Green functions and their phenomenology," Phys. Rev. D **99** (2019) no.11, 114015.

[85] G. Ecker, A. Pich and E. de Rafael, Phys. Lett. B **237** (1990), 481-487.

[86] I. Rosell, J. J. Sanz-Cillero and A. Pich, JHEP **08** (2004), 042 doi:10.1088/1126-6708/2004/08/042.

[87] V. Mateu and J. Portolés, "Form-factors in radiative pion decay," Eur. Phys. J. C **52** (2007), 325-338.

[88] D. G. Dumm, P. Roig, A. Pich and J. Portolés, "Hadron structure in tau → K K pi nu (tau) decays," Phys. Rev. D **81** (2010), 034031.

[89] D. G. Dumm, P. Roig, A. Pich and J. Portolés, "tau → pi pi pi nu(tau) decays and the a(1)(1260) off-shell width revisited," Phys. Lett. B **685** (2010), 158-164.

[90] O. Shekhovtsova, T. Przedzinski, P. Roig and Z. Was, "Resonance chiral Lagrangian currents and τ decay Monte Carlo," Phys. Rev. D **86** (2012), 113008.

[91] D. Gómez Dumm and P. Roig, "Resonance Chiral Lagrangian analysis of $\tau^- \to \eta^{(\prime)}\pi^-\pi^0\nu_\tau$ decays," Phys. Rev. D **86** (2012), 076009.

[92] I. M. Nugent, T. Przedzinski, P. Roig, O. Shekhovtsova and Z. Was, "Resonance chiral Lagrangian currents and experimental data for $\tau^- \to \pi^-\pi^-\pi^+\nu_\tau$," Phys. Rev. D **88** (2013), 093012.

[93] A. Guevara, G. López Castro and P. Roig, "Weak radiative pion vertex in $\tau^- \to \pi^-\nu_\tau\ell^+\ell^-$ decays," Phys. Rev. D **88** (2013) no.3, 033007.

[94] P. Roig, A. Guevara and G. López Castro, "$VV'P$ form factors in resonance chiral theory and the $\pi - \eta - \eta'$ light-by-light contribution to the muon $g-2$," Phys. Rev. D **89** (2014) no.7, 073016.

[95] A. Guevara, G. López-Castro and P. Roig, "$\tau^- \to \eta^{(\prime)}\pi^-\nu_\tau\gamma$ decays as backgrounds in the search for second class currents," Phys. Rev. D **95** (2017) no.5, 054015.

[96] A. Guevara, P. Roig and J. J. Sanz-Cillero, "Pseudoscalar pole light-by-light contributions to the muon $(g-2)$ in Resonance Chiral Theory," JHEP **06** (2018), 160.

[97] P. Roig and P. Sánchez-Puertas, "Axial-vector exchange contribution to the hadronic light-by-light piece of the muon anomalous magnetic moment," Phys. Rev. D **101** (2020) no.7, 074019.

[98] J. A. Miranda and P. Roig, "New τ-based evaluation of the hadronic contribution to the vacuum polarization piece of the muon anomalous magnetic moment," Phys. Rev. D **102** (2020), 114017.

[99] W. Qin, L. Y. Dai and J. Portolés, "Two and three pseudoscalar production in e^+e^- annihilation and their contributions to (g - 2)$_\mu$," JHEP **03** (2021), 092.

[100] J. Portolés, "Basics of Resonance Chiral Theory," AIP Conf. Proc. **1322**, no.1, 178-187 (2010).

[101] V. Cirigliano, A. Crivellin and M. Hoferichter, "No-go theorem for nonstandard explanations of the $\tau \to K_S \pi \nu_\tau$ CP asymmetry," Phys. Rev. Lett. **120** (2018) no.14, 141803.

[102] J. P. Lees *et al.* [BaBar Collaboration], "Search for CP Violation in the Decay $\tau^- - > \pi^- K^0_S (>= 0\pi^0)\nu_\tau$," Phys. Rev. D **85** (2012) 031102 Erratum: [Phys. Rev. D **85** (2012) 099904].

[103] D. Epifanov *et al.* [Belle Collaboration], "Study of $\tau^- \to K_S \pi^- \nu_\tau$ decay at Belle," Phys. Lett. B **654** (2007) 65.

[104] H. Z. Devi, L. Dhargyal and N. Sinha, "Can the observed CP asymmetry in $\tau \to K \pi \nu_\tau$ be due to nonstandard tensor interactions?," Phys. Rev. D **90** (2014) no.1, 013016.

[105] L. Dhargyal, "Full angular spectrum analysis of tensor current contribution to $A_{cp}(\tau \to K_s \pi \nu_\tau)$.

[106] L. Dhargyal, "New tensor interaction as the source of the observed CP asymmetry in $\tau \to K_S \pi \nu_\tau$," Springer Proc. Phys. **203** (2018) 329.

[107] I. I. Bigi and A. I. Sanda, "A 'Known' CP asymmetry in tau decays," Phys. Lett. B **625** (2005) 47.

[108] G. Calderón, D. Delepine and G. L. Castro, "Is there a paradox in CP asymmetries of $\tau^\pm \to K_{L,S} \pi^\pm \nu_\tau$ decays?," Phys. Rev. D **75** (2007) 076001.

[109] Y. Grossman and Y. Nir, "CP Violation in $\tau \to \nu \pi K_S$ and $D \to \pi K_S$: The Importance of $K_S - K_L$ Interference," JHEP **1204** (2012) 002.

[110] A. D. Sakharov, "Violation of CP Invariance, C asymmetry, and baryon asymmetry of the universe," Pisma Zh. Eksp. Teor. Fiz. **5** (1967) 32 [JETP Lett. **5** (1967) 24] [Sov. Phys. Usp. **34** (1991) no.5, 392] [Usp. Fiz. Nauk **161** (1991) no.5, 61].

[111] A. G. Cohen, D. B. Kaplan and A. E. Nelson, "Progress in electroweak baryogenesis," Ann. Rev. Nucl. Part. Sci. **43** (1993) 27.

[112] A. Riotto and M. Trodden, "Recent progress in baryogenesis," Ann. Rev. Nucl. Part. Sci. **49** (1999) 35.

[113] M. Bischofberger *et al.* [Belle Collaboration], "Search for CP violation in $\tau \to K^0_S \pi \nu_\tau$ decays at Belle," Phys. Rev. Lett. **107** (2011) 131801.

[114] B. Moussallam, "Analyticity constraints on the strangeness changing vector current and applications to $\tau^- \to K\pi\nu_\tau$, $\tau \to K\pi\pi\nu_\tau$," Eur. Phys. J. C **53** (2008) 401.

[115] M. Jamin, A. Pich and J. Portolés, "What can be learned from the Belle spectrum for the decay $\tau^- \to \nu_\tau K_S \pi^-$," Phys. Lett. B **664** (2008) 78.

[116] D. R. Boito, R. Escribano and M. Jamin, "K pi vector form-factor, dispersive constraints and $\tau^- \to \nu_\tau K\pi$ decays," Eur. Phys. J. C **59** (2009) 821.

[117] D. R. Boito, R. Escribano and M. Jamin, "K π vector form factor constrained by $\tau - > K\pi\nu_\tau$ and K_{l3} decays," JHEP **1009** (2010) 031.

[118] M. Antonelli, V. Cirigliano, A. Lusiani and E. Passemar. "Predicting the τ strange branching ratios and implications for V_{us}". JHEP 1310 (2013) 070.

[119] D. Kimura, K. Y. Lee and T. Morozumi, "The Form factors of $\tau \to K\pi(\eta)\nu$ and the predictions for CP violation beyond the standard model," PTEP **2013** (2013) 053B03 Erratum: [PTEP **2014** (2014) no.8, 089202].

[120] V. Bernard, "First determination of $f_+(0)|V_{us}|$ from a combined analysis of $\tau \to K\pi\nu_\tau$ decay and πK scattering with constraints from $K_{\ell 3}$ decays," JHEP **1406** (2014) 082.

[121] R. Escribano, S. González-Solís, M. Jamin and P. Roig, "Combined analysis of the decays $\tau^- \to K_S \pi^- \nu_\tau$ and $\tau^- \to K^- \eta \nu_\tau$," JHEP **1409** (2014) 042.

[122] M. Jamin, A. Pich and J. Portolés, "Spectral distribution for the decay $\tau^- \to \nu_\tau K\pi$," Phys. Lett. B **640** (2006) 176.

[123] L. A. Jiménez Pérez and G. Toledo Sánchez, "Absorptive corrections for vector mesons: matching to complex mass scheme and longitudinal corrections," J. Phys. G **44** (2017) no.12, 125003.

[124] M. Jamin, J. A. Oller and A. Pich, "Strangeness changing scalar form-factors," Nucl. Phys. B **622** (2002) 279.

[125] M. Jamin, J. A. Oller and A. Pich, "S wave K pi scattering in chiral perturbation theory with resonances," Nucl. Phys. B **587** (2000) 331.

[126] E. A. Garcés, M. Hernández Villanueva, G. López Castro and P. Roig, "Effective-field theory analysis of the $\tau^- \to \eta^{(\prime)}\pi^-\nu_\tau$ decays," JHEP **1712** (2017) 027.

[127] J. A. Miranda and P. Roig, "Effective-field theory analysis of the $\tau^- \to \pi^-\pi^0\nu_\tau$ decays," JHEP **11**, 038 (2018).

[128] V. Cirigliano, A. Falkowski, M. González-Alonso and A. Rodríguez-Sánchez, "Hadronic tau decays as New Physics probes in the LHC era," Phys. Rev. Lett. **122** (2019) no.22, 221801.

[129] T. Bhattacharya, V. Cirigliano, S. D. Cohen, A. Filipuzzi, M. González-Alonso, M. L. Graesser, R. Gupta and H. W. Lin, "Probing Novel Scalar and Tensor Interactions from (Ultra)Cold Neutrons to the LHC," Phys. Rev. D **85**, 054512 (2012).

[130] V. Cirigliano, M. González-Alonso and M. L. Graesser, "Non-standard Charged Current Interactions: beta decays versus the LHC," JHEP **1302** (2013) 046.

[131] V. Cirigliano, S. Gardner and B. Holstein, "Beta Decays and Non-Standard Interactions in the LHC Era," Prog. Part. Nucl. Phys. **71** (2013) 93.

[132] H. M. Chang, M. González-Alonso and J. Martín Camalich, "Nonstandard Semileptonic Hyperon Decays," Phys. Rev. Lett. **114** (2015) no.16, 161802.

[133] A. Courtoy, S. Baessler, M. González-Alonso and S. Liuti, "Beyond-Standard-Model Tensor Interaction and Hadron Phenomenology," Phys. Rev. Lett. **115** (2015) 162001.

[134] M. González-Alonso and J. Martín Camalich, "Global Effective-Field-Theory analysis of New-Physics effects in (semi)leptonic kaon decays," JHEP **1612** (2016) 052.

[135] M. González-Alonso and J. Martín Camalich, "New Physics in $s \to u\ell^-\bar{\nu}$: Interplay between semileptonic kaon and hyperon decays," arXiv:1606.06037 [hep-ph].

[136] S. Alioli, V. Cirigliano, W. Dekens, J. de Vries and E. Mereghetti, "Right-handed charged currents in the era of the Large Hadron Collider," JHEP **1705** (2017) 086.

[137] M. González-Alonso, O. Naviliat-Cuncic and N. Severijns, "New physics searches in nuclear and neutron β decay," Prog. Part. Nucl. Phys. **104** (2019) 165.

[138] J. Rendón, P. Roig and G. Toledo Sánchez, "Effective-field theory analysis of the $\tau^- \to (K\pi)^-\nu_\tau$ decays," Phys. Rev. D **99**, no.9, 093005 (2019).

[139] J. Rendón, "Effective-field theory analysis of the $\tau^- \to (K\pi)^-\nu_\tau$ decays," PoS **LHCP2019**, 030 (2019).

[140] M. Jamin, J. A. Oller and A. Pich, "Light quark masses from scalar sum rules," Eur. Phys. J. C **24** (2002) 237.

[141] M. Jamin, J. A. Oller and A. Pich, "Order p^6 chiral couplings from the scalar $K\pi$ form-factor," JHEP **0402** (2004) 047.

[142] M. Jamin, J. A. Oller and A. Pich, "Scalar K pi form factor and light quark masses," Phys. Rev. D **74** (2006) 074009.

[143] K. M. Watson, "The Effect of final state interactions on reaction cross-sections," Phys. Rev. **88**, 1163 (1952).

[144] R. Escribano, S. Gonzàlez-Solís and P. Roig, "$\tau^- \to K^-\eta^{(\prime)}\nu_\tau$ decays in Chiral Perturbation Theory with Resonances," JHEP **1310** (2013) 039.

[145] R. Escribano, S. Gonzàlez-Solís and P. Roig, "Predictions on the second-class current decays $\tau^- \to \pi^-\eta^{(\prime)}\nu_\tau$," Phys. Rev. D **94** (2016) no.3, 034008.

[146] I. Baum, V. Lubicz, G. Martinelli, L. Orifici and S. Simula, "Matrix elements of the electromagnetic operator between kaon and pion states," Phys. Rev. D **84**, 074503 (2011).

[147] S. Gonzàlez-Solís and P. Roig, "A dispersive analysis of the pion vector form factor and $\tau^- \to K^- K_S \nu_\tau$ decay," Eur. Phys. J. C **79** (2019) no.5, 436.

[148] D. Aston *et al.*, "A Study of $K-\pi^+$ Scattering in the Reaction $K^- p \to K^- \pi^+ n$ at 11 GeV/c," Nucl. Phys. B **296** (1988) 493.

[149] P. Estabrooks, R. K. Carnegie, A. D. Martin, W. M. Dunwoodie, T. A. Lasinski and D. W. G. S. Leith, "Study of $K\pi$ Scattering Using the Reactions $K^\pm p \to K^\pm \pi^+ n$ and $K^\pm p \to K^\pm \pi^- \Delta^{++}$ at 13 GeV/c," Nucl. Phys. B **133** (1978) 490.

[150] P. Buettiker, S. Descotes-Genon and B. Moussallam, "A new analysis of pi K scattering from Roy and Steiner type equations," Eur. Phys. J. C **33** (2004) 409.

[151] L. Beldjoudi and T. N. Truong, "tau to pi K neutrino decay and pi K scattering," Phys. Lett. B **351** (1995) 357.

[152] D. N. Gao and X. F. Wang, "On the angular distributions of $\tau^- \to K_S \pi^- \nu_\tau$ decay," Phys. Rev. D **87** (2013) 073016.

[153] Y. Amhis *et al.* [HFLAV Collaboration], "Averages of b-hadron, c-hadron, and τ-lepton properties as of summer 2016," Eur. Phys. J. C **77** (2017) no.12, 895.

[154] P. Roig, "Semileptonic τ decays: powerful probes of non-standard charged current weak interactions," EPJ Web Conf. **212** (2019), 08002.

[155] S. Gonzàlez-Solís, A. Miranda, J. Rendón and P. Roig, "Effective-field theory analysis of the $\tau^- \to K^-(\eta^{(\prime)}, K^0)\nu_\tau$ decays," Phys. Rev. D **101**, no.3, 034010 (2020).

[156] J. P. Lees *et al.* [BaBar], "Measurement of the spectral function for the $\tau^- \to K^- K_S \nu_\tau$ decay," Phys. Rev. D **98**, no.3, 032010 (2018).

[157] M. A. Arroyo-Ureña, G. Hernández-Tomé, G. López-Castro, P. Roig and I. Rosell, "Radiative corrections to $\tau \to \pi(K)\nu_\tau[\gamma]$: a reliable new physics test," [arXiv:2107.04603 [hep-ph]].

[158] Z. H. Guo and P. Roig, Phys. Rev. D **82** (2010), 113016.

[159] J. C. Hardy and I. S. Towner, "Superallowed $0^+ \to 0^+$ nuclear β decays: 2020 critical survey, with implications for V_{ud} and CKM unitarity," Phys. Rev. C **102** (2020) no.4, 045501.

[160] R. Decker and M. Finkemeier, "Short and long distance effects in the decay tau —> pi tau-neutrino (gamma)," Nucl. Phys. B **438**, 17-53 (1995).

[161] V. Cirigliano and I. Rosell, "pi/K —> e anti-nu(e) branching ratios to O(e**2 p**4) in Chiral Perturbation Theory," JHEP **10**, 005 (2007).

[162] J. L. Rosner, S. Stone and R. S. Van de Water, "Leptonic Decays of Charged Pseudoscalar Mesons - 2015." [arXiv:1509.02220 [hep-ph]]. Prepared for the PDG 2016.

[163] M. Fujikawa *et al.* [Belle], "High-Statistics Study of the tau- —> pi-pi0 nu(tau) Decay," Phys. Rev. D **78**, 072006 (2008).

[164] K. Inami *et al.* [Belle], "Precise measurement of hadronic tau-decays with an eta meson," Phys. Lett. B **672**, 209-218 (2009).

[165] J. P. Lees *et al.* [BaBar], "Study of high-multiplicity 3-prong and 5-prong tau decays at BABAR," Phys. Rev. D **86**, 092010 (2012).

[166] G. D'Ambrosio, G. F. Giudice, G. Isidori and A. Strumia, "Minimal flavor violation: An Effective field theory approach," Nucl. Phys. B **645** (2002), 155-187.

[167] F. Guerrero and A. Pich, "Effective field theory description of the pion form-factor," Phys. Lett. B **412**, 382-388 (1997).

[168] A. Pich and J. Portolés, "The Vector form-factor of the pion from unitarity and analyticity: A Model independent approach," Phys. Rev. D **63** (2001), 093005.

[169] D. Gómez Dumm and P. Roig, "Dispersive representation of the pion vector form factor in $\tau \to \pi\pi\nu_\tau$ decays," Eur. Phys. J. C **73** (2013) no.8, 2528.

[170] D. Gómez Dumm, A. Pich and J. Portolés, "The Hadronic off-shell width of meson resonances," Phys. Rev. D **62** (2000), 054014.

[171] R. Omnès, "On the Solution of certain singular integral equations of quantum field theory," Nuovo Cim. **8** (1958), 316-326.

[172] R. García-Martín, R. Kaminski, J. R. Peláez, J. Ruiz de Elvira and F. J. Ynduráin, "The Pion-pion scattering amplitude. IV: Improved analysis with once subtracted Roy-like equations up to 1100 MeV," Phys. Rev. D **83**, 074004 (2011).

[173] Z. H. Guo and J. A. Oller, "Resonances from meson-meson scattering in U(3) CHPT," Phys. Rev. D **84**, 034005 (2011).

[174] Z. H. Guo, J. A. Oller and J. Ruiz de Elvira, "Chiral dynamics in form factors, spectral-function sum rules, meson-meson scattering and semi-local duality," Phys. Rev. D **86** (2012), 054006.

[175] Z. H. Guo, L. Liu, U. G. Meißner, J. A. Oller and A. Rusetsky, "Chiral study of the $a_0(980)$ resonance and $\pi\eta$ scattering phase shifts in light of a recent lattice simulation," Phys. Rev. D **95**, no. 5, 054004 (2017).

[176] S. Descotes-Genon and B. Moussallam, "Analyticity of $\eta\pi$ isospin-violating form factors and the $\tau \to \eta\pi\nu$ second-class decay," Eur. Phys. J. C **74** (2014), 2946.

[177] E. Arganda, M. J. Herrero and J. Portolés, JHEP **06** (2008), 079.

[178] A. Celis, V. Cirigliano and E. Passemar, Phys. Rev. D **89** (2014), 013008.

[179] A. Lami, J. Portolés and P. Roig, Phys. Rev. D **93** (2016) no.7, 076008.

[180] J. Rendón, tesis de maestría, Polarization effects in $\tau^- \to \pi^-\ell^+\ell^-\nu_\tau$ decays. Departamento de física del Cinvestav, 2016.

[181] A. Guevara, G. López Castro and P. Roig, Phys. Rev. D **88**, no.3, 033007 (2013).

[182] C. Dib, J. C. Helo, M. Hirsch, S. Kovalenko and I. Schmidt, Phys. Rev. D **85** (2012) 011301.

[183] Talk given by D. Epifanov, Tau Michel parameters at Belle II, KEK-FF2014FALL/B2TiP, 28-31 October 2014.

[184] A. Guevara Escalante, Tesis de maestría, El vértice $W^*\gamma^*\pi^-$ en la teoría quiral de resonancias y la desintegración $\tau^- \to \pi^-\ell^+\ell^-\nu_\tau$. Departamento de física del Cinvestav, 2013.

[185] Z. H Guo and P. Roig, Physical Review, D82 (2010) 113016, arXiv: 1009.2542 [hep-ph], and references therein.

[186] A. Flores Tlalpa, Tesis de Doctorado, Modelo de dominancia de mesones para decaimientos semileptónicos de sabores pesados. Departamento de física del Cinvestav, 2008.

[187] J. Gutierrez, Tesis de Maestría, Estudio de los decaimientos semileptónicos $\tau^- \to \nu_\tau \pi^- \pi^0$ y $\tau^- \to \nu_\tau \pi^- \pi^0 \ell^+ \ell^-$. Departamento de física del Cinvestav, 2016.

[188] F. J. Escrihuela, L. J. Flores, O. G. Miranda and J. Rendón, JHEP **07** (2021), 061.

[189] R. Barate *et al.* [ALEPH], Phys. Lett. B **420**, 127-139 (1998).

[190] R. Barate *et al.* [ALEPH], Phys. Lett. B **429**, 201-214 (1998).

[191] A. Heister *et al.* [ALEPH], Eur. Phys. J. C **28**, 1-13 (2003).

[192] P. Abreu *et al.* [DELPHI], Eur. Phys. J. C **17**, 53-65 (2000).

[193] M. Acciarri *et al.* [L3], Phys. Lett. B **415**, 299-310 (1997).

[194] M. Acciarri *et al.* [L3], Phys. Lett. B **444**, 503-515 (1998).

[195] M. Acciarri *et al.* [L3], Phys. Lett. B **470**, 268-280 (1999).

[196] K. Ackerstaff *et al.* [OPAL], Eur. Phys. J. C **2**, 607-625 (1998).

[197] G. Abbiendi *et al.* [OPAL], Eur. Phys. J. C **8**, 23-40 (1999).

[198] G. Abbiendi *et al.* [OPAL], Eur. Phys. J. C **18**, 253-272 (2000).

[199] P. Vilain *et al.* [CHARM-II], Phys. Lett. B **302**, 351-355 (1993).

[200] M. Deniz *et al.* [TEXONO], Phys. Rev. D **81**, 072001 (2010).

[201] J. Dorenbosch *et al.* [CHARM], Phys. Lett. B **180**, 303-307 (1986).

[202] J. V. Allaby *et al.* [CHARM], Z. Phys. C **36**, 611 (1987).

[203] A. Blondel, P. Bockmann, H. Burkhardt, F. Dydak, A. L. Grant, R. Hagelberg, E. W. Hughes, W. Krasny, A. Para and H. Taureg, *et al.* Z. Phys. C **45**, 361-379 (1990).

[204] G. P. Zeller *et al.* [NuTeV], Phys. Rev. Lett. **88**, 091802 (2002). [erratum: Phys. Rev. Lett. **90**, 239902 (2003).]

[205] S. Gonzàlez-Solís, A. Miranda, J. Rendón and P. Roig, Phys. Lett. B **804** (2020), 135371.